Alkynes and Late Transition Metals - Theory, Reactions and Mechanism

Ahlquist, Mårten Sten Gösta

Publication date:
2007

Document Version
Publisher's PDF, also known as Version of record

Mårten Ahlquist

Alkynes and Late Transition Metals – Theory, Reactions and Mechanism

Ph. D. Thesis
DTU, Lyngby, January 2007

DTU

Preface

The first persons I would like to acknowledge are my two supervisors Per-Ola Norrby and David Tanner. Per-Ola, who became my primary supervisor, has been a great mentor and I am especially grateful for the freedom I have been given to develop my own ideas. Above all the ideas I have had on my own Per-Ola is a machine of them, some better than others. There is a saying from a previous member of the group that "If Per-Ola tells you what to do once – don't do it. But if he tells you about the same idea three times, you'd better start working on it". Another thing that Per-Ola taught me was *how* to write a paper and *when* to write it, and without him I would never have the eight published papers or all the manuscripts that are currently under preparation. David has had the role as my co-supervisor, and my experimental supervisor. Even though the experimental work became a minor part of my thesis David has had invaluable input on my work, and nowadays we have discussions on pure theoretical chemistry.

Another person at DTU that I would like to give a special acknowledgement to is my former group member and friend Peter Fristrup. As our collaboration has become closer and our discussions more and more frequent, my inspiration for finding and solving chemical problems has grown.

During my time as a PhD student I have had the privilege to work with several groups outside of DTU. The first such collaboration was with Prof. Sandro Cacchi and his group at La Sapienza in Rome. With some COST money in my pocket I went to Rome in October 2004, to work in the Cacchi group. This great collaboration has resulted in two publications and more is probably coming.

Another very good collaboration I have had was with Prof. Troels Skrydstrup and his co-workers at Aarhus University. The work resulted in a publication in Angewandte Chemie which was picked to as a "Hot Paper" by the publisher.

In March 2006 my second and longest external stay started. I had the great privilege to go to work in the group of Profs. K. Barry Sharpless and Valery V. Fokin at The Scripps Research Institute in La Jolla, California. Looking back on my three years of PhD studies I must say that the six months at Scripps were probably the most memorable. The charisma and inspiration of Barry was unprecedented to me. He is truly a character in its best sense and I am very thankful for the time I was allowed to spend in his group. I also miss the mechanistic discussions with Valery which were always interesting and inspirational. After an hour or so in his office I usually came out with a pile of paper filled with ideas and mechanistic proposals. At the time when I was working in the Sharpless group, Prof. Sukbok

Chang was a guest in the group. Our collaboration was truly great, and as I am writing we are still collaborating.
A special thanks is directed to my good friend Helena Ohlsson who designed the cover of this thesis.
I would also like to thank all current and previous members and visitors of the Norrby group for making work a fun place. Henriette Holm is especially acknowledged for helping out with all the little things, the things that the rest of us are pretty lousy at.
For the translation of the abstract from English to Danish I had invaluable help from Mette Fanefjord and Thomas Jensen. Thanks guys!
During the preparation of this thesis I have been frustrated, annoyed and bored many times. I would therefore thank Erika for being a great company.
Finally I would like to thank everyone who has been working in building 201 during my time at DTU.

Mårten Ahlquist
March 30, 2007

Abstract

The work described in this thesis is focused on reactions of organic molecules with transition metals. The field of organometallic chemistry has been growing rapidly the last decades and two recent Nobel Prizes were awarded for discoveries in transition metal catalyzed reactions.

A short introduction to organometallic chemistry and the mechanisms behind it is given in the first part. Several of the most common methods for studying reaction mechanisms are described, and their advantages and disadvantages are discussed.

In the second chapter the reaction mechanism of stannylcupration of α,β-acetylenic carbonyl compounds is described. By a combination of experimental methods and theoretical modeling the unexpected stereoselectivity of the addition of stannylcuprates to ynones was studied and compared to the corresponding carbocupration.

The work described in the third chapter is on coupling reactions catalyzed by palladium. After a brief introduction to the field, the mechanism of the hydroarylation/vinylation reaction is described. For the investigation mainly theoretical methods were used, but for investigating the regiochemical outcome of the reaction it was combined. Thereafter the observation by Skrydstrup and co-workers is discussed, that under some conditions internal vinyl electrophiles yielded products with the rearranged terminal vinyl group. The mechanism for the rearrangement was proposed to proceed via a palladium(II)-hydride-acetylene intermediate. The final part of the chapter describes an investigation of the stability and reactivity of palladium(0) phosphine complexes. Oxidative addition of aryl halides was found to proceed via an S_NAr like mechanism at a mono-coordinate complex PdL.

The final chapter deals with a type of reaction which has gained much attention lately, Huisgen's 1,3-dipolar cycloaddition of azides and alkynes. The copper catalyzed version of the reaction has become *the* central reaction in "Click Chemistry". It was found to be very robust and produced the 1,4-triazole exclusively. Herein is described how dinuclear copper acetylides react more readily than the previously studied mononuclear analogs. Next the reaction with *N*-sulfonyl azides is described with focus on the mechanisms for breakdown of the intermediates. For selective synthesis of 1,5-triazoles a ruthenium(II) catalyst has been used, and based on computational results the selectivity and reactivity was rationalized.

Resumé

Denne afhandling fokuserer på reaktioner mellem organiske molekyler og overgangsmetaller. Området metalorganisk kemi har udviklet sig hastigt indenfor de sidste årtier. For nyligt er der således uddelt to Nobelpriser for opdagelser indenfor metalorganisk kemi.

Det første kapitel giver en kort introduktion til metalorganisk kemi og mekanismerne bag. Flere af de mest almindelige metoder for mekanistiske studier beskrives, og deres fordele og ulemper diskuteres.

Andet kapitel beskriver reaktionsmekanismen for stannylkuprering af α,β-acetylen karbonyl forbindelser. Stereoselektiviteten af addition af stannylkuprater til ynoner er blevet undersøgt og sammenlignet med den tilsvarende karbokuprering ved hjælp af eksperimentelle og teoretisk metoder.

Kapitel tre omhandler palladium-katalyserede koblingsreaktioner, og efter en introduktion til dette felt beskrives mekanismen for hydroarylering/vinylering. Denne reaktion blev undersøgt hovedsagligt med teoretiske metoder, dog blev en kombination af eksperimentelle og teoretiske metoder brugt til bestemmelsen af regiokemien. Troels Skrydstrups gruppe har observeret, at under nogle betingelser omlejres den interne vinylelektrofil til en terminal vinylgruppe, mekanismen herfor foreslås at forløbe via et palladium(II)-hydrid-acetylen intermediat. Den sidste del af kapitlet beskriver resultaterne fra en undersøgelse af stabiliteten og reaktiviteten af palladium(0)-phosphin komplekser. Oxidativ addition af arylhalider blev fundet til at forløbe via en S_NAr lignende mekanisme på et mono-koordineret PdL-kompleks.

Det sidste kapitel behandler en reaktion som på det seneste har fået stor opmærksomhed, Huisgens 1,3-dipolære cykloaddition af azider til alkyner. Den kobber-katalyserede version af denne reaktion er blevet *den* centrale reaktion i "Click Chemistry". Denne reaktion er konstateret at være ekstremt robust og danner udelukkende 1,4-triazolen. Kapitlet beskriver hvordan dikobber acetylider reagerer hurtigere end de tidligere studerede monokobber acetylid-analoger. Reaktionen af *N*-sulfonyl azider beskrives med fokus på mekanismen for intermediaternes nedbrydning. For selektiv syntese af 1,5-triazolerne anvendes en ruthenium(II)-katalysator, og ved hjælp af beregnede resultater rationaliseres både selektiviteten og reaktiviteten af denne reaktion.

Table of Contents

Articles

Papers included in this thesis

1. "*An Experimental and Theoretical Study of the Mechanism of Stannylcupration of α,β-Acetylenic Ketones and Esters*"
   Mårten Ahlquist, Thomas E. Nielsen, Sebastian Le Quement, David Tanner, and Per-Ola Norrby
   Chem. Eur. J. **2006**, 2866.

2. "*Palladium(0) alkyne complexes as active species: A DFT-investigation*"
   Mårten Ahlquist, Giancarlo Fabrizi, Sandro Cacchi, and Per-Ola Norrby
   Chem. Commun. **2005**, 4196.

3. "*The Mechanism of the Phosphine Free Palladium Catalyzed Hydroarylation of Alkynes*"
   Mårten Ahlquist, Giancarlo Fabrizi, Sandro Cacchi, and Per-Ola Norrby
   J. Am. Chem. Soc. **2006**, *128*, 12785.

4. "*Heck Coupling with Nonactivated Alkenyl Tosylates and Phosphates. Examples of Effective 1,2-Migrations of the Alkenyl Palladium(II) Intermediates*"
   Anders L. Hansen, Jean-Philippe Ebran, **Mårten Ahlquist**, Per-Ola Norrby, and Troels Skrydstrup
   Angew. Chem. Int. Ed. **2006**, *45,* 3349.

5. "*Theoretical evidence for low-ligated palladium(0): [Pd-L] as the active species in oxidative addition reactions*"
   Mårten Ahlquist, Peter Fristrup, David Tanner, and Per-Ola Norrby
   Organometallics **2006**, *25,* 2066.

6. "*Oxidative Addition of Aryl Chlorides to Monoligated Palladium(0) - A DFT-SCRF Study.*"
   Mårten Ahlquist and Per-Ola Norrby
   Organometallics **2007**, *26*, 550.

7. "*Copper-Catalyzed Synthesis of N-Sulfonyl-1,2,3-triazoles: Controlling Selectivity* "
   Eun Jeong Yoo, **Mårten Ahlquist**, Seok Hwan Kim, Imhyuck Bae, Valery V. Fokin, K. Barry Sharpless, and Sukbok Chang
   Angew. Chem. Int. Ed. **2007**, *In press – Available online*

8. "*Enhanced Reactivity of Dinuclear Copper(I) Acetylides in Dipolar Cycloadditions*"
   Mårten Ahlquist, and Valery V. Fokin **2007**
   Submitted for publication

Papers not included in this thesis

9. "*On the Performance of Continuum Solvation Models for the Solvation Energy of Small Anions*"
   Mårten Ahlquist, Sebastian Kozuch, Sason Shaik, David Tanner, and Per-Ola Norrby
   Organometallics **2006**, *25*, 45.

10. "*Palladium Chemistry from a Computational Perspective."*
    Peter Fristrup, **Mårten Ahlquist**, David Tanner, and Per-Ola Norrby
    Manuscript in preparation for invited perspective article in Organic and Biomolecular Chemistry.

Outline

Chapter 1 – Introduction.

An introduction to organometallic chemistry is presented herein with focus on the reaction mechanisms of transition metals and different methods for mechanistic investigation.

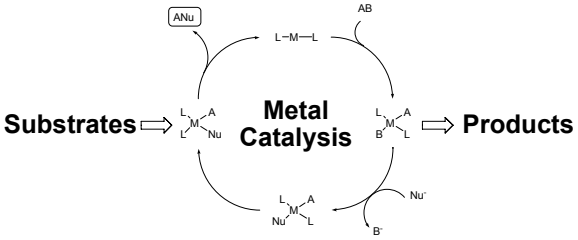

Chapter 2 – Cuprate Additions.

The nature of organocuprate reactions, with a focus on the reactivity and selectivity of stannylcuprates with α,β-acetylenic carbonyl compounds. The experimentally observed fact that stannylcuprates behave differently from that of the corresponding carbocuprates is rationalized.

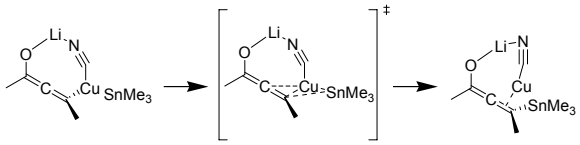

Chapter 3 – Palladium Catalyzed Coupling Reactions.

A short introduction to the field of palladium chemistry is followed by a discussion of the mechanism of the palladium catalyzed hydroarylation, and the regiochemical outcome is rationalized. This is followed by a computational study of the observed isomerization of internal vinyl palladium(II) intermediates to terminal vinyl complexes. Finally the stability and reactivity towards oxidative addition of palladium(0) phosphine complexes is described.

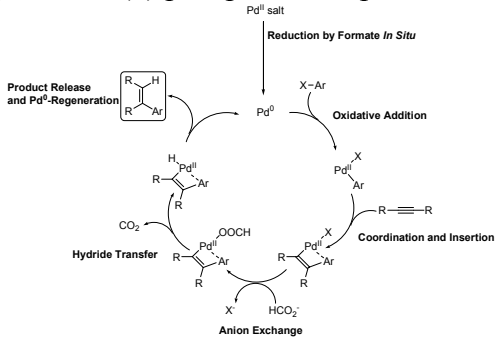

Chapter 4 – Metal Catalyzed Ligation of Azides and Alkynes.

Herein is described how two copper centers cooperatively catalyze the 1,3-dipolar cycloaddition of organic azides and alkynes to selectively give the 1,4-triazoles. A further study on the reactivity of the intermediates from the corresponding reaction of *N*-sulfonyl azides is then presented. Finally it has been found that the 1,5-triazoles are selectively produced with a ruthenium(II) catalyst. The selectivity and reactivity of this catalytic transformation is discussed.

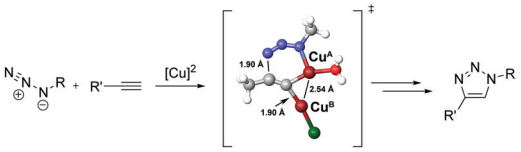

Chapter I

Introduction

Organometallic Chemistry

In the early days of modern chemistry Berzelius defined chemical compounds as either organic or inorganic,[1] and since then chemists routinely make a distinction between the fields of organic and inorganic chemistry. However, much of the recent development in both organic and inorganic chemistry has been made in what can be described as a cross-breed between the two fields, namely organometallic chemistry, the chemistry of metal-carbon bonds. The first organotransition metal complex to be synthesized was $K[Pt(C_2H_4)Cl_3]$.[2] It was discovered in 1827 by the Danish chemist William Christopher Zeise by boiling a mixture of $PtCl_4$, $PtCl_2$ and KCl in ethanol. It is nowadays known as Zeise's salt (Figure 1), and it should be noted that the first synthesis of an organic compound was not made until the year after, when Wöhler in 1828 made his ground breaking synthesis of urea.[3] Today organometallic chemistry is one of the most active fields in chemistry. As a measure of the current impact it is noted that two of the Nobel Prizes since 2000 have been given for development in organometallic chemistry.[4]

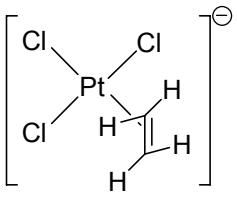

Figure 1 Anion of Ziese's salt

After the discovery of Zeise's salt the development in the field was quite slow. Actually it was not until the 20th century that the true structure of Zeise's salt was elucidated by X-ray crystallography.[5] In 1890 the zero-valent nickel carbonyl complex $Ni(CO)_4$ was discovered,[6] and this was one of the first organometallic complexes with an industrial use. By exposing impure nickel metal to carbon monoxide at 50 °C the volatile $Ni(CO)_4$ is formed (boiling point 43 °C). The nickel containing gas (which is now separated from the impurities) is then heated to above 220 °C upon which carbon monoxide is released again and the pure nickel metal is isolated. The process was developed a few years after the original discovery by Ludwig Mond and hence it is called the Mond process. Despite the long history of organometallic chemistry it was not until the 1950s that the interest in organotransition metal complexes would really emerge. A few of the 1950s landmarks include: the synthesis of ferrocene by Kealy and Pauson in 1951;[7] the discovery of titanium catalyzed polymerization of ethylene by Karl Ziegler in 1953[8] and Giulio Natta's further development[9] of the

process now known as Ziegler-Natta polymerization; the development of the Wacker process for oxidation of ethylene to acetaldehyde by Jürgen Smidt in 1959 (Figure 2).[10]

1951: Ferrocene synthesis by Keany and Pauson

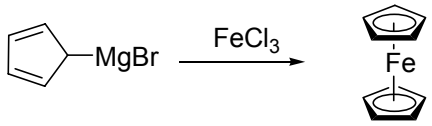

1953: Ethylene polymerization by Karl Ziegler

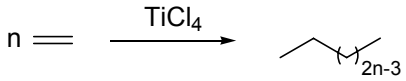

1959: Wacker process by Jürgen Schmidt

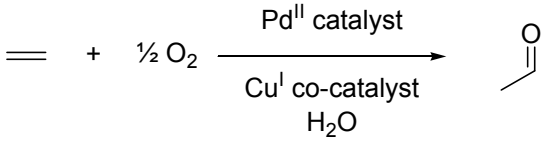

Figure 2. Three of the important discoveries in organometallic chemistry in the 1950's.

substrates ferrocene

Today transition metal catalyzed reactions are among the most important in organic synthesis. The majority of the transition metals are employed in different transformations, and interestingly one of the metals that is currently attracting most attention is gold, a metal which was previously regarded as one of the more chemically inert elements.[11] The main reason for the high interest in transition metals is the rich chemistry of these, which originates from the involvement of easily accessible d-orbitals in their interactions. The following section will discuss further some of the most common reactions at transition metals.

Mechanisms at Transition Metal Centers

The rich chemistry of transition metals involves a multitude of different types of transformations, and still new reactivities are being discovered. There are however, a few steps which are more frequent and by which a majority of the mechanisms of the synthetically interesting reactions can be explained. A few selected transformations will therefore be discussed in more detail in this section.[12]

Oxidative Addition and Reductive Elimination

Many transformations in synthetic organic chemistry are two electron processes, meaning that they involve rearrangement of electron pairs rather than only single electrons. It is therefore not hard to see the great importance of the two electron process of oxidative addition of transition metals. The overall process can be described as the addition of a fragment A-B to a metal M^n to yield a complex $A\text{-}M^{n+2}\text{-}B$. Several types of mechanisms have been characterized for oxidative addition reactions and some of these are outlined in Figure 3. The first is the three-center concerted mechanism where the A-B bond is broken simultaneously with the formation of the M-A and the M-B bond. The second type of mechanism is the nucleophilic displacement, where the M-A bond is formed first with the release of B^- in a process similar to an S_N2 type reaction. B^- then associates with the $M\text{-}A^+$ fragment to give the product complex. The third type of mechanism in Figure 3 is a radical reaction, which involves two one electron processes to give an overall two electron process.

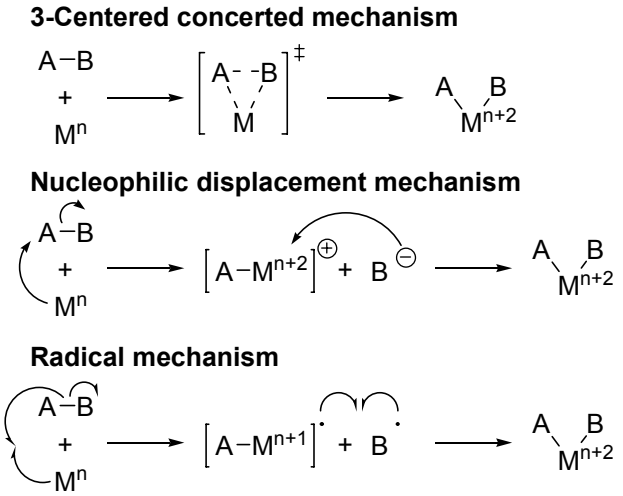

Figure 3. Different mechanisms for oxidative addition.

Reductive elimination is the final step in many transition metal catalyzed reactions. Mechanistically it is simply the reverse of the oxidative addition. Reductive elimination of A-M^{n+2}-B yields A-B and M^n, which clearly shows why this step is often the one where the final product is formed.

Insertion

There are different types of insertion reactions, but the two most common are the 1,1-insertion and the 1,2-insertion. The 1,1-insertion most frequently involves carbon monoxide. When a metal center is bonding to a nucleophilic group, e.g. an alkyl group or a hydride, and a carbonyl ligand, the carbonyl can insert into the metal-nucleophile bond (Figure 4). Sometimes the reaction is described as a migration of the nucleophilic group rather than an insertion, and therefore the reaction is often termed *migratory insertion*. A similar reaction can take place with alkenes and alkynes as the inserting groups. The reaction is then termed a 1,2-insertion. This transformation is one of the most important from an industrial point of view, since it is the key step in the metal catalyzed polymerizations such as the Ziegler-Natta polymerization of olefins.[8, 9]

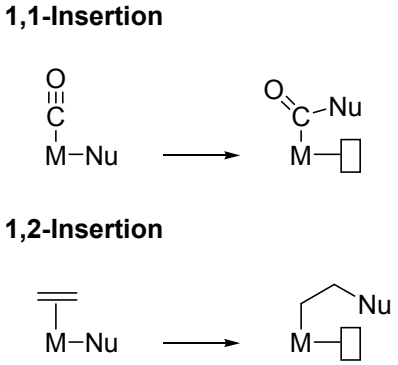

Figure 4. Above: 1,1-insertion of carbon monoxide. Below: 1,2-insertion of ethylene.

β-Hydride Elimination

Transition metal alkanes frequently show low kinetic stability, and the most common reason for their breakdown is that they undergo a process known as β-hydride elimination (Figure 5). The process is basically a reverse of a 1,2-insertion of an alkene into a metal hydride bond. For β-hydride elimination to occur a few requirements need to be fulfilled. Firstly, the alkyl chain must contain a β-hydrogen, meaning that groups such as methyl or benzyl cannot decompose by this mechanism. Secondly, the metal must have a free coordination site to which the hydride can be transferred. Thirdly, the metal should have accessible d-electrons that it can donate into the C-H σ*-

orbital for the reaction to proceed rapidly. This requirement is one of the factors responsible for the high efficiency of the Ziegler-Natta process. Since the d^0 metal fragment rarely undergoes β-hydride elimination the polymerization can proceed to yield the desired high molecular weight polymers.

β-Hydride elimination

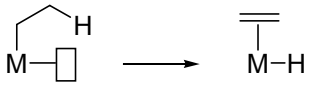

Figure 5. β-Hydride elimination is the reverse insertion of an olefin in an metal-hydride bond.

Substitution Reactions

A step which occurs in most catalytic transformations, if one considers that the reactants are ligands, is the ligand substitution reaction. It is in principle a very simple group of reactions, M-A + B → M-B + A, but in reality the intimate mechanism is often quite complex. There are two major mechanisms for the ligand exchange reactions. The most frequent one at coordinatively saturated complexes, e.g. octahedral geometry, is the dissociative exchange (Figure 6). Since the metal center is already sterically very crowded one of the ligands must dissociate before another can take its place. At coordinatively unsaturated complexes it is frequently observed that ligand exchange occurs via an associative mechanism. This means that the new metal ligand bond starts forming before the dissociating ligand has lost its bond to the metal. Square planar complexes frequently undergo associative ligand substitution.

Dissociative ligand substitution

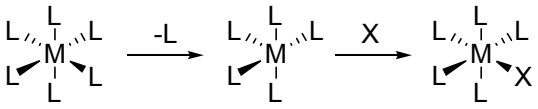

Associative ligand substitution

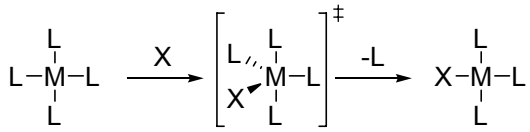

Figure 6 Above: Dissociative ligand exchange is common at coordinatively saturated complexes. Below: Associative substitution is common at complexes with more open geometries.

An important phenomenon which was initially observed for ligand substitution on square planar platinum(II) complexes, is the *trans*-effect. It is the observed rate of substitution of ligands in *trans* position to another ligand, meaning that exchange of A *trans* to B proceeds with a higher rate if B has a large *trans*-effect. The *trans*-effect is believed to originate in mainly two different factors, the ability of the ligand to stabilize the transition state and the ability of the ligand to destabilize the bond *trans* to it. The latter is also termed the *trans*-influence and is a purely thermodynamic phenomenon,[13] while the *trans*-effect is a kinetic one.[14] Highly electron donating ligands, e.g. hydride and phosphines, tend to have strong *trans*-influences. Some ligands with very low *trans*-influences have been found to have the highest *trans*-effects, though. These are ligands with high electron accepting ability through back-donation e.g. ethylene and carbonyl, which are believed to stabilize the trigonal bipyramidal transition state. In Figure 7 the relative *trans*-influences and *trans*-effects of some selected ligands are outlined.

***Trans*-influence**

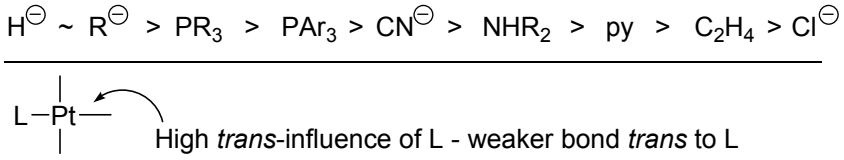

***Trans*-effect**

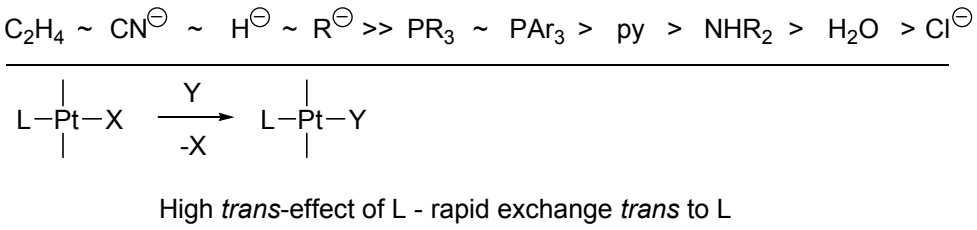

Figure 7 Above: *Trans*-influence of some selected ligands. Below: *Trans*-effect of some selected ligands.

Metathesis

Metathesis reactions can be described as two couples exchanging partners, AB + CD → AC + BD. In organometallic chemistry there are two main types of metathesis reactions, σ-bond metathesis and π-bond metathesis. While σ-bond metathesis has had relatively limited use π-bond metathesis has bloomed in both organic synthesis as well as in polymer science. It typically involves a metal fragment which is doubly bonded to a carbon, a so called metal carbenoid, and an alkene. The metal

fragment then reacts with the hydrocarbon and exchanges its carbenoid group for one part of the hydro carbon. In Figure 8 an illustrative example is outlined of how norbornene is polymerized by this mechanism. The reaction is nowadays one of the most important organic transformations and in 2005 Grubbs, Schrock and Chauvin were awarded the Nobel Prize in chemistry for their work on metathesis chemistry.[15]

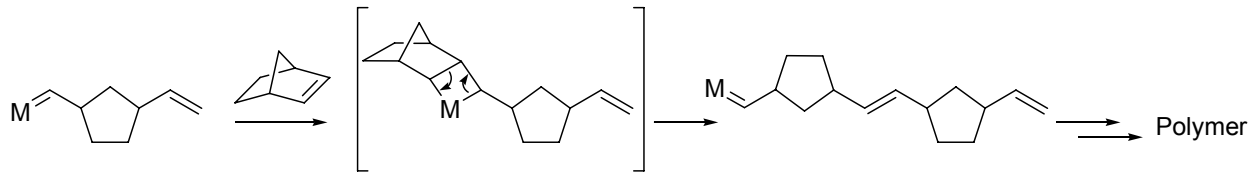

Figure 8 Ring opening metathesis polymerization (ROMP) of norbornene.

Electron Transfer Reactions

Electron transfer reactions constitute an important class of reactions, since transition metals often have easily accessible electronic levels they are often able to both accept and donate electrons. In many oxidative and reductive reactions electron transfer reactions play a crucial role, e.g. the copper co-catalyst in the Wacker process.[10] The copper(II) is here reduced to copper(I) by palladium(0) to produce palladium(II) which is the active catalyst. Once the copper(I) is formed it is re-oxidized to copper(II) by aerobic oxidation. The Wacker process example is shown in Figure 9.

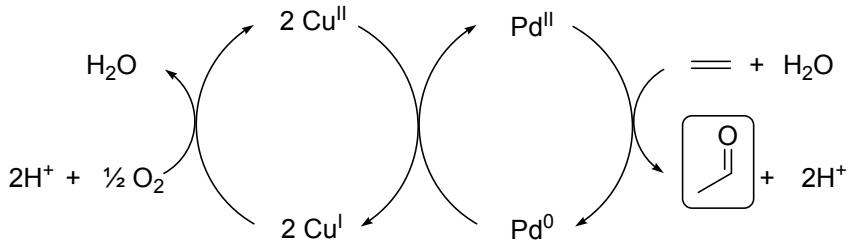

Figure 9 Electron transfer from copper to palladium is a key step in the Wacker Process.

Catalysis

Several examples of catalysis aided by transition metals have already been discussed and it is surely catalysis which plays the central role of organotransition metal chemistry. Therefore this part will briefly discuss and exemplify catalytic reactions. The phenomenon of catalysis was first observed by Berzelius in 1835 when he noted that addition of certain chemicals could speed up reactions. This is basically what a catalyst does: it increases the rate of a reaction without being consumed itself. Another way of putting it would be that the catalyst can take the reactants through a low activation energy path to give the products (Figure 10). When the catalyst has done its job it should be unchanged relative to the species that started the reaction.

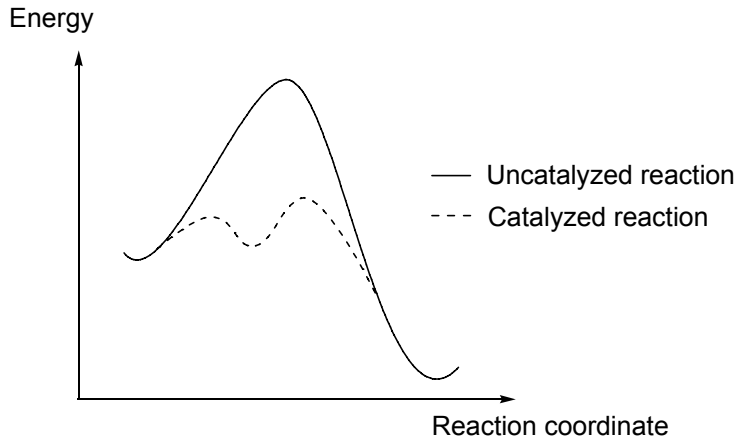

Figure 10 The dashed line illustrates the low energy path of a catalyzed reaction in comparison to the non-catalyzed reaction (solid line).

The most well known catalysts are probably the catalytic converters in cars. These are solid catalysts that catalyze the combustion of carbon monoxide and non-combusted hydrocarbons to carbon dioxide. Herein the focus will be on a different type of catalysts, though. Several different reactions on transition metal complexes were described above, and it was stated that the chemistry of such complexes is very rich. This rich chemistry has been applied extensively in the field of homogeneous catalysis, where the catalyst is dissolved in the same phase as the reactants. A typical catalytic cycle involving transition metal complexes is constituted of several steps, most frequently including several of the reactions described previous section. As an example a hydrogenation of an olefin catalyzed by a cationic rhodium catalyst is described and outlined in Figure 11.[16] The first step is ligand substitution where two solvent ligands are displaced by the substrate olefin. Oxidative addition of dihydrogen then produces a rhodium(III) dihydride species. The first hydrogen is then transferred to the olefin via an insertion of the olefin into one of the Rh-H bonds. Reductive

elimination then produces the hydrogenated product and finally another ligand exchange regenerates the active catalyst species.

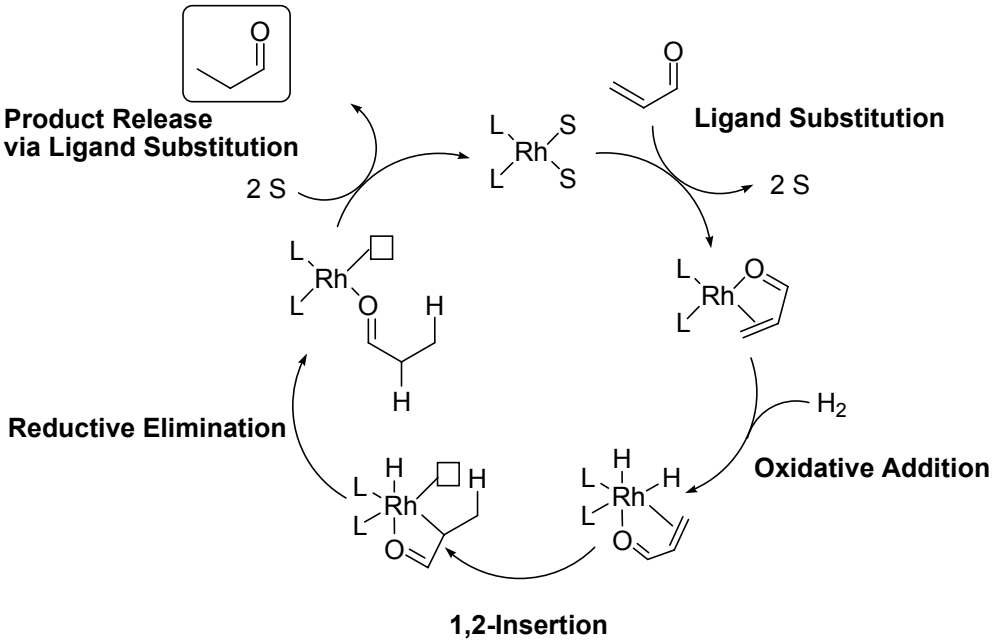

Figure 11 Illustration of rhodium catalyzed hydrogenation of α,β-unsaturated carbonyl compounds.

The asymmetric version of the rhodium catalyzed hydrogenation is one of the most efficient and important reactions of metal catalyzed reactions in organic chemistry, and in 2001 Noyori and Knowles shared one half of the Nobel Prize in chemistry for the discovery and development of these reactions.[17] The other half was awarded to Sharpless for his contributions to asymmetric metal catalyzed oxidation reactions.[18]

The efficiency of catalytic reactions is crucial for the success. There are a few different ways of measuring the efficiency, and the most common way to quantify it is by measuring the turnover number (TON) and the turnover frequency (TOF) of the catalyst. The turnover number is the measurement of how many catalytic conversions each catalyst molecule can undergo before it becomes inactive. Typical values for good catalysts range from a few hundred to extreme values of 10^9 (see chapter III on palladium catalysis). Turnover frequency is a measure of how many catalytic conversions each catalyst can perform in a certain amount of time. A catalyst that shows high turnover frequency as well as turnover number is thus usually desired.

Methods for Mechanistic Investigations on Transition Metal Reactions

There are many different methods for investigating reaction mechanisms of transition metal reactions. Numerous different experimental techniques as well as computational methods have been applied extensively to gain insight into the mechanistic details of chemical reactions. They all have different advantages and disadvantages which will be discussed for some selected methodologies.

Product Studies

One of the most straightforward and simple tools for mechanistic investigations is investigation of the products. Under most reaction conditions more than one product can be formed. By simply modifying the reactants, the reaction conditions, the catalyst, using additives etc, it is often observed that the reactivity changes. For example, if a certain additive, which is known to hamper one type of reaction suspected to be responsible for formation of one of the products, gives a product distribution with lower amounts of this particular product it is an indication of the proposed mechanism. This is illustrated in the following example. The formation of 1,4-triazoles has been found to be catalyzed by copper (Figure 12). In a protocol by Sharpless and co-workers the copper source was a copper(II) salt ($CuSO_4$) which in combination with ascorbate was believed to give copper(I) which catalyzed the reaction.[19] A control experiment to see if this hypothesis was correct was then just to simply perform the reaction with $CuSO_4$ but without the ascorbate reducing agent. The result was that no significant amounts of 1,4-triazole was formed without ascorbate, clearly indicating that it is copper(I) that is active in the catalytic cycle.

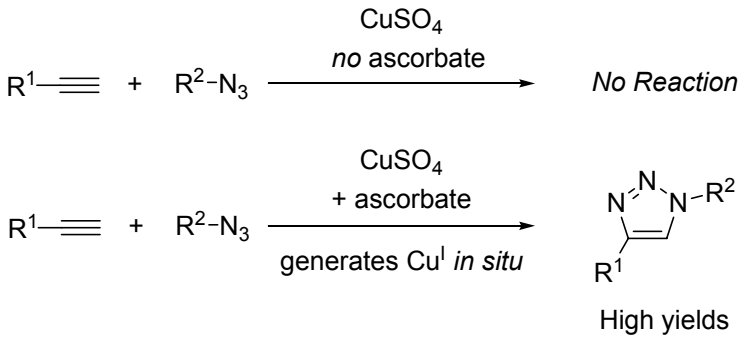

Figure 12. An example of product studies as a tool to gain mechanistic insight. This experiment showed that the active catalyst is most likely Cu^I.

Kinetic Experiments

In kinetic experiments one measures the rate at which a certain reaction proceeds. There are two major types: relative kinetics and absolute kinetics. In absolute kinetics the rate of the reaction is measured in different experiments where one parameter is altered. This could be the concentration dependence of one of the reactants or the catalyst. From these experiments the order of the species, for which the concentration is varied, can be determined. A first order dependence indicates that one molecule of the varied species is involved in the rate limiting step. A second order dependence indicates that there are two molecules involved in the rate limiting step. Another parameter which is often varied is the temperature. Varied temperature can give important thermochemical data such as the enthalpy and entropy of activation. Despite the many interesting data of absolute kinetics one should be careful when interpreting the results. Firstly, the methods are highly sensitive for variations other than the intended one. Secondly, however correct the collected data are, the interpretation might be less straightforward and frequently there is more than one way to interpret the results.

A far less sensitive type of kinetics is the relative kinetic measurement. In a relative kinetic experiment the absolute rates are not measured but rather the relative rates. The most common way to accomplish this is simply to use two similar substrates, and to monitor the product distribution while the reaction is running. This gives invaluable information of the rate limiting step *OR* an irreversible selectivity-determining step other than the rate limiting step.

Detection of Reactive Intermediate

Much of the effort in mechanistic investigations is made to understand more of the reactive intermediates of the reaction. With knowledge of the intermediates it is supposedly more facile to manipulate the reaction in a desired direction. It is therefore not surprising that numerous groups have tried to either isolate or detect the intermediates. However, when studying catalytic reactions intermediate detection is risky business. Most catalytic reaction use only minute amounts of the catalyst and in many cases only a fraction of the added catalyst is actually active. The concentrations of the reactive intermediates are therefore most often extremely low. In most reactions involving transition metals large amounts of the metal are involved in different unproductive dead-end equilibria. If one then tries to detect an intermediate it is more likely one which is not involved in the catalytic cycle. One of the most famous examples of this phenomenon is the mechanistic investigation by Landis and Halpern on the enantioselective hydrogenation with

rhodium.[16a] Under the reaction conditions one intermediate could be detected. However the detected intermediate was not participating in the catalytic cycle giving the major product, but was instead an intermediate of the cycle leading to the minor product. All intermediates in the cycle towards the major product were too short lived to be detected.

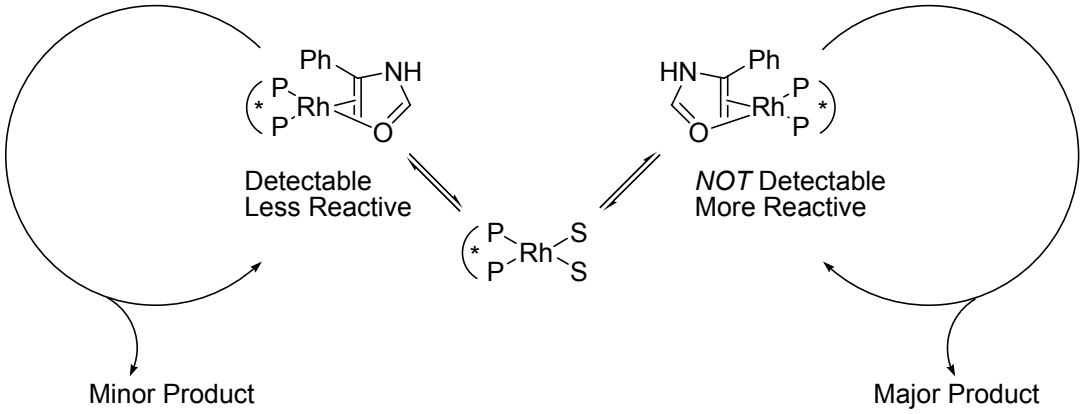

Figure 13. Landis and Halpern's observed that the detectable intermediate was not part of the catalytic cycle which yielded the major product.

Computational Studies[20]

With the explosive development of computers the field of computational chemistry and molecular modeling has evolved more rapidly than most fields. From rather primitive calculations on small model systems it is today possible to look at the reactions with full systems without too severe approximations. The most commonly employed methods will be discussed briefly here.

Molecular Mechanics

One of the simplest ways to represent molecules theoretically is by regarding the atomic centers of the molecule as balls connected together by springs. The potential for the distance between to atoms in the molecule is then simply described by Hooke's law, or in some cases the harmonic oscillator equation. In a similar fashion other parameters such as angular bends and torsional strain are described. Non-bonding interactions such as van der Waals and electrostatic interactions are described by additional terms. Each of the terms includes parameters that are derived from empirical data, makes this method very reliable for calculations on known structures and closely related structures. On unknown structures the methods are not particularly useful, though. The focus of this thesis, transition metal complexes, tend to be problematic since the bonding is much more complex than for most organic molecules. The main interest of calculations on transition metals is

the reactivity of these, and here most methods based on molecular mechanics fail. For these calculations more elaborate methods are needed. It should be noted though, that for excessively large systems such as biological macromolecules there are no other methods than molecular mechanics that are able to perform the calculations within a reasonable time limit.

Quantum Chemical Methods

For around two hundred years most physical phenomena were described successfully using Newton's laws of physics. Then in the second half of the 19th century physicists noted that some observed behaviors of matter did not seem to obey the established laws. One of the most studied systems at the time was the light emission of hot objects, the *black-body radiation*. It was not until the German physicist Max Planck's proposal in 1900 that energy emitted by an oscillator could not take an arbitrary value but was limited to discrete values, that the black-body radiation could be explained. This finding is by many regarded as the birth of quantum mechanics. In 1926 *the* central equation of quantum mechanics was proposed by the Austrian physicist Erwin Schrödinger. [21, 22] In his proposal, any system could be described by a wave function Ψ. By applying an operator on the wave function the eigenvalue of the operator would represent a property of the system. One operator is the Hamiltonian operator H, which will return the energy of the system E. The Schrödinger equation then takes the form:

$$\mathbf{H\Psi = E\Psi}$$

For description of most chemically interesting systems the Hamiltonian typically includes five terms to describe the energy of the system. The first describes the kinetic energy of the electrons; the second describes the kinetic energy of the nuclei; the third describes the attraction between electrons and the nuclei; the fourth describes the interelectronic repulsion; and finally the fifth describes the internuclear repulsion. One of the most common and least harsh approximations made for chemically relevant problems is that the second term, which describes the kinetic energy of the nuclei, is excluded. This approximation known as the Born-Oppenheimer approximation is made upon the assumption that the much higher mass of the nuclei compared to the electrons renders the contribution of the term insignificant.[23] Assuming that the Born-Oppenheimer approximation does not affect the system significantly, the Schrödinger equation can be solved exactly for H_2^+. For any larger systems further approximations need to be made. Some of these will be discussed further below.

One of the most important developments in quantum chemistry applied to many electron systems was the *ab initio* Hartree-Fock molecular orbital theory (HF).[24] HF assumes that the motion of the

electrons is not correlated, so that the energy of each electron is calculated with the electron-electron repulsion term of the Hamiltonian for an average of all electrons. In reality the interelectronic interactions *are* correlated, still the HF-theory can account for around 98 % of the energy. The problem is that the last two percent of the energy is often highly significant for describing chemical problems. Therefore methods which include correlation have been developed which methods are founded on the equation:

$$\mathbf{E_{Total} = E_{Correlation} + E_{HF}}$$

Numerous post-HF methods have been developed, where less advanced methods, i.e. MP2,[25] have been widely applied on systems of reasonable size with varying success, while more advanced methods, i.e. CCSD(T),[26] are usually very accurate but can only be applied to minimal systems due to high computational cost.

Density Functional Theory

A different approach to describe the electronic structure of different systems has lately appeared more and more frequently in the literature. It is the Density Functional Theory – DFT.[27] In DFT one does not work with the mysterious wave function, but rather with the physically observable electron density. One of the major advantages of DFT methods is that they include some correlation, yet computationally they are not more costly than HF methods. The accuracy of the DFT methods have been found to often be close to that of correlated *ab initio* methods e.g. MP2. For description of transition metals DFT has often yielded better results than the lower lever correlated *ab initio* methods, and one would need to go to the very advanced methods such as coupled cluster (CCSD(T)) to get equal or better results than DFT. Interestingly, some of the most widely used methods today are the hybrid methods, which include some exchange between DFT and HF. One of the most widely used hybrid functional is B3LYP,[28] but numerous different functionals have been developed for different applications.

Despite the popularity and recent success of DFT there are some drawbacks. One is that DFT is in principle incapable of correctly describing the weak non-bonding interactions which is always present in intermolecular interactions, the dispersion interactions. Some recently developed functionals are claimed to be able to account for dispersion interactions (M05, M05-2X, M06-L),[29] but these need to be tested more extensively before their capabilities are proven. Another issue with DFT-methods resides in the description of exited states. However, some methods (time dependent DFT) have been developed which have proven useful in certain cases.[30]

In this thesis a number of reactions involving the transition metals copper, palladium and ruthenium have been studied by mainly DFT methods, but always in combination with experiments performed by me or my collaborators. For the calculations the hybrid functional B3LYP has been used through out the work. It is one of the most widely used DFT methods and has proven to generally give results in good agreement with exeperiments.[31]

Chapter II

Cuprate Additions

Background

The field of organocopper chemistry commenced in 1923 when the first synthesis of an organocopper complex was described by Reich.[32] Kharasch later discovered that Grignard reagents undergo 1,4-addition to enones, rather than the normally observed 1,2-addition, when performed in presence of a copper(I) salt (Figure 14).[33] Organocopper reagents of the type CuR displayed low reactivity and poor solubility in ethereal solvents, and it was not until the discovery of highly reactive cuprates with the composition R_2CuLi, i.e. Gilman reagents,[34] that the synthetic utility could be explored.

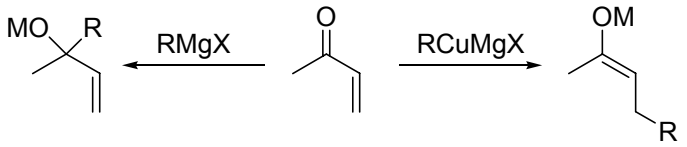

• Figure 14. In presence of copper(I) Grignard reagents adds in a 1,4-fashion (right) instead of the normal 1,2-fashion.

In the early work by House and coworkers they described a convenient way to prepare Me_2CuLi from a copper salt and methyl lithium,[35] and the reactivity towards enones was found to be highly selective for 1,4-addition, in agreement with Kharasch's work. Me_2CuLi as well as other alkyl and aryl analogs, was then shown by both Corey[36] and House[37] to work well in S_N2 reactions with organic halides, where they were appreciated for their much greater tolerance towards functional groups than the previously employed organolithiums, and the greater reactivity than zinc and magnesium reagents. Despite the advantages of the Gilman cuprates, one major disadvantage remained - the fact that one of the organic groups did not react and was just wasted in the work-up. This disadvantage is especially evident when the organic part of the cuprate is expensive and a maximum yield of 50 % is not acceptable. A solution to this problem came in 1972 when Corey showed the synthesis of mixed cuprates, from which one group could be transferred selectively.[38] By preparing a copper acetylide with a stoichiometry of 1:1 in copper and acetylide, and then reacting it with an organolithium reagent a mixed cuprate with a formula RCu(Acetylide)Li was formed. Due to the higher nucleophilicity of the alkyl/aryl group compared to the acetylide moiety, 1,4-addition of the more nucleophilic group could be accomplished selectively. Later a number of other dummy ligands have been shown to function in the same way as the acetylide, with cyanide, iodide and thiophenolate being some of the more widely used examples. In 1986 a highly enantioselective carbocupration was achieved by Corey.[39] By making a cuprate reagent with a chiral dummy ligand enantiomeric excesses up to 95% could be achieved (Figure 15).

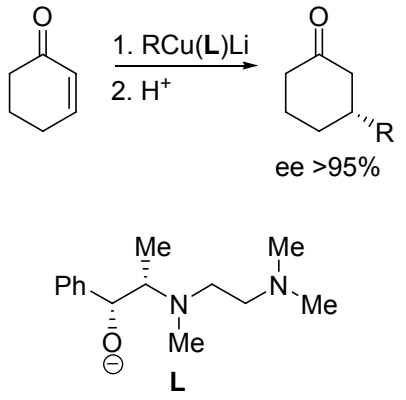

• Figure 15 Asymmetric carbocupration developed by Corey and coworkers. Complexation of the cuprate to the dummy ligand **L** afforded a cuprate capable of reacting with high enantioselectivity.

Higher order cuprates also known as "Lipshutz reagents" were found to be even more reactive than Gilman cuprates.[40] Reacting copper cyanide with two equivalents of an organolithium reagent yield compounds with the formula $R_2Cu(CN)Li_2$. The true solution phase structure of higher order cuprates has been under debate, where some researchers suggested a tricoordinate copper[41] and others suggested that the cyanide is not bonded to copper but that the reagent is better described as a complex of the structure $R_2CuLi{\cdot}LiCN$.[42] Lately both experimental and theoretical investigations seem to favor the latter in which the copper is coordinated to two alkyl/aryl groups.[43] The tendency towards clustering is very high for most copper reagents, and for the organocuprates multimeric structures such as the one shown in Figure 16. Depending on the stoichiometry in the organocuprates different clusters form.[44] have been proposed. Gschwind has investigated the tendency towards clustering and the effect of clustering on the reactivity.[44] It was observed that clustering above dimers had a negative impact on the rate, while dimers and monomers displayed similar reactivity.

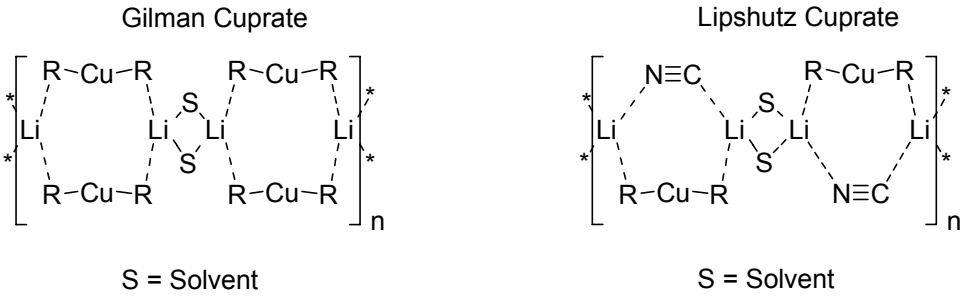

• Figure 16. Depending on the stoichiometry in the organocuprates different clusters form.[44]

1,4-addition to enones was shown by Corey[45] and Ullenius[46] to proceed via initial formation of a d-π-complex (Figure 17). Later studies by Krause of C-C coupling constants further supported the presence of π-complexes.[47] Corey proposed this intermediate to be a formal copper(III) complex, from which reductive elimination could occur to form the new carbon-carbon bond. Protonolysis of the enone would then lead to formation of the Michael addition product. Nakamura later investigated the reaction between acrolein and the Gilman lithium organocuprate cluster $[Me_2CuLi]_2$.[48] This dimeric species had been observed experimentally and was believed to be the active species. An outline of the mechanism is shown in Scheme 1 and it proceeds as follows 1) π-complexation of the copper to the double bond 2) reductive elimination to form the carbon-carbon bond which results in the formation of an enolate where the copper atom is coordinating to the C1-C2 double bond 3) dissociation of the resulting CuMe. The rate determining step was suggested to be the reductive elimination. All in all, the mechanism was in agreement with the proposed one by Corey. A more detailed analysis of the orbitals in the d-π-complex showed that the copper binds to C3 with a sigma-bond and the interaction to C2 is more of a π-complexation to the enolate double bond, which further indicates that the description of the intermediate as a copper(III) complex is correct. Even though copper in the oxidation state +3 is relatively rare a few examples of copper(III) species are known, and some have been characterized by X-ray crystallography.[49]

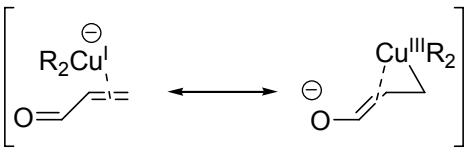

• Figure 17 π-complexes between enones and cuprates have been proposed to be copper(III) complexes.

• Scheme 1. Mechanism for carbocupration of acrolein by $[Me_2CuLi]_2$ as proposed by Nakamura.

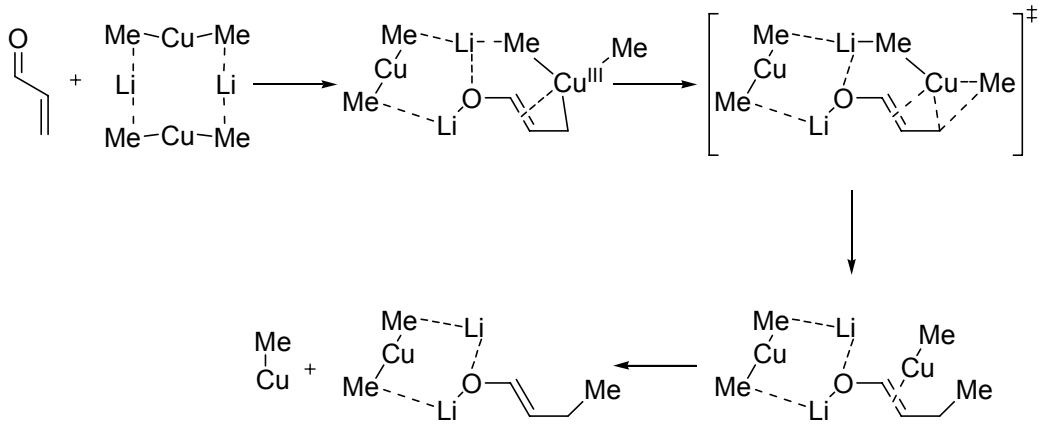

An analogous d-π-complex was shown by NMR methods to form between cuprates and ynones/ynoates.[50] Later a DFT study was conducted by Nakamura to investigate the reactivity of model acetylenic carbonyls (ynone and ynoate) with the cuprate cluster $Me_2CuLi{\cdot}LiCl$.[51] As in the reaction with enones, ynones and ynoates form a π-complex which can be described as a copper(III)[52] complex formed from an oxidative β-addition to the Michael accepting α,β-acetylenic carbonyl compound. The following step is the reductive elimination in which the carbon-carbon bond is formed. Regardless of the substrate the intermediate produced in this step was shown to be the syn-addition vinylcuprate, which could then rearrange to the anti-addition vinylcuprate via an allenolate intermediate. The reaction is outlined in Scheme 2.

• Scheme 2. Theoretically determined mechanism between an ynone and the organocuprate cluster $Me_2CuLi{\cdot}LiCl$.[51] The initially formed syn-addition vinylcuprate rearranges via an allenolate to the anti-addition analog.

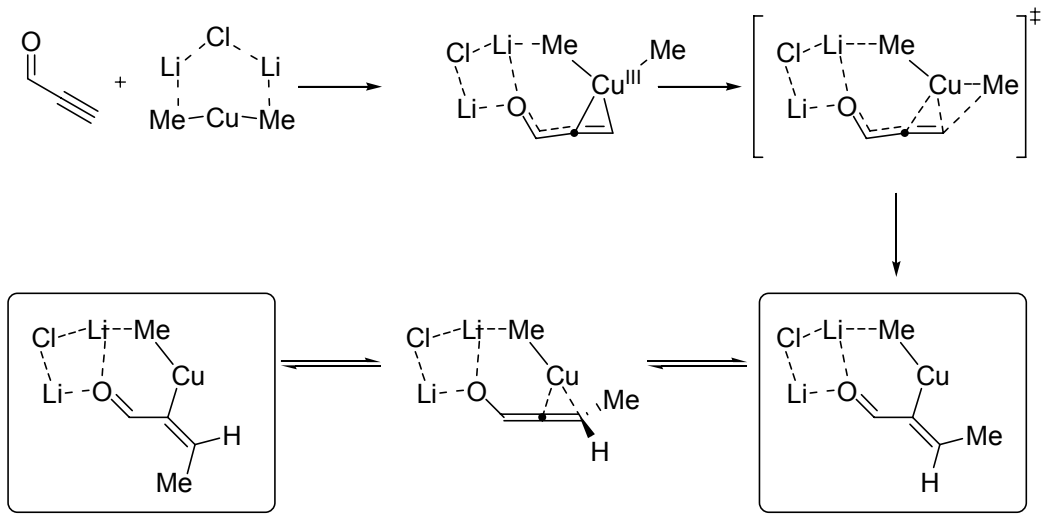

Stannylcupration of α,β-acetylenic ketones and esters.

Organotin compounds have been widely utilized in organic synthesis mainly in two types of reactions. The first type is radical reactions, since carbon radicals are readily produced from homolytic cleavage of carbon-tin bonds. The second type of reaction is the palladium catalyzed coupling with an organic electrophile, e.g. an aryl halide, a reaction known to most as the Stille coupling.[53] Numerous examples of total syntheses involving Stille couplings have emerged, yet industrially the use of the reaction has been limited to pre-production stages, mainly due to the high toxicity of organotin compounds. A few of the more popular methods for synthesizing organotin compounds are shown in Figure 18.[54]

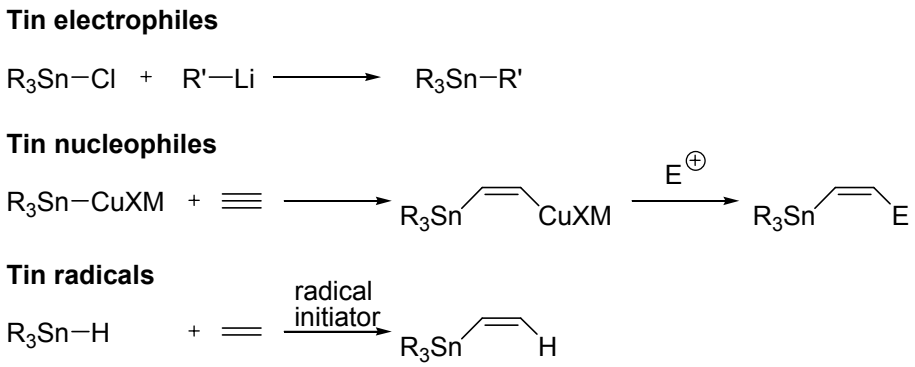

• Figure 18. Some different methods for producing organotin compounds.

A route for the total synthesis of the marine alkaloid Zoanthamine was proposed by Tanner et al. in 1994,[55] involving the key fragments A and B (Figure 19). Fragment A was to be synthesized from the α,β-acetylenic ketone by 1,4-addition of a stannyl cuprate reagent. Earlier work by Piers and coworkers demonstrated reaction conditions for selective formation of the syn-addition product in the closely related stannylcupration of α,β-acetylenic esters (Figure 20).[56] By simply varying the temperature the outcome could be controlled, so that reacting with methanol as a proton source at -78 °C gave the syn-addition product while performing the reaction at higher temperature and adding the proton source in the work-up yielded the anti-addition product.

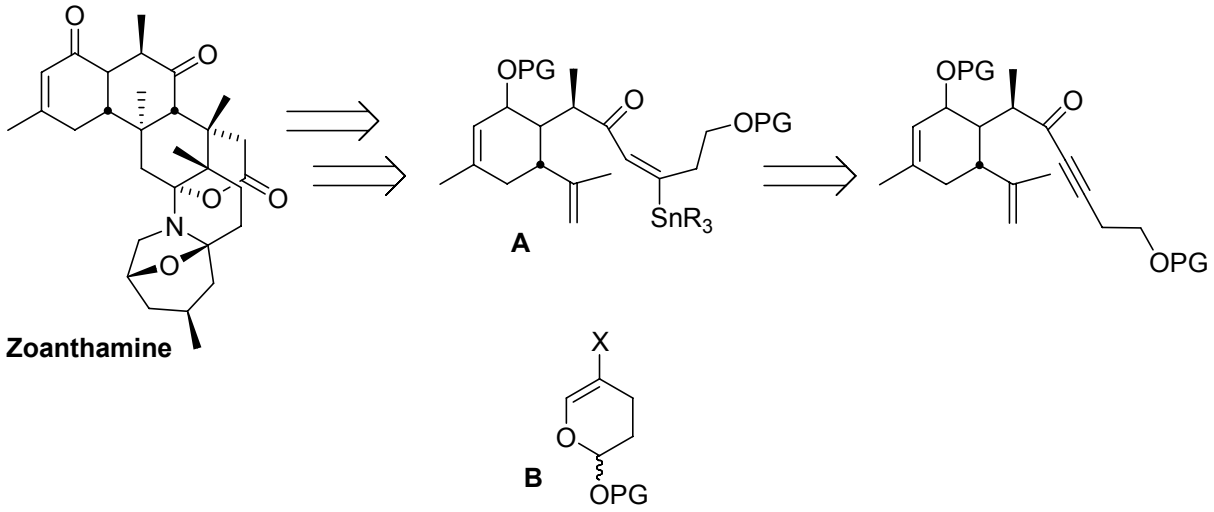

• Figure 19. Retrosynthetic analysis of Zoanthamine by Tanner involves a stannylcupration of an ynone.

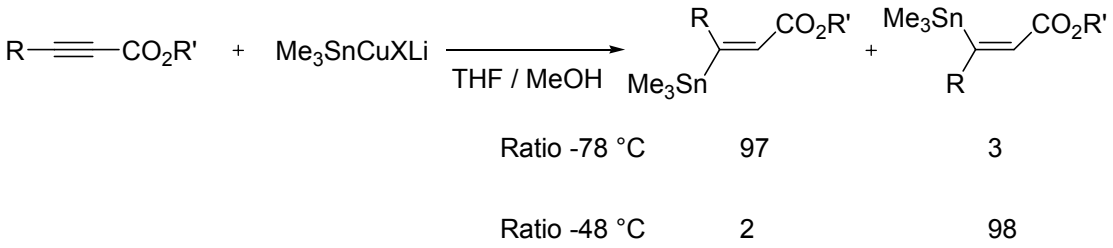

• Figure 20. Regioselective stannylcupration of ynoates.

Stannylcupration of a model compound for fragment A was performed under conditions expected to give the syn-addition product selectively according to Piers's protocol, yet the only product observed was the isomerized anti-addition product.[57] A number of substrates, copper reagents and stannyl groups were tested (Table 1), all giving the anti-addition products exclusively.

• Table 1 Stannylcupration of ynones selectively give anti-addition products as shown by Nielsen et al..

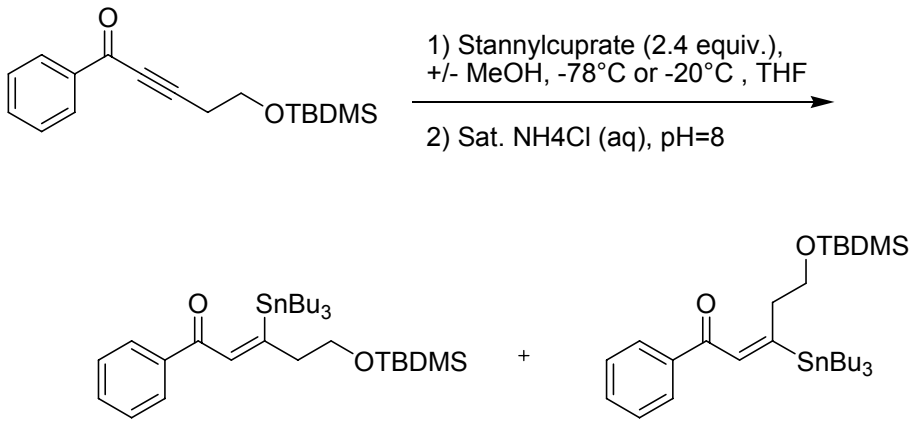

Entry	Stannylcuprate	MeOH (+/-)	Temp (°C)	Yield Anti / Syn
1	$(Bu_3Sn)Cu(SPh)Li$	-	-78	95 / -
2	$(Bu_3Sn)Cu(SPh)Li$	+	-78	75 / -
3	$(Bu_3Sn)Cu(SPh)Li$	+	-20	58 / -
4	$(Bu_3Sn)Cu(CN)Li$	-	-78	95 / -
5	$(Bu_3Sn)Cu(CN)Li$	+	-78	77 / -
6	$(Bu_3Sn)Cu)SMe_2)$	-	-78	44 / -
7	$(Bu_3Sn)Cu(SMe_2)$	+	-78	36 / -

To gain further insight to the unexpected change in selectivity when exchanging the α,β-acetylenic esters for the corresponding ketones, a model system was selected. Ideally both the acetylenic substrates and the stannylcuprate should be picked so that the reactions can be investigated by both experimental as well as theoretical methods. Therefore the choice of ketone was the simple pent-3-yn-2-one (**1**) and the ester methyl 2-butynoate (**2**). Due to its simple structure and known reactivity the stannylcuprate reagent $Me_3SnCu(CN)Li$ (**3**) was the reagent of choice. Piers showed that the E/Z-selectivity could be controlled by varying the temperature.[56] To probe the temperature dependence the reactions were performed in presence of a proton source (MeOH), or in absence of a proton source at low temperature with subsequent work-up with saturated ammonium chloride at higher temperature. In Scheme 3 are shown the results. Just like in the previous study the reaction of the ketone **1** with **3** yielded the anti-addition products exclusively, regardless of the temperature when the proton source is added. For the ester the outcome is somewhat different. When methanol is present during the reaction the only product observed is the syn-addition product **syn-5**. Performing the reaction in absence of a proton source with aqueous work-up yielded a mixture of **syn-5** and **anti-5** with **anti-5** as the major product.

Scheme 3. Product distribution of stannylcuprations of ynones and ynoates.

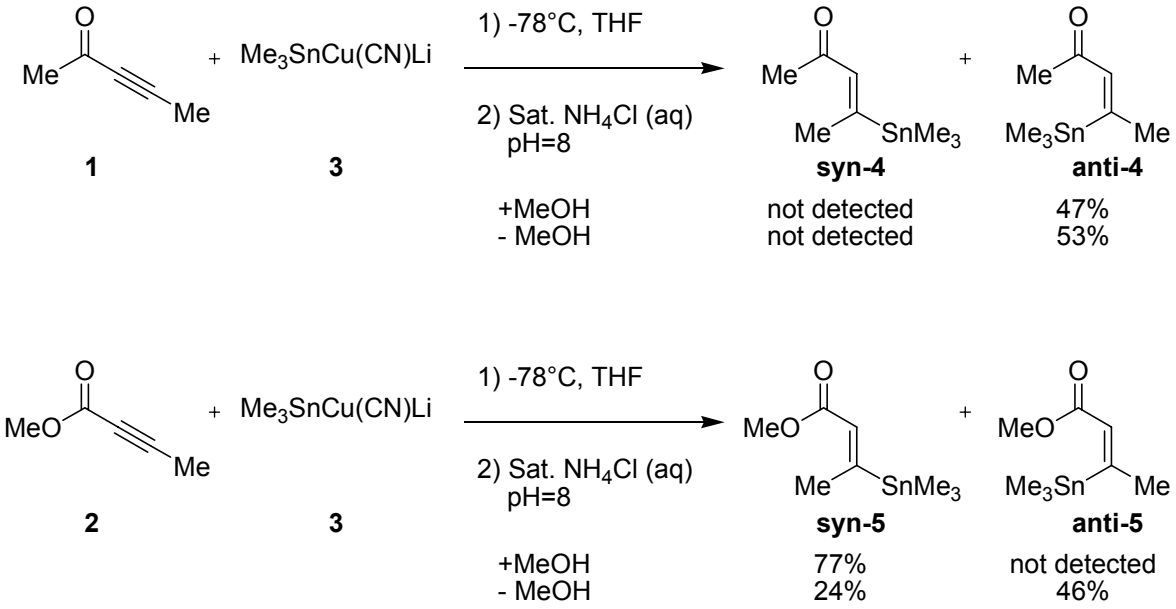

The fact that the closely related carbocupration reaction has been studied in more detail, both experimentally and theoretically, prompted us to perform the reaction between the same acetylenic substrates as for the stannylcupration but with the stannylcuprate reagent replace by a carbocuprate. The carbo-analog of **3** *t*BuCu(CN)Li (**6**) was chosen so that the steric properties of the carbocuprate reagent should be as similar as possible to the stannylcuprate **3**. As shown in Scheme 4 the reaction yielded the syn-addition product **syn-7**, even though the reaction was performed without any proton source at low temperature, with protonation during the aqueous work-up. The reaction was performed with opposite substitution pattern, meaning *t*Bu group on the acetylene and a methyl cuprate, but the reaction did not give any substantial amounts of product, possibly due to formation of higher order, less reactive cuprate clusters.

Scheme 4. Carbocupration of the ynone **1** shows opposite stereoselectivity than the corresponding stannylcupration.

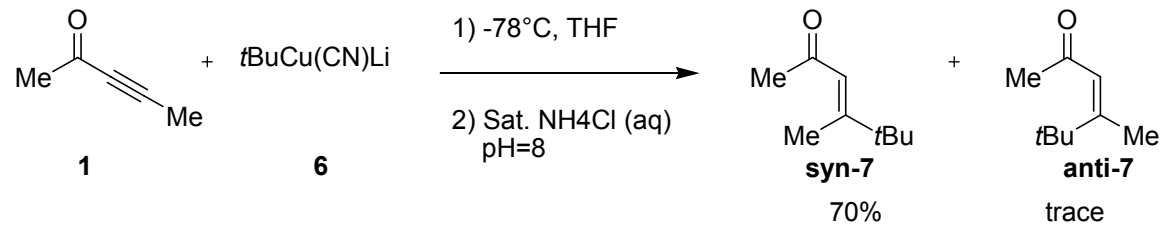

Experimental studies by Ullenius[46, 50] and theoretical work by Nakamura[51] have shown that when mixing a cuprate with a α,β-acetylenic carbonyl compound a π-complex between the acetylene and

the copper atom is formed. It was hence assumed that a complex with similar structure is formed in the reaction between **1** and **3**. The complex **8** was therefore the starting point of the computational study (Figure 21). X can either be drawn as a copper(I) complex where copper is coordinating to the acetylene, or as the resonance form where copper is formally a copper(III) with a σ-bond to the β-carbon. From the intermediate **8** the reaction proceeds via the reductive elimination type transition state **9ts** to yield the allenolate **10**. **10** then isomerizes via identical barriers to **syn-12** and **anti-12**. The initial step differentiates the reaction from the carbocupration which has been shown to give the syn-addition vinyl cuprate as the intermediate following the reductive elimination. As a consequence one would not expect to observe the syn-addition product as the major product even at low temperature.

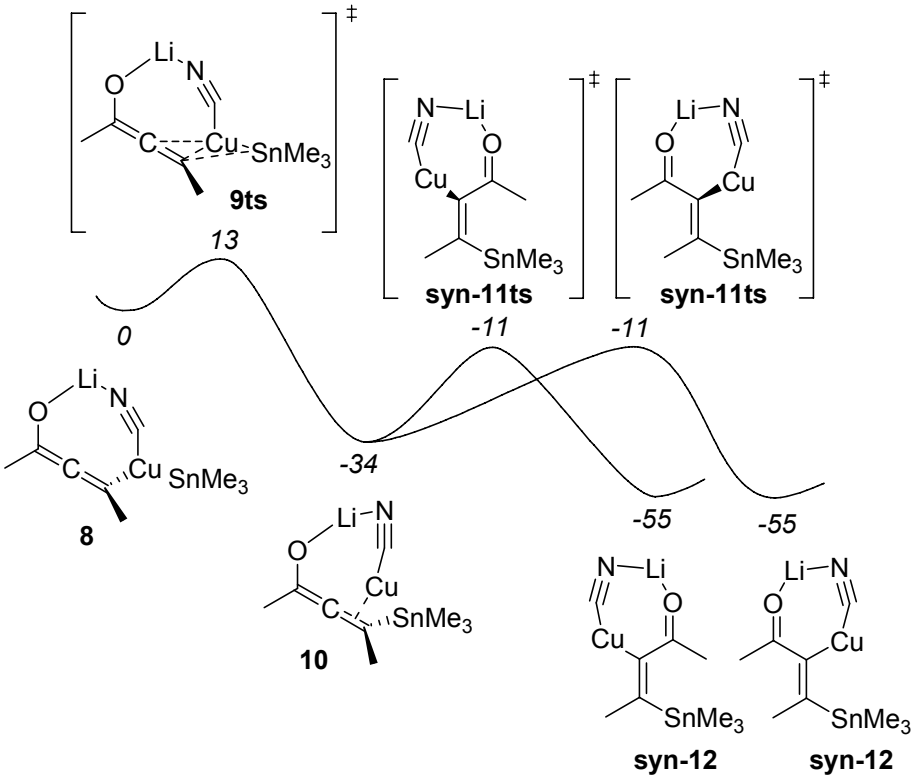

Figure 21. Reaction coordinate of the stannylcupration of ynone **33**.

Experimentally only one product is observed, yet the mechanism in Figure 21 depicts equal amounts of the E/Z-isomers. But since the reaction is conducted in THF, at least partial dissociation of the Li^+ ion is likely to occur. Without the Li^+ ion a Lewis-acid/Lewis-base interaction between the tin of the stannyl group and the carbonyl oxygen can contribute to favor of the anti-addition product. The two isomeric anionic complexes were modeled and as shown in Figure 22 there is a strong preference for the anti-addition complex.

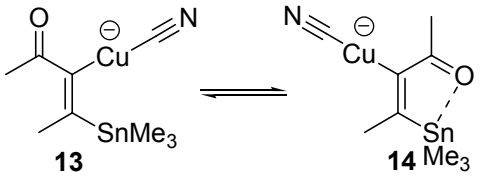

Relative Energies:		
Gas	30 kJ/mol	0 kJ/mol
THF	22 kJ/mol	0 kJ/mol

Figure 22. A Lewis acid/Lewis base interaction favors the anti-addition product (right).

As for the ketone **1** the mechanistic investigation of the ester **2** starts with a copper(III) complex **15** (Figure 23). The barrier for reductive elimination from this complex was calculated to 23 kJ/mol and affords the vinylcuprate from the syn-addition over the π-bond, which differentiates the mechanism from the one described for the ketone. Rearrangement to the anti-addition intermediate **anti-17** can then occur with a barrier of 74 kJ/mol via an allenolate transition state **18ts** and the formation of **anti-17** was calculated to be exothermic by 13 kJ/mol. The barrier for the rearrangement between the two isomeric vinylcuprates is substantially higher than the one found for the ketone analog **12** (44 kJ/mol).

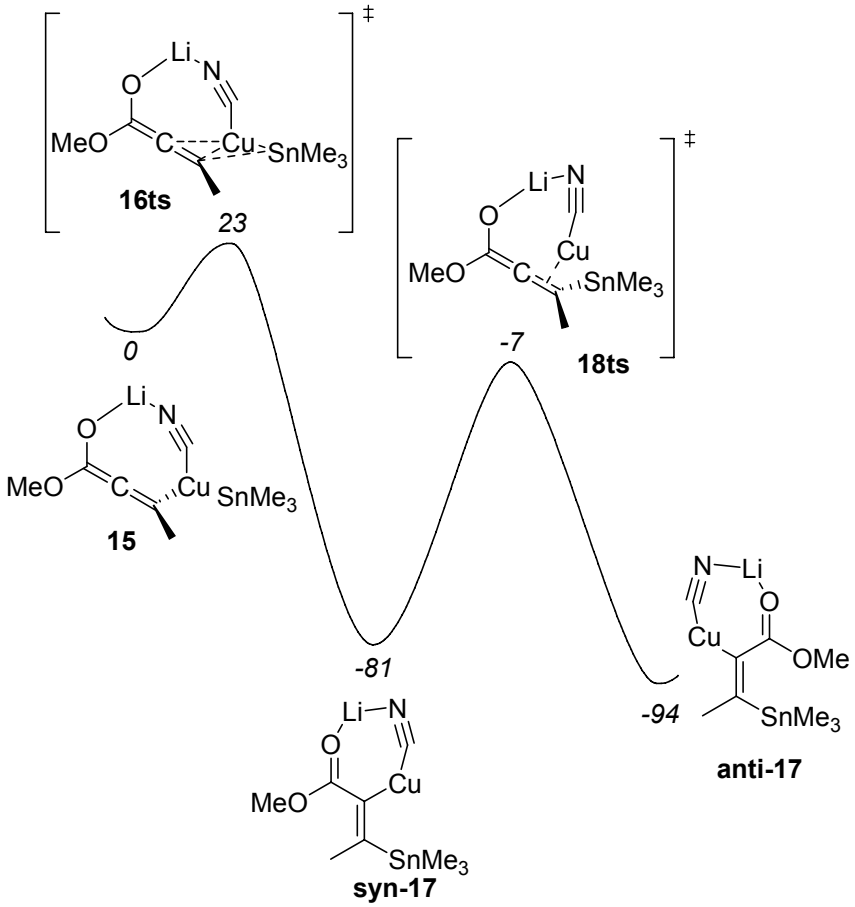

Figure 23. Reaction coordinate for stannylcupration of ynoate **2**.

The experiment with the carbocuprate **6** gave the opposite result in terms of E/Z-selectivity compared to the structurally very similar stannylcuprate **3**, and therefore the reaction between **1** and **6** was also modeled (Figure 24). As for the two stannylcuprations the starting point for the carbocupration was a copper(III) complex **19**. Reductive elimination then occurs via **20ts** with a barrier of 39 kJ/mol which is slightly higher than for the stannyl addition but still a very low barrier. As for the stannylcupration of the ester **2**, and in agreement with earlier theoretical studies, the resulting intermediate is the syn-addition complex **syn-21**. The exothermicity of the step was found to be substantially higher than for the stannylcupration of **1**, 169 kJ/mol for the carbocupration compared to 55 kJ/mol for the stannylcupration. Rearrangement then takes place via the allenolate with a barrier of 33 kJ/mol to the anti-addition complex, but the reaction is endothermic by 9 kJ/mol and the syn-addition vinylcuprate is therefore likely to be the most abundant species.

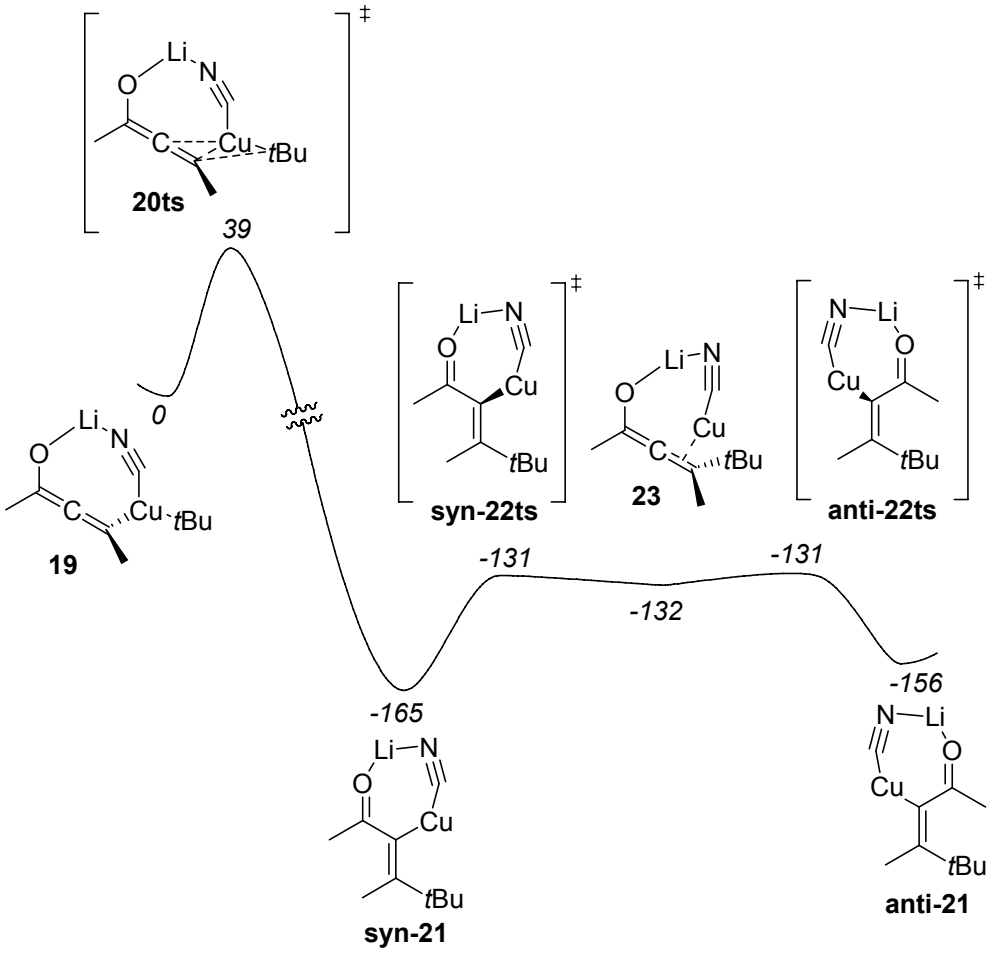

Figure 24. Reaction coordinate of the carbocupration of ynone **1**.

Conclusions

The stereochemical outcome of the stannylcupration of ynones and ynoates was studied by both theoretical and experimental methods in order to understand the factors governing the selectivity. The high selectivity towards anti-addition to ynones was found to be due to facile isomerization and a favorable Lewis-base/Lewis-acid interaction in the anti-addition vinylcuprate intermediate. For ynoates the isomerization between the syn- and anti-addition intermediates had a higher barrier, but with the anti-addition vinylcuprate intermediate being more stable, which is in agreement with the temperature dependent stereoselectivity. This study underlines the utility of modern computational methods to aid the understanding of the mechanistic details of organic transformations.

Chapter III

Palladium Catalyzed Coupling Reactions

Introduction

Palladium catalyzed reactions are among the most important transformations in homogeneous catalysis and organic synthesis.[53] Introduction of these reactions made some of the most challenging tasks in organic chemistry possible, e.g. construction of carbon(sp^2)-carbon(sp^2) bonds. Often these catalytic reactions can be performed under mild reaction conditions and are tolerant to a wide variety of functional groups. Extreme turnover numbers (TON) up to 10^9 have been reported[58] and multiple research groups have been involved in development of highly active palladium catalysts.[59] In asymmetric synthesis palladium plays a central role with asymmetric versions of the Tsuji-Trost[60] (Figure 25) and the Heck reactions[61] (Figure 26) as two prominent examples.

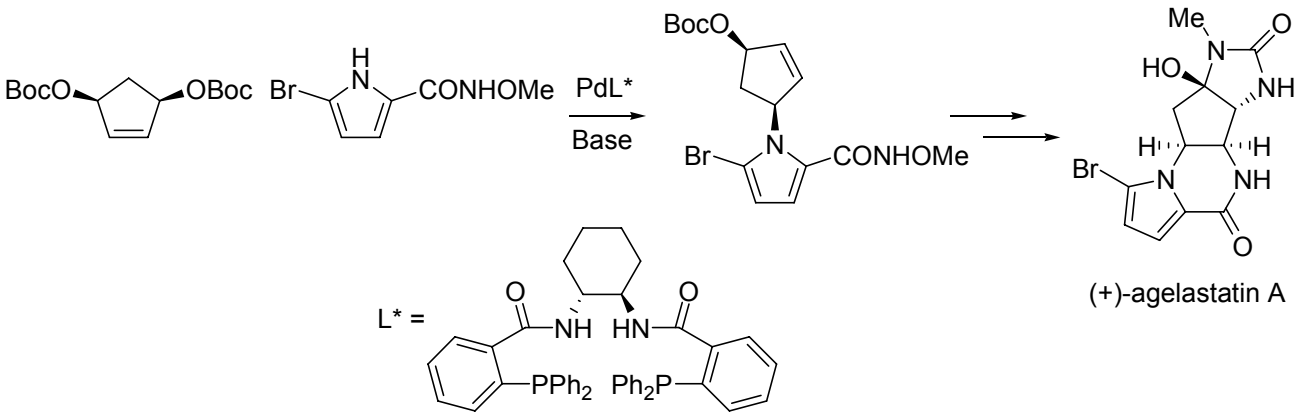

Figure 25. Total synthesis with an asymmetric Tsuji-Trost reaction as a key step.[60]

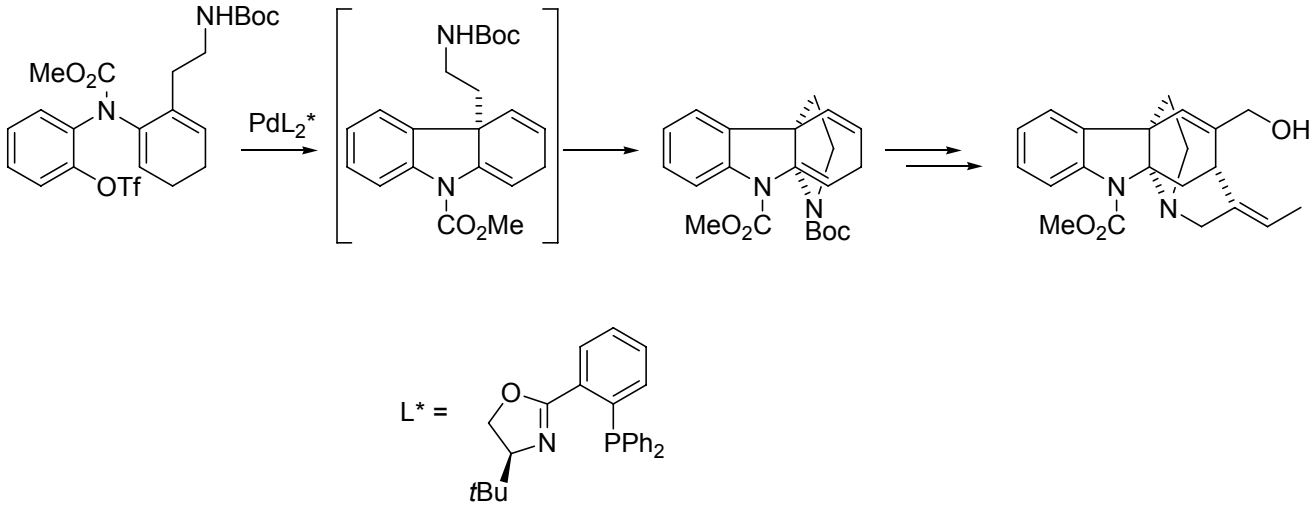

Figure 26. Construction of a chiral quaternary center using an asymmetric Heck reaction is one of the key-steps in this total synthesis by Overman et al.. [61]

In 2006 more than 3500 scientific papers were published on palladium chemistry which illustrates the huge impact palladium chemistry currently has.[62] While there are many advantages with palladium chemistry there are also a few drawbacks which ought to be mentioned. Firstly, palladium is one of the more expensive elements,[63] and even when used in catalytic amounts the metal can constitute a major part of the cost. One way of getting around the cost of the catalyst has been by using minute amounts of catalyst where down to parts per billion amounts have been reported. Most of these examples require much harsher reaction conditions and are limited to rather simple substrates.[64] Secondly, it is often challenging to remove all of the catalyst in the purification process, which makes the use of palladium more complicated in e.g. production of pharmaceuticals.[65] Thirdly, many of the transformations work very well with relatively reactive substrates like aryl- or vinyl iodides but with more difficulty for the more readily available chloride or vinyl tosylate analogs. Since a few years a number of protocols are available for coupling of aryl chlorides and other challenging substrates and it remains a highly active research area.[66] The final challenge in palladium chemistry that I would like to mention is the issue of selectivity. Many organic transformations can produce more than one product and in several of the palladium catalyzed reactions regio- and stereoisomers are produced. To some extent these issues have been overcome in asymmetric synthesis by the use of chiral ligands which bind to palladium and thereby induce chirality in the product.[53] In some transformations regioselectivity has been induced by having bidentate ligands with two different types of atoms binding to the metal.[67] Despite the drawbacks palladium chemistry is one of the most active focus areas within the fields of catalysis and organic synthesis.

Before the 1960s only few palladium catalyzed reactions were known. Then in 1959 one of the industrially most important reactions of the 20th century was reported. This is nowadays known as the Wacker process or the Wacker-Smidt process, after the inventor Jürgen Smidt who discovered the process while employed at Wacker Chemie.[68] The original reaction was an oxidative process which converted ethylene gas into acetaldehyde. Further development by Tsuji resulted in a reaction known as the Wacker-Tsuji oxidation, which converted terminal alkenes to ketones.[69] In spite of the great industrial importance of the Wacker process it was a different type of transformation that was to revolutionize organic synthesis. When Tsuji in 1964 first found that palladium allyl complexes react with malonates to form allyl malonates one of the first seeds was planted that would later bloom into the now enormous field of organic transformations catalyzed by palladium.[70] The catalytic version developed by Trost[71] was later applied in an elegant asymmetric fashion[72] and the reaction is commonly referred to as the Tsuji-Trost reaction.

In 1968 Richard F. Heck described the reaction between an organomercury compound with an olefin in presence of a palladium(II) salt.[73] The product was an olefin where one of the hydrogen atoms of the substrate olefin had been replaced by the organic moiety of the organomercury substrate. In the following paper the mechanism for the insertion of an olefin into an palladium-carbon bond was described, and the final conclusion of the paper was "*These results illustrate further the extraordinary usefulness of organopalladium compounds in organic synthesis*".[74] Today this rather bold statement seems more like an understatement. Only a few years after the initial discoveries a greatly improved protocol for hydrogen substitution on olefins was reported by the groups of Mizoroki[75] and Heck.[76] In the new protocol the synthetically unattractive organomercury substrate had been exchanged for a much more readily available aryl halide, and nowadays this reaction is known as the Heck-reaction or the Mizoroki-Heck reaction (Figure 27).

Figure 27. The Heck reaction.

Following the discovery of the Heck reaction a number of other palladium catalyzed carbon-carbon coupling reactions were developed. They differed from the Heck reaction in that the nucleophilic coupling partner was an organometallic reagent instead of an olefin, and in one case a heteroatom nucleophile. A few of the most famous named coupling reactions are the Stille,[77]

Hiyama,[78] Kumada,[79] Negishi,[80] Suzuki,[81] Sonogashira[82] and more recently the carbon-heteroatom bond forming Buchwald-Hartwig[83] coupling (Figure 28).

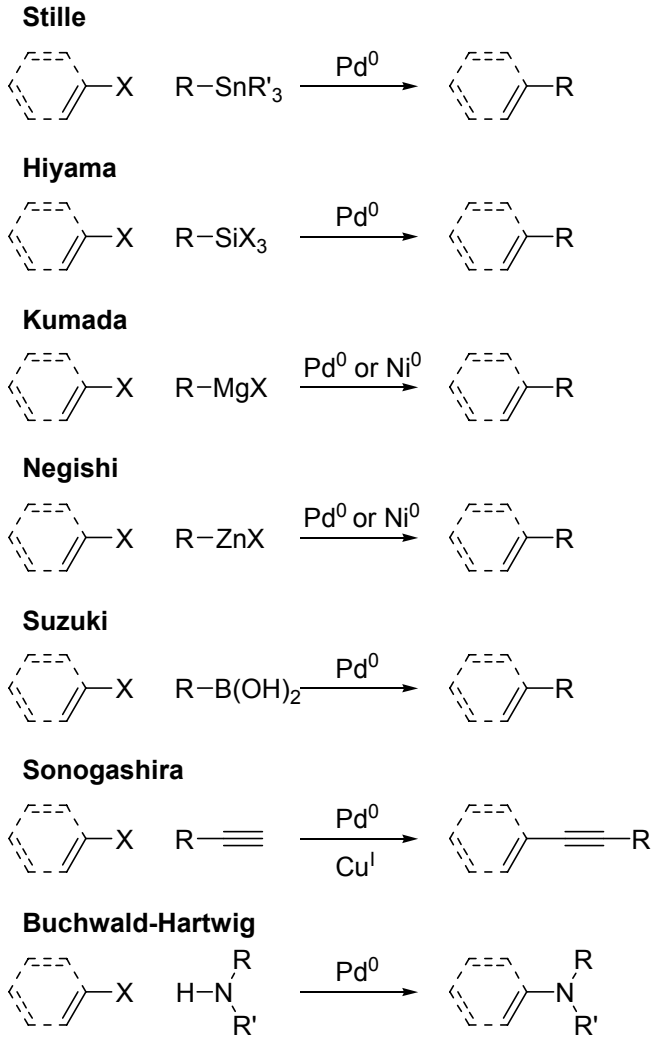

Figure 28. Examples of named palladium catalyzed cross-coupling reactions. Some reactions require more additives such as a base to run efficiently.

The mechanisms of these reactions have a few common denominators and a generalized mechanism is outlined in Figure 29. It starts with a zero-valent palladium species to which an organic electrophile (e.g. aryl halide) can be oxidatively added. The palladium(II) species formed can then react with the nucleophilic substrate, and via an intramolecular reaction the bond between the nucleophile and the electrophile is formed, the product is released and the active palladium(0) species is regenerated.

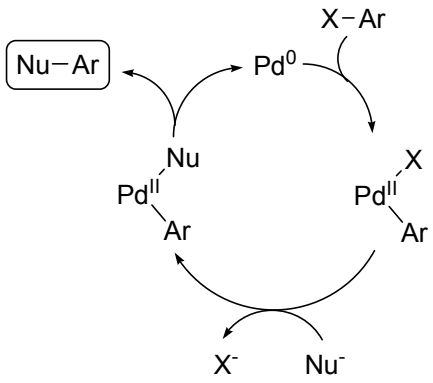

Figure 29. Generalized mechanism for catalytic cycles involving the Pd^0/Pd^{II}-couple.

Among the carbon-carbon bond forming coupling reactions in Figure 28 the Sonogashira coupling differentiates from the other by having the organometallic coupling partner generated in situ from a terminal alkyne and a copper(I) salt. Recently another protocol that applied a similar methodology was developed by Goossen for coupling of aryl reagents instead of alkynes (Figure 30).[84] In Goossen's reaction the aryl nucleophile is added as an aryl-carboxylate. Decarboxylation by copper generates an aryl-copper species in situ which transmetalates the aryl group to palladium and reductive elimination then generates the biaryl product. The authors argue that the advantage with this methodology is that there is no need for stoichiometric amounts of costly organometallic reagents since both palladium and copper are present in catalytic amounts. Compared to the Sonogashira reaction the main advantage is that the product formed is not an aryl acetylene but a biaryl which is a highly interesting structural motif in pharmaceuticals. One of the obvious drawbacks is the rather harsh reaction conditions. In the original paper the reaction was performed at 160 °C under basic conditions in NMP (N-methylpyrrolidone) with 2% palladium catalyst. For substrates that tolerate the reaction conditions it appears to be a very attractive protocol. The reaction was reported in 2006 and is a prominent example of current development in palladium catalysis.

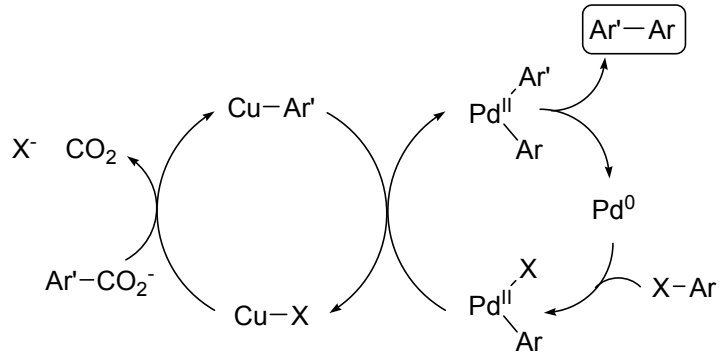

Figure 30. Goossen's decarboxylative biaryl coupling of aryl halides and benzoic acid derivatives.

Mechanistic Work on Some Selected Reactions

This thesis is focused on the mechanisms of metal assisted reactions and therefore a more detailed description will be given of the recent work by other groups in that area. The main focus is on the computational work on elementary steps of the reactions. Some of the discussion is presented later in relation to my own work.

Oxidative Addition

For most palladium catalyzed coupling reactions, the mechanism is generally believed to start with oxidative addition of an aryl or vinyl electrophile to the active palladium(0) species.[85] There are several methods for generating soluble palladium(0). Either it is added as zero-valent palladium stabilized by a ligand such as phosphines or dibenzylidene acetone (dba).[86] Alternatively palladium is added as a palladium(II) salt in combination with a reducing agent to generate the active palladium(0) *in situ*.[87] The main advantage of generating palladium(0) *in situ* is that palladium(II) salts are easier to handle due low sensitivity towards aerobic oxidation.

The nature of the oxidative addition has been studied by numerous groups,[88] and still much of the details are unknown. One of the problems is that the coordination of palladium(0) is not fully understood. In crystal structures, coordination numbers of two, three and four are frequent,[89] but in solution it is still disputed which is the more favored mode of coordination.[90]

Phosphines are widely used in organometallic chemistry since they tend to form strong metal-phosphine bonds and the introduction of large organic phosphines can make otherwise insoluble metals soluble in a wide variety of solvents.[91] For example phosphines containing water soluble

groups e.g. $-SO_3^-$ can form metal complexes with high solubility in water, thus making it possible to perform some reactions without using environmentally hostile solvents.[92] However, while many advantages with performing reactions in water can be listed, most reactions within synthetic chemistry are performed in organic solvents. In palladium(0) catalyzed reactions addition of ligands that keep palladium from precipitating as palladium metal is most often necessary, where one of the most commonly used ligands is triphenyl phosphine (PPh_3). The low price and the relatively high stability towards oxidation in air are the main factors for its popularity. Lately several new phosphines have been developed for coupling of less reactive electrophilic substrates. Common features of these phosphines are that they are electron rich and are sterically very demanding. The drawback of the high electron density on the phosphorus atom is that aerobic oxidation is then a very rapid process.

One of the first experimental studies on palladium(0)-phosphine complexes was a ^{31}P-NMR study at low temperature by Mann and Musco.[93] In case of sterically non-demanding phosphines the complexes added had the general formula $Pd(PR_3)_4$. For $Pd(PPh_3)_4$ two signals at δ=22.6 ppm and δ=18.4 ppm were observed which were assigned to $Pd(PPh_3)_4$ and $Pd(PPh_3)_3$. Later studies by Fauvarque et al. observed an inverse dependence of the PPh_3 concentration on the rate of oxidative addition of aryl iodides.[85] The explanation for this behavior was that the main species in solution was $Pd(PPh_3)_3$ with the active species being the 14-e complex $Pd(PPh_3)_2$. Extensive experimental studies by Amatore and Jutand came to the same conclusion. [94]

Many cross-coupling reactions have been found to proceed more efficiently when performed in presence of halide or carboxylate anions.[95] Amatore and Jutand found that addition of halide to a solution $Pd(PPh_3)_4$ induced the formation of a new palladium(0) species. The primary product in the oxidative addition to the anionic palladium species was found to be another complex than the one resulting from oxidative addition to the neutral analog. It was suggested that the presence of anions resulted in the formation of a tricoordinate species $[Pd(PPh_3)_2X]^-$, to which oxidative addition was more efficient as an effect of the anionic character of the complex. It was also proposed that the primary product of the oxidative addition was a pentacoordinate anionic complex, rather than a square planar one. Based on this interpretation a new type of catalytic cycle was proposed in which the square planar palladium(II) complexes were replaced by trigonal bipyramidal intermediates (Figure 31).

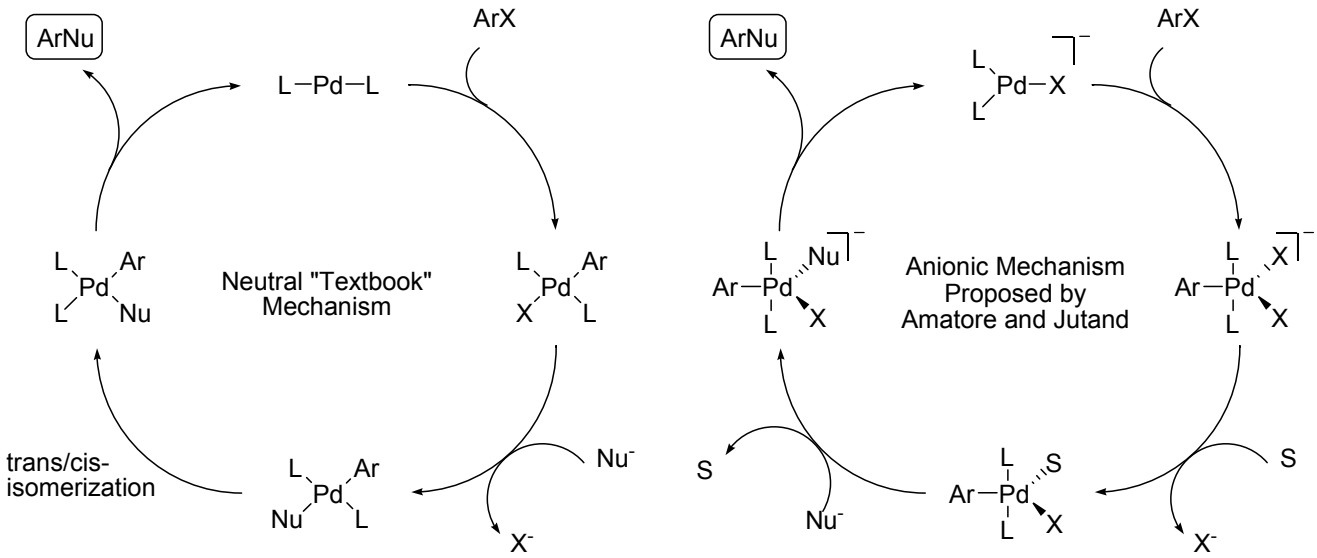

Figure 31. Amatore and Jutand proposed a catalytic cycle involving anionic intermediates (right) to proceed more efficiently than the neutral one (left).[95]

DFT studies by Shaik et al. showed that the tricoordinate anionic complexes, e.g. $[Pd(PPh_3)_2Cl]^-$, suggested by Amatore and Jutand were indeed minima on the potential energy surface.[96] Goossen et al. studied the similar complex $[Pd(PMe_3)_2OAc]^-$ and found that dissociation of one of the phosphines to $[Pd(PMe_3)OAc]^-$was a favored process in terms of free energy, although they assume that $[Pd(PMe_3)_2OAc]^-$ is the major species in solution from the potential energy calculations.[97] Oxidative addition of phenyl iodide to the tricoordinate anionic complex $[Pd(PMe_3)_2OAc]^-$ was preceded by dissociation of the acetate (Figure 32). The resulting complex was a square planar one where the phosphines were *cis* to each other with the acetate and the phenyl group occupying the remaining two sites. The iodide dissociated and did not coordinate to palladium, and thus no pentacoordinate palladium(II) complex was formed. Any attempt to minimize a pentacoordinate complex with the ligands used in their study failed. This suggests that the anionic mechanism proposed by Amatore and Jutand which involved pentacoordinate palladium(II) complexes is an incorrect interpretation of the experimental results.

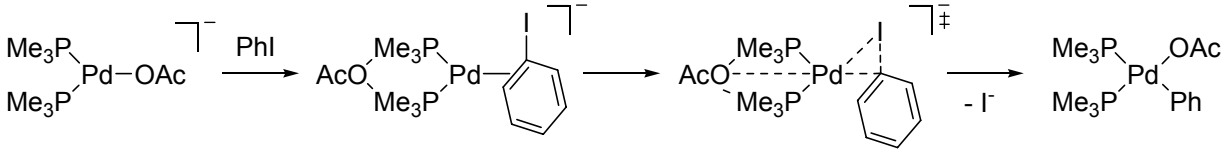

Figure 32. Simplified version of the oxidative addition mechanism proposed by Goossen et al..[97]

In all the studies described so far the geometries were optimized without applying a solvent model throughout the geometry optimization. Senn and Ziegler studied the oxidative addition of aryl halides to palladium(0) species coordinated by bidentate phosphine ligands.[98] The central point in their report is that the oxidative addition transition states found in gas phase calculations were not transition states when the reactions were fully optimized with a continuum model to describe solvent. Instead, another type of transition state was located where the halide was not interacting directly with the palladium center in the transition state, but was described as a dissociative transition state of S_NAr type (Figure 33). The structure then collapsed to a palladium(II) complex with the iodide coordinated to palladium.

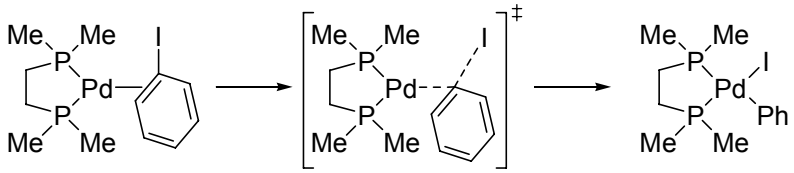

Figure 33. Oxidative addition mechanism proposed by Senn and Ziegler.[98]

Migratory Insertion

The Heck reaction was discussed to some extent earlier in this chapter. This is the palladium catalyzed substitution of a hydrogen atom for an organic group in an olefin. The generally accepted mechanism is outlined in Figure 34 and involves coordination of an alkene to palladium and subsequent insertion of the alkene into the palladium-carbon bond to give a palladium-alkyl intermediate. β-Hydride elimination then gives the product olefin and deprotonation of the palladium-hydride regenerates palladium(0). For the final regeneration of the active palladium(0) species to be a favored reaction, a base needs to be added to the reaction mixture. In this section earlier work on the migratory insertion step will be described in more detail.

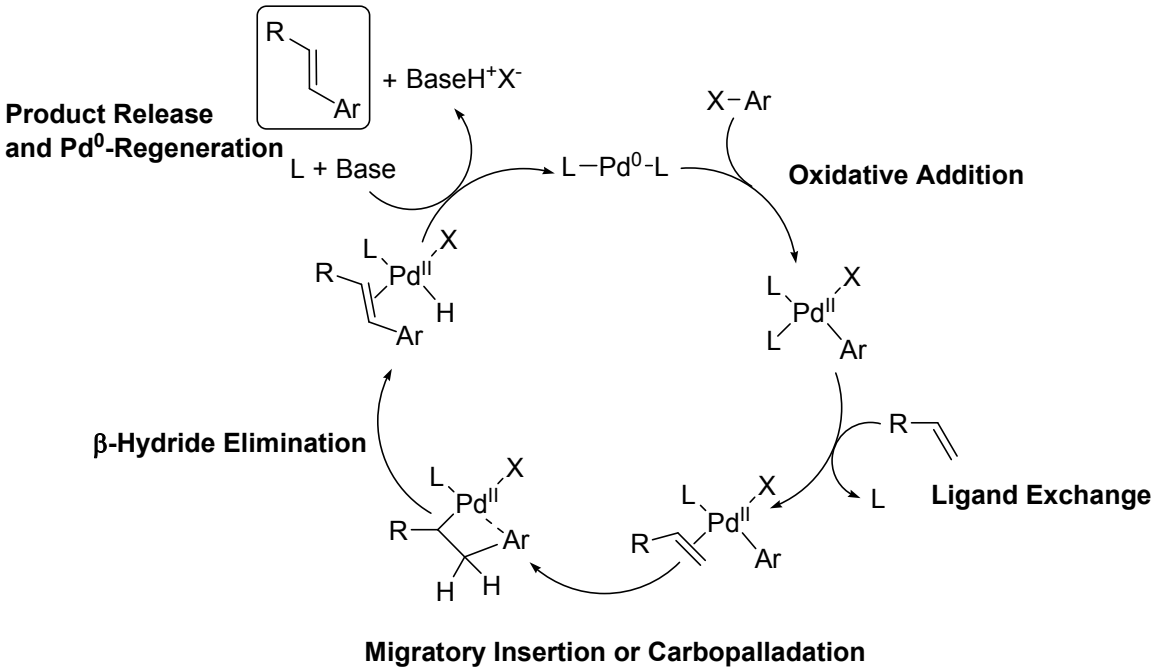

Figure 34. Simplified mechanism of the Heck reaction.

After the palladium(II) complex has been formed in the oxidative addition step a carbon-carbon bond can be formed by migratory insertion of an olefinic substrate. Depending on the reaction conditions this step can take place with either a cationic or neutral palladium(II) complex. The main impact of the charge of the system is believed to be the regiochemical outcome of the reaction. Recently a study by Deeth et al. described in detail how the electronics influence the regioselectivity.[99] A relationship between the experimentally observed product and the orbitals as well as the partial charge was found. By adding ΔE_{orb}, which is derived from the energy of the HOMO:s and LUMO:s of the coordinated alkene and the migrating group (here a vinyl group), with the difference in partial charge between the reacting carbon centers Δq (multiplied by a constant), a selectivity factor **Ω** was derived (eq. 1). When the values of **Ω** were in a certain range the selectivity was for one regioisomer, in another range the other regioisomer was favored, and in between a mixture would be expected.

$$\mathbf{\Omega = \Delta E_{orb} + 4.33 \Delta q} \qquad \text{Eq. 1}$$

β-hydride elimination

Following the migratory insertion in the Heck reaction is the β-hydride elimination which generates the product alkene. One of the first theoretical studies on β-hydride elimination was reported by Siegbahn et al. in 1996.[100] In their study the migrating group was modeled by a methyl group and the olefin was ethylene. They found that a 14-electron complex was formed after the insertion where the fourth coordination site is occupied by the β-hydrogen which interacted with an agostic bond to the palladium center. β-Hydride elimination from this complex had a barrier of merely 12 kJ/mol, and the step was found to be essentially thermoneutral. The main implication of the thermoneutrality is for the related polymerization of ethylene, where the reversibility of this step causes branching of the polymer. It is likely that the thermodynamics of the step are altered if a migrating group with higher coordinating ability than a methyl group is used. In many organic transformations the group would be an aryl or a vinyl group where both, and in particular the vinyl group, are likely to form reasonably strong bonds to palladium.

Transmetalations

Most of the coupling reactions that follow the general protocol outlined in Figure 28 involve an organometallic nucleophile as a coupling partner instead of the olefin in the Heck reaction. Following the oxidative addition of the aryl- or vinyl electrophile in these transformations is the delivery of the nucleophile from the coupling partner, the transmetalation step. Several protocols have been developed with different organometallic reagents, including Stille coupling with organotin reagents, Kumada coupling with organomagnesium reagents, Negishi with organozinc reagents, Suzuki with organoboron reagents and Sonogashira with copper acetylides (see Figure 28).

Recent studies by Goossen et al.[101] and Maseras et al.[102] have dealt with the transmetalation of an aryl or vinyl group from boronic acids to palladium(II) complexes, one of the key steps in the Suzuki coupling. The two groups studied slightly different versions of the reaction, where Goossen's study focused on the coupling between acetic acid anhydride with phenyl boronic acid, while Maseras has investigated the standard Suzuki coupling between a vinyl halide and vinyl boronic acid (Figure 35). The two groups have come to some common conclusions. In both Goossen's and Masereas' study prereactive complexes are described where the hydrocarbon moiety to be transferred is coordinating in an η^2-fashion to the palladium center. The boron is tetracoordinate with either a base or a halide occupying the fourth coordination site. The

palladium-carbon σ-bond is then formed simultaneously with the breaking of the boron-carbon bond, in what appears to be a dissociation of the boronic acid moiety. Once the aryl or vinyl group is transferred to palladium reductive elimination via a concerted three-center transition state closes the catalytic cycles (this step is described further later in this section).

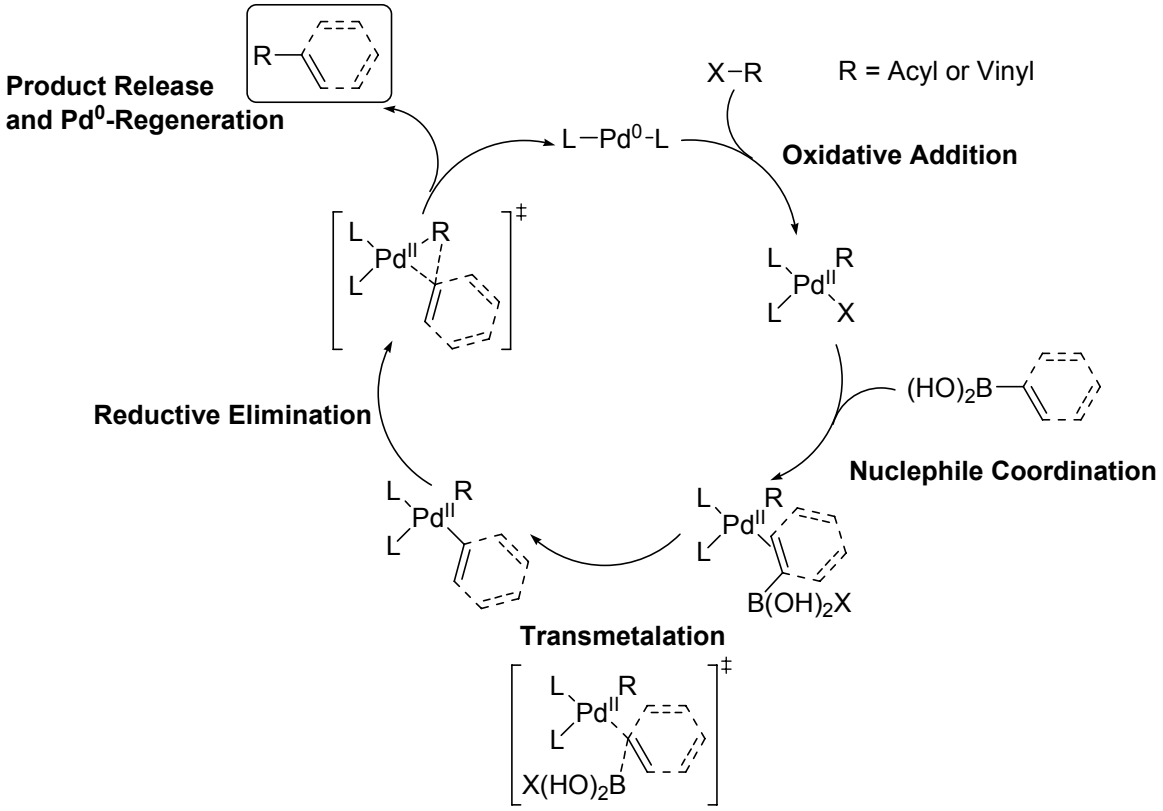

Figure 35. Simplification of the mechanistic proposals for the Suzuki reaction reported by Goossen et al. and Maseras et al..[101, 102]

Except for the studies just mentioned the number of theoretical studies on the other coupling reactions involving transmetalation is quite limited. Two recent examples by Napolitano et al.[103] and Alvárez et al.[104] were focused on the transmetalation step from an organotin reagent to a palladium(II) complex, the transmetalation steps of the Stille coupling. Two similar cyclic transition states were presented by the two research groups (Figure 36), where the hydrocarbon moiety is delivered to palladium simultaneously with the formation of a tin-halide bond. Napolitano also found an alternative path for transfer of the hydrocarbon group from tin to palladium. This involved hypervalent tin coordinated by four hydrocarbons and one Lewis base, in their study an amine. This Lewis base-assisted path was found to be favored energetically for the model system studied, which could rationalize the experimentally observed rate acceleration when performed in presence of base.[105]

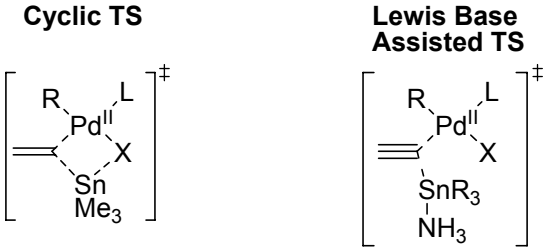

Figure 36. Two possible transition states for transmetalation from a stannane to palladium.

Most catalytic cycles of reactions involving transmetalation are closed by the reductive elimination step in which the carbon-carbon bond is formed and the active palladium(0) catalyst is regenerated. Several groups have studied this step, and all have come to the conclusion that the transition state is a three-centered concerted one (Figure 37).[101, 102, 106] Some studies have observed that decoordination of one of the spectator ligands may have a favorable impact. In most cases where the reaction has been studied as a part of an investigation of the entire catalytic cycle, the conclusion has been that the reductive elimination step is not the rate limiting one.

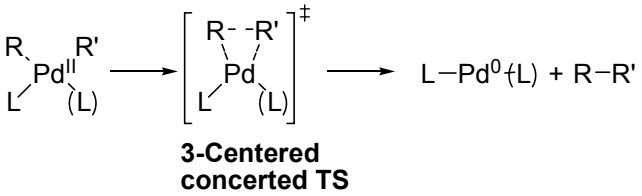

Figure 37. Reductive elimination as the final step in the catalytic cycle of many palladium catalyzed reactions.

Hydroarylation/vinylation of Alkynes

Background

Much like the Heck reaction, the hydroarylation reaction is a reaction between an aryl halide and a C-C π-bond (Figure 38).[107] The two reactions differ in that in the hydroarylation, the olefinic substrate of the Heck reaction has been replaced by an alkyne, and in the hydroarylation no base is needed but rather the mild reducing agent formate. The presence of a reducing agent allows for the alkyne to be reduced to an alkene. In the non-reductive Heck-reaction the degree of unsaturation remains the same throughout the reaction.

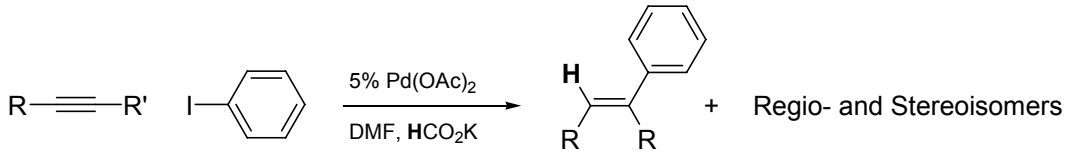

Figure 38. Typical reaction conditions for the hydroarylation reaction.[108]

The hydroarylation and hydrovinylation reactions have been applied to construct a variety of different target structures. In the initial studies mono- and disubstituted alkynes were used to produce simple alkenes.[107] The general observation was that the reaction was non-regioselective, meaning that the migratory insertion of the alkyne into the palladium-carbon bond could go two ways with similar barriers. Even for acetylenes substituted with an aryl and a *tert*-butyl group it has proven to be difficult to control the regioselectivity despite the large steric bulk of the *tert*-butyl group. Introduction of a hydroxyl group in the α-position was found to have a favorable impact on the regioselectivity yielding products from insertion at the remote carbon relative to the hydroxyl group (Table 2).[108] Isomerization of the double bond was observed in many cases thus yielding not only two regioisomers but also E/Z-stereoisomers. Later it was observed that exchanging the aryl electrophiles for cyclohexenyl analogs a higher regioselectivity could be obtained, and in most cases the syn-addition isomer was obtained exclusively.[109] Examples are outlined in Table 2.

Table 2 Some selected hydroarylation reactions.

Entry	Alkyne	Electrophile	Product
1	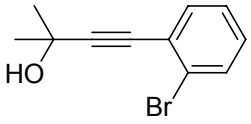	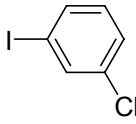	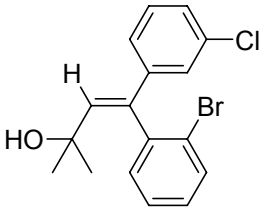
2	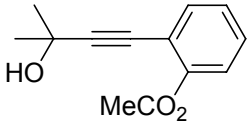	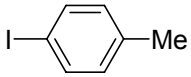	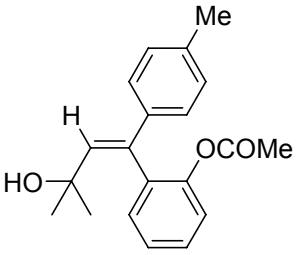
3	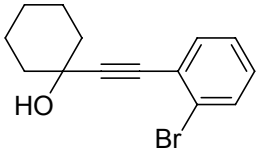	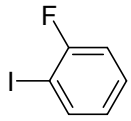	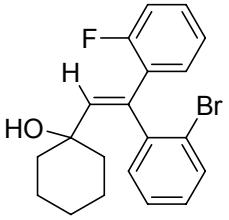
4	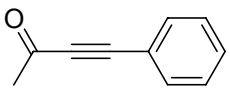	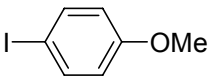	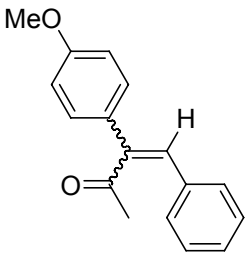
5	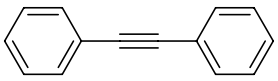	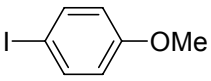	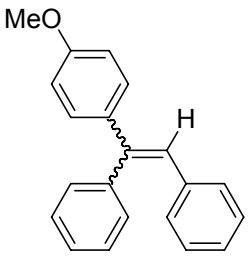

Sequential hydroarylation/vinylation and cyclization have successfully been used to produce a number of heterocyclic compounds. A general procedure is outlined in Figure 39. The reaction is an addition of an aryl or vinyl group to an acetylene substituted with an aryl group containing an nucleophile in the *ortho*-position. The other substituent on the acetylene contains a leaving group

(LG). The position of the nucleophile and leaving group can also be reversed. Two examples of syntheses of heterocycles reported by the Cacchi group will be described below.

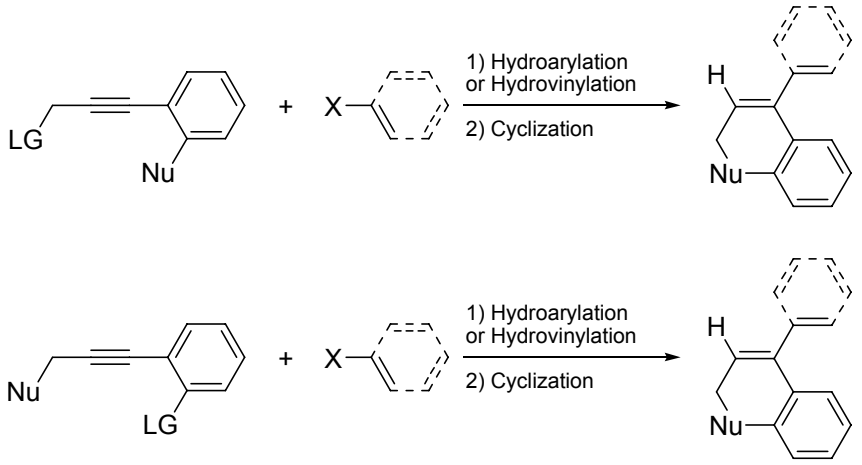

Figure 39. Sequential hydroarylation and cyclization have been used for construction of heterocyclic compounds.

The method for synthesizing bicyclic heterocyclic compounds have been successfully applied for the synthesis of chromenes.[110] From tertiary 3-(o-bromophenyl)propynols a series of 4-aryl and 4-vinyl-2,2-dialkyl-3-chromes were synthesized in a two-step protocol (Figure 40). First the alkyne is hydroarylated or hydrovinylated, then in the second step the chromene ring system is formed via an intramolecular Buchwald-Hartwig etherification. The overall yields were good and the first hydroarylation/vinylation step was found to be highly regioselective.

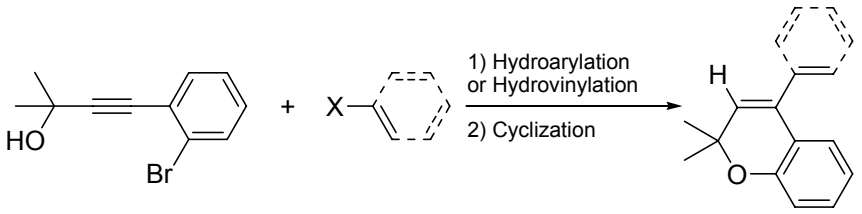

Figure 40. Synthesis of chromenes.

Quinolines represent another group of heterocycles where the hydroarylation reaction has been applied successfully as a synthetic strategy.[111] The one-pot tandem reaction which is shown in Figure 41 has the nucleophilic group in the form of a protected amine on the aryl group. At the other end of the acetylene the electrophilic part is an aldehyde protected as an acetal. The reaction was performed in an ionic liquid with a recyclable palladium catalyst, a procedure that allowed for the catalyst to be used in six consecutive runs without decreased activity.

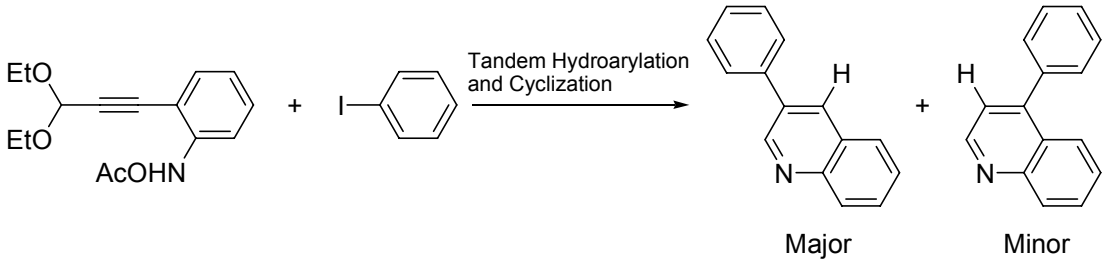

Figure 41. Quinoline synthesis.

Mechanistic Investigation

Little was known about the mechanism and the proposed one is based on knowledge of related reactions.[107] In Figure 42 an outline of the steps is presented: 1) reduction of the added palladium(II) salt to form the active palladium(0) species; 2) oxidative addition of the aryl halide giving a palladium(II) intermediate; 3) coordination and subsequent insertion of the alkyne into the Pd-Aryl bond, yielding a vinyl-palladium intermediate; 4) exchange of the halide for a formate; 5) hydride transfer from the formate moiety, and finally 6) reductive elimination to give the product alkene and regenerate the active palladium(0).

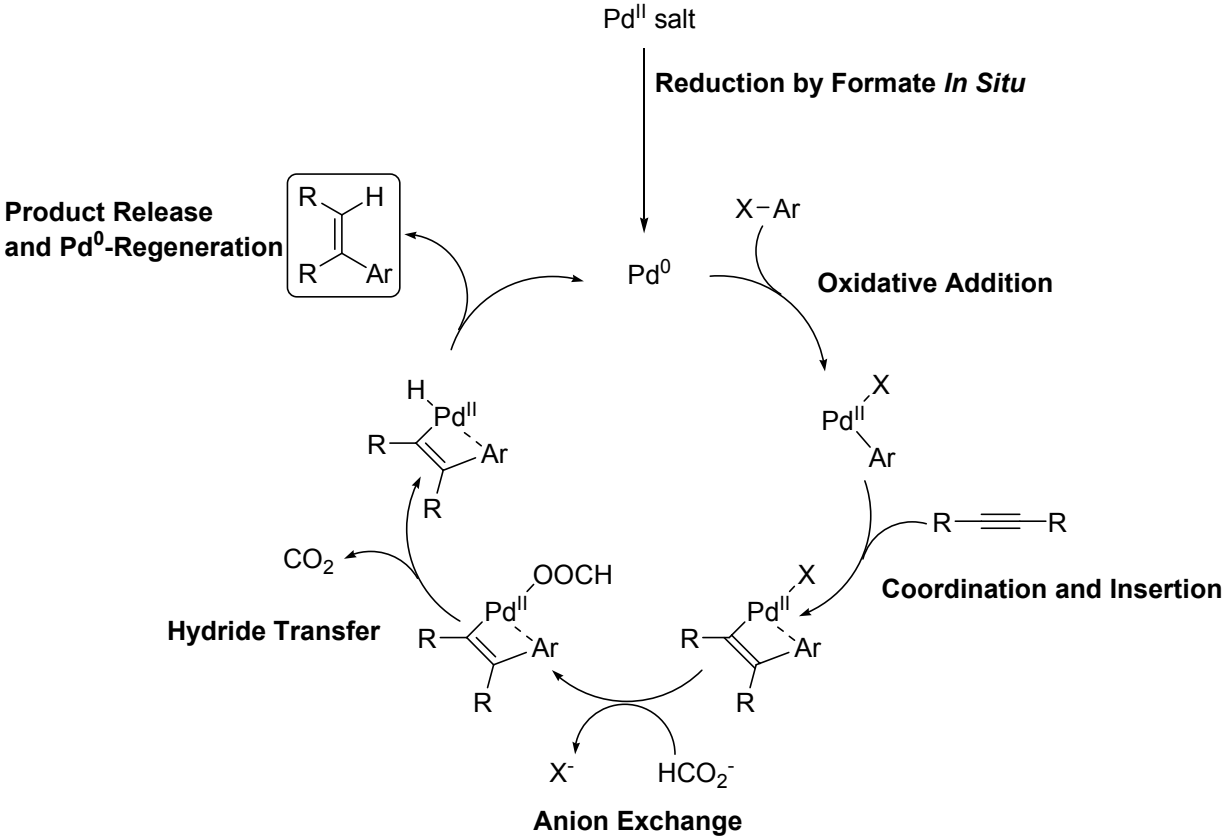

Figure 42. Proposed mechanism for the palladium catalyzed hydroarylation of alkynes.

In the first protocol for the hydroarylation it was performed in presence of a phosphine ligand to keep palladium from precipitating as palladium metal, a standard procedure in palladium catalysis. Later development demonstrated that the reaction could equally well be performed without the addition of phosphines, thus eliminating problems associated with phosphines such as oxygen sensitivity and tedious separation. Although synthetically very practical the absence of phosphine complicates the situation for a mechanistic investigation. Since the mechanism is believed to involve a palladium(0) species to which the aryl halide is oxidatively added and the catalytic cycle is commenced, something that can keep palladium from precipitating as metallic palladium must be present. Of the possible candidates the acetylenic substrates are the most probable due to the possible d-π-backdonation as a stabilizing interaction (Figure 43). Experimentally it was observed by Cacchi et al. that when the reaction was started five minutes before any alkyne is added, whereafter the alkyne was added dropwise, no product could be isolated.[109] When the reaction was run with 5% alkyne from the start and then the alkyne was added dropwise the yield was close to identical to when the reaction was run with all alkyne present from the start. This observation suggests that alkynes can act as stabilizers of dissolved palladium(0) species.

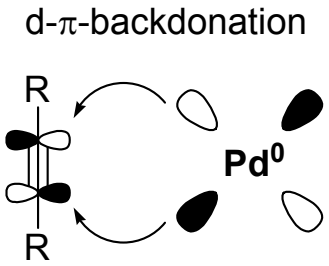

Figure 43. d-π*-backdonation from the electron rich palladium(0) center.

DFT calculations on ligand exchange equilibria of neutral palladium(0) complexes showed that alkynes are highly potent stabilizers for palladium(0).[112] The stabilities of the alkyne complexes were similar to the commonly employed palladium phosphine complexes (Table 3). The greatest stabilization is seen for the electron deficient alkynes, likely due to the greater capability of these alkynes to accept electron density from the metal center via backdonation as illustrated in Figure 43. Interestingly, the complex formed by an electron deficient alkyne and the simple phosphine PH_3 does not addopt a linear but a bent geometry, indicating the formation of pallada(II)cyclopropene (Figure 44). The more electron rich alkynes such as acetylene form complexes with a close to linear geometry.

Table 3. Relative potential energies of some $Pd^0L^1L^2$ complexes

Entry	L^1	L^2	Relative Energy (kJ/mol)
1	H-C≡C-H	H-C≡C-H	0
2	Ph-C≡C-Ph	Ph-C≡C-Ph	26
3	Me-C≡C-Me	Me-C≡C-Me	40
4	OHC-C≡C-H	OHC-C≡C-H	10
5	OHC-C≡C-CHO	OHC-C≡C-CHO	1
6	H-C≡C-H	PH_3	26
7	H-C≡C-H	PPh_3	13
8	OHC-C≡C-CHO	PH_3	-3
9	OHC-C≡C-H	PPh_3	0

Figure 44. The geometry of the complex with an electron deficient alkyne (left) is bent, which is an indication of the formation of a pallada(II)cycle. When the alkyne is more electron rich the preffered geometry is a linear one (right).

When reactions are conducted in presence of anions, formation of anionic palladium(0) complexes have been proposed to be the active species. Therefore anionic complexes were also optimized. The general structure was $[(HCO_2)PdL]^-$ where L is the neutral ligand (acetylene or phosphine ligand) and the anionic ligand was chosen to be formate since it is present in high concentrations under typical hydroarylation conditions. Here the effect of the π-accepting ability of the neutral ligand is much greater than in the neutral complexes (Table 4). The most stable complex was found to be the one containing the electron deficient butyn-dial ligand. This complex adopts a structure where the formate anion is coordinating to palladium in a bidentate fashion, indicating that the d-π-backdonation is of such magnitude that the complex is best described as a palladium(II) complexes (Figure 45). Anionic phosphine complex are strongly disfavored compared to the complexes containing acetylenic ligands, likely due to the much lower ability of phosphines to accept electrons compared to the acetylene ligands.

Table 4. Relative potential energies of some $[HCO_2Pd^0L]^-$ complexes

Entry	L	X^-	Relative Energy (kJ/mol)
1	H-C≡C-H	$^-$OOCH	0
2	Me-C≡C-Me	$^-$OOCH	23
3	Ph-C≡C-Ph	$^-$OOCH	20
4	PPh_3	$^-$OOCH	30
5	OHC-C≡C-H	$^-$OOCH	-40
6	OHC-C≡C-CHO	$^-$OOCH	-53

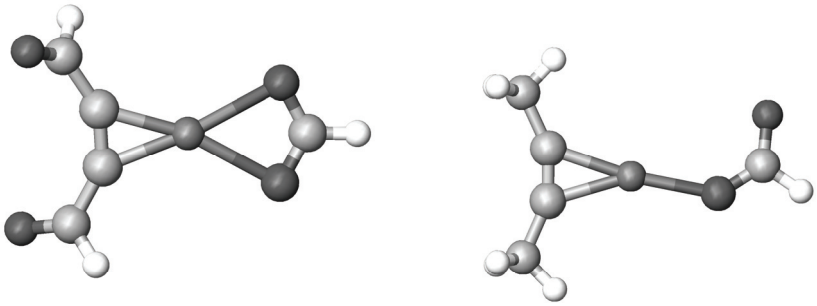

Figure 45. In the complex with an electron deficient alkyne (left) the formate coordinates with both oxygen atoms, an indication of the formation of a pallada(II)cylcle. When the alkyne is more electron rich the preffered geometry is a linear one (right) and the formate coordinates with one oxygen atom.

For modeling the reaction mechanism of the hydroarylation the acetylene chosen was diphenyl acetylene, a frequently employed experimental model substrate. Both anionic and neutral paths were investigated, but not directly compared since the methods are less reliable when comparing species of different charge.[113] The starting complex **24** of the neutral path was bis(diphenyl actenylene)palladium(0) in which the two alkynes are coordinating in a perpendicular fashion to allow for backdonation from two orthogonal d-orbitals (Figure 46).[112a] Exchange of one of the acetylenes for phenyl iodide, possibly via a solvent complex **25**, leads to the formation of the prereactive complex **26**. Oxidative addition can then take place via **27ts** with an overall barrier from **24** of 55 kJ/mol to yield the palladium(II) complex **28**. Coordination of a solvent molecule to the free site is highly favored and the oxidative addition transformation is calculated to be exothermic by 50 kJ/mol (**29**). A similar path was found for the anionic complex **32** for which an

overall barrier of 32 kJ/mol was calculated. Here a palladium(II) complex is formed where the formate anion is coordinating in a bidentate fashion (**34**). In this case the reaction is highly exothermic by as much as 117 kJ/mol.

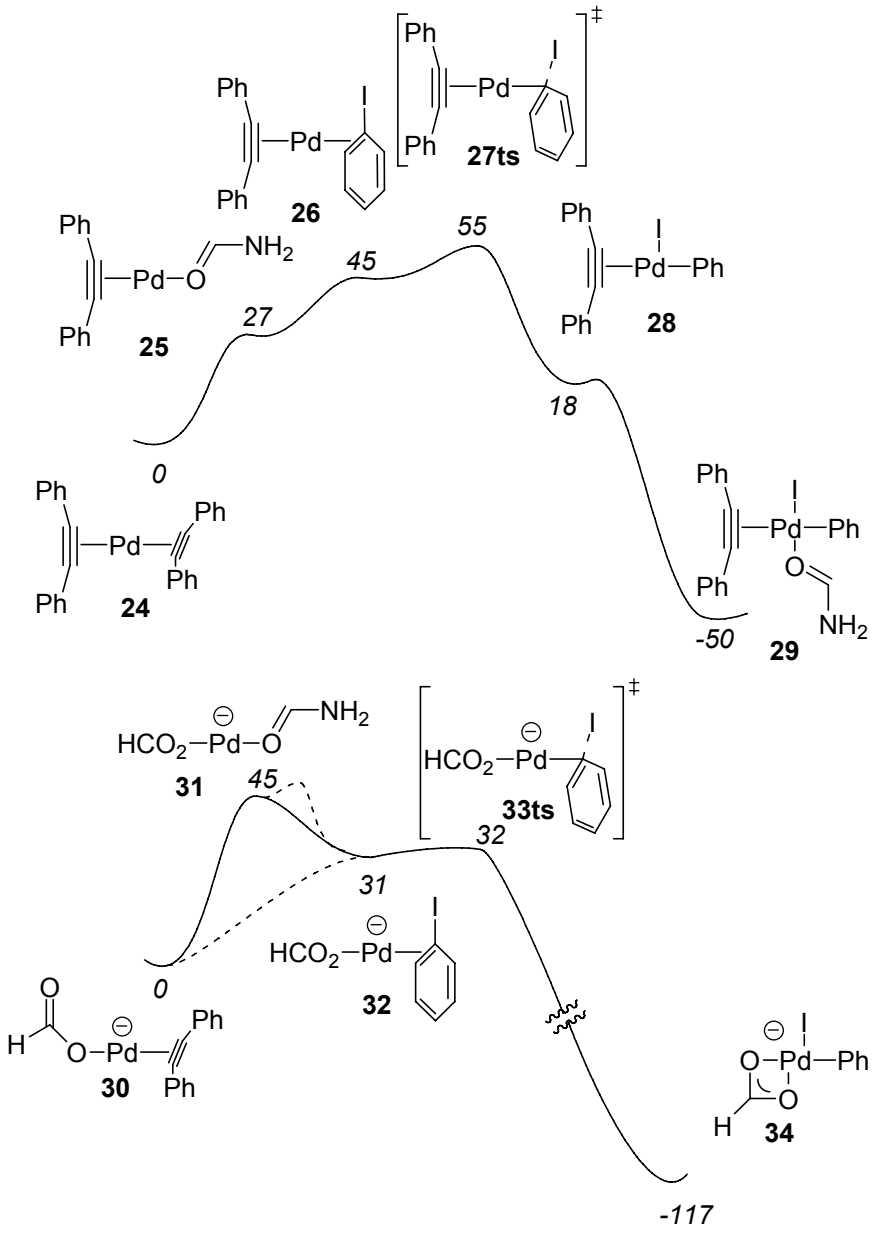

Figure 46. Oxidative addition paths to a neutral (above) and an anionic (below) palladium(0) complex.

Prior to the migratory insertion of the alkyne substrate a *cis*-acetylene-phenyl palladium(II) species must form. Exchange of the ligands is likely to be rapid and we believe that a complex like **35** is a possible intermediate under the reaction conditions. In **35**, the migrating phenyl and the inserting alkyne are situated in a *cis* fashion. The two remaining coordination sites are

occupied by a formate and a coordinating solvent molecule, here a formamide as a model for DMF. Two *cis*/*trans* isomers are possible with respect to the position of the spectator ligands and both were considered. The phenyl group in **35** is coordinating in a fashion so that the ring is perpendicular to the coordination plane of palladium. Also the alkyne coordinates out of the coordination plane. In the following transition state the alkyne rotates so that it almost in the coordination plane of palladium. The barrier for the step was calculated to 85 kJ/mol independent of the position of the spectator ligands. In the resulting vinyl-palladium complex **37** the migrated phenyl group coordinates in what seems to be an η^1-fashion to the *ortho*-carbon of the phenyl ring. Before the product can be formed the hydride needs to be transferred from the formate moiety to palladium to give a palladium-hydride species. Two paths were characterized for the hydride transfer. In the first **38ts**, the formate and the vinyl are positioned *trans* to each other. The hydride is then transferred to the site where the migrated phenyl group was coordinating, which after dissociation of CO_2 yields the *cis*-hydride-vinyl palladium complex **39**. The barrier for the reaction step was calculated to 71 kJ/mol (95 kJ/mol relative to the more stable complex with formate is in *cis*-position to the vinyl). From the vinyl palladium complex with the formate in *cis*-position to the vinyl group another path was located. This path starts with the formate rotating to give a complex where the coordination of the formate is via the hydrogen instead of one of the oxygen atoms. The barrier was calculated to 99 kJ/mol. Dissociation of CO_2 then occurs with virtually no barrier to give a palladium hydride complex similar to **39**. An interesting feature of both paths is that they yield the *cis*-hydride-vinyl palladium complex, which is set for product formation via reductive elimination. No transition state could be located which would give the trans-hydride-vinyl palladium, and a quick comparison of the stability of a *cis*- versus a *trans*-complex showed a strong preference for the *cis*-complex of 90 kJ/mol in potential energy. The strong *trans*-influence of both the hydride and the vinyl group makes it much more favorable to have these positioned *cis* to each other, a feature which also favors the reaction. Reductive elimination of the hydride and the vinyl moieties was found to be a facile process, which takes place with a barrier of 40 kJ/mol (**40ts**). The resulting complex **41** is a palladium(0) species coordinating to the product alkene and a solvent molecule, and palladium has been regenerated to the zero-valent oxidation state which can enter a new catalytic cycle. The reaction is outlined in Figure 47.

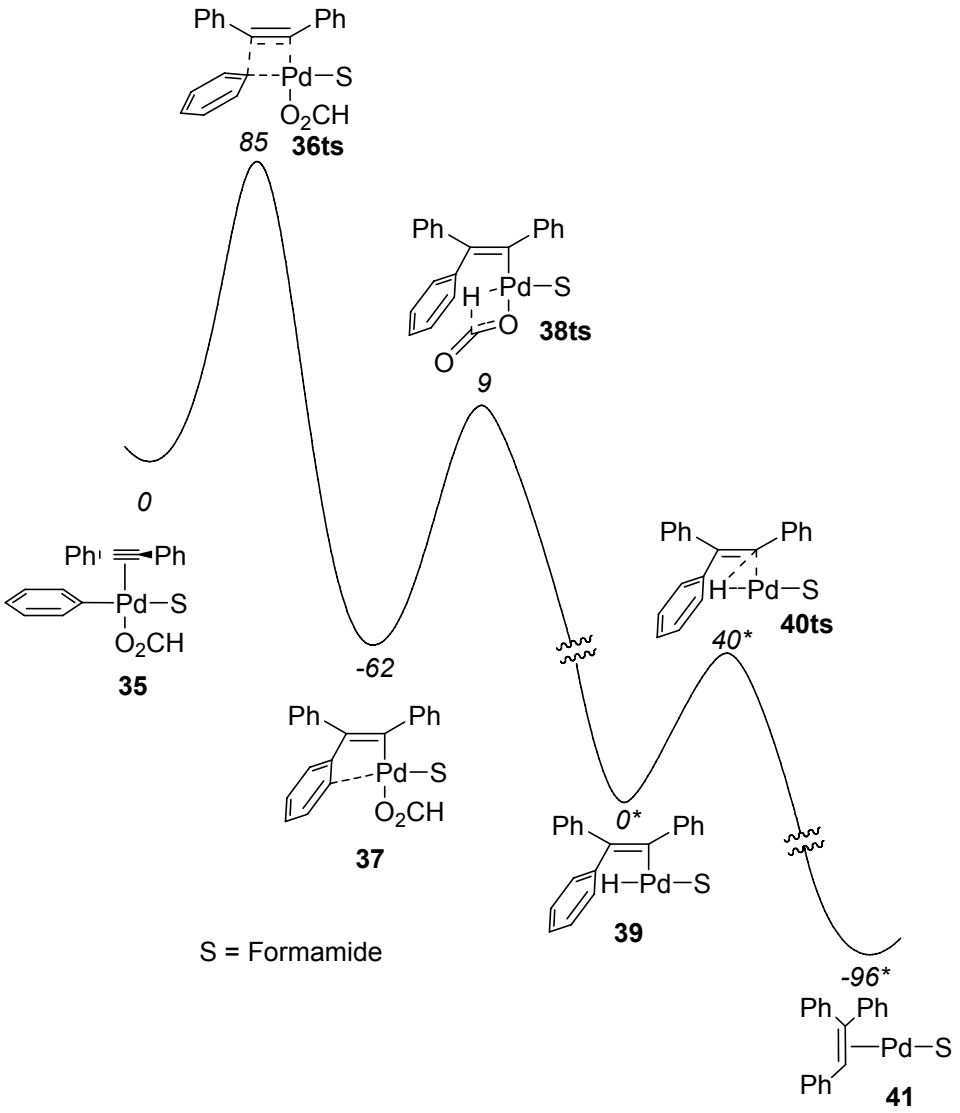

Figure 47. Proposed mechanism for the migratory insertion, hydride transfer from formate and the reductive elimination steps.

In the reaction path described above the migratory insertion step is where the regiochemical outcome of the reaction is determined. We therefore decided to look more closely at this step since several interesting observations have been made in terms of the regioselectivity of the reaction. First it had been observed that hydroarylation of Ar-C≡C-*t*Bu tends to yield statistical mixtures of the four possible regio- and stereoisomers. On the contrary hydrovinylation of the same type of alkyne, using 4-phenyl-cyclohexenyl triflate instead of the aryl iodide in the hydroarylation, gave one product exclusively (Figure 48).

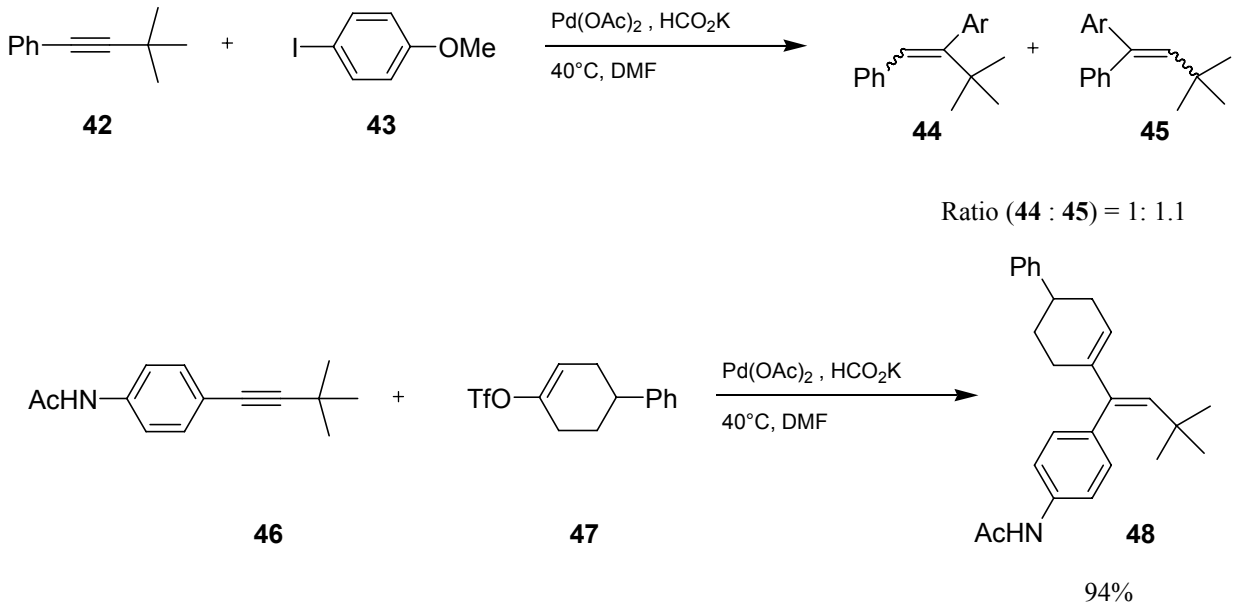

Figure 48. Regiochemsitry in the hydroarylation is unselective (above), while the hydrovinylation is highly regioselective.

The major differences between the two reactions are the exchanges of aryl to vinyl and iodide to triflate. To understand which of the changes that is responsible for the change in product outcome, an experiment was conducted with 4-phenyl-cyclohexenyl iodide as the electrophilic substrate. Reactivity similar to that of the cyclohexenyl triflate would then indicate that the aryl-vinyl change is responsible for the change in reactivity, while reactivity like aryl iodide would indicate that the change from iodide to triflate is the one making the outcome different. In Figure 49 are shown two reactions. In the first the electrophile is 4-phenyl-cyclohexenyl iodide and in the second 4-phenyl-cyclohexenyl triflate is used with added potassium iodide. In both experiments the outcome was identical to that of the reaction with 4-phenyl cyclohexenyl triflate in absence of iodide. This is a strong indication that the vinyl group is responsible for the change in reactivity, and not the triflate.

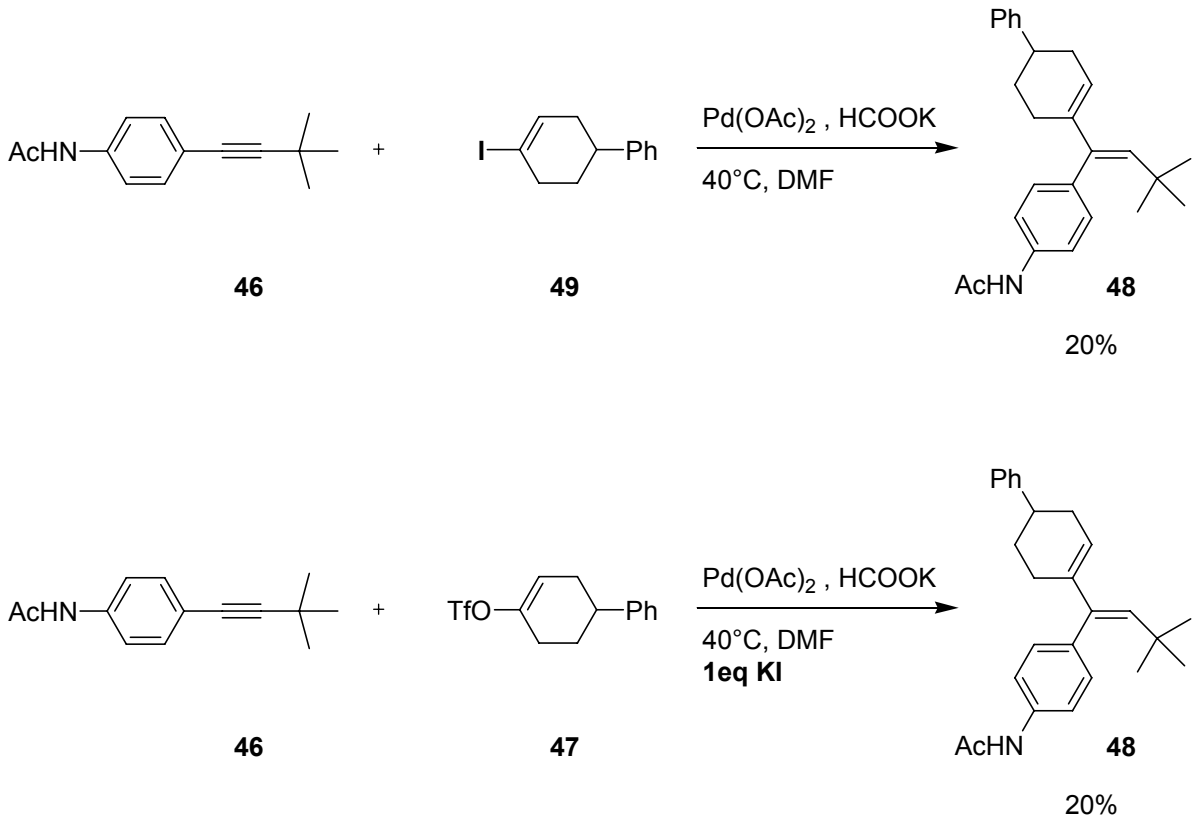

Figure 49. Control experiments show that the vinyl-aryl shift is responsible for the shift in regioselectivity rather than the iodide-triflate change.

To understand the underlying details of the regioselectivity the migratory insertion step was modeled computationally. The alkyne was chosen to Ph-C≡C-*t*Bu and the aryl group a simple phenyl group. The vinylic moiety was 2-butenyl to incorporate the sterics and electronic effects of the methylene groups of the cyclohexenyl substrate. For each transition state two *cis*/*trans* isomers with respect to the position of spectator ligands formate and formamide were modeled. In Figure 50 the lowest energy transition states for each regioisomeric insertion are shown with the relative energies. The hydroarylation reaction has isoelectronic transition states in excellent agreement with the experiments. Also for the vinyl the agreement is good where the regioisomeric transition state leading to the experimentally observed product was calculated to be 19 kJ/mol lower in energy than the transition state which would give the non-observed product.

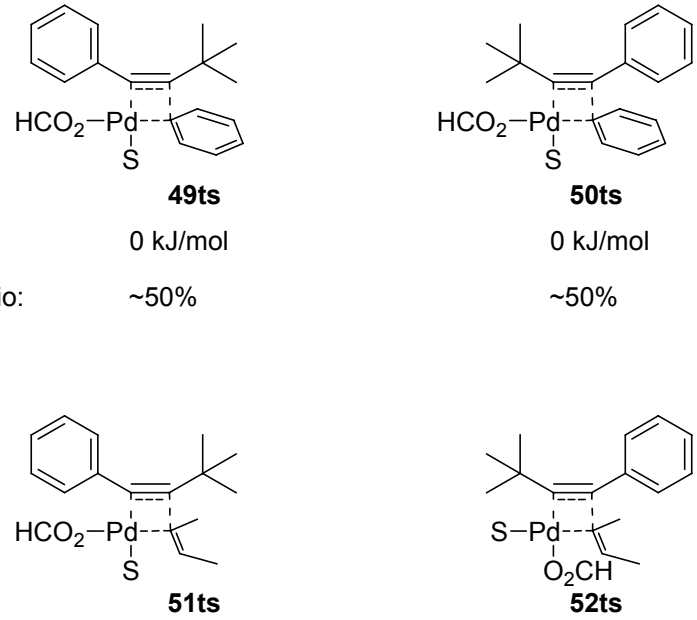

Figure 50. DFT calculations are in agreement with the experimental results.

Despite the good agreement between the experimental and the modeled results the explanation for the regioselectivity was not straightforward. Electronic effects are likely to have an impact on the reaction, but exchanging an aryl group for a vinyl should not alter the electronic situation much. A closer look at the transition state geometries reveals another difference, namely the introduction of steric bulk in α-position on the vinyl from the protons of the methyl group. So if it is the steric bulk of the methyl group that makes the difference, a substrate with the electronic properties of a vinyl but the sterics of a phenyl should have isoelectronic transition states. Therefore the regioisomeric transition states for the migration of 2-butadienyl were located. The transition states were indeed isoelectronic (Figure 51), thus confirming the hypothesis that the main difference between the aryl and cyclohexenyl is the steric properties of these.

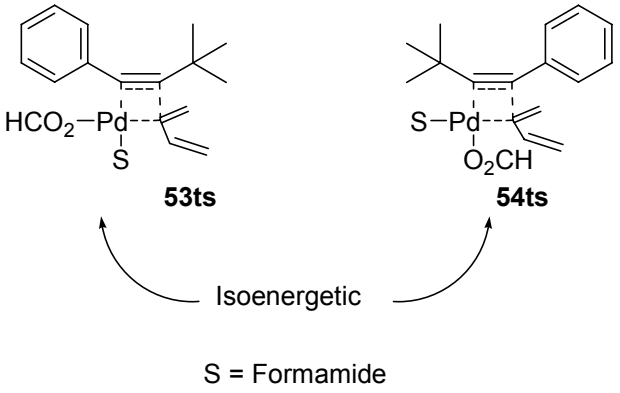

Figure 51. Transition states were calculated to be when the inserting group was 2-butadienyl.

The second interesting regiochemical feature of the hydroarylation/vinylation that drew our attention was the fact that α,β-acetylenic carbonyl compounds tend to insert into the Pd-C bond to give the α-addition product selectively (Figure 52).[108, 114] For the similar Heck reaction of typical Michael acceptors such as benzylideneacetone the outcome is the more intuitive β-addition product.[108] To get a better understanding of the background of the reactivity, the transition states leading to two regioisomeric products in the reaction with phenyl-propargyl aldehyde were modeled. Again good agreement with the experiments was obtained and the transition state leading to the α-addition product was favored by 17 kJ/mol (Figure 53).

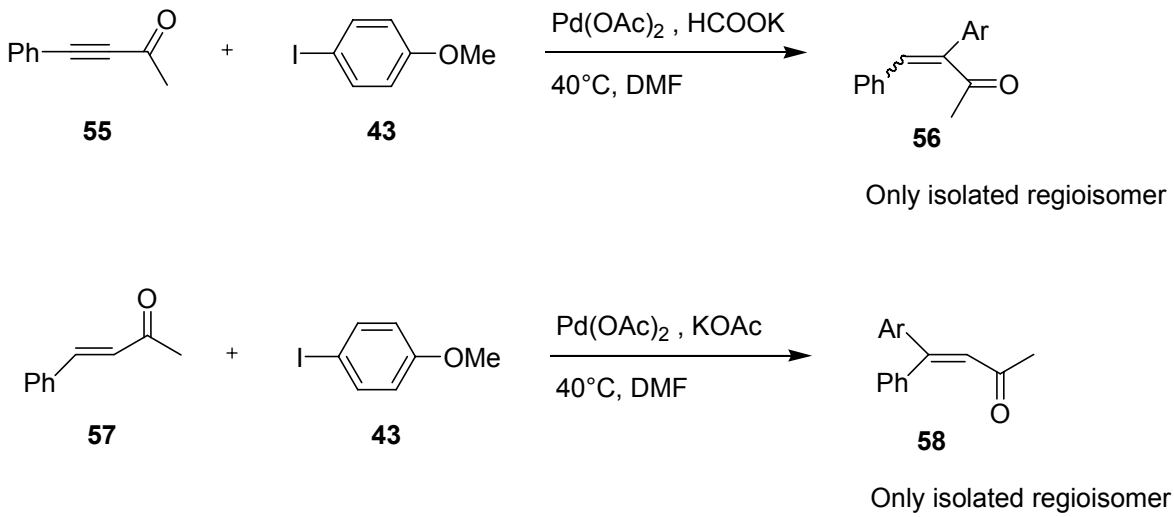

Figure 52. Above: Hydroarylation gives the α-addition product Below: Heck reaction gives the β-addition product.

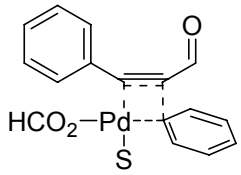

59ts

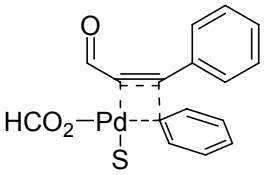

60ts

Relative Energy:	0 kJ/mol	17 kJ/mol
Experimental Ratio:	~100%	-

Figure 53. DFT calculations of the regioisomeric transition states agree well with the experiments.

The most obvious difference between alkene and alkyne substrates is the extra π-bond. When observing the transition state geometries for the insertion of the α,β-acetylenic aldehyde, it appears as if the reacting π-system is not in conjugation with the carbonyl group nor with the phenyl group (Figure 54). Addition of the polarized Pd-C bond to a polarized Michael acceptor π*-orbital is expected to give the β-addition product. For an alkyne the reaction is very different since the reacting π*-orbital is not in conjugation with the carbonyl group, and therefore one must look at the distribution of this non-conjugated orbital rather than the conjugated one. NBO-analyses[115] of the two π*-orbitals of phenyl-propargyl aldehyde show a clear difference in the distribution of the π*-orbitals. Whereas the conjugated orbital is mainly located at the β-carbon the non-conjugated orbital has a slightly larger coefficient on the α-carbon. The very small difference in the value of the coefficients of the π*-orbital combined with the partial charge distribution mainly concentrated on the β-carbon indicate that electronics are not the most important factor for the regiochemical outcome. Since the phenyl group is in coordination with the non-reacting π-system its steric bulk is maximized, and compared to a carbonyl group the phenyl group is then substantially larger.

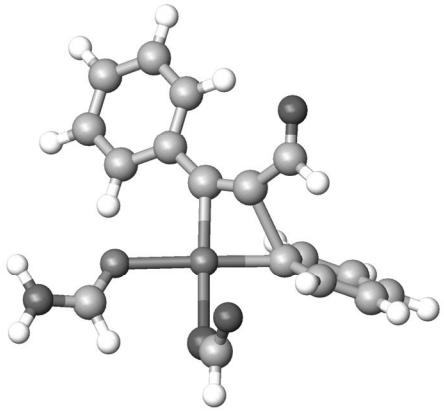

Figure 54. Geometry of **59ts**

Conclusions

A feasible mechanism for the hydroarylation reaction was characterized computationally. The active species is likely a palladium(0) species stabilized by coordination of alkynes. Oxidative addition proceeds with a relatively low barrier. The following insertion of the alkyne was calculated to have a barrier of 85 kJ/mol, with a four-center cyclic transition state. The resulting complex was a vinyl-palladium species with the migrating aryl coordinating to the metal-center with its π-electrons. When regioisomeric transition states were calculated, agreement with experiments was excellent. It was found that the regiochemical outcome was largely dependent on the steric bulk of the alkyne substituents and the inserting aryl/vinyl-group. Two mechanisms for the hydride transfer were characterized, and interestingly both yield a palladium species with the hydride and the vinyl in *cis*-position. With the hydride transferred the reductive elimination could take place with a low barrier.

Isomerization of Vinyl Electrophiles in the Heck Reaction

Much of the recent efforts in the research on palladium coupling have focused on using cheaper, more readily available and more stable electrophilic substrates e.g. aryl chlorides and vinyl tosylates.[66, 116] Unactivated vinyl-tosylates and vinyl-phosphates represent some of the more challenging electrophilic substrates, but they are very attractive substrates due to the facile preparation from the corresponding ketones.[116] Most examples of vinyl tosylate coupling applied activated substrates and only a few studies have reported protocols for coupling of the unactivated analogs. A highly efficient protocol was developed by Skrydstrup and co-workers for coupling of electron rich vinyl tosylates as well as vinyl phosphates with alkenes in a Heck type reaction (Figure 55).

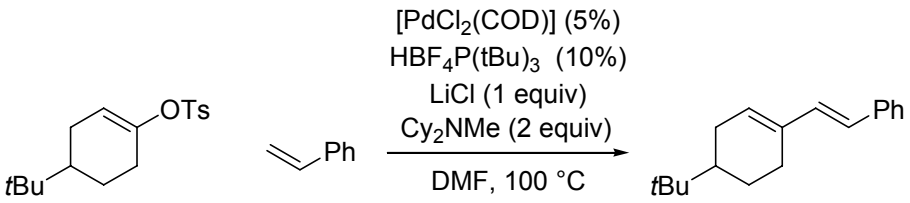

Figure 55. Protocol by Skrydstrup for coupling of unactivated vinyl tosylates.

When the reaction was applied on a vinyl substrate with a *tert*-butyl group in α-position rearrangement of the vinyl was observed, with the consequence that the internal vinyl tosylate yielded a product where the new carbon-carbon-bond was formed to the terminal carbon (Figure 56). A possible path for this rearrangement involves a β-hydride elimination to give a hydride-(*t*Bu-acetylene)-palladium intermediate. Subsequent rotation and reinsertion of the alkyne would then yield an intermediate with the rearranged vinyl-group (Figure 57). When the reaction was performed on a deuterium labeled vinyl tosylate substrate the product expected from the proposed mechanism was the observed one (Figure 58).

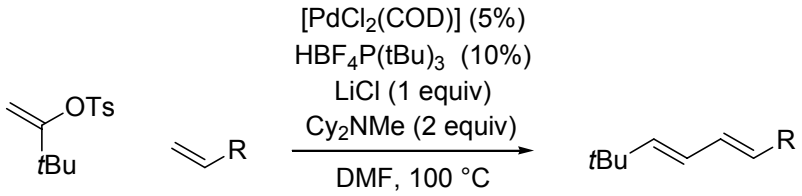

Figure 56. *t*Bu-vinyl tosylates rearrange to yield the terminal vinyl product.

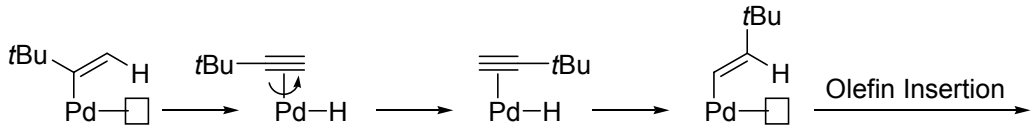

Figure 57. Proposed mechanism for the vinyl-rearrangement via β-elimination.

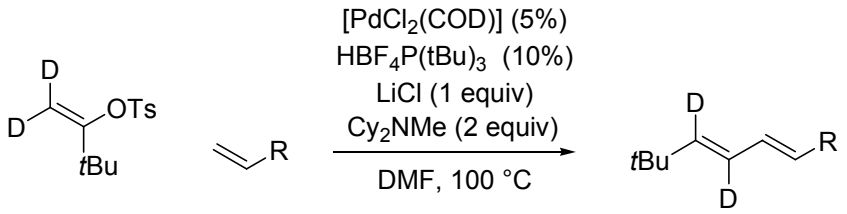

Figure 58. Deuterium labeling yielded the product in this figure exclusively.

To further investigate the proposed mechanism we undertook a DFT investigation. The starting complex was chosen to be the T-shaped 14-e complex **61**, where palladium is coordinating to the *t*Bu-vinyl group, a tri-*t*Bu-phosphine and a chloride. Complexes of this type have been isolated and characterized by X-ray crystallography, hence **61** was considered a reasonable choice. β-Hydride elimination on vinyl groups is rarely observed. For such a reaction to occur a free site of coordination is required, and we therefore believed that the observed system was optimal since the steric bulk of the phosphine and the vinyl would leave one site open. In addition to the favored coordination, the fact that two groups with large *trans*-influences are in *trans* position to each other in **61**, could favor β-elimination since that would yield a complex with a hydride and the phosphine positioned *cis* to each other. A β-elimination transition state from **61** was located **62ts** and the process was calculated to have a barrier of 62 kJ/mol. The alkyne-hydride-palladium intermediate formed (**63**) was calculated to be 27 kJ/mol above **61** in potential energy. The following reinsertion of the alkyne into the palladium-hydride bond was found to have a very low barrier of 21 kJ/mol, yielding the rearranged vinyl-palladium intermediate **65** in an overall thermoneutral reaction (+1 kJ/mol). The values of the calculated barriers suggest that the process is facile under the reaction conditions. For this mechanism to be operating it still needs to have a lower activation energy than the competing olefin insertion. Coordination of acrylamide at **61** yielded **66** which was calculated to be 18 kJ/mol higher than **61** in potential energy. Insertion can then take place via **67ts** and the overall barrier from **61** was calculated 87 kJ/mol. The corresponding transformations at the isomerized complex were calculated to be substantially more facile. Coordination of acrylamide was endothermic by 1 kJ/mol (**68**) and the insertion had an activation energy of 66 kJ/mol (**69ts**), which means a 19 kJ/mol lower barrier than the one for

insertion at the non-isomerized complex **67ts**. Both insertion transition states are further disfavored relative to the isomerization path by 20-40 kJ/mol due to the unfavorable entropy of a bimolecular reaction contra a unimolecular one. The current reaction is thus an example of typical Curtin-Hammett situation, where the two intermediates **61** and **65** are in rapid equilibrium with a subsequent irreversible step with a higher barrier. The reaction is outlined in Figure 59.

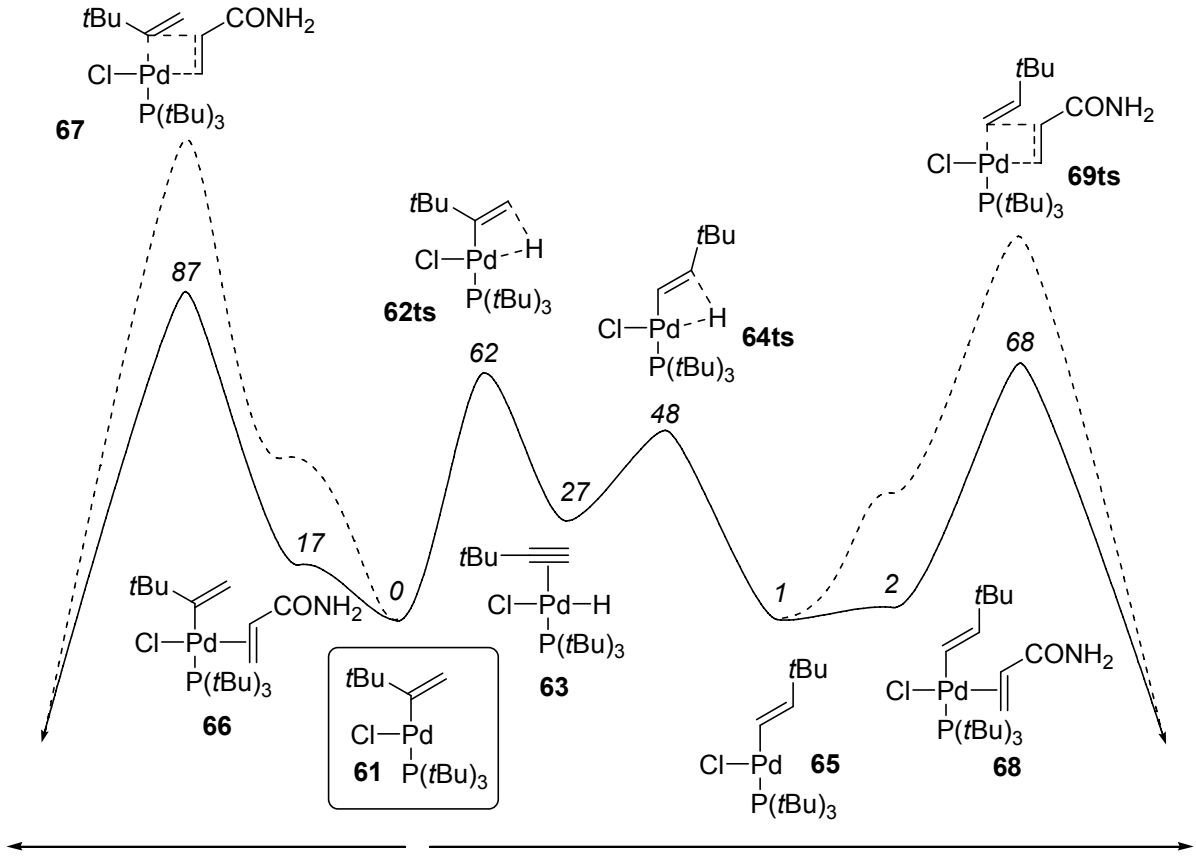

Figure 59. The mechanism for the vinyl rearrangement characterized by DFT. The rearrangement and insertion is favored over direct insertion. Dashed lines represent approximate energies including entropic contributions for the bimolecular insertion. Relative energies in kJ/mol.

Theoretical Studies on Coordination and Reactivity of Pd^0 Complexes.

The studies on the reactivity of the palladium(0) alkyne complexes revealed a higher reactivity of monocoordinate palladium PdL towards oxidative addition of aryl halides. These findings are not in agreement with the earlier proposed mechanism for oxidative addition to palladium phosphine complexes.[85-87] For these complexes the oxidative addition was suggested to occur at a dicoordinate palladium species PdL_2, except when extremely bulky ligands were used e.g. P*t*Bu_3.[117]

To get a deeper understanding of the coordination and reactivity of palladium(0) several neutral as well as anionic complexes were modeled, most containing the experimentally relevant ligand PPh_3. All geometries were fully optimized applying a continuum to simulate solvent.[118] For the neutral complexes free energies were calculated in the gas phase to get an estimate on the entropic contribution to equilibria with different molecularity.[119] In Table 5 are outlined the relative free and potential energies of a number of neutral complexes believed to be involved in the preequilibria of the oxidative addition.

Table 5. Relative potential energies of a series of neutral Pd^0-complexes. All numbers are in kJ/mol.

Entry	***Complex***	***CN***[a]	ΔG_{gas}	ΔE_{DMF}	"ΔG_{DMF}"[b]
1	$Pd(PPh_3)$	1	82	102	53
2	$Pd(PPh_3)_2$	2	**0**	**0**	**0**
3	$Pd(PPh_3)$(PhI)	2	60	53	46
4	$Pd(PPh_3)$DMF	2	63	40	43
5	$Pd(PPh_3)_3$	3	44	26	84
6	$Pd(PPh_3)_2$(PhI)	3	100	68	124

(a) Coordination number of Pd. (b) See computational details in paper 5.

According to the results in Table 5 the dicoordinate complexes were highly favored over the mono- and tricoordinate ones. A striking result is that $Pd(PPh_3)_2$ was calculated to be very much more stable than the tricoordinate $Pd(PPh_3)_3$, in sharp contrast to the earlier interpretations of the experimental measurements.[85] Further studies on anionic complexes containing either formate or chloride as the anionic ligand show similar trends (Table 5 and Table 7). For both types of anionic complexes dissociation of one phosphine from $[Pd(PPh_3)_2X]^-$ was calculated to be a favored process. In the chloride complex $[Pd(PPh_3)_2Cl]^-$ the Pd-Cl bond distance was calculated to 2.73 Å

compared to 2.47 Å in the dicoordinate $[Pd(PPh_3)Cl]^-$, indicating a much weaker interaction in the tricoordinate complex.

Table 6 Relative potential energies of $[PdL_nCl]^-$. All numbers are in kJ/mol.

Entry	Complex	CN[a]	ΔE_{DMF}	"$\Delta G_{Estimate}$"[b]
1	$[Pd(PPh_3)Cl]^-$	2	**0**	**0**
2	$[Pd(PhI)Cl]^-$	2	35	35
3	$[Pd(DMF)Cl]^-$	2	50	50
4	$[Pd(PPh_3)_2Cl]^-$	3	32	72
5	$[Pd(PPh_3)(PhI)Cl]^-$	3	50	90

(a) Coordination number of Pd. (b) See computational details in paper 5.

Table 7. Relative potential energies of $[PdLOOCH]^-$. All numbers are in kJ/mol.

Entry	Complex	CN[a]	ΔE_{DMF}	"$\Delta G_{Estimate}$"[b]
1	$[Pd(PPh_3)(OOCH)]^-$	2	**0**	**0**
2	$[Pd(PhI)(OOCH)]^-$	2	25	25
3	$[Pd(DMF)(OOCH)]^-$	2	33	33
4	$[Pd(PPh_3)_2(OOCH)]^-$	3	10	50

(a) Coordination number of Pd. (b) See computational details in paper 5.

Oxidative addition transition states were also located to gain further insight into the paths that have been previously proposed as well as alternative ones. For the neutral complexes two transition states were modeled - one dicoordinate with one phosphine and one tricoordinate containing two. It was found that the dicoordinate one was highly favored in potential energy and even more in free energy. For the anionic paths only dicoordinate complexes were considered since the prereactive complex $[Pd(PhI)(PPh_3)Cl]^-$ was already highly disfavored compared to the prereactive complex without the phosphine $[Pd(PhI)Cl]^-$. Oxidative addition of phenyl iodide was found to be a very facile process with very low barriers relative to the prereactive complexes $[Pd(PhI)Cl]^-$. The barriers of the different complexes are summarized in Table 8.

Table 8. Transition state energies relative to the respective prereactive complexes. All numbers are in kJ/mol.

Entry	**OA TS State Complex**	**CN[a]**	**ΔE_{DMF}**
1	$Pd(PPh_3)_2(PhI)$	3	13
2	$Pd(PPh_3)(PhI)$	2	2
3	$[PdCl(PhI)]^-$	2	1.2
4	$[Pd(OOCH)(PhI)]^-$	2	0.2

(a) Coordination number of the corresponding pre-reactive complex.

The results from the DFT study on the stabilities of palladium(0) triphenyl phosphine complexes do not agree with the earlier interpretations of the experimental observations, where $Pd(PPh_3)_3$ was concluded to be the resting state of palladium(0).[85] Neither do the current results support the hypothesis of the tricoordinate anionic complexes $[Pd(PPh_3)_2X]^-$ as the more stable intermediates.[95, 96a] Instead the dicoordinate analogs $[Pd(PPh_3)X]^-$ were found to be more stable. There are several possible explanations for the disagreement between the experimental and theoretical results. Firstly, the DFT methods cannot describe dispersion forces. However, one could argue that the sum of the dispersion forces are similar for the free ligand in solution as in the complex and therefore do not affect the equilibria much. Secondly, the implicit solvent model is a severe oversimplification of the solvent, even though such models have often been shown to be very successful in describing the condensed phase. Thirdly, the interpretation of the experimental results could be incorrect, despite correctly performed experiments. The cause of the disagreement between experiment and theory is thus currently difficult to state.

As mentioned earlier in this section and in the introduction to this chapter the use of bulky electron rich phosphines e.g. P*t*Bu$_3$ has been found to facilitate coupling of less electrophilic substrates such as aryl chlorides and vinyl tosylates. Due to the large steric bulk of these phosphines they form linear dicoordinate 14-e complexes even in the solid phase. Experimental work by Jutand et al. and Hartwig et al. on oxidative addition of aryl halides to these systems have shown that the reaction most likely goes via a monocoordinate Pd^0L complex. It has frequently been observed that electron deficient aryl chlorides react more readily than the electron rich ones. Since these reactions are highly interesting we decided to investigate in more detail what factors are responsible for the change in reactivity. The modeled system was the full system with the synthetically relevant phosphines P*t*Bu$_3$.

As in the previous study both a neutral and an anionic path was investigated. The starting complex for the neutral path was the dicoordinate $Pd(PtBu_3)_2$. Prereactive complexes and transition states for six aryl chorides with different substituents in para position were modeled. Relative energies of the complexes and transition states are outlined in Table 9. The largest effect of the electron withdrawing groups are in the formation of the prereactive complexes with a difference of 17 kJ/mol between p-OHC-C_6H_4Cl and p-MeO-C_6H_4Cl. In the transition state the difference is down to 10 kJ/mol.

Table 9. Energies of pre-reactive complexes $Pd(ArCl)PtBu_3$ and the subsequent oxidative addition transition states, relative to $Pd(PtBu_3)_2$, in kJ/mol.

p-Cl-Ph-X	**Pre-reactive complexes**	**Transition states**
-CHO	64.9	104.6
-CN	65.7	104.8
-H	75.8	112.5
$-NH_2$	74.2	107.0
-Me	76.8	112.6
-OMe	81.7	114.2

The starting point for the anionic reactions was the chloride complex $[Pd(PtBu_3)Cl]^-$, where prereactive complexes formed from exchange of the phosphine for an aryl chloride were optimized. Energies of the prereactive complexes with the general formula $[Pd(ArCl)Cl]^-$ and the following oxidative addition transition states are outlined in Table 10. A similar but more profound effect of the substitution on the stability of the prereactive complexes as for the neutral analogs is observed for the anionic path. Also here the effect is larger for the prereactive complexes than for the transition states, but there is still a profound influence of the para-substituent on the barrier.

Table 10. Energies of pre-reactive complexes $[Pd(ArCl)Cl]^-$ and the subsequent oxidative addition transition states relative to $[Pd(PtBu_3)Cl]^-$ in $kJmol^{-1}$. In parenthesis are values from single point calculations including diffuse functions on all heavy elements.

p-Cl-Ph-X	**Pre-reactive complexes**	**Transition states**
-CHO	39.6 (35.3)	78.9 (72.3)
-CN	41.0 (37.6)	78.8 (72.8)
-H	58.8 (56.2)	90.7 (84.9)
$-NH_2$	52.9 (52.0)	90.6 (87.2)
-Me	58.9 (57.6)	91.7 (87.6)
-OMe	59.3 (57.6)	92.9 (88.2)

A good correlation between the reaction barriers of the anionic complexes and the Hammett σ^--values indicates that the reaction is related to S_NAr type reactions (Figure 60). Viewing the bond dissociation energies (BDE) of the C-Cl bonds in the aryl chlorides a trend similar trend as the reaction barriers is observed (Figure 61), meaning that electron rich aryl chlorides have higher BDE:s than the electron deficient ones. There are some differences, though. Firstly, the difference in BDE is smaller than the difference in reaction barrier. Secondly, the BDE:s of the C-Cl bonds correlate with the σ^{para} while the reaction barriers correlate with σ^-. Based on these facts we conclude that the main factor for the difference in reactivity is not mainly governed by the C-Cl bond strength, but more the ability of the ability of phenyl ring to accept electrons. This effect is more profound in the prereactive complexes which coordinate via a π-coordination, but the effect remains to some extent in the transition state.

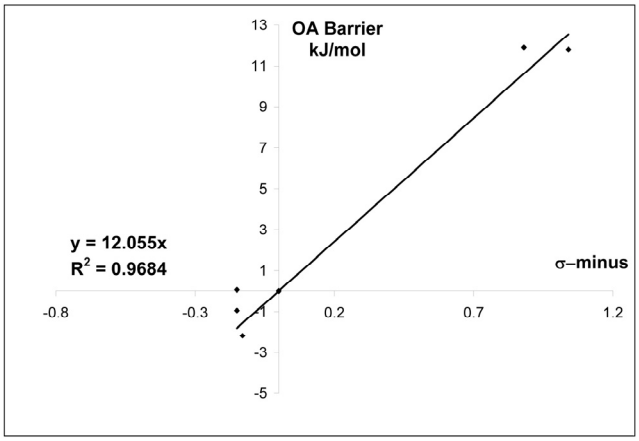

Figure 60. Correlation between σ^- and oxidative addition transition states.

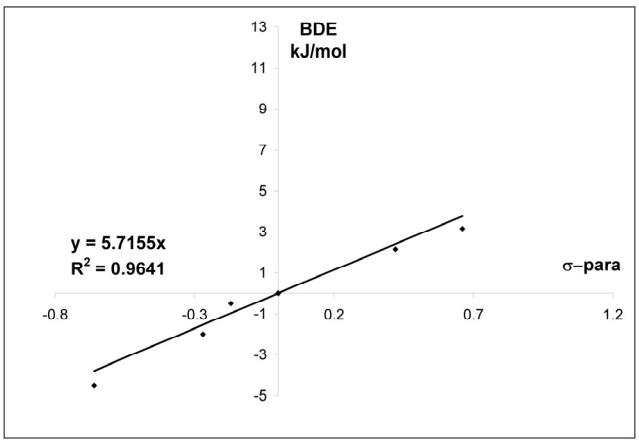

Figure 61. Correlation between σ^{para} and BDE:s of C-Cl bonds in aryl chorides.

Conclusions

Calculations of the stabilities and reactivities of palladium(0) complexes have suggested the dicoordinate complexes to be more stable as well as more reactive than the tricoordinate analogs. While the higher reactivity of the dicoordinate complexes was not unexpected, the higher stability of the dicoordinate compared to the tricoordinate complexes does not agree with the generally accepted picture. More theoretical as well as experimental work is needed to fully understand these reactions. For the systems where bulky ligands are used it is well known that the path for

oxidative addition goes via a dicoordinate complex with palladium coordinating only to one ligand and the reacting aryl halide. These systems were investigated in more detail to get a deeper understanding of the mechanism. It was found that the mechanism is best described as an S_NAr mechanism. The fact that electron poor aryl halides react with higher rates was concluded to be due to their higher ability to accept electrons in the transition state.

Chapter IV

Metal Catalyzed Ligation of Azides and Alkynes

Introduction

Click Chemistry

As organic synthesis has evolved and more advanced methods for constructing molecules have been developed the complexity of drug-targets has increased. Together with a revolutionary development in molecular biology that has given us much deeper understanding of the mechanisms operating in living organisms the expectations for discovery of new drugs have been high. It is therefore with disappointment that researchers and pharmaceutical companies have actually seen the number of new drugs on the market *decreasing*. Convinced that drug discovery suffered from fundamental conceptual issues K. Barry Sharpless and his coworkers Hartmuth Kolb and M.G. Finn presented a new concept. Inspired by Nature and the obscure sci-fi novel "Out of control"[120] Sharpless, Kolb and Finn created "Click Chemistry".[121]

In the ground breaking paper by Sharpless and co-workers from 2001 a detailed background, the criteria for, and a number of examples of click chemistry were presented. Earlier as well as today a substantial part of the work in organic synthesis focused on the construction of carbon-carbon bonds, where one of the most widely applied methods has been the use of aldol addition reactions. This method is Nature's main route for construction of C-C bonds, but for synthetic purposes it suffers from unfavorable thermodynamics.[122] Often the exothermicity of the reaction is <12 kJ/mol and therefore additional driving forces needs to be added to make the reaction efficient. In biological systems only a minor part of the molecules are built up by long chains of C-C bonds. Instead small building blocks are linked together to oligomers, and depending on which building blocks are linked together and in what order, different function is attained. The way the oligomers are linked together is always through carbon-heteroatom bonds. In this way enzymes, proteins, polysaccharides and polynucleic acids are constructed, and thus a large part of the structures and functions of all biological systems is built up by these natural polymers. The concept of click chemistry was built on a similar approach, namely construction of functional structures by combining fragments via C-X bonds, but by using more favored reactions from a synthetic perspective.

The criteria required for a reaction to qualify as a click reaction are:

- It must be modular
- It must be wide in scope
- It must be high yielding
- It should generate only inoffensive byproducts that can be removed by nonchromatographic methods
- It should be stereospecific (if stereoisomeric products are possible).

Characteristics of the processes include:

- Simple reaction conditions – Insensitive to oxygen and water
- Readily available starting materials and reagents
- If purification is needed it has to be done by nonchromatographic methods such as distillation or recrystallization
- The product must be stable under physiological conditions

The points listed here may seem very restrictive at first glance, but the authors argue that the chemical space of molecules with reasonable structures for pharmaceutical purposes is enormous. With about 10^{63} possible structures the efforts to make more and more complex structures makes little sense,[123] and the search should instead be focused on function and in the introduction to the 2001 paper George S. Hammond is cited: "*The most fundamental and lasting objective of synthesis is not production of new compounds but production of properties*".[124] Discovery of new functions could in principle be accomplished by use of only a few highly efficient reactions for connecting small modules into larger structures. A number of reactions which could qualify as click reactions were listed (Figure 62).[125] A common feature of the reactions is that they were all "spring-loaded" with energy, meaning that they all are highly exothermic. The substrates best suited for such highly exothermic reactions were concluded to be unsaturated hydrocarbons - alkenes and alkynes.

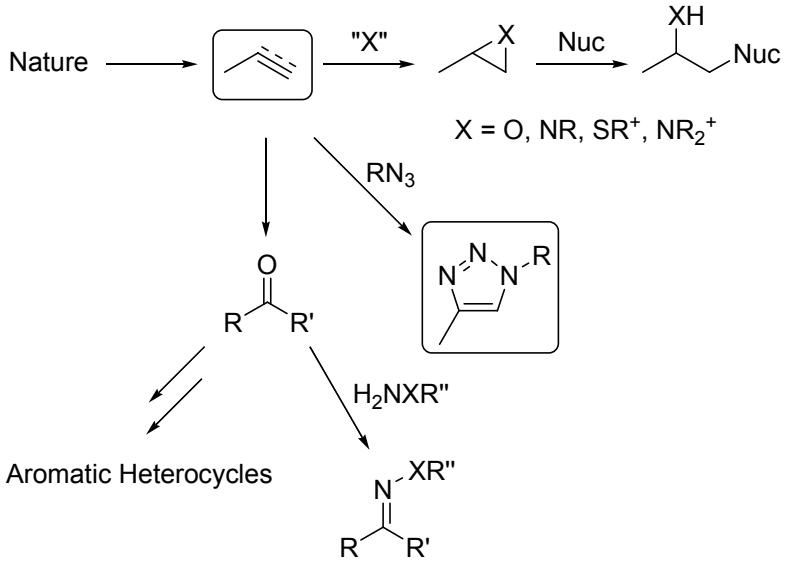

Figure 62. Examples of reactions that could qualify as Click reactions according to Sharpless and co-workers. Huisgen's triazole formation is the most successful so far.

Of the reactions presented in Figure 62 it is the reaction between an alkyne and an azide which has become the central reaction in click chemistry. It was originally discovered by Huisgen already in the 1960's, and is a highly exothermic reaction ~60 kcal/mol.[126] The two reacting groups are orthogonal to most functional groups and react selectively to give the triazole product. The major drawback is that the reaction requires elevated temperatures in order to react with reasonable rates. Furthermore, the two possible regioisomeric products are normally produced in equimolar amounts. The solution to these problems came soon after the click chemistry concept was presented. As with many other highly desired but problematic reactions, the solution involved transition metal catalysis.

Cu-catalyzed Azide Alkyne Cycloadditon – CuAAC

Soon after the first concept article on click chemistry was published one of the most important developments on the reaction between alkynes and azides were discovered in the groups of Meldal[127] and Sharpless[128] independently. It was found that when Huisgen's 1,3-dipolar cycloaddition of azides and terminal alkynes was performed in presence of a copper(I) catalyst, the reactions could be performed at ambient temperature, was completed within hours and selectively yielded the 1,4-triazole with no trace of the 1,5-triazole. A very efficient protocol developed in the Sharpless group is shown in Figure 63.[128] The solvent was a mixture of water and *tert*-butanol and the copper catalyst was added as the copper(II) salt $CuSO_4$ which was reduced *in situ* to copper(I) by ascorbate. A wide variety of substrates were tried and in all cases the yields were excellent and

since the reaction was performed in an aqueous system the non-soluble products could be purified by simple filtration and washing with water.

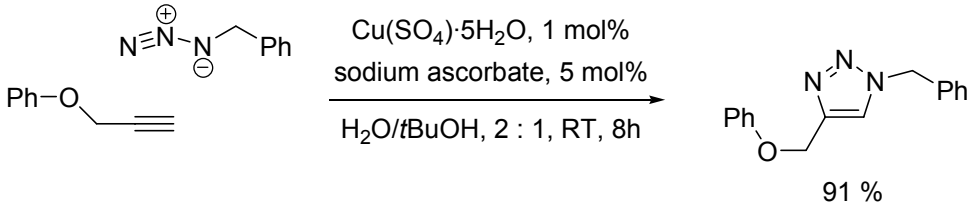

Figure 63. The protocol for CuAAC by Sharpless and co-workers.

With this highly effective reaction in hand, click chemistry could start the rapid development we witness today. Even though the concept was initially presented as an alternative way of finding new pharmaceuticals more efficiently, click chemistry has been applied in a wide range of fields within the chemical sciences. Applications include highly efficient dendrimer synthesis,[129] functionalization of biological macromolecules,[130] construction of polymers,[131] efficient synthesis of rotaxanes,[132] metal ligands,[133] functionalization of surfaces[134] etc. New applications still appear frequently and by looking at the development of the number of citations of the original CuAAC paper it is clear that the field is highly active (Figure 64).[135]

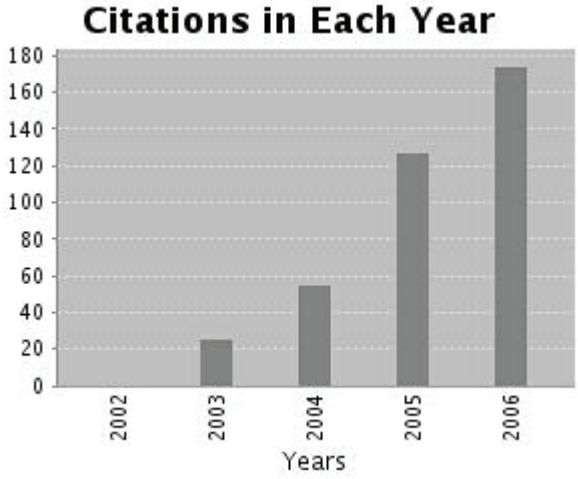

Figure 64. Citations 2002-2006 of the first CuAAC paper by Sharpless et al..

Mechanistic Work[136]

Simultaneously with the experimental findings in the Sharpless group the copper catalyzed reaction was investigated computationally by Fahmi Himo in Louis Noodleman's group in close

collaboration with the Sharpless group. The mechanistic proposal was presented already in the first paper of the CuAAC reaction but it was not until 2005 that the full computational study was published.[137] The starting point for the calculations was a copper(I) complex with an acetylide ligated to copper and the remaining coordination sites occupied by solvent molecules (Figure 65), either water or acetonitrile.[138] The first step was then exchange of one of the solvent ligands for an azide coordinating via the nitrogen bonded to the organic moiety (N^1). A stepwise mechanism for the cycloaddition was then characterized, starting with the formation of a C-N bond between the terminal nitrogen of the azide (N^3) and the second carbon of the acetylide (C^2). The resulting complex of this transformation was a six-membered cupracycle which was described as a copper(III) species. In this copper(III) species the copper was doubly bonded to C^1 of and formed a single bond to N^1. A second transition state was located for the formation of the second C-N bond, which resulted in a triazolyl copper(I) complex. It was concluded that the first step, the formation of the cupracylic intermediate was the rate determining step. Compared to the uncatalyzed reaction the barrier was lowered significantly from 26.0 to 18.7 kcal/mol (109 to 78 kJ/mol) in water and from 25.7 to 14.9 in acetonitrile (107 to 62 kJ/mol). The computational study clearly illustrated how a copper(I) can enhance reaction rates by forming copper(I) aceylides which react more readily with organic azides. Furthermore the mechanism correlated very well with the observed selectivity for formation of the 1,4-triazole.

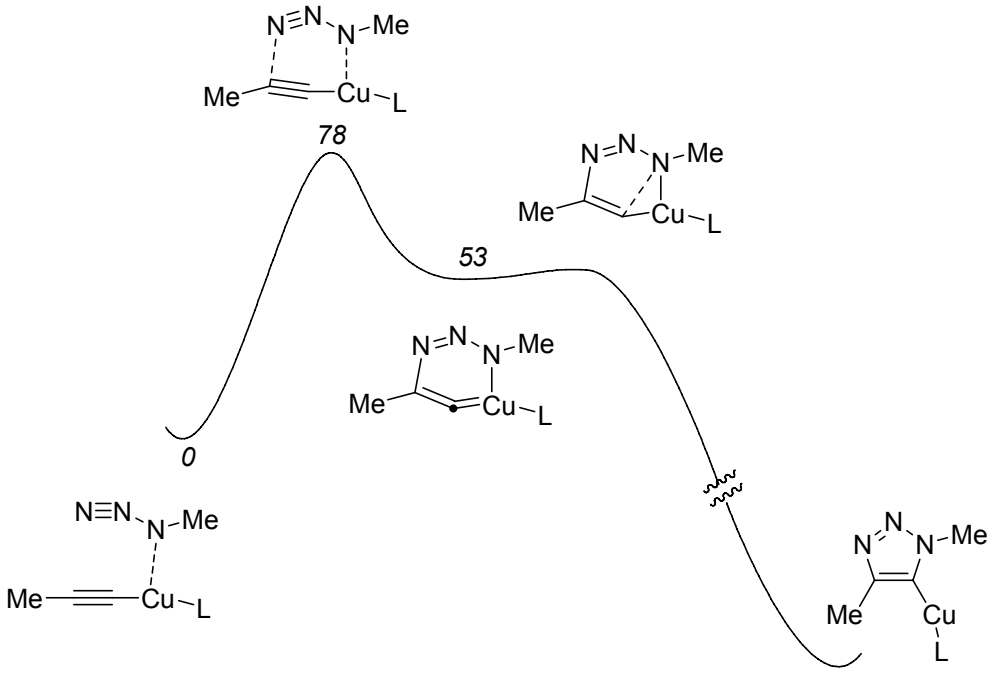

Figure 65. Reaction coordinate proposed by Himo et al..

Not long after the computational study Rodionov et al. published an investigation of the kinetics of the reaction.[139] One of the most striking findings in that report was that a second order rate dependence on the concentration of copper was found, thus suggesting that two copper atoms were in some way involved in the catalytic cycle. One suggestion of the role of the second copper was that the acetylide was coordinated to the first copper and that the second copper could assist in binding of the azide (Figure 66).

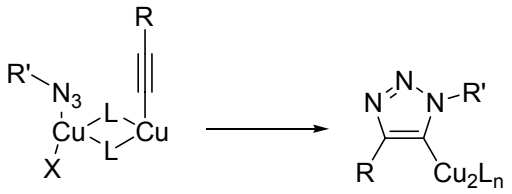

Figure 66. Possible assistance from a second copper suggested by Rodionov et al..

Dinuclear Copper Acetylides

It is well known that copper tends to form oligomeric structures in solution and also in the solid phase.[140, 141] Often the separation between the copper centers is relatively short and it has been suggested that there is a stabilizing interaction between the copper atoms.[142]

The original mechanism by Himo et al. suggested the formation of a cupracyclic intermediate to be the rate limiting step in the mechanism. This intermediate could in principle also be drawn as the charge separated resonance form, with a formal negative charge on C^1 (Figure 67). One could then envision a stabilizing effect from an introduction of a second copper atom in close proximity to C^1. Despite the fact that the copper centers are of the same charge, it seems likely that a second copper could be placed in proximity of the first one without unfavorable repulsion.

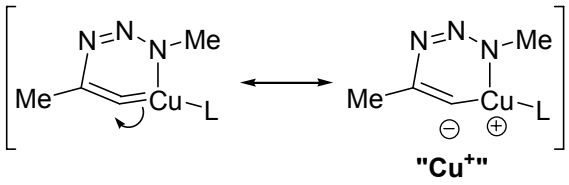

Figure 67. The cupracyclic intermediate could be more favored by a second copper center in proximity.

Visualization of the orbitals of a cupric(III)cyclic complex shows that a high-lying orbital (HOMO-1) is concentrated on the C^1 and to some extent on the copper center (Figure 68). Interaction with and a second copper center is thus likely to be stabilizing by an orbital interaction as well as by the electrostatic interaction described in Figure 67.

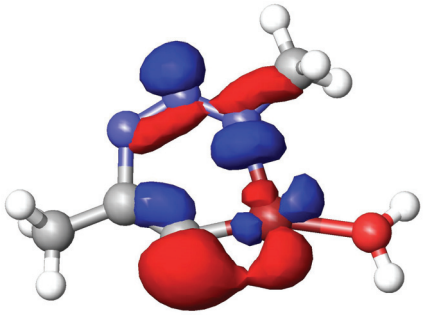

Figure 68. HOMO-1 of a cupra(III)cylic intermediate.

To probe the hypothesis of the stabilizing effect of the second copper, transition states with a second copper center were modeled. Two different systems were investigated, one where the second copper was bonded to an acetylide, and another where it was bonded to a chloride. In both systems the second copper center was found to be tightly bonded to C^1 with a bond length of 1.93 Å and 1.90 Å for **70ts** and **71ts** respectively. The distance between the copper center bonded to the azide (Cu^A) and the second copper center (Cu^B) was calculated to 2.64 Å and 2.54 Å in **70ts** and **71ts** respectively. The calculated geometries are shown in Figure 69.

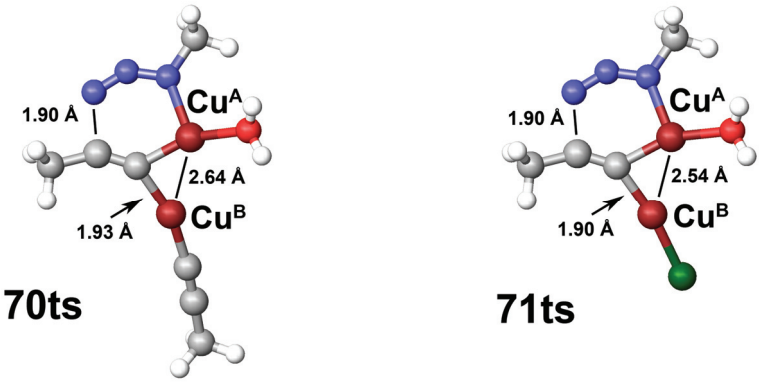

Figure 69.

The interaction in the transition state indicates that Cu^B could have a favorable impact on the reaction but for the reaction to be accelerated the barrier of the reactions of the dinuclear copper acetylides with the organic azide needs to be compared to the analogous reaction of the mononuclear copper acetylide. To get an estimate of the effect the overall barriers from the separated copper acetylide complexes and methyl azide were calculated. The geometries of the

dinuclear copper acetylides are shown in Figure 70. They appear to adopt a structure where the acetylides form a σ-bond to the more electropositive copper center (Cu^A) and the second copper is coordinating on the side of the acetylide. Cu^B seems to mainly interact with C^1, with possible stabilization also from the interaction with C^2 and the copper center. Cycloadditions of methyl azide to the dinuclear copper acetylides were calculated to have barriers of 54 and 44 kJ/mol for **72** and **73** respectively. A barrier of 71 kJ/mol was calculated for cycloaddition at the mono-nuclear acetylide **74** which clearly illustrates that the introduction of a second copper has a very favorable effect on the reactivity. The greatest enhancement is observed when Cu^B is bonded to a chloride, likely due to the much lower *trans* influence of chloride compared to acetylide.

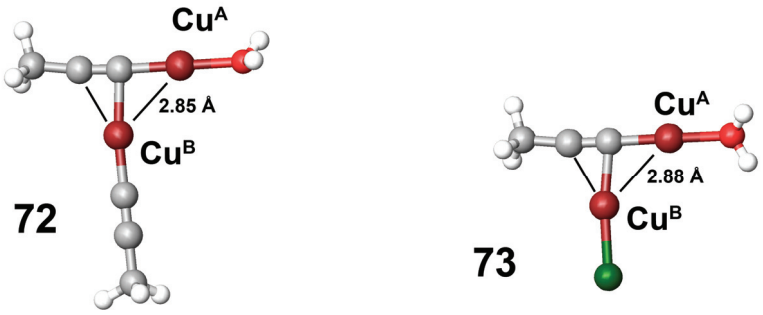

Figure 70.

To get an estimate of the stability of the dinuclear copper complexes relative to the mononuclear complexes, calculations on the free energy of the formation of **72** from **74** were performed. It was found that the equilibrium outlined in Figure 71 was strongly in favor of the dinuclear species by 32 kJ/mol. Hence, the dinuclear complexes are both more reactive *AND* more stable than the mononuclear analogs.

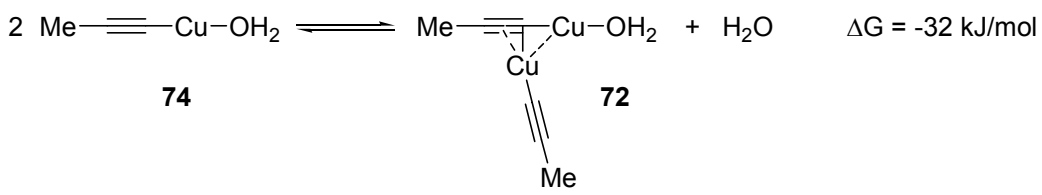

Figure 71. Equilibrium between the mono and dinuclear copper acetylide was calculated to be in favor of the dinuclear complex (right).

Resulting from the transformation is a cyclic intermediate similar to the cupra(III)cycle described before, just with an additional copper to stabilize the electron density on C^1. An endothermicity of 47 kJ/mol was calculated in the mono-copper case, while in the cases of the dinuclear complexes the endothermicities were as low as 25 and 15 for **75** and **76** respectively. This further illustrates the favorable impact of the second copper in close proximity of C^1 in this transformation. Structures are shown in Figure 72.

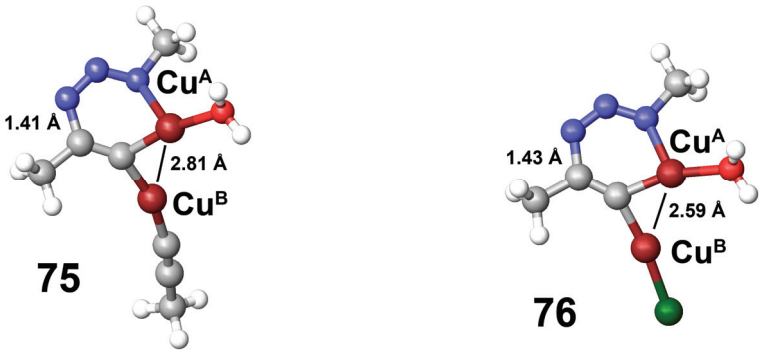

Figure 72

For modeling of the entire reaction a slightly different system was chosen. The dinuclear copper acetylide was the simple $MeCC(CuCl)_2^-$ (**77**) to facilitate the modeling without losing information. Geometrically this copper acetylide differs slightly from the dinuclear copper acetylides described earlier **72** and **73**. Since the copper centers are equivalent the acetylide prefers a μ^2-bridging structure (Figure 73).

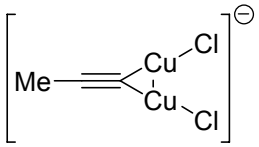

77

Figure 73.

Prior to the formation of the first C-N bond a prereactive complex **78** is formed where the azide is coordinating one of the copper centers (Cu^A) via the internal nitrogen N^1. The coordination of methyl azide was calculated to be exothermic by 9 kJ/mol (still most likely endergonic due to unfavorable entropic contributions in an associative process).[119] The distribution of the frontier

orbitals of the prereactive complex **78** clearly indicates that interaction between the HOMO and the LUMO will result in formation of the first C-N bond (Figure 74).

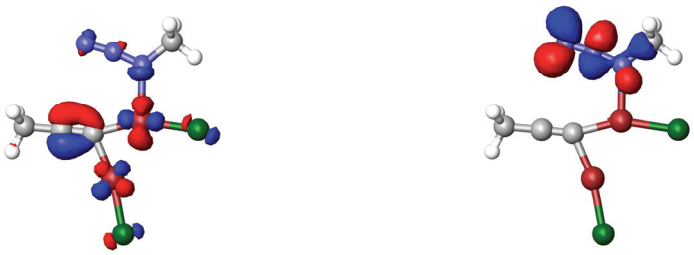

Figure 74. Left: HOMO of **78**. Right. LUMO of **78**.

Just as for the dinuclear complexes described above the cycloaddition at **78** proceeds with a low barrier of 48 kJ/mol (39 kJ/mol overall barrier from the separated reactants **77** and **79**). The cupracyclic intermediate formed **81** was calculated to be 12 kJ/mol higher in energy than **78** and endothermic by merely 3 kJ/mol relative to the separated reactants. For the reaction to be complete the second C-N bond must form. This step was found to be very facile for mono-nuclear copper complexes, and proceeded with virtually no barrier. A transition state (**82ts**) was localized for the formation of the second C-N bond. The barrier was calculated to 21 kJ/mol which is higher than the corresponding reaction at the mono-nuclear copper complexes, but still a low enough barrier so that the reaction step should not have any impact on the rate, since the potential energy of **82ts** is substantially below that of **80ts**. The transformation results in a triazolyl intermediate **83** (Figure 75) where the triazolyl moiety coordinates to the two copper chloride moieties in a μ^2-bridging structure, similar to the acetylide complex **77**. Overall the reaction was calculated to be highly exothermic, 235 kJ/mol. A profile of the reaction is outlined in Figure 76.

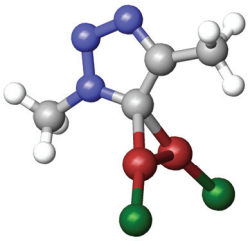

Figure 75. Dinuclear triazolyl complex **83.**

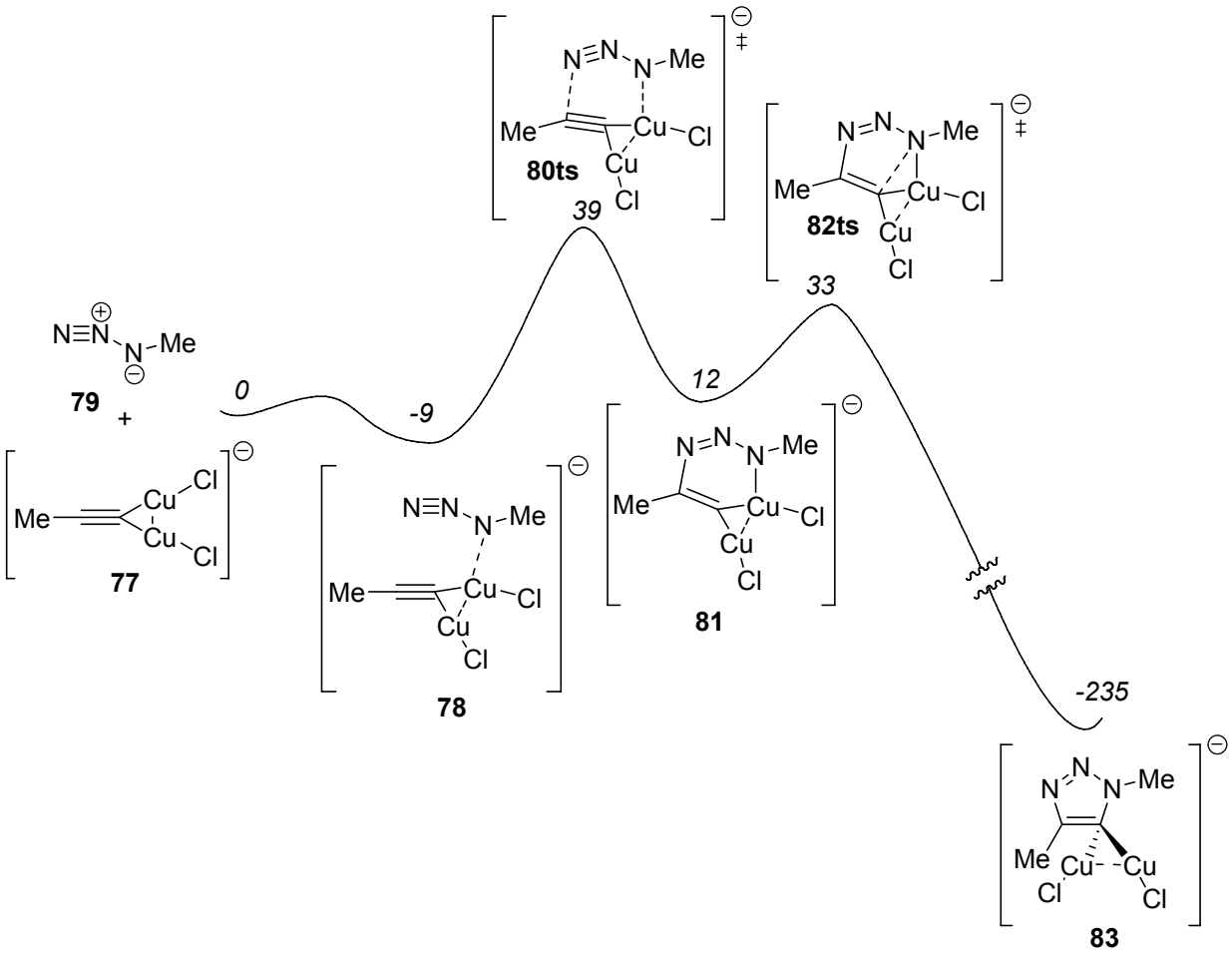

Figure 76. Reaction coordinate of the cycloaddition of MeN_3 and the dinuclear copper complex **77**.

Copper Catalyzed Reaction of N-Sulfonyl Azides and Alkynes.

The copper(I) catalyzed azide and alkyne coupling is known to be tolerant of most functional groups, and a wide variety of alkynes and azides have been applied. An interesting finding by Chang and co-workers was that when sulfonyl azides were used in the reaction the isolated product was *not* the expected sulfonyl triazoles.[143] Instead they isolated *N*-sulfonylamidines as the major products in excellent yields (Figure 77). It was suggested that the sulfonyl azide and the alkyne reacted to give a keteneimine intermediate in a process involving N_2-loss. The amino group in the product originated from an amine base, a common additive in the CuAAC. The same methodology was later applied to the formation of *N*-sulfonyl-amides, in a protocol where the amine base was simply exchanged for water. Whiting and Fokin later used the methodology of sulfonyl azides to form tetracycles,[144] which was accomplished by either dimerization of the keteneimine or by trapping the keteneimine intermediate with an imine to give *N*-sulfonyl azetidinimine (Figure 78).

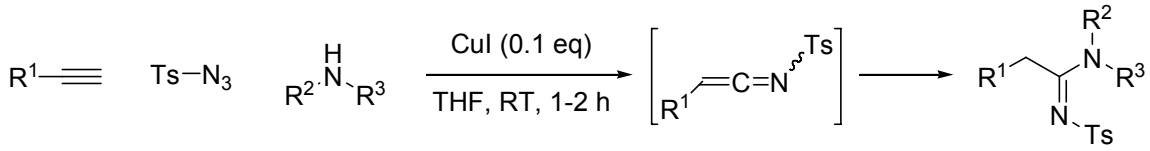

Figure 77

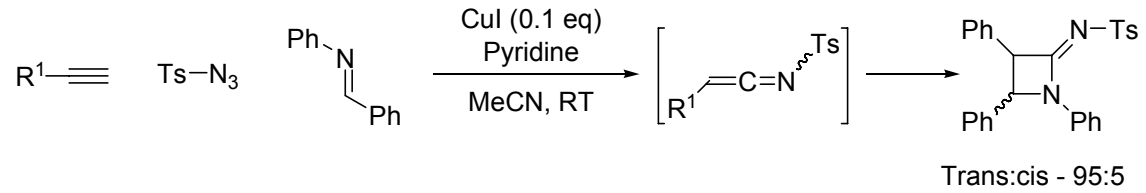

Figure 78

Fokin and co-workers have suggested a path in which an *N*-sulfonyl triazolyl intermediate was initially formed.[144, 145] Two possible paths for the breakdown were then suggested, either via concerted loss of N_2 or sequential breaking of the N^1-N^2 and C^4-N^3 bonds (Scheme 5). Both paths would lead to the formation of a keteneimine intermediate. The mechanism via the triazolyl intermediate was supported by a trapping experiment, in which the addition of allyl iodide that lead to formation of the allyl substituted *N*-sulfonyl triazole in good yield. The *N*-Sulfonyl triazole was also often observed as a byproduct in most of the reactions described above.

• Scheme 5. Proposed mechanism for the formation of the *N*-sulfonyl keteneimine.

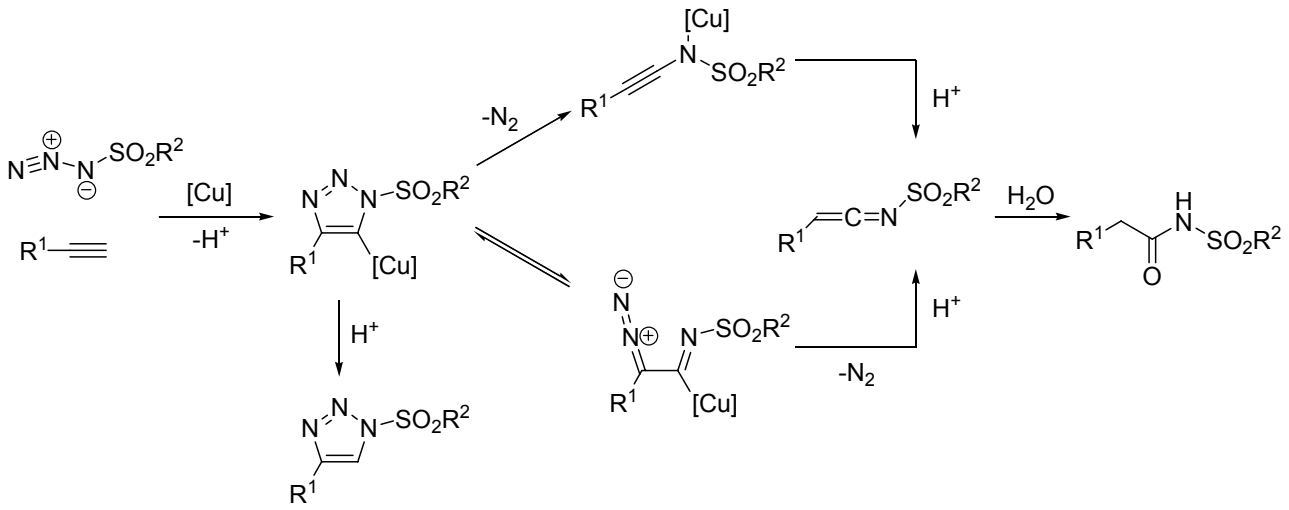

To get a deeper understanding and to possibly being able to direct the reaction of sulfonyl azides and alkynes to the desired product, a computational study of the reaction was initiated. The initial step, the formation of a cupracyclic intermediate from a copper acetylide and a sulfonyl azide was modeled both with dinuclear as well as mononuclear copper acetylides. The sulfonyl azide was chosen as a mesyl azide. Starting with the mono-nuclear copper acetylide MeC≡CCu(OH_2) the overall barrier for the cycloaddition was calculated to be 42 kJ/mol, which is substantially lower than for the addition of methyl azide (71 kJ/mol). A cupracyclic intermediate **86** is formed in the reaction step and the endothermicity was calculated to 11 kJ/mol. Addition to the dinuclear complex **73** was calculated to even more facile, and the barrier for the formation of the cupracylic intermediate was calculated to 27 kJ/mol. Formation of the dinuclear cupracyclic intermediate was found to be *exothermic* by 10 kJ/mol, in contrast to the other cupracycle formations described in this chapter which are all endothermic. The following step, the formation of the second C-N bond, has only been modeled for the mononuclear case where it proceeds with a barrier of merely 2 kJ/mol to give the triazolyl intermediate in a highly exothermic step. Overall the reaction from the separated reactants was calculated to be exothermic by 206 kJ/mol. A reaction profile of the cycloaddition of mesyl azide to copper acetylides is shown in Figure 79.

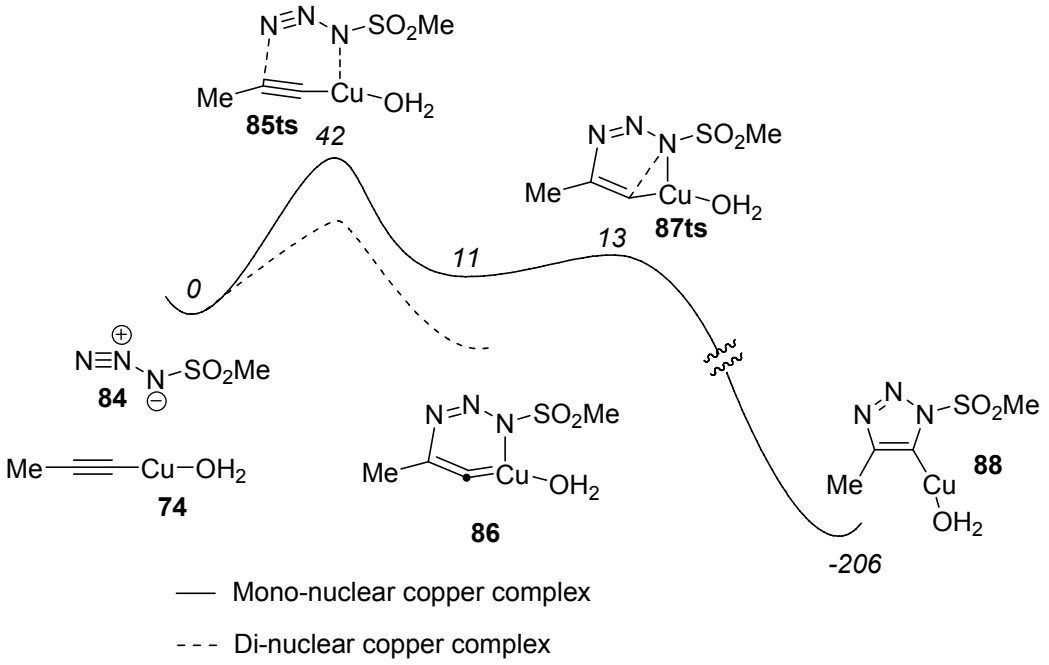

Figure 79. Reaction coordinate for the formation of the *N*-sulfinyl triazolyl intermediate X.

The formation of the *N*-sulfonyl triazolyl intermediate shows that it is not only possible, but also appears to be even more facile than the highly effective coupling of alkyl azides. The next task was then to study the breakdown of the triazolyl intermediate. Fokin has suggested two different paths for the loss of N_2, one concerted and another stepwise process. The stepwise mechanism was characterized and will be described in more detail below, while the concerted mechanism could not be localized though several attempts were made.

Triazoles containing electron withdrawing groups on the nitrogen are known to ring open easily. When the triazoles are substituted on the 5-position with an amine the ring opening can be followed by rearrangement and ring-closing to the other amine nitrogen in a process known as the Dimroth rearrangement (Figure 80).[146]

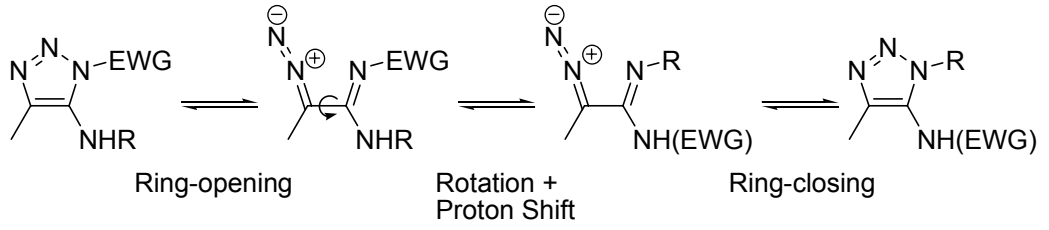

Figure 80. Dimroth rearrangement.

Ring opening of the triazolyl intermediate **88** takes place via a transition state **89ts** with a calculated barrier of 64 kJ/mol (Figure 81). The intermediate formed in this process is a diazoimine type intermediate and the process is endothermic by 27 kJ/mol. Since alkyl and aryl triazoles have not been observed to lose N_2 the corresponding reaction at the methyl triazolyl intermediate **91** was characterized. The ring opening is highly disfavored at **91** compared to the electron poor **88**, and activation energy required for this transformation was calculated to 148 kJ/mol. It is thus clear that the ring opening is strongly accelerated by the sulfonyl group.

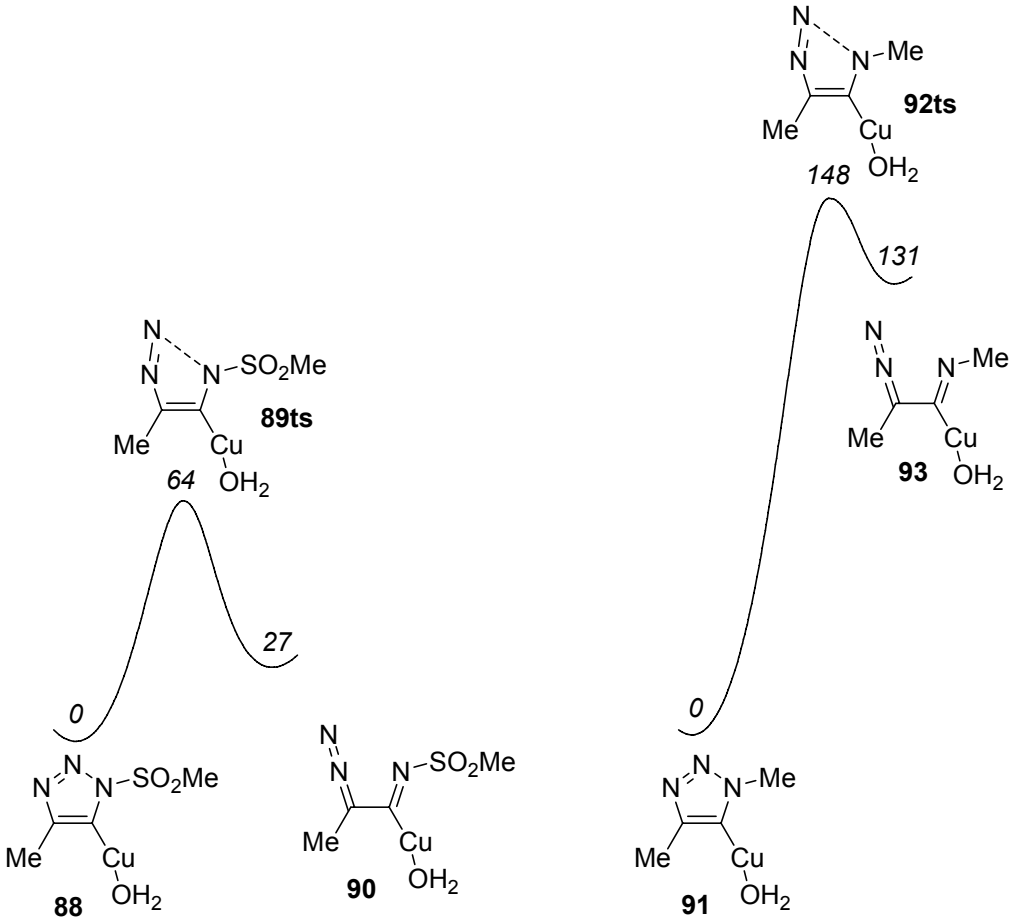

Figure 81. Ring-opening of triazolyl intermediates

The ring-opening is followed by dissociation of N_2 in the stepwise mechanism. A transition state with a 51 kJ/mol higher energy than **90** was localized **94ts**, which means an overall barrier of 78 kJ/mol relative to the triazolyl intermediate **88** (Figure 82). The influence of another copper center in proximity of the carbon atom bonded to N_2, was modeled by using the protonated analog. The corresponding reaction at was found to have a substantially higher barrier of 107 kJ/mol relative to the diazoimine intermediate **96**. Thus it seems as if the copper moiety can have an accelerating effect on the rate of N_2 dissociation.

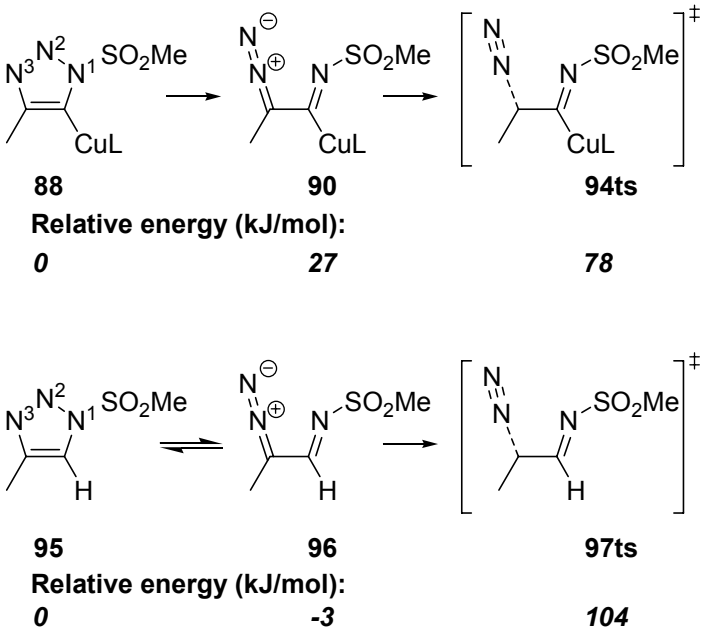

Figure 82. N_2-dissociation from diazoimine intermediates.

Ruthenium Catalyzed Formation of 1,5-triazoles.

In the field of transition metal catalyzed organic transformations there are a few metals which are the real "working horses". Without a doubt ruthenium is one of these,[147] with applications in hydrogenations,[148] oxidations,[149] metathesis,[150] allylations[151] etc. In this section will be described another success of ruthenium, the selective formation of 1,5-triazoles.

With the CuAAC reaction one of the most efficient synthetic transformations were available. One of the strengths with the reaction was the high selectivity towards formation of 1,4-triazoles. Still, however good the CuAAC reaction was, a reaction for the formation of 1,5-triazoles was lacking. Then in a collaboration between the Jia and the Sharpless/Fokin groups one of the landmark findings in 1,3-dipolar cycloadditions of alkynes and azides was made.[152] They showed that in presence of a ruthenium(II) catalyst ligated to cyclopentadienyl group (CP), the 1,5-triazole was formed to some extent, even though the 1,4-triazole was still produced to a significant extent. Exchanging the CP ligand for the pentamethyl-cyclopentadienyl ligand (CP*), made the reaction completely selective and the isolated product was pure 1,5-triazole. The CP*-ruthenium catalyst was not only observed to be more selective, but also more reactive. The product distribution of the reaction is outlined in Figure 83.

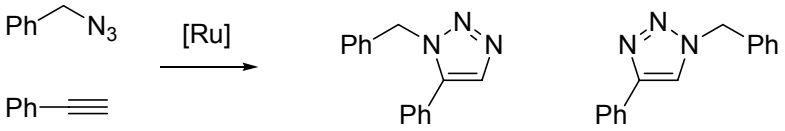

$CpRuCl(PPh_3)_2$	85%	15%
$Cp^*RuCl(PPh_3)_2$	100%	-

Figure 83. Ruthenium catalyzed formation of 1,5-triazoles.

A DFT study of the reaction was initiated to understand the reaction mechanism, especially the influence of the CP* ligand, which seemed to be crucial for the reaction to run efficiently and selectively. The starting complex was one where the azide and the alkyne are ligated to the ruthenium center. The remaining coordination sites were occupied by the CP or CP* ligand and a chloride. Transition states for the formation of the first C-N bond were localized for the formation of both regioisomers, for complexes with both the CP and CP* ligand. In the CP complex the

barriers was calculated to 22 kJ/mol and 28 kJ/mol for the formation towards the 1,5- and 1,4-triazole, respectively. This energy difference corresponds to an 86 : 14 distribution at 333 K, which corresponds very well to the experimentally observed 85 : 15 ratio. At the CP* complex the formation of the intermediate towards the 1,5-triazole was calculated to proceed with a barrier of 16 kJ/mol. The slightly lower barrier compared to the CP complex is likely due to the higher electron density of the CP* which favors the oxidative process (ruthenium(II) to ruthenium(IV)). The regioisomeric transition state was on the other hand found to have a higher reaction barrier of 32 kJ/mol. Here the explanation lies in the steric properties (Figure 85). The substituent of the alkyne is in this transition state positioned so that it comes in close contact with the methyl groups of the CP*. Such an unfavorable interaction is not present to the same extent in the CP catalyst. The energy difference of 16 kJ/mol corresponds to a ratio of 99.6 : 0.4 in agreement with the experiments. A reaction profile is outlined in Figure 84.

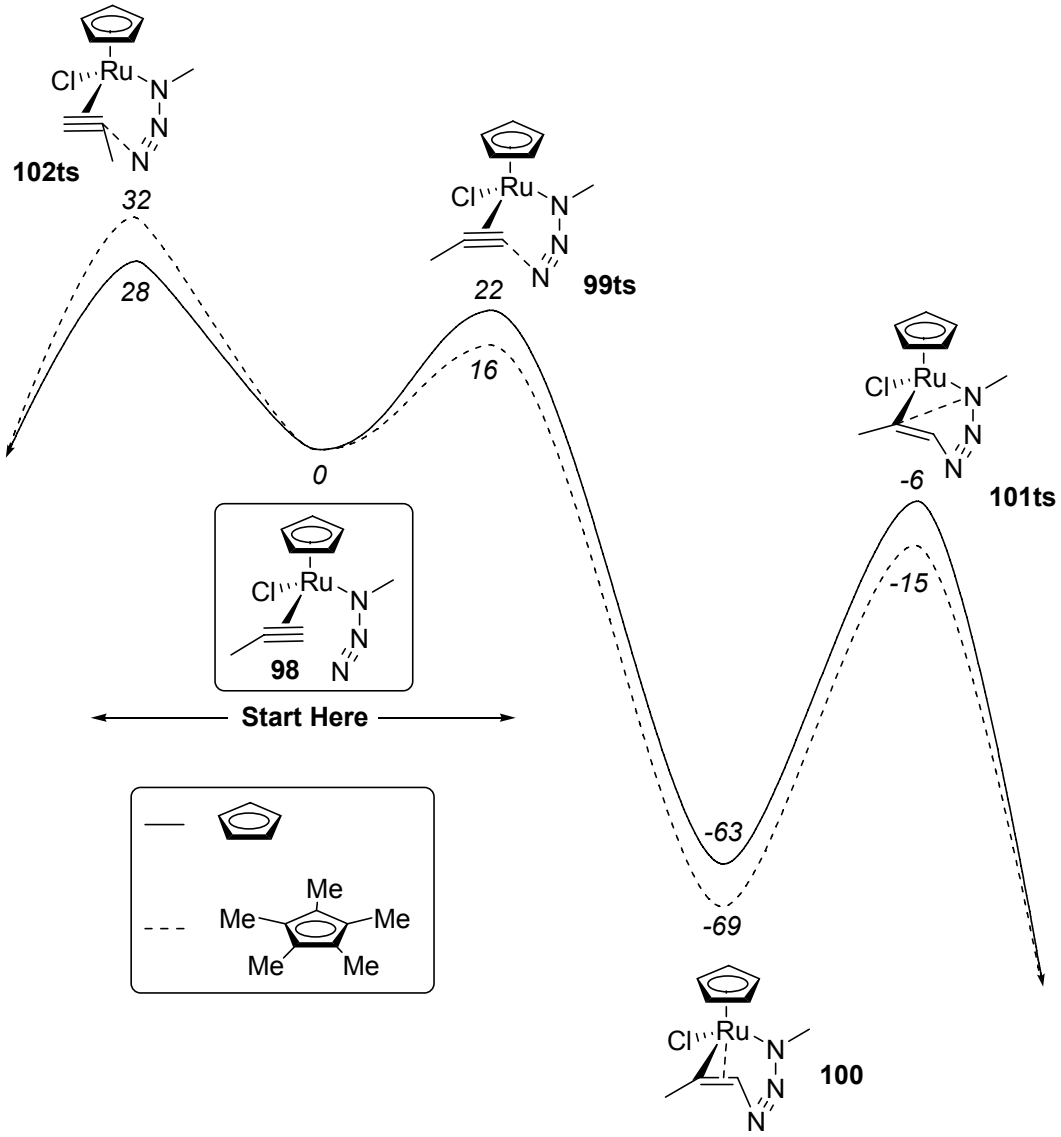

Figure 84. Reaction coordinate for the ruthenium catalyzed formaition of triazoles.

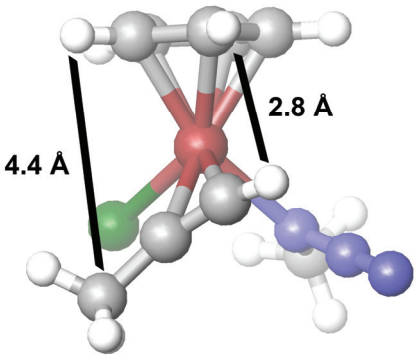

Figure 85. The geometry of **98** shows the different influence of steric bulk from the CP ligand on the two positions of the alkyne.

As shown in Figure 84 the formation of the second C-N bond seems to be the rate limiting step, while the formation of the first C-N bond is the selectivity determining step. There is a slight difference between the CP and the CP* catalyst in the barrier, still only a minor difference that is

unlikely to account for the much more efficient catalysis of the CP*-catalyst. Another crucial step in the reaction is the dissociation of the phosphine ligands from the added pre-catalyst. The phosphine ligands are there to stabilize the catalyst in solution and to keep it from precipitating. However, too much of the phosphine will hinder the reaction and thus poison the catalyst. Another possible explanation for the difference in reactivity of the CP and CP* catalysts could perhaps be the ease of dissociation of phosphine. In Figure 86 are shown the equilibria for dissociation of one phosphine from the bisphosphine complex. It is clear that the steric bulk of the CP* ligand favor the dissociation, thus it is likely to increase the amounts of active species of the catalyst in solution.

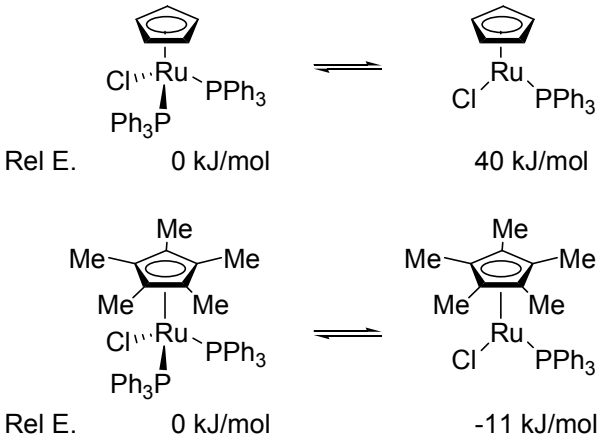

Figure 86. Ligand dissociation equilibria shows the favorable impact of the CP* ligand.

Conclusions

Using computational methods a plausible model for the role of dinuclear copper acetylides in the copper(I) catalyzed azide alkyne coupling reaction was found. It was shown that stabilization by a second copper atom of the electron density which is build up on C^1 of the earlier suggested cupracyclic intermediate, resulted in enhanced reactivity. The second copper center was found to be more efficient in stabilizing the cupracyclic intermediate when having spectator ligands with low *trans* influence, e.g. chloride.

Sulfonyl azides were found to react even more efficiently with copper acetylides than the alkyl azides. Once the *N*-sulfonyl triazolyl intermediate is formed it can break down via a stepwise mechanism with relatively low activation energy. The mechanism was shown to be accelerated by the presence of the sulfonyl group as well as by the copper center in proximity of the carbon from which N_2 dissociates.

A theoretical study on the ruthenium catalyzed formation of 1,5-triazoles was made to understand the impact of the CP* ligand. It was found that the CP* ligand induces higher regioselectivity than the CP-ligand, both by lowering the barrier of the desired path as well as increasing the barrier of the undesired one. The steric bulk of the CP* ligand also facilitates the dissociation of triphenyl phosphine from the catalyst, hence increases the amount of active catalyst in reaction mixture.

References

[1] Tansjö, L. In *Nationalencyklopedin,* Vol. 2, Bra Böcker, Höganäs, **1990**, p. 483. (The Swedish National Encyklopedia; in Swedish).

[2] Zeise, W. C. *Annalen der Physik und Chemie* **1831**, *21*. 497.

[3] Wöhler, F. *Ann. Phys. Chem.* **1828**, *88*, 253.

[4] For more information on the Nobel Prizes in chemistry see http://www.nobelprize.org

[5] Love, R. A.; Koetzle, T. F.; Williams, G. J. B.; Andrews, L. C.; Bau, R. *Inorg. Chem.* **1975**, *14*, 2653.

[6] Mond, L.; Langer, C.; Quincke, F. *J. Chem. Soc.* **1890**, *57*, 749.

[7] Kealy, T. J.; Pauson, P. L. *Nature* **1951**, *168*, 1039

[8] (a) Nobel lecture with an historical background by Karl Ziegler available online at http://www.nobelprize.org (b) Ziegler, K.; Holzkamp, E.; Breil, H.; Martin, H. *Angew. Chem. Int. Ed.* **1955**, *67*, 541.

[9] (a) Nobel lecture with an historical background by Giulio Natta available online at http://www.nobelprize.org (b) Natta, G.; Pino, P.; Corradini, P.; Danusso, F.; Mantica, E.; Mazzanti, G.; Moraglio, G. *J. Am. Chem. Soc.* **1955**, *77*, 1708. (c) Natta, G. *Angew. Chem. Int. Ed.* **1956**, *68*, 393.

[10] Smidt, J.; Hafner, W.; Jira, R.; Sedlmeier, J.; Sieber, R.; Ruttinger, R.; Kojer, J. *Angew. Chem. Int. Ed.* **1959**, *71*, 176.

[11] (a) Hammer, B.; Nørskov, J. K.; *Nature* **1995**, *376*, 238 b) Hashmi, A. S. K.; Hutchings, G. J. *Angew. Chem. Int. Ed.* **2006**, *45*, 7896.

[12] For more general descriptions of mechanisms in organometallic chemistry I recommend: Organometallic Chemistry Spessard, G. O.; Miessler, G. L. 1997 Prentice-Hall, Upper Saddle River, New Jersey 07458

[13] Appleton, T. G.; Bennett, M. A. *Inorg. Chem.* **1978**, *17*, 738.

[14] (a) Tobe, M. L., Treadgold, A. T., Cattalini, L. *J. Chem. Soc., Dalton. Trans.* **1988**, 2349. (b) Gosling, R.; Tobe, M. L. *Inorg. Chem.* **1983**, *22*, 1235.

[15] (a) Nobel lectures with historical backgrounds by the laureates available online at http://www.nobelprize.org (b) Grubbs, R. H.; Chang, S. *Tetrahedron* **1998**, *54*, 4413. (c) Schrock, R. R. *Acc. Chem. Res.* **1990**, *23*, 158.

[16] (a) Landis, C. R.; Halpern, J. *J. Am. Chem. Soc.* **1987**, *109*, 1746. (b) Feldgus, S.; Landis, C. R. *J. Am. Chem. Soc.* **2000**, *122*, 12714.

[17] Nobel lectures with historical backgrounds by the laureates available online at http://www.nobelprize.org (b) Noyori, R.; Takaya, H. *Acc. Chem. Res.* **1990**, *23*, 345. (c) Knowles, W. S. *Acc. Chem. Res.* **1983**, *16*, 106.

[18] Nobel lecture with an historical background by K. Barry Sharpless available online at http://www.nobelprize.org (b) Katsuki, T.; Sharpless, K. B. *J. Am. Chem. Soc.* **1980**, 102, 5974.

[19] Rostovtsev, V. V.; Green, L. G.; Fokin, V. V.; Sharpless, K. B. *Angew. Chem. Int. Ed.* **2002**, *41*, 2596.

[20] For a more detailed description on quantum chemistry see: Cramer, C. J. *Essentials of computational chemistry: theories and models, 2nd Edition*, Wiley, New York, **2004**.

[21] (a) Schrödinger, E. *Ann. Physik* **1926**, *79*, 361. (b) Schrödinger, E. *Ann. Physik* **1926**, *79*, 489. (c) Schrödinger, E. *Ann. Physik* **1926**, *80*, 437. (d) Schrödinger, E. *Ann. Physik* **1926**, *81*, 109.

[22] The matrix mechanics theory was published by Heisenberg in 1925, is another equally good way of describing quantum mechanical phenomena as the Schrödinger equation: Heisenberg, W. *Z. Phys.* **1925**, *33*, 879.

[23] Born, M.; Oppenhiemer, R. *Ann. Physik* **1927**, *84*, 457.

[24] (a) Hartree, D. R. *Proc. Cambridge Phil. Soc.* **1927**, *24*, 89. (b) Fock, V. *Z. Phys.* **1930**, *61*, 126.

[25] MP2 is an abbreviation for Möller-Plesset second order perturbation theory. Møller, C.; Plesset, M. S. *Phys. Rev.* **1934**, *46*, 618.

[26] (a) Coester, F.; Kümmel, H. *Nuc. Phys.* **1958**, *9*, 225. (b) Čižek, J. *J. Chem. Phys.* **1966**, *45*, 4256.

[27] Hohenberg, P.; Kohn, W. *Phys. Rev.* **1964**, *136*, B864 (b) Kohn, W.; Sham, L. J. *Phys. Rev.* **1965**, *140*, A1133

[28] (a) Becke**,** A. D. *J. Chem. Phys.* **1993**, *98***,** 5648 (b) Lee, C.; Yang, W.; Parr, R. G. *Phys. Rev.* **1988**, *B37*, 5648.

[29] (a) Zhao, Y.; Schultz, N. E.; Truhlar, D. G. *J. Chem. Theory Comput.* **2006**, *2*, 364. (b) Zhao, Y.; Truhlar, D. G. *J. Chem. Phys.* **2006**, *125*, 194101.

[30] Stratmann, R. E.; Scuseria, G. E. Frisch, M. J. *J. Chem. Phys.* **1998**, *109*, 8218.

[31] Ziegler, T.; Autschbach, J. *Chem. Rev.* **2005**, *105*, 2695

[32] Reich, R.; Hebd, C. R. *Seances Acad. Sci.* **1923**, *177*, 322.

[33] Kharasch, M. S.; Tawney, P. O. *J. Am. Chem. Soc.* **1941**, *63*, 2308.

[34] Gilman, H.; Jones, R. G.; Woods, L. A. *J. Org. Chem.* **1952**, *17*, 1630.

[35] House, H. O.; Respess, W. L.; Whitesides, G. M. *J. Org. Chem.* **1966**, *31*, 3128.

[36] Corey, E. J.; Posner, G. H. *J. Am. Chem: Soc.* **1967**, *89*, 3911.

[37] Whitesides, G. M.; Fischer, W. F., Jr.; Filippo, J. S., Jr.; Bashe, R. W.; House, H. O. *J. Am. Chem. Soc.* **1969**, *91*, 4871.

[38] Corey, E. J.;Beames, D. J. *J. Am. Chem: Soc.* **1972**, *94*, 7210.

[39] Corey, E. J.;Naef, R.; Hannon, F. J. *J. Am. Chem: Soc.* **1986**, *108*, 7114.

[40] (a) Lipshutz, B. H.; Wilhelm, R. S. *J. Am. Chem. Soc.* **1981**, *103*, 7672. (b) Lipshutz, B. H.; Kozlowski, J.; Wilhelm, R. S. *J. Am. Chem. Soc.* **1982**, *104*, 2305.

[41] Lipshutz, B. H.; Sharma, S.; Ellsworth, E. L. *J. Am. Chem. Soc.* **1990**, *112*, 4032.

[42] Bertz, S. H. *J. Am. Chem. Soc.* **1990**, *112*, 4031.

[43] (a) Stemmler, T. L.; Barnhart, T. M.; Penner-Hahn, J. E.; Tucker, C. E.; Knochel, P.; Böhme, M.; Frenking, G. *J. Am. Chem. Soc.* **1995**, *117*, 12489 (b) Boche, G.; Bosold, F.; Marsch, M.; Harms, K. *Angew. Chem. Int. Ed.* **1998**, *37*, 1684. (c) Krause, N. *Angew. Chem. Int. Ed.* **1999**, *38*, 79. (d) John, M.; Auel, C.; Behrens, C.; Marsch, M.; Harms, K.; Bosold, F.; Gschwind, R. M.; Rajamohanan, P. R.; Boche, G. *Chem. Eur. J.* **2000**, *6*, 3060.

[44] (a) Gschwind, R. M.; Rajamohanan, P. R.; John, M.; Boche, G. *Organometallics* **2000**, *19*, 2868. (b) Xie, X.; Auel, C.; Henze, W.; Gschwind, R. M. *J. Am. Chem. Soc.* **2003**, *125*, 1595. (c) Gschwind, R. M.; Xie, X.; Rajamohanan, P. R.; Auel, C.; Boche, G. *J. Am. Chem. Soc.* **2001**, *123*, 7299. (d) Henze, W.; Vyater, A.; Krause, N.; Gschwind, R. M. *J. Am. Chem. Soc.* **2005**, *127*, 17335.

[45] Corey, E. J.; Boaz, N. W. *Tetrahedron Lett.* **1985**, *26*, 6015.

[46] Hallnemo, G.; Olsson, T.; Ullenius, C. *J. Organomet. Chem.* **1985**, *282*, 133.

[47] Krause, N. *Tetrahedron Lett.* **1989**, *30*, 5219.

[48] (a) Nakamura, E.; Mori, S.; Morokuma, K. *J. Am. Chem. Soc.* **1997**, *119*, 4900. (b) Yamanaka, M.; Nakamura, E. *Organometallics* **2001**, *20*, 5675. (c) Nakamura, E.; Mori, S. *Angew. Chem. Int. Ed.* **2000**, *39*, 3750. (d) Yamanaka, M.; Nakamura, E. *J. Am. Chem. Soc.* **2005**, *127*, 4697.

[49] Furuta, H.; Maeda, H.; Osuka, A. *J. Am. Chem. Soc.* **2000**, *122*, 803.

[50] Nilsson, K.; Ullenius, C.; Krause, N. *J. Am. Chem. Soc.* **1996**, *118*, 4194.

[51] Mori, S.; Nakamura, E.; Morokuma, K. *Organometallics* **2004**, *23*, 1081.

[52] Yamanaka, M.; Inagaki, A.; Nakamura, E. *J. Comput. Chem.* **2001**, *24*, 1401.

[53] Palladium couplings are described further in Chapter III. For a recent review see: Nicolaou, K. C. *Angew. Chem. Int. Ed.* **2005**, *44*, 4442.

[54] Stille, J. K. *Angew. Chem. Int. Ed.* **1986**, *25*, 508.

[55] Tanner, D.; Andersson, P. G.; Tedenborg, L.; Somfai, P. *Tetrahedron* **1994**, *50*, 9135.

[56] (a) Piers, E. ; Chong, J. M.; Morton, H. E. *Tetrahedron* **1989**, *45*, 363. (b) Piers, E.; Morton, H. E. *J. Org. Chem.* **1980**, *45*, 4263.

[57] (a) Nielsen, T. E.; Tanner, D. *J. Org. Chem.* **2002**, *67*, 6366. (b) Nielsen, T.E.; Cubillo de Dios, M. A.; Tanner, D. *J. Org. Chem.* **2002**, *67*, 7309.

[58] Gruber, A. S.; Pozebon, D.; Monteiro, A. L.; Dupont, J.*Tetrahedron Lett.* **2001**, *42*, 7345.

[59] (a) Dupont, J.; Consorti, C. S.; Spencer, J. *Chem. Rev.* **2005**, *105*, 2527. (b) deVries, A. H. M.; Mulders, J. M. C. A.; Mommers, J. H. M.; Henderickx, H. J. W.; de Vries, J. G. *Org. Lett.* **2003**, *5*, 3285.

[60] Trost, B. M.; Dong, G.; *J. Am. Chem. Soc.* **2006**, *128*, 6054.

[61] Dounay, A. B.; Overman, L. E.; Wrobleski, A. D. *J. Am. Chem. Soc.* **2005**, *127*, 10168.

[62] ISI Web of Science, December 2006, http://isiknowledge.com

[63] The price of palladium metal was $339/oz. January 19 2007.

[64] Herrmann, W. A.; Böhm, V. P. W.; Reisinger, C. –P. *J. Organomet. Chem.* **1999**, *576*, 23.

[65] Herrmann, W. A.; Cornils, B. *Angew. Chem. Int. Ed.* **1997**, *36*, 1048.

[66] (a) Littke, A. F.; Dai, C.; Fu, G. C. *J. Am. Chem. Soc.* **2000,** *122,* 4020. (b) Barder, T. E.; Walker, S. D.; Martinelli, J. R.; Buchwald, S. L. *J. Am. Chem. Soc.* **2005**, *127,* 4685. (c) Barrios-Landeros, F.; Hartwig, J. F. *J. Am. Chem. Soc.* **2005**, *127*, 6944. (d) Roy, A.H.; Hartwig, J. F. *J. Am. Chem. Soc.* **2003**, *125*, 8704. (d) Zapf, A.; Beller, M. *Chem. Commun.* **2005**, 431.

[67] Helmchen, G.; Pfaltz, A. *Acc. Chem. Res.* **2000**, *33*, 336.

[68] Smidt, J.; Hafner, W.; Jira, R.; Sedlmeier, J.; Sieber, R.; Rüttinger, R.; Kojer, H. *Angew. Chem. Int. Ed.* **1959**, 71, 176.

[69] Tsuji, J. *Synthesis* **1984**, 369.

[70] Tsuji, J.; Kiji, J.; Imamura, S.; Morikawa, M. *J. Am. Chem. Soc.* **1964**, *86*, 4350.

[71] Trost, B. M.; Fullerton, T. J. *J. Am. Chem. Soc.* **1973**, *95*, 292.

[72] Trost, B. M. *Acc. Chem. Res.* **1980**, *13*, 385.

[73] Heck, R. F. *J. Am. Chem. Soc.* **1968**, *90*, 5518

[74] Heck, R. F. *J. Am. Chem. Soc.* **1968**, *90*, 5538

[75] Mizoroki, T.; Mori, K.; Ozaki, A. *Bull. Chem. Soc. Jpn.* **1971**, *44*, 581.

[76] Heck, R. F.; Nolley, J. P. *J. Org. Chem.* **1972**, *37*, 2320.

[77] (a) Milstein, D.; Stille, J. K. *J. Am. Chem. Soc.* **1978**, *100*, 3636. (b) Milstein, D.; Stille, J. K. *J. Am. Chem. Soc.* **1979**, *101*, 4992.

[78] Hatanaka, Y.; Hiyama, T. *J. Org. Chem.* **1988**, *53*, 918.

[79] Tamao, K.; Sumitani, K.; Kumada, M. *J. Am. Chem. Soc.* **1972**, *94*, 4374.

[80] Negishi, E.; King, A. O.; Okukado, N. *J. Org. Chem.* **1977**, *42*, 1821.

[81] (a) Miyaura, N.; Yamada, K.; Suzuki, A. *Tetrahedron Lett.* **1979**, *50*, 3437. (b) Miyaura, N.; Suzuki, A. *Chem. Rev.* **1995**, *95*, 2457.

[82] Sonogashira, K.; Tohda, Y.; Hagihara, N. *Tetrahedron Lett.* **1975**, *36*, 4467.

[83] (a) Louie, J.; Hartwig, J. F.; *Tetrahedron Lett.* **1995**, *36*, 3609. (b) Guram, A. S.; Rennels, R. A.; Buchwald, S. L. *Angew. Chemie Int. Ed. Engl.* **1995**, *34*, 1348.

[84] Goossen, L. J.; Deng, G.; Levy, L. M. *Science* **2006**, *313*, 662.

[85] Fauvarque, J. -F.; Pflüger, F.; Troupel, M. *J. of Organomet. Chem.*. **1981**, *208*, 419.

[86] Amatore, C.; Jutand, A. *Coord. Chem. Rev.* **1998**, *178*, 511.

[87] Amatore, C.; Jutand, A.; M'Barki, M. A. *Organometallics* **1992**, *11*, 3009.

[88] (a) Low, J. J.; Goddard III, W. A. *J. Am. Chem. Soc.* **1986**, *108*, 6115. (b) Ananikov, V. P.; Musaev, D. G.; Morokuma, K. *Organometallics* **2005**, *24*, 715. (c) Sakaki, S.; Biswas, B.; Sugimoto, M.; *J. Chem. Soc., Dalton Trans.* **1997**, 803. (d) Sakaki, S.; Kai, S.; Sugimoto, M.; *Organometallics* **1999**, *18*, 4825. (e) Sumimoto, M.; Iwane, N.; Takahama, T.; Sakaki, S. *J. Am. Chem. Soc.* **2004**, *126*, 10457.

[89] Negishi, E. I., Ed., *Handbook of Organopalladium Chemistry for Organic Synthesis*, Wiley-Interscience, New York, **2002**. Section II.2.3.

[90] See discussion on page 74 of this thesis.

[91] For a theoretical discussion of the nature of phosphine-transition metal bonds see: Bessac, F.; Frenking, G. *Inorg. Chem.* **2006**, *45*, 6956.

[92] Herrmann, W. A.; Kohlpaintner, C. W. *Angew. Chemie Int. Ed. Engl.* **1993**, *32*, 1524.

[93] Mann, B. E.; Musco, A. *J. Chem. Soc. Dalton Trans.* **1975**, *16*, 1673.

[94] Amatore, C.; Pflüger, F. *Organometallics* **1990**, *9*, 2276.

[95] (a) Amatore, C.; Azzabi, M.; Jutand, A. *J. Am. Chem. Soc.* **1991**, *113*, 8375. (b) Amatore, C.; Jutand, A. *Acc. Chem. Res.* **2000**, *33*, 314.

[96] (a) Kozuch, S.; Shaik, S.; Jutand, A.; Amatore, C. *Chem. Eur. J.* **2004**, *10*, 3072. (b) Kozuch, S.; Amatore, C.; Jutand, A.; Shaik, S. *Organometallics*. **2005**, *24*, 2319.

[97] (a) Goossen, L. J.; Koley, D.; Hermann, H. L.; Thiel, W. *Chem. Commun.* **2004,** 2141. (b) Goossen, L. J.; Koley, D.; Hermann, H. L.; Thiel, W. *Organometallics* **2005**, *24*, 2398.

[98] Senn, H. M.; Ziegler, T. *Organometallics* **2004**, *23*, 2980.

[99] Deeth, R. J.; Smith, A.; Brown, J. M. *J. Am. Chem. Soc.* **2004**, *126*, 7144.

[100] Siegbahn, P. E. M.; Strömberg, S.; Zetterberg, K. *Organometallics* **1996**, *15*, 5542.

[101] (a) Goossen, L. J.; Koley, D.; Hermann, H. L.; Thiel, W. *J. Am. Chem. Soc.* **2005**, *127*, 11102. (b) Goossen, L. J.; Koley, D.; Hermann, H. L.; Thiel, W. *Organometallics* **2006**, *25*, 54.

[102] Braga, A. A. C.; Ujaque, G.; Maseras, F. *Organometallics* **2006**, *25*, 3647.

[103] Napolitano, E.; Farina, V.; Persico, M. *Organometallics* **2003**, *22*, 4030.

[104] Alvarez, R.; Faza, O. N.; Lopez, C. S.; de Lera, A. R. *Org. Lett.* **2006**, *8*, 35.

[105] Miyaura, N.; Yanagi, T.; Suzuki, A. *Synth. Commun.* **1981**, *11*, 513.

[106] (a) Low, J. J.; Goddard III, W. A. *J. Am. Chem. Soc.* **1986**, *108*, 6115. (b) Ananikov, V. P.; Musaev, D. G.; Morokuma, K. *Organometallics* **2005**, *24*, 715. (c) Sakaki, S.; Biswas, B.; Sugimoto, M.; *J. Chem. Soc., Dalton Trans.* **1997**, *5*, 803. (d) Sakaki, S.; Kai, S.; Sugimoto, M.; *Organometallics* **1999**, *18*, 4825. (e) Sumimoto, M.; Iwane, N.; Takahama, T.; Sakaki, S. *J. Am. Chem. Soc.* **2004**, *126*, 10457.

[107] Cacchi, S.; Felici, M.; Pietroni, B. *Tetrahedron Lett.* **1984**, *25*, 3137.

[108] Cacchi, S.; Fabrizi, G.; Marinelli, F.; Moro, L.; Pace, P. *Tetrahedron* **1996**, *52*, 10225.

[109] Arcadi, A.; Cacchi, S.; Fabrizi, G.; Marinelli, F.; Pace, P. *Eur. J. Org. Chem.* **1999**, *12*, 3305.

[110] Arcadi, A.; Cacchi, S.; Fabrizi, G.; Marinelli, F.; Pace, P. *Eur. J. Org. Chem.* **2000**, *13*, 4099.

[111] Cacchi, S.; Fabrizi, G.; Goggiamani, A.; Moreno-Mañas, M.; Vallribera, A.. *Tetrahedron Lett.* **2002**, 4*3*, 5537.

[112] Palladium acetylene complexes have previously been studied but not in relation to their relative stabilities and their reactivity towards aryl halides: (a) Wang, X.; Andrews, L. *J. Phys. Chem. A* **2003**, *107*, 337 (b) Cui, Q.; Musaev, D. G.; Morokuma, K. *Organometallics* **1998**, *17*, 1383

[113] Ahlquist, M.; Kozuch, S.; Shaik, S.; Tanner, D.; Norrby, P.-O. *Organometallics* **2006**, *25*, 45.

[114] Similar observations have been made by Larock: Larock, R. C.; Yum, E. K.; Doty, M. J.; Sham, K. K. C. *J. Org. Chem.* **1995**, *60*, 3270.

[115] NBO 4.0, Glendening, E. D.; Badenhoop, J.K.; Reed, A.E.; Carpenter, J.E.; Weinhold, F. Theoretical Chemistry Institute, University of Wisconsin, Madison, WI, **1996**.

[116] (a) Limmert, M. E.; Roy, A. H.; Hartwig, J. F. *J. Org. Chem.* **2005**, *70*, 9364. (b) Coe, J. W. *Org. Lett.* **2000**, *2*, 4205. (c) Fu, X.; Zhang, S.; Yin, J.; McAllister, T. L.; Jiang, S. A.; Chou-Hong, T.; Thiruvengadam, K.; Zhang, F. *Tetrahedron Lett*. **2002**, *43*, 573. (d) Hansen, A. L.; Skrydstrup, T. *J. Org. Chem.* **2005**, *70*, 5997. (e) Hansen, A. L.; Skrydstrup, T. *Org. Lett.* **2005**, *7*, 5585.

[117] Galardon, E.; Ramdeehul, S.; Brown, J. M.; Cowley, A.; Hii, K. K.; Jutand, A. *Angew. Chemie Int. Ed.* **2002**, *41*, 1760.

[118] Marten, B.; Kim, K.; Cortis, C.; Friesner, R. A.; Murphy, R. B.; Ringnalda, M. N.; Sitkoff, D.; Honig, B. *J. Phys. Chem.*, **1996**, *100*, 11775.

[119] Entropic contributions of bimolecular reactions have been studied experimentally and theoretically by: (a) Searle, M. S.; Westwell, M. S.; Williams, D. H.; *J. Chem. Soc., Perkin Trans. 2* **1995**, *1*, 141. (b) Woo, T. K.; Blöchl, P. E.; Ziegler, T. *J. Phys. Chem. A* **2000**, *104*, 121. (c) Seth, M.; Senn, H. M.; Ziegler, T. *J. Phys. Chem. A* **2005**, *109*, 5136.

[120] Kelley, K. *Out of Control, the Rise of Neo-Biological Civilization* 1990, available online at http://www.kk.org/outofcontrol

[121] Kolb, H. C.; Finn. M. G.; Sharpless, K. B. *Angew. Chemie Int. Ed.* **2001**, *40*, 2004.

[122] Voet, D.; Voet, J. G.; Pratt, C. W. *Fundamentals of Biochemistry* **1999**, John Wiley & Sons, Inc.

[123] Bohacek, R. S.; McMartin, C.; Guida, W. C. Med. Res. Rev. **1996**, *16*, 3.

[124] George S. Hammond, Norris Award Lecture, **1968**

[125] Kolb, H. C.; Sharpless, K. B. *Drug Discov. Today* **2003**, *8*, 1128.

[126] Huisgen, R. *Angew. Chemie Int. Ed.* **1963**, *75*, 604.

[127] Tornøe, C. W.; Christensen, C.; Meldal, M. *J. Org. Chem.* **2005**, *67*, 3057.

[128] Rostovtsev, V. V.; Green, L. G.; Fokin, V. V.; Sharpless, K. B. *Angew. Chem. Int. Ed.* **2002**, *41*, 2596.

[129] Wu, P.; Feldman, A. K.; Nugent, A. K.; Hawker, C. J.; Scheel, A.; Voit, B.; Pyun, J.; Frechet, J. M. J.; Sharpless, K. B.; Fokin, V. V. *Angew. Chem. Int. Ed.* **2004**, *43*, 3928.

[130] Wang, Q.; Chan, T. R.; Hilgraf, R.; Fokin, V. V.; Sharpless, K. B.; Finn, M. G. *J. Am. Chem. Soc.* **2003**, *125,* 3192.

[131] Hawker, C. J.; Wooley, K. L.; *Science* **2005**, *309*, 2000.

[132] Dichtel, W. R.; Miljanic, O. S.; Spruell, J. M.; Heath, J. R.; Stoddart, J. F. *J. Am. Chem. Soc.* **2006**, *128*, 10388.

[133] Liu, D.; Gao, W. Z.; Dai, Q.; Zhang, X. M. *Org. Lett.* **2005**, *7*, 4907.

[134] Devaraj, N. K.; Dinolfo, P. H.; Chidsey, C. E. D.; Collman, J. P. *J. Am. Chem. Soc.* **2006**, *128*, 1794.

[135] ISI Web of Science, December 2006, http://isiknowledge.com

[136] For a review on the mechanism of CuAAC: Bock, V. D.; Hiemstra, H.; van Maarseveen, J. H. *Eur. J. Org. Chem.* **2006**, 51.

[137] (a) Himo, F.; Lovell, T.; Hilgraf, R.; Rostovtsev, V. V.; Noodleman, L.; Sharpless, K. B.; Fokin, V. V. *J. Am. Chem. Soc.* **2005**, *127*, 210. Related reactions were reported in: (b) Himo, F.; Demko, Z. P.; Noodleman, L. *J. Org. Chem.* **2003**, *68*, 9076. (c) Himo, F.; Demko, Z. P.; Noodleman, L.; Sharpless, K. B. *J. Am. Chem. Soc.* **2002**, *124*, 12210.

[138] The chemistry of copper acetylides was first studied by Glaser: Glaser, C. *Chem. Ber.* **1869**, *2*, 422.

[139] Rodionov, V. O.; Fokin, V. V.; Finn, M. G. *Angew. Chem. Int. Ed.* **2005**, *44*, 2210.

[140] (a) Karlin, K. D.; Hayes, J. C.; Gultneh, Y.; Cruse, R. W.; McKown, J. W.; Hutchinson, J. P.; Zubieta, J. *J. Am. Chem. Soc.* **1984**, *106*, 2121. (b) Karlin, K. D.; Zhu, Z.-Y.; Karlin, S. *J. Biol. Inorg. Chem.* **1998**, *3*, 172. (c) Chen, P.; Solomon, E. I. *Proc. Natl. Acad. Sci. U. S. A.* **2004**, *101*, 13105. (d) Liao, Y.; Novoa, J. J.; Arif, A.; Miller, J. S. *Chem. Comm.* **2002**, 3008. (e) Zheng, S.-L.; Messerschmidt, M.; Coppens, P. *Angew. Chem. Int. Ed.* **2005**, *44*, 4614. (f) Siegbahn, P. E. M. *Faraday Discuss.* **2003** *124*, 289. (f) Company, A.; Lamata, D.; Poater, A.; Sola, M.; Rybak-Akimova, E. V.; Que, L.; Fontrodona, X.; Parella, T.; Llobet, A.; Costas, M. *Inorg. Chem.* **2006**, *45*, 5269. (g) Li, Z.; Barry, S. T.; Gordon, R. G. *Inorg. Chem.* **2005**, *44*, 1728. (h) Liao, Y.; Novoa, J. J.; Arif, A.; Miller, J. S. *Chem. Commun.* **2002**, 3008.

[141] For a review on copper complexes see: Mykhalichko, B. M.; Temkin, O. N.; Mys'kiv, M. G. *Russ. Chem. Rev.* **2001**, *69*, 957.

[142] Pyykkö, P. *Chem. Rev.* **1997**, *97*, 597.

[143] (a) Bae, I.; Han, H.; Chang, S. *J. Am. Chem. Soc.* **2005**, *127*, 2038. (b) Cho, S. H.; Yoo, E. J.; Bae, I.; Chang, S. *J. Am. Chem. Soc*. **2005**, *127*, 16046 (c) Yoo, E. J.; Bae, I.; Cho, S. H.; Han, H.; Chang, S. *Org. Lett.* **2006**, *8*, 1347 (d) Chang, S.; Lee, M.; Jung, D. Y.; Yoo, E. J.; Cho, S. H.; Han, S. K. *J. Am. Chem. Soc*. **2006**, *128*, 12366

[144] Whiting, M.; Fokin, V. V. *Angew. Chem. Int. Ed.* **2006**, *45*, 3157.

[145] Cassidy, M. P.; Raushel, J.; Fokin, V. V. *Angew. Chem. Int. Ed.* **2006**, *45*, 3154.

[146] (a) Dimroth, O. *Liebigs Ann. Chem.* **1909**, *364*, 183. (b) Katritzky, A. R.; Ji, F. -B.; Fan, W. -Q.; Gallos, J. K.; Greenhill, J. V.; King, R. W.; Steel, P. J. *J. Org. Chem.* **1992**, 57, 190.

[147] Naota, T.; Takaya, H.; Murahashi, S. -I. *Chem. Rev.* **1998**, *98*, 2599.

[148] Noyori, R.; Hashiguchi, S. *Acc. Chem. Res.* **1997**, *30*, 97.

[149] Carlsen, P. H. J.; Katsuki, T.; Martin, V. S.; Sharpless, K. B. *J. Org. Chem.* **1981**, 46, 3936.

[150] Nicolaou, K. C.; Buger, P. G.; Sarlah, D. *Angew. Chem. Int. Ed.* **2005**, *44*, 4490.

[151] Zhang, S. -W; Mitsudo, T.; Kondo, T.; Watanabe, Y. *J. Organomet. Chem.* **1993**, *450*, 197.

[152] Zhang, L.; Chen, X.; Xue, P.; Sun, H. H. Y.; Williams, I. D.; Sharpless, K. B.; Fokin, V. V.; Jia, G. *J. Am. Chem. Soc*. **2005**, *127*, 15998

Articles

CHEMISTRY
A EUROPEAN JOURNAL

DOI: 10.1002/chem.200501229

An Experimental and Theoretical Study of the Mechanism of Stannylcupration of α,β-Acetylenic Ketones and Esters

Mårten Ahlquist, Thomas E. Nielsen, Sebastian Le Quement, David Tanner,* and Per-Ola Norrby*[a]

Abstract: The title reaction has been investigated by experimental and computational (DFT) techniques, and subsequently compared to the corresponding carbocupration reaction, with particular emphasis on the stereoselectivity. For stannylcupration of an ynone substrate, only the *anti*-addition product is observed, whereas for the corresponding ynoate substrate, the stereoselectivity can be affected by the reaction conditions: in the presence of methanol as proton donor, the initial *syn*-addition product can be trapped, whereas a *syn*/*anti* mixture is obtained in a non-protic solvent. This is in sharp contrast to the carbocupration of the same ynone substrate with a cyanocuprate (RCu(CN)Li), which is highly selective for *syn*-addition. The product selectivities can be understood from a detailed computational characterization of the reaction paths, and in particular from the relative stabilities of the vinyl cuprate and allenolate intermediates. It is suggested that the stereodetermining step is protonation of vinyl cuprate intermediates.

Keywords: alkynes · cuprates · density functional calculations · stannylcupration · stereoselectivity

Introduction

Heteroatomcuprates, especially stannylcopper and silylcopper species, are versatile reagents for organic synthesis.[1] For example, trialkylstannyl cuprates, $(R_3Sn)(X)_nCuLi_n$, react with a wide range of organic substrates, particularly alkynes. This stannylcupration process provides convenient entry to structurally diverse alkenyl stannanes which are themselves very useful building blocks for further elaboration, including the formation of vinyllithiums and vinyl iodides or as coupling partners in the Stille reaction.[2] The pioneering work of Piers[3] on the stannylcupration of α,β-acetylenic esters, which has been extended to α,β-acetylenic *N*,*N*-dimethylamides[4] and α,β-acetylenic acids,[5] provides highly stereoselective routes to either (*E*)- or (*Z*)-β-stannylated α,β-unsaturated moieties, by simple variation of the reaction conditions (Scheme 1).

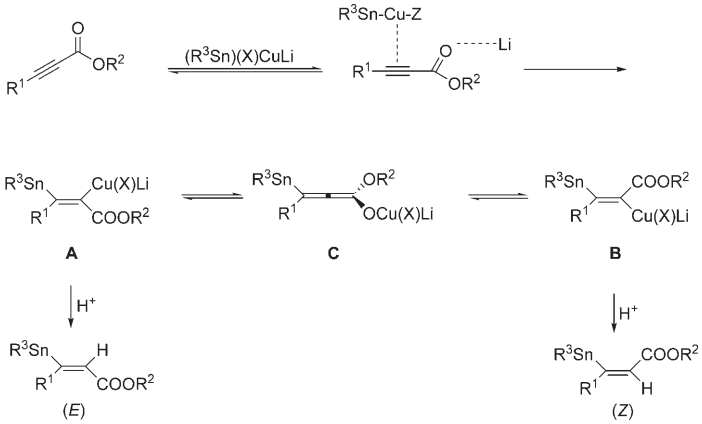

Scheme 1. Proposed mechanism for addition of stannylcuprates to α,β-acetylenic esters (adapted from ref. [3a]).

For α,β-acetylenic esters, the reaction has been envisioned to occur via regio- and stereoselective addition across the triple bond to give **A** which, if protonated under kinetic conditions (the ester is mixed in THF with an alcohol as a proton source prior to exposure to the cuprate at −78 °C), gives mainly or exclusively (up to >99:1 selectivity) the *E* isomer. Warming the reaction mixture to ca. −50 °C before the addition of a proton source provides the thermodynamically more stable *Z* isomer (typically around 98:2 selectivity) after equilibration to **B** via the allenolate **C**.

[a] M. Ahlquist, Dr. T. E. Nielsen, S. Le Quement, Prof. Dr. D. Tanner, Prof. Dr. P.-O. Norrby
Department of Chemistry
Technical University of Denmark, Building 201 Kemitorvet
2800 Kgs. Lyngby (Denmark)
Fax: (+45) 4593-3968
E-mail: dt@kemi.dtu.dk
pon@kemi.dtu.dk

Supporting information for this article is available on the WWW under http://www.chemeurj.org/ or from the author.

Recently, as part of a total synthesis project,[6] we became interested in the development of synthetic methodology enabling the stereoselective production of (*E*)-β-trialkylstannyl α,β-unsaturated ketones. Based on analogy with the work of Piers, the obvious route would be regio- and stereoselective stannylcupration of the corresponding α,β-acetylenic ketones, and we were surprised to find only one report[7] of such a reaction being used in the context of total synthesis. Accordingly, we screened a range of stannylcupration reactions of various acetylenic ketones with different combinations of solvent, reaction temperature, stannylcuprate and proton source.[8] To our surprise, in all these experiments the

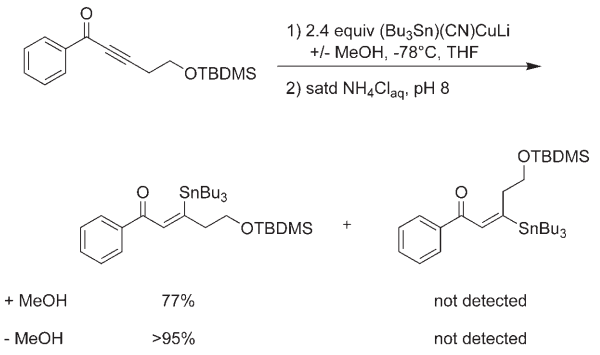

Scheme 2. High *Z* selectivity in the stannylcupration of alkynones, both in the presence and absence of methanol (taken from ref. [8]).

(*Z*)-β-trialkylstannyl α,β-unsaturated ketones were consistently formed as the major product in high yield and with excellent stereoselectivity (>95%), often without even a trace of the *E* isomers, as exemplified in Scheme 2.

There is thus a very different reactivity/selectivity pattern for the stannylcupration of α,β-unsaturated alkynoic esters and ketones, respectively, We also noted that (in line with the work of others[9]) the corresponding reactions of the Gilman or Lipshutz organocuprates with our alkynones were non-stereoselective,[8] thus providing more food for mechanistic thought. Important mechanistic studies of this type of reaction, involving the "classical" organocuprates, have been reported by Ullenius[10] and Krause,[11] while Nakamura[12] has recently contributed with extensive computational studies; Hall[13] has made a systematic study of the effect of additives on the stereochemical outcome of the reaction involving acetylenic esters. In detailed NMR studies of the carbocupration of α,β-acetylenic substrates, Ullenius[10] noted distinct differences between the behavior of ynoates and ynones, the latter forming only allenolates as observable intermediates (corresponding to **C** in Scheme 1) which are subsequently protonated with only low (or no) stereoselectivity. This further prompted the question as to why the stannylcupration reactions of alkynones are so highly stereoselective. A possible answer to that question, and an explanation of the different reactivity/selectivity pattern of alkynones versus alkynoates in stannylcupration reactions, is the subject of this report.

Results

Experimental results

A model system was chosen to be as simple as possible to facilitate a study by both experimental and computational methods. Therefore, the ketone chosen here was pent-3-yn-2-one (**1**), the ester methyl 2-butynoate (**2**), and the stannylcuprate $Me_3SnCu(CN)Li$ (**3**). The reactions were performed in THF at −78°C in the presence (+MeOH) or absence (−MeOH) of methanol as proton source. When performed in absence of methanol the reaction mixture was worked up with saturated aqueous ammonium choride (Scheme 3).

To parallel the stannylcupration with the related carbocupration, **1** was subjected to the corresponding carbocuprate *t*BuCu(CN)Li (**6**). The opposite substitution pattern was also investigated to probe the influence of the sterics of the acetylene substituent and the carbocuprate. Therefore the *t*Bu-substituted alkyne **7** was treated with the carbocuprate MeCu(CN)Li (**8**). In both cases the reaction mixtures were worked up with saturated ammonium chloride. The results are presented in Scheme 4.

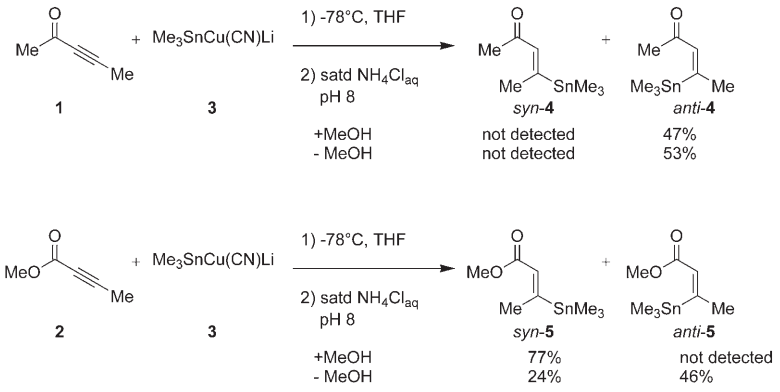

Scheme 3. Stannylcupration of ynone **1** and ynoate **2**.

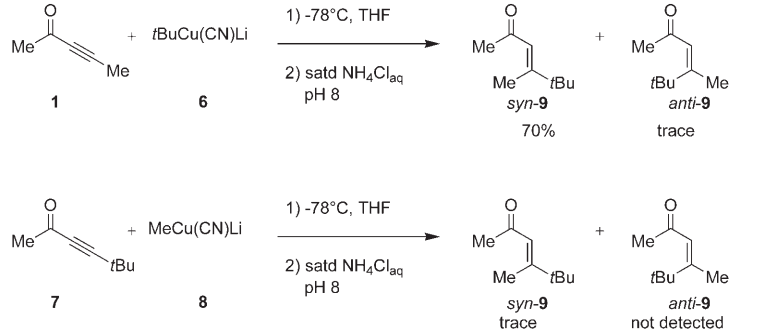

Scheme 4. Results from carbocupration of ynones **1** and **7**.

Under these conditions the cuprate **8** surprisingly proved to be very unreactive towards **7**, and after three hours of reaction most of the starting material was recovered. This is possibly due to formation of less reactive clusters of reagent **8**, a factor which is not an issue for the cuprate **6**.[14]

Computational results

Stannylcupration of pent-3-yn-2-one: The starting point for the calculations is the complex **10**, which has been shown by experimental and computational methods to be the initially formed complex when ynones/ynoates are reacted with cuprates.[10,12b] This can be viewed as being either a copper(III) species, or a copper(I) coordinated to an alkyne (Figure 1). We have chosen the copper(III) description since it is more in line with the calculated geometry of intermediates **10** and **15**.

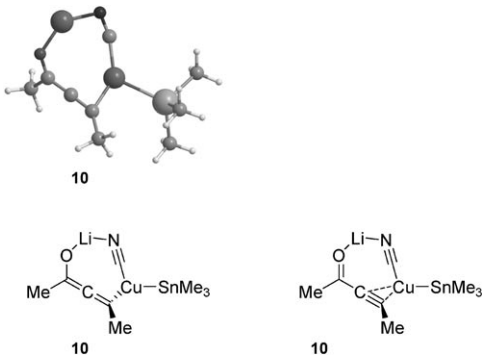

Figure 1. Calculated structure of the "Cu^{III}"-complex **10**.

The Cu^{III} species **10** can undergo a reductive elimination type reaction in which the carbon–tin bond is formed via the transition state **11ts**, with a low barrier of 13 kJ mol^{-1} (Figure 2). After the carbon–tin bond is formed the complex collapses to an allenolate intermediate **12**, in which the Cu^{I} is coordinated to the α,β-double bond. The reaction path was confirmed by a relaxed scan of the C–Sn distance, as well as by displacement followed by energy minimization, in both cases yielding the allenolate **12**. We note that this mechanism is different from the one proposed for the carbocupration of ynones, in which the reductive elimination of the Cu^{III} species always leads to a vinylcuprate type structure.[12b]

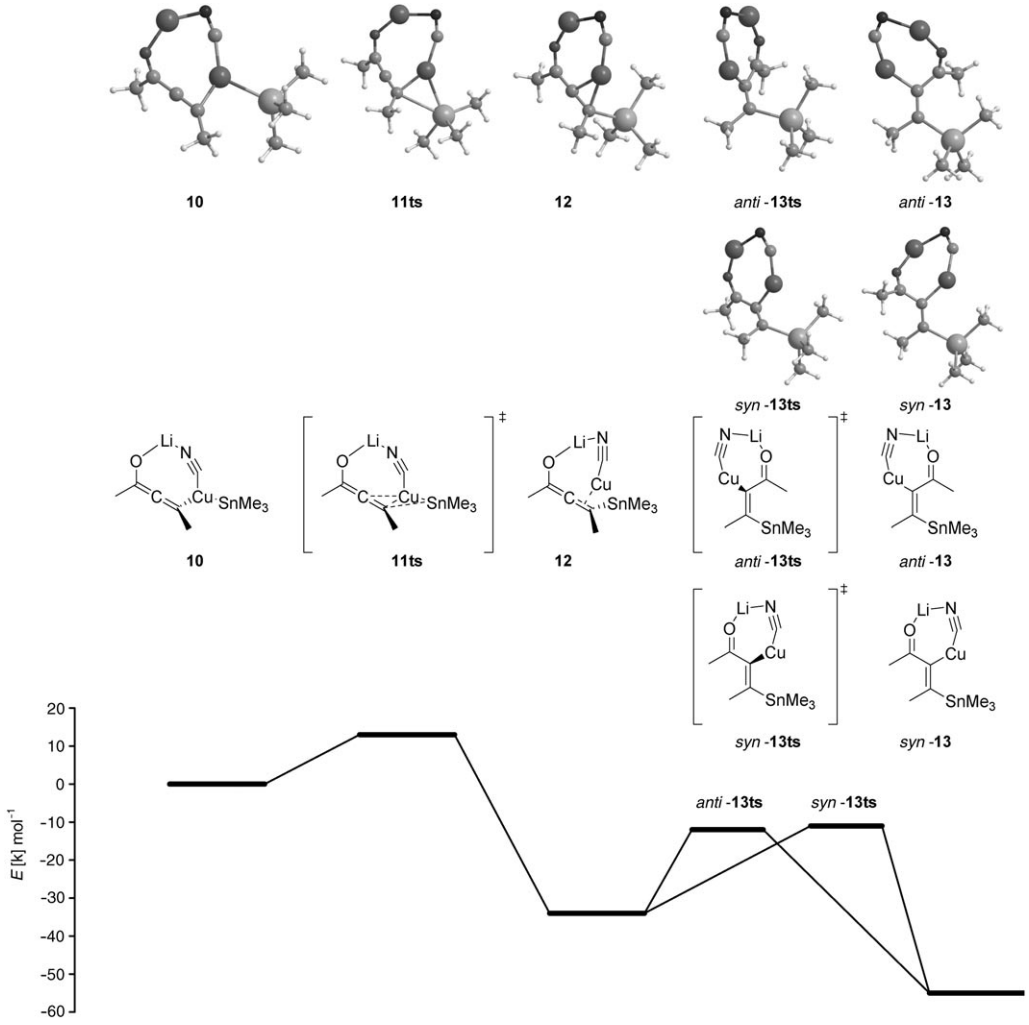

Figure 2. Energy profile for stannylcupration of ynone **1**.

Isomerizations of the allenolate **12** to the *syn*-addition vinylcuprate *syn*-**13** or the *anti*-addition vinylcuprate *anti*-**13** occur via basically identical barriers, 22 kJ mol^{-1} for *syn*-**13ts** and 23 kJ mol^{-1} *anti*-**13ts**. The resulting vinylcuprates *syn*-**13** and *anti*-**13** are isoenergetic, and the overall reactions from **10** (Cu^{III} complex) are calculated to be exothermic by 55 kJ mol^{-1} (Figure 2). The energy required for isomerization between *syn*-**13** and *anti*-**13** is thus calculated to be 44 kJ mol^{-1}, with the allenolate intermediate **12** being 21 kJ mol^{-1} less stable than the vinylcuprates.

Since the reaction is conducted in THF it is possible that the lithium ion is dissociated to yield an anionic vinylcuprate intermediate, in analogy with earlier observations for lithium dialkylcuprates,[15] which then is protonated to yield the products. Due to the stabilizing effect of an oxygen–tin (Lewis base/Lewis acid) interaction the *anti*-addition complex *anti*-**14** is calculated to be stabilized by as much as 30 kJ mol^{-1} in the gas phase, relative to the *syn*-addition complex *syn*-**14** (Figure 3). In the *syn*-addition complex there is also a destabilizing interaction between the carbonyl oxygen and the anionic copper. Calculations with a solvation model were therefore performed. These yielded a difference of 22 kJ mol^{-1} in favor of *anti*-**14**. Thus only in the presence of Li^+ ions are the *syn* and *anti* intermediates isoenergetic, and decomplexation leads to a preference for the complex leading to the *anti*-addition product.

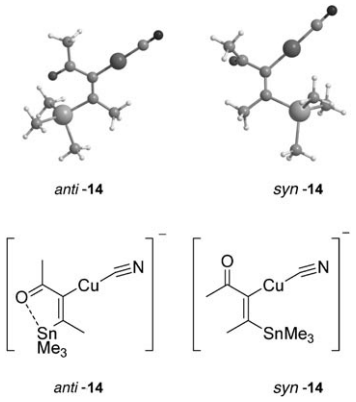

Figure 3. Calculated structures of *anti*-**14** (left) and *syn*-**14** (right).

Stannylcupration of methyl-2-butynoate: Cu^{III}-complex **15** analogous to **10** was the starting point for the mechanistic study of the stannylcupration of methyl-2-butynoate (Figure 4). This complex can undergo reductive elimination

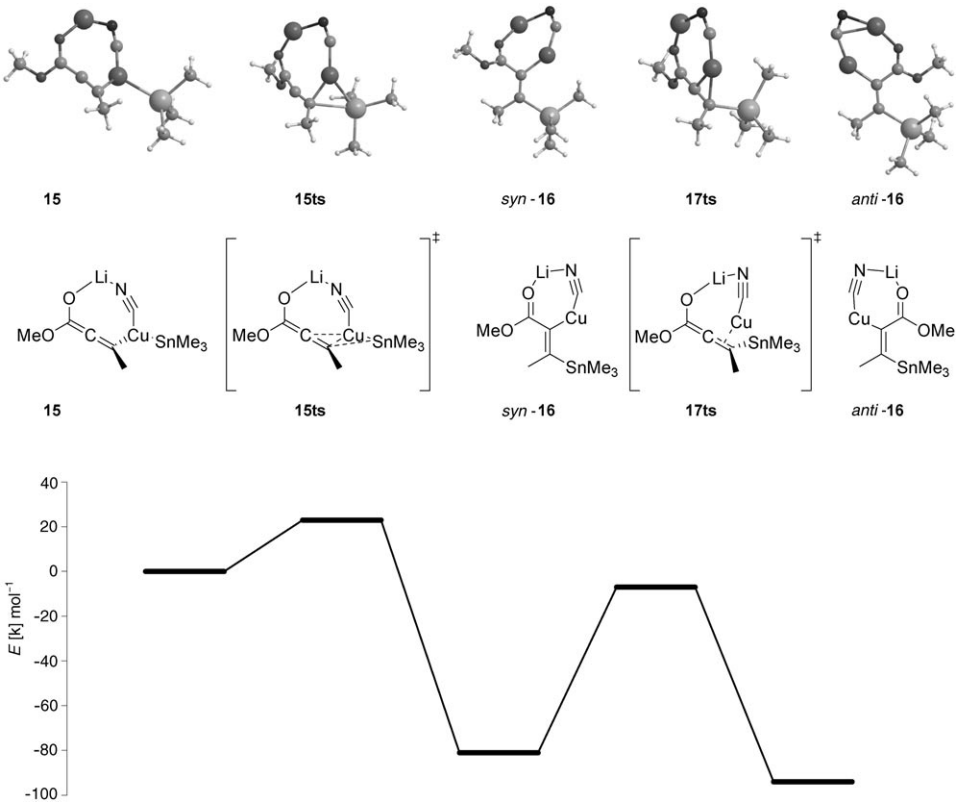

Figure 4. Energy profile for stannylcupration of ynoate **2**.

to yield the *syn*-addition vinylcuprate *syn*-**16**. The mechanism is analogous to the one for carbocupration of ynones/ynoates proposed by Nakamura et al.,[12b] and proceeds with a barrier which is calculated to be slightly higher than for the reaction of pent-3-yn-2-one described above (23 kJ mol^{-1}) and the overall reaction is exothermic by 81 kJ mol^{-1}. This complex can then rearrange to isomeric vinylcuprate *anti*-**16**, via an allenolate type transition state **17ts** with a barrier of 74 kJ mol^{-1}. From **15** the overall reaction is exothermic by 94 kJ mol^{-1}. It is the stabilizing oxygen–tin (Lewis base/Lewis acid) interaction in the *anti*-addition vinylcuprate *anti*-**16** that makes it more energetically favorable than the *syn*-addition vinylcuprate *syn*-**16**.

Another *anti*-addition vinylcuprate complex (**18**) was also found in which the ester moiety had been rotated 180° (Figure 5). This complex was calculated to be less stable than *anti*-**16** by 39 kJ mol^{-1}.

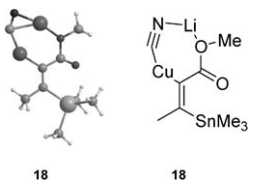

Figure 5. Calculated structure of **18**, a less stable isomer of *anti*-**16**.

Carbocupration of ynones: Carbocupration of pent-3-yn-2-one (**1**) by *t*BuCu(CN)Li **6** has been investigated for comparison with the stannylcupration (Figure 6). The reaction starts with a Cu^{III} species analogous to the ones described above for the stannylcuprations. The complex **19** formed from **1** and **6**, undergoes reductive elimination to yield the vinylcuprate *syn*-**21** with a barrier of 39 kJ mol^{-1} (**20ts**). *syn*-**21**, the initially formed intermediate in the reaction between **1** and **6**, isomerizes to the allenolate **22** with a barrier which is only slightly above the energy of **22** (0.1 kJ mol^{-1}). Formation of **22** is endothermic by 33 kJ mol^{-1}. The transition state for formation *anti*-**21** (*anti*-**23ts**) is also low, 0.4 kJ mol^{-1}, and the overall reaction from the vinylcuprate *syn*-**21** to the isomeric vinylcuprate *anti*-**21** is calculated to be endothermic by 9 kJ mol^{-1} (Figure 6). This difference in potential energy of the two intermediates is due to the unfavorable steric interaction between the *tert*-butyl group and the methyl group bonded to the carbonyl in *anti*-**21**. The favorable Lewis acid/Lewis base interaction in the analogous stannylcupration intermediates has no counterpart in the carbocupration case. This important feature will be discussed in more detail below.

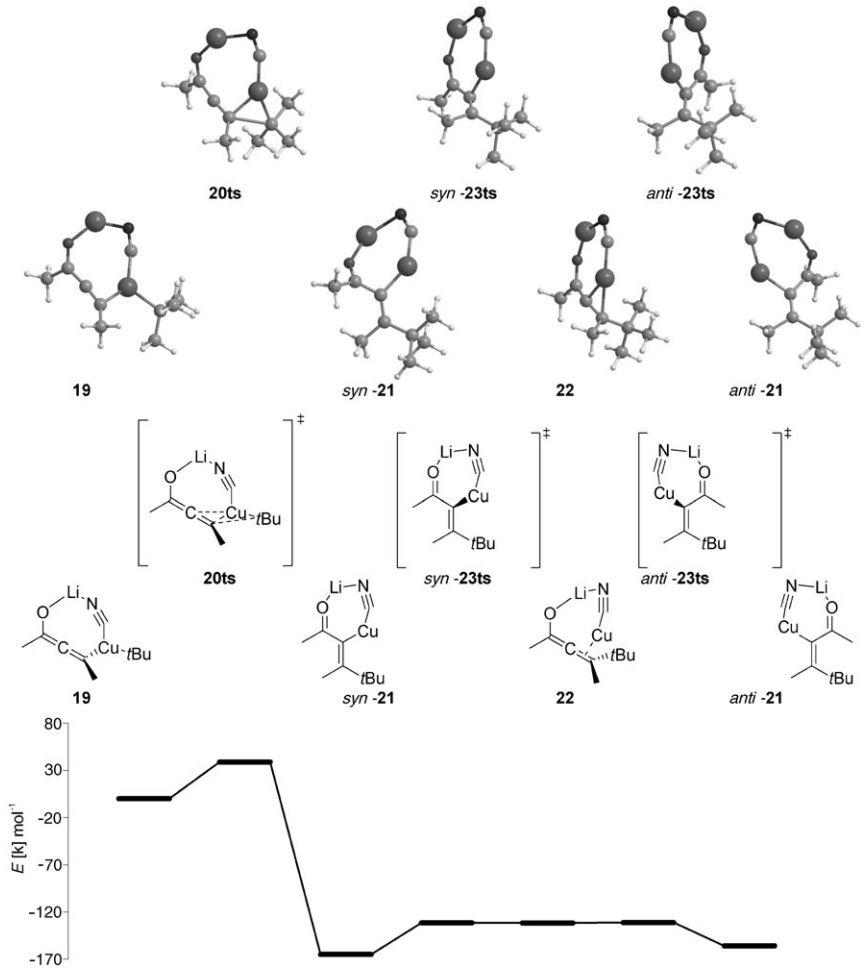

Figure 6. Energy profile for carbocupration reaction of **1** and **6**.

Discussion

The observed stereochemical outcome of the stannylcupration of ketones was at first surprising. Previous observations have shown stannylcupration of esters to yield *syn*-addition products at low temperature.[3] The stereochemical outcome of our model system, ketone **1** and stannylcuprate **3**, was always the *anti*-addition product *anti*-**4**, independent of both the quenching temperature and the nature of the proton source.

Previous investigations of the related carbocupration of ynones and ynoates made a link between the conjugate addition and insertion of the triple bond into the Cu–C bond.[12b] It was shown that the carbon–carbon bond is formed in a reductive elimination from a copper(III) species, after which the complex collapsed to the alkyne *syn*-insertion vinylcuprate analogous to *syn*-**21**. In the present study another mechanism has been observed for the stannylcupration of ynones. Also here the initial complex formed is a Cu^{III} species **10** (Figure 2). Reductive elimination from this complex takes place via a low energy transition state **11ts**, with a calculated barrier of merely 13 kJ mol^{-1}. From here the mechanism of the stannylcupration differs from the one found for the carbocupration. After **11ts** the complex does not form a *syn*-addition vinylcuprate but instead the allenolate **12**. This has some fundamental consequences for the expected outcome of the reaction. Whereas one would expect pure *syn*-addition products at low temperature for carbocuprations and a mixture when performed at higher temperatures, the stannylcupration reaction would be expected to yield mixtures even at low temperature since the initial intermediate **12** could in principle yield both products, either by direct protonation of **12** or protonation of the vinylcuprates *syn*-**13** and *anti*-**13**. Formation of *syn*-**13** and *anti*-**13** takes place via similar barriers and the two isomers are calculated to be isoenergetic, wherefore direct protonation of the isomers of **13** would be expected to lead to a mixture of stereoisomeric products. We are thus left with two possible rationalizations for the experimentally observed stereochemical outcome of the reaction. The first is that the species which is pro-

tonated is the allenolate **12**. The steric bulk of the stannyl group could then hinder the protonation which would yield the *syn*-addition product **4**, while protonation from the other side would yield the observed product. The other possibility is that the complexes which are protonated are not the isomers of **13**, but instead those in which the lithium ion has dissociated to give *syn*-**14** and *anti*-**14** (Figure 3). Of these, *anti*-**14** is strongly favored (30 kJ mol^{-1} in the gas phase) due to a strong Lewis acid/Lewis base interaction between the tin and the carbonyl oxygen, and direct protonation of *anti*-**14** would lead to the observed product.

While the stereochemical outcome of the stannylcupration of ynone **1** was surprising, the product distribution of the corresponding reaction between **3** and ynoate **2** followed literature precedence.[3] Protonation at low temperature results in only *syn*-addition product and at higher temperature a mixture of *syn*- and *anti*-addition products. The computational investigation of the stannylcupration of ynoate **2** by stannylcuprate **3** starts with the Cu^{III}-complex **15** (Figure 4) from which reductive elimination of the stannyl group and the β-carbon of the ynoate occurs with a calculated barrier of 23 kJ mol^{-1} which is only slightly higher than for the corresponding reaction at **10**. From here the reaction takes a different path compared with the ynone reaction, and the product of the reductive elimination is the *syn*-addition vinylcuprate *syn*-**16**, which can then isomerize to *anti*-**16**. For this reaction no allenolate intermediate was found but instead a transition state **17ts** with an allenolate type structure. The energy required for this isomerization was found to be 74 kJ mol^{-1} which is substantially higher than for the corresponding reaction of the ynone (44 kJ mol^{-1}). Due to a stabilizing interaction between the alkoxy oxygen and the tin atom, *anti*-**16** is stabilized relative to *syn*-**16** by 13 kJ mol^{-1}. These results are in agreement with the experimental observations that at low temperature the kinetic product *syn*-**5** is formed in 77% yield, while in the case where the reaction is quenched with aqueous ammonium chloride (thus increasing the temperature), both the kinetic product *syn*-**5** and the thermodynamic product *anti*-**5** are observed, in 24 and 46% percent yields, respectively.

The corresponding carbocupration reaction between **1** and **6** resulted in formation of the *syn*-addition product *syn*-**9** exclusively (Scheme 4), in sharp contrast to the *anti*-addition observed in the stannyl cupration reaction between **1** and **3** (Scheme 3). Our carbocupration results with cyanocuprate **6** are also in sharp contrast to earlier studies where mixtures were obtained when ynoates were reacted with Gilman or Lipshutz reagents.[8–10] Mechanistically the reaction is found to be similar to the one reported by Nakamura and co-workers for carbocuprations with the cuprate Me_2CuLi.[12b] The Cu^{III}-species **19** (Figure 6) reductively eliminates via the transition state **20ts**, which then collapses to the vinylcuprate *syn*-**21**. *syn*-**21** can isomerize to *anti*-**21** via the allenolate intermediate **22**. Energetically, the most favorable of the two vinylcuprates is *syn*-**21** (by 9 kJ mol^{-1}), due to a steric interaction between the tert-butyl group and the α protons in *anti*-**21**. The allenolate **22** via which the isomerization between the vinylcuprates occurs, is 33 kJ mol^{-1} higher in potential energy than *syn*-**21**. The transition states *syn*-**23ts** and *anti*-**23ts** are slightly higher than **22** in potential energy (0.1 and 0.4 kJ mol^{-1}, respectively). An intermediate flanked by such low energy barriers should not be considered a true minimum, but rather a transient point on the potential energy surface, but the energy is still indicative of the barrier the molecule must pass over during isomerization of the vinylcuprates.

Carbocupration reagent **6** was originally chosen for its steric similarity to stannylcupration reagent **3**, and yet, the stereochemical outcome of their reactions with ynone **1** were completely different (Schemes 3 and 4). As mentioned above there are two possibilities for the origin of the stereochemistry, the first being stereoselective protonation of the allenolate intermediate where protonation on the same face as the bulkier group would be hindered (Figure 7). The second possibility is then protonation of the more stable vinylcuprate (Figure 8), which assumes a rapid equilibrium between the two isomers.

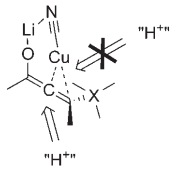

Figure 7. Selective protonation of allenolate (X = Sn or C).

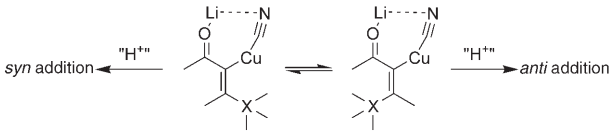

Figure 8. Protonation of the more stable vinylcuprate (X = Sn or C).

If the stereochemistry is set by selective protonation of an allenolate intermediate the outcome would be expected to be the same in both stannyl- and carbocupration. However the experimental results show that this it not the case: carbocupration of **1** yields the *syn*-addition product whereas the stannylcupration of one yields the *anti*-addition product (Schemes 3 and 4). It is thus likely that in both cases the species being protonated are the vinylcuprate intermediates, and that the stereochemistry is determined by the relative stability of these. For the carbocupration reaction the calculations are in good agreement with the experiments, *syn*-**21** that would lead to *syn*-**9** is energetically more favorable than *anti*-**21** by 9 kJ mol^{-1} (Figure 6). For the stannylcupration of **1** the situation is slightly more complex. Since the two vinylcuprates *syn*-**13** and *anti*-**13** in which the lithium ion is still coordinated have been calculated to be isoenergetic, another explanation is needed to rationalize the stereochemistry. The reaction is conducted in THF and therefore it is possible that the lithium ion is dissociated from the vinylcuprate intermediate. This yields the two anionic complexes *syn*-**14** and *anti*-**14**, where *anti*-**14** (which would lead to the observed product upon protonation) is found to be 30 kJ mol^{-1} more stable (22 kJ mol^{-1} with a solvent model). That *anti*-**14** is strongly favored is due to the interaction be-

tween the carbonyl oxygen and the stannyl moiety. The real situation may well be intermediate between the two sets of gas-phase calculations. Even if the lithium ion is still associated in solution, it will be at least partially solvated, bringing the system closer to model **14** than to **13**, and thus into good agreement with the experimentally observed selectivity.

The stereochemical outcome of the stannylcupration of ynoate **2** is in agreement with the computational results. When the protonation occurs at low temperature the only product observed is the kinetic product *syn*-**5**, while when the protons are added as an aqueous solution, and thus the temperature is increased, both the thermodynamic (*anti*-**5**) and the kinetic (*syn*-**5**) products are observed.

Conclusion

A difference in the stereochemical outcome between stannylcupration of ynones and ynoates has been observed, as well as a difference between stannylcupration and carbocupration of ynones. The mechanisms for the transformations have been studied by DFT methods. Combination of the experimental observations and the computational results has led to a rationalization of the differences in mechanism that give rise to the different product distributions. Firstly, the mechanism for the stannylcupration of ynones has been found to be different from the one suggested for carbocuprations. The stereochemical outcome was found to be due to a vinylcuprate intermediate with an interaction between the carbonyl oxygen and the stannyl group. Due to a low barrier for the interconversion between the two vinylcuprate isomers the reaction yields only the thermodynamic product, even at −78 °C. Secondly, the outcome of stannylcupration of ynoates was rationalized to be due to a mechanism in which the kinetic vinylcuprate intermediate is first formed. The barrier for isomerization to the thermodynamic vinylcuprate is large enough for this not to occur at −78 °C, but at higher temperature both the products from the thermodynamic and kinetic intermediates were observed. Thirdly, the carbocupration of ynone **1** was found to yield the opposite product compared to the stannylcupration. This strongly suggests that the stereochemical outcome of these reactions is determined by the relative stabilities of the vinylcuprates, rather than by stereoselective protonation of the allenolate intermediates.

Experimental Section

General methods: ^{1}H (500 MHz) and ^{13}C (125 MHz) NMR spectra were recorded by using $CDCl_3$ as the solvent, and signal positions (δ values) were measured relative to the signals for $CHCl_3$ (7.27) and $CDCl_3$ (77.0), respectively. Tin–hydrogen coupling constants, J(Sn,H), are given as the average of the ^{117}Sn and ^{119}Sn values. IR spectra were obtained for thin films on AgCl plates, and only the strongest/structurally most important peaks (ν_{max}/cm^{-1}) are listed. HRMS was performed at the Department of Chemistry, University of Copenhagen, Denmark. Molecular mass determinations (high-resolution mass spectrometry) for substances containing Me_3Sn are based on ^{120}Sn and made on $[M-R]^+$. All compounds on which HRMS were performed exhibited clean ^{1}H NMR spectra and showed one spot on TLC analysis. TLC analyses were performed on Merck aluminum-backed F254 silica gel plates using UV light, and a solution of 5–10 % phosphomolybdic acid for visualization. All chromatography was performed with the use of Merck silica gel (40–63 μm).Prior to use, THF was distilled under nitrogen from Na/benzophenone. Commercially available compounds were used as received unless otherwise indicated. Saturated ammonium chloride (pH ~ 8) was prepared by addition of aqueous ammonia (25 %; 60 mL) to saturated ammonium chloride (950 mL). Commercial copper(I) cyanide was oven-dried overnight at 150 °C and used without further purification. All reactions were carried out under an atmosphere of dry argon in carefully flame-dried glassware and Schlenk tubes, rigorously excluding oxygen from the reaction mixture. Argon gas was dried by passage through phosphorus pentoxide and silica gel.

General procedure for stannylcupration of α,β-acetylenic ketone and ester: A solution of hexamethylditin (328 mg, 1.0 mmol) in THF (9 mL) was cooled to −20 °C and methyllithium (1.4 M in Et_2O, 0.7 mL, 1.0 mmol) was added dropwise via syringe, and stirring was continued at −20 °C for 15 min to afford a pale yellow solution of trimethylstannyllithium. The mixture was cooled to −78 °C and solid copper(I) cyanide (90 mg, 1.0 mmol) was added in one portion. After 10 min of stirring, the reaction mixture was heated to −45 °C for 10 min to afford a bright orange solution of lithium (cyano)(trimethylstannyl)cuprate. The reaction mixture was cooled to −78 °C before dropwise addition of pent-3-yn-2-one or methyl propiolate (0.33 mmol) in THF (1 mL). The reaction mixture was monitored by TLC, and when all starting material had reacted the reaction was quenched by addition of saturated ammonium chloride (pH ~ 8). The organic phase was washed with brine, dried over magnesium sulfate, and filtered. The solvent was evaporated and the residue purified by flash column chromatography on silica gel (hexane/ethyl acetate) to give the stannylcupration products as colorless oils.

Addition of MeOH: Following the general procedure, with the modification that MeOH (0.6 mmol) and the acetylenic substrate (0.33 mmol) dissolved in the same THF solution (1.0 mL) were added dropwise to the stannylcuprate reaction mixture.

Analytical data for products

(*Z*)-4-(Trimethylstannyl)-pent-3-en-2-one: ^{1}H NMR (500 MHz, $CDCl_3$): δ = 6.85 (m, J(Sn,H) = 120 Hz, 1H), 2.21 (s, 3H), 2.16 (d, J = 2, J(Sn,H) = 46 Hz, 3H), 0.13 (s, J(Sn,H) = 55 Hz, 9H); ^{13}C NMR (125 MHz, $CDCl_3$): δ = 197.4, 172.8, 136.0, 29.9, 26.7, −7.8; IR (neat): $\tilde{\nu}$ = 2967, 1682, 1575, 1431, 1358, 1198 cm^{-1}; HRMS (EI): m/z: calcd for $C_7H_{13}OSn$: 232.9990, found 232.9995 $[M-CH_3]^+$.

(*Z*)-3-(Trimethylstannyl)but-2-enoic acid methyl ester: ^{1}H NMR (500 MHz, $CDCl_3$): δ = 6.40 (m, J(Sn,H) = 118 Hz, 1H), 3.72 (s, 3H), 2.15 (d, J = 2, J(Sn,H) = 45 Hz, 3H), 0.18 (s, J(Sn,H) = 55 Hz, 9H); ^{13}C NMR (125 MHz, $CDCl_3$): δ = 171.8, 168.2, 128.6, 51.4, 26.9, −7.8; IR (neat): $\tilde{\nu}$ = 2950, 1706, 1602, 1435, 1324, 1202 cm^{-1}; HRMS (EI): m/z: calcd for $C_7H_{13}O_2Sn$ 248.9939, found 248.9943 $[M-CH_3]^+$.

(*E*)-3-(Trimethylstannyl)but-2-enoic acid methyl ester: ^{1}H NMR (500 MHz, $CDCl_3$): δ = 5.99 (m, J(Sn,H) = 74 Hz, 1H), 3.69 (s, 3H), 2.39 (d, J = 2, J(Sn,H) = 50 Hz, 3H), 0.18 (s, J(Sn,H) = 54 Hz, 9H); ^{13}C NMR (125 MHz, $CDCl_3$): δ = 168.6, 164.8, 127.4, 50.7, 21.4, −10.0; IR (neat): $\tilde{\nu}$ = 2949, 1718, 1601, 1433, 1344, 1174 cm^{-1}; HRMS (EI): m/z: calcd for $C_7H_{13}O_2Sn$: 248.9939, found 248.9935 $[M-CH_3]^+$.

General procedure for carbocupration of α,β-acetylenic ketone: A mixture of CuCN (90 mg, 1 mmol) in THF (10 mL) was cooled to −40 °C. To the mixture was added alkyl lithium (1 mmol) carefully with stirring. The solution was then stirred at −40 °C for 15 min, and was then cooled to −78 °C, whereafter a solution of the ynone in 1 mL THF was added dropwise. After 10 min of stirring at −78 °C the reaction was quenched by addition of saturated ammonium chloride. The organic phases were separated and the aqueous phase was extracted with Et_2O. The combined organic phases were washed with saturated ammonium chloride and brine, dried over $MgSO_4$ and evaporated to dryness. The crude product was purified by flash chromatography.

Analytical data for 4,5,5-trimethyl-3-hexen-2-one: ^{1}H NMR (500 MHz, $CDCl_3$): δ = 6.13 (m, 1H), 2.19 (s, 3H), 2.10 (s, 3H,), 1.10 (s, 9H). These data are in agreement with literature values.[16] The stereochemistry was further confirmed by NOESY experiments.

Computational details: To include both steric interactions as well as the correct electronics the complete system has been investigated. All calculations were performed with the Jaguar 4.2 build 77 program package[17] using the hybrid functional B3LYP. The basis set used was the LACVP* which applies the 6-31G* for all light elements and the Hay–Wadt ECP and basis set for copper and tin.[18] To simulate solvent the Poisson-Boltzmann self consistent reaction field (PB-SCRF) incorporated in Jaguar 4.2 was used.[18] PB-SCRF is a continuum solvation model, where the molecule is put into a reaction field consisting of surface charges on a solvent accessible surface constructed using a hypothetical spherical solvent probe molecule with the indicated radius. The wavefunction and the reaction field charges are solved iteratively until self-consistency is reached. The parameters for the solvent have been set to ε = 7.43, probe radius = 2.52372 to simulate THF. All transition state structures were confirmed to have one negative frequency. The reaction path from **11ts** was checked by two methods. The first involved gradual decrease of the C–Sn distance by steps of 0.1 Å, fully relaxing all other coordinates at each point, starting with the Cu^{III}-species **10**. In the second method the transition state structure **11ts** was moved in the direction of the imaginary vibration and then minimized with a small trust radius. Both methods led to the allenolate structure **12**.

[1] For a recent review, see: R. K. Dieter in *Modern Organocopper Chemistry* (Ed.: N. Krause), Wiley-VCH, Weinheim **2003**, pp. 79–144.
[2] For examples, see: T. E. Nielsen, S. Le Quement, M. Juhl, D. Tanner, *Tetrahedron* **2005**, *61*, 8013.
[3] a) E. Piers, J. M. Chong, H. E. Morton, *Tetrahedron* **1989**, *45*, 363; b) E. Piers, H. E. Morton, *J. Org. Chem.* **1980**, *45*, 4263.
[4] E. Piers, J. M. Chong, B. A. Keay, *Tetrahedron Lett.* **1985**, *26*, 6265.
[5] J. Thibonnet, V. Launay, M. Abarbri, A. Duchene, J.-L. Parrain, *Tetrahedron Lett.* **1998**, *39*, 4277.
[6] T. E. Nielsen, D. Tanner, *J. Org. Chem.* **2002**, *67*, 6366.
[7] P. Wipf, S. Lim, *J. Am. Chem. Soc.* **1995**, *117*, 558.
[8] T. E. Nielsen, M. A. Cubillo de Dios, D. Tanner, *J. Org. Chem.* **2002**, *67*, 7309.
[9] For examples, see: a) T. J. Houghton, S. Choi, V. H. Rawal, *Org. Lett.* **2001**, *3*, 3615; b) S. Hashimoto, M. Sonegawa, S. Sakata, S. Ikegami, *J. Chem. Soc. Chem. Commun.* **1987**, 24.
[10] K. Nilsson, T. Andersson, C. Ullenius, A. Gerold, N. Krause, *Chem. Eur. J.* **1998**, *4*, 2051.
[11] S. Mori, M. Uerdingen, N. Krause, K. Morokuma, *Angew. Chem.* **2005**, *117*, 4795; *Angew. Chem. Int. Ed.* **2005**, *44*, 4715.
[12] a) N. Yoshikai, T. Yamashita, E. Nakamura, *Angew. Chem.* **2005**, *117*, 4799; *Angew. Chem. Int. Ed.* **2005**, *44*, 4721; b) S. Mori, E. Nakamura, K. Morokuma, *Organometallics* **2004**, *23*, 1081; c) M. Yamanaka, E. Nakamura, *Organometallics* **2001**, *20*, 5675; d) M. Yamanaka, A. Inagaki, E. Nakamura, *J. Comput. Chem.* **2003**, *24*, 1401; e) M. Yamanaka, E. Nakamura, *J. Am. Chem. Soc.* **2005**, *127*, 4697; f) For a recent review, see: S. Mori, E. Nakamura in *Modern Organocopper Chemistry* (Ed.: N. Krause), Wiley-VCH, Weinheim **2003**; pp. 315–340.
[13] N. Zhu, D. G. Hall, *J. Org. Chem.* **2003**, *68*, 6066.
[14] A. Gerold, J. T. B. H. Jastrzebski, C. M. P. Kronenburg, N. Krause, G. van Koten, *Angew. Chem.* **1997**, *109*, 778; *Angew. Chem. Int. Ed. Engl.* **1997**, *36*, 755.
[15] M. John, C. Auel, C. Behrens, M. Marsch, K. Harms, F. Bosold, R. M. Gschwind, P. R. Rajamohanan, G. Boche, *Chem. Eur. J.* **2000**, *6*, 3060.
[16] R. K. Dieter, L. A. Silks, *J. Org. Chem.* **1986**, *51*, 4687.
[17] Jaguar 4.2 program package from Schrödinger Inc., Portland, Oregon: http://www.schrodinger.com.
[18] P. J. Hay, W. R. Wadt, *J. Chem. Phys.* **1985**, *82*, 299.
[19] B. Marten, K. Kim, C. Cortis, R. A. Friesner, R. B. Murphy, M. N. Ringnalda, D. Sitkoff, B. Honig, *J. Phys. Chem.* **1996**, *100*, 11775.

Received: October 6, 2005
Published online: January 19, 2006

Palladium(0) alkyne complexes as active species: a DFT investigation†

Mårten Ahlquist,[a] Giancarlo Fabrizi,[b] Sandro Cacchi[b] and Per-Ola Norrby*[a]

Received (in Cambridge, UK) 2nd June 2005, Accepted 5th July 2005
First published as an Advance Article on the web 20th July 2005
DOI: 10.1039/b507784b

Alkynes have been found to be excellent ligands for Pd(0); the stability of a range of alkyne–Pd(0) complexes, and their reactivity in oxidative addition, have been investigated by DFT methods.

Palladium is one of the most frequently employed transition metals in catalytic organic transformations, in particular for formation of new C–C and C–X bonds.[1] For many catalytic cycles, the resting state is Pd(0), necessitating the use of ligands able to stabilize Pd(0) in solution. By far the most frequently employed ligands are phosphines. These have many excellent properties, but also drawbacks like sensitivity to air and water, and separation problems. Some palladium catalyzed reactions have been proven to proceed as well without as with added phosphines.[2,3] Two closely related examples of reactions that run well without phosphines are the hydroarylation[4] and hydrovinylation[5] reactions, which were first conducted in presence of triphenyl phosphine, but later performed under ligand free conditions (Scheme 1).

It was observed that under these conditions the hydrovinylation reaction did not yield the desired product when the alkyne was added subsequent to the other reagents,[2,3] but proceeded well if as little as five percent of alkyne was present at the initial stage and the rest was added successively. This indicates that alkynes are crucial for stabilization of the presumed active Pd(0) catalyst. Investigations of Pd(0) alkyne complexes as active species are rare,[4] and in no case have the stability and reactivity of the palladium(0) alkyne complexes been studied. Herein we report a systematic DFT investigation of the stability of Pd(0) complexes with several model ligands, both alkynes and other types of frequently employed ligand classes. We also investigate the ability of model complexes to partake in oxidative addition to a model substrate, phenyl iodide.[6]

Palladium(0) has an electron-rich d^{10} electronic configuration, with only one s-orbital available for accepting electrons from the ligand. Recent work has indicated that transition metals do not employ p-orbitals for bonding, but higher coordinations (termed "hypervalent") can be achieved through formation of 3-center-4-electron bonds (ω-bonds).[7] Backbonding forms an essential part of coordination to Pd(0), wherefore good ligands should be π-acceptors. Like electron-deficient alkenes,[8] alkynes have the possibility to interact with filled d-orbitals *via* one of the π*-orbitals (Fig. 1).

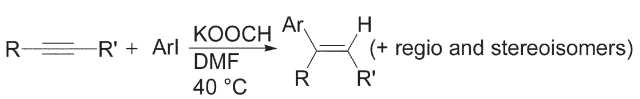

Scheme 1 Typical reaction conditions for the hydroarylation reaction.

Palladium(0) diacetylene has previously been studied by both experimental and theoretical methodologies.[9] The ideal structure was found to be one where the acetylenes are coordinating in a perpendicular fashion, allowing for backdonation from two orthogonal d-orbitals.

In the current study, the structure found for $Pd(HC{\equiv}CH)_2$ is basically identical to the one described by Wang and Andrews (Fig. 1).[9] The effect of replacing one or both of these acetylenes with other ligands is summarized in Table 1. We have included both electron-rich and electron-poor alkynes, formamide as a model for the solvent (DMF), ammonia as a model for simple amines, and both a model phosphine and the real ligand PPh_3.

It is clear that simple alkynes are strongly stabilizing ligands for Pd(0). Replacing one alkyne with any other ligand leads to a strong energy increase (Table 1, entries 6–9), well beyond the expected

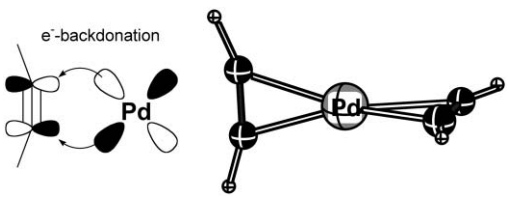

Fig. 1 Backbonding in Pd-acetylenes, and $Pd(H–C{\equiv}C–H)_2$ optimal geometry.

Table 1 Relative potential energies of $Pd^0L^1L^2$ complexes

Entry	L^1	L^2	Relative energy(kJ/mol)
1	H–C≡C–H	H–C≡C–H	0
2	Ph–C≡C–Ph	Ph–C≡C–Ph	26
3	Me–C≡C–Me	Me–C≡C–Me	40
4	OHC–C≡C–H	OHC–C≡C–H	10
5	OHC–C≡C–CHO	OHC–C≡C–CHO	1
6	H–C≡C–H	$HCONH_2$	52
7	H–C≡C–H	NH_3	55
8	H–C≡C–H	PH_3	26
9	H–C≡C–H	PPh_3	13
10	Me–C≡C–Me	PH_3	58
11	Ph–C≡C–Ph	PH_3	33
12	OHC–C≡C–H	PH_3	7
13	OHC–C≡C–CHO	PH_3	−3
14	OHC–C≡C–H	PPh_3	0

[a]*Technical University of Denmark, Kemitorvet Building 201, Dk-2800, Lyngby, Denmark. E-mail: pon@kemi.dtu.dk; Fax: +45 4593 3968; Tel: +45 4525 2123*
[b]*Dipartimento di Studi di Chimica e Tecnologia delle Sostanze Biologicamente Attive, Università degli Studi "La Sapienza", P. le A. Moro 5, 00185, Rome, Italy. E-mail: sandro.cacchi@uniroma1.it; Fax: +39 (06) 4991 2780; Tel: +39 (06) 4991 2795*
† Dedicated to Professor David Tanner on the occasion of his 50th birthday.

confidence range of the methods employed here (*ca.* 10 kJ/mol). In the mixed phosphine/alkyne system (Table 1, entry 8), when the alkyne is substituted with formyls as a model of electron withdrawing groups, the net effect is a strong stabilization, by as much as 29 kJ/mol for butynedial (Table 1, entry 8 *vs.* 13). As expected, electron donating substituents instead destabilize the complex, by 32 kJ/mol for 2-butyne (Table 1, entry 8 *vs.* 10). This is fully in line with the postulate that the most important contribution to the bond strength comes from the backbonding, Fig. 1; electron withdrawing substituents lower the LUMO of the alkyne, thus increasing the energy gain from backbonding.

The structures of these palladium phosphine alkyne complexes have some interesting features. Whereas the ones with more electron-rich alkynes adopt a nearly linear structure, the ones containing the electron-poor alkynes are bent (Fig. 2). This bending effect is most profound for the most electron-poor alkyne butynedial. The backdonation in this complex is so strong that it is more correctly described as a pallada(II)cyclopropene, which should adopt a square planar structure with one open coordination site. Coordination of one more ligand would lead to a complex highly reminiscent of that observed by Elsevier and coworkers for an electron-deficient alkene complex.[8]

Anionic complexes similar to the ones described by Amatore and Jutand have also been studied.[10] To simulate the hydroarylation conditions, we have concentrated on the formate anion, but we have also included one example with an iodide.‡ The results are summarized in Table 2. The trends are similar to those for the neutral complexes. Alkynes substituted with electron withdrawing groups yield more stable complexes (Table 2, entries 4 & 5) and also give pallada(II)cyclopropene structures. This is especially clear in the presence of the potentially bidentate formate ligand: with an electron-rich alkyne, a linear complex is formed, whereas with the electron-poor alkyne, the structure optimizes to a square-planar pallada(II)cyclopropene with a bidentate formate ligand. (Fig. 3).

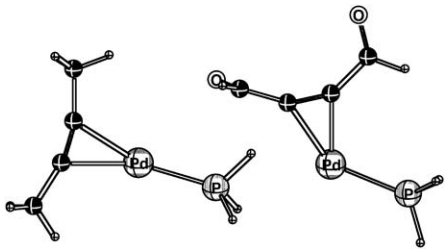

Fig. 2 Left: Pd(Me–C≡C–Me)PH_3, Right: Pd(OHC–C≡C–CHO)PH_3.

Table 2 Relative potential energies of anionic Pd^0LX^- complexes

$$^-OOCH + \left[\text{|||}—Pd—I\right]^- \rightleftharpoons \left[\text{|||}—Pd—OOCH\right]^- \rightleftharpoons \left[L—Pd—OOCH\right]^- + \text{|||}$$

Entry	L	X^-	Relative energy(kJ/mol)
1	H–C≡C–H	$^-$OOCH	0
2	Me–C≡C–Me	$^-$OOCH	23
3	Ph–C≡C–Ph	$^-$OOCH	20
4	OHC–C≡C–H	$^-$OOCH	−40
5	OHC–C≡C–CHO	$^-$OOCH	−53
6	H–C≡C–H	I^-	49
7	(H–C≡C–H)$_2$	$^-$OOCH	−17
8	(OHC–C≡C–H)$_2$	$^-$OOCH	−54

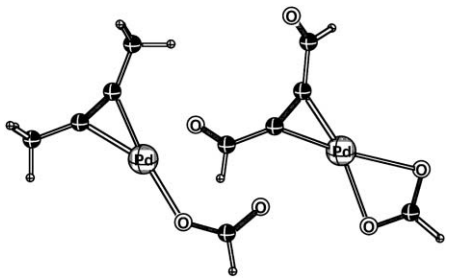

Fig. 3 Left: Pd(Me–C≡C–Me)$OOCH^-$, Right: Pd(OHC–C≡C–CHO)$OOCH^-$.

In the recently introduced nomenclature of Weinhold and Landis,[7] dicoordinate Pd(0) complex can formally be regarded as hypervalent, since both ligands donate into the same orbital on Pd. A third ligand can only be stabilized by backbonding. Two examples of tricoordinated complexes are included in Table 2, entries 7 & 8, which are stabilized by 14–17 kJ/mol relative to the dicoordinated analogs, entries 1 & 4. We note that association is disfavored entropically, by *ca.* 30 kJ/mol at ambient temperature, making dicoordination the favored binding mode, in good agreement with the binding model of Weinhold and Landis.[7]

In many Pd-catalyzed reactions, Pd(0) enters the catalytic cycle through an oxidative addition to yield a Pd(II) complex. Some DFT studies of this reaction step in the presence of phosphine ligands have recently appeared.[11–14] Building on the earlier studies and new results, we have studied four plausible pathways for oxidative addition of model alkyne complexes to phenyl iodide.

Goossen *et al.* have shown that oxidative addition to PhI proceeds *via* initial coordination of I to Pd, followed by rearrangement to a pre-reactive complex where one phenyl C–C bond coordinates to Pd, which then transfers the aryl group from I to Pd.[11] The same path has been located here starting from Pd diacetylene.[6] Formation of the I-coordinated intermediate is calculated to be endothermic by 39 kJ/mol, and rearrangement to the pre-reactive complex **1** costs another 2 kJ/mol.

The actual oxidative addition then takes place *via* a dissociation of the iodide, TS1. This transition state is similar to the ones described by Senn and Ziegler for addition to palladium diphosphines,[12] although it is an earlier transition state with a C–I distance of 2.47 Å. The iodide is only weakly interacting with palladium in the transition state, Pd–I = 3.16 Å. The barrier for oxidative addition from **1** is 54 kJ/mol, which yields an overall barrier of 95 kJ/mol from the separated reactants.

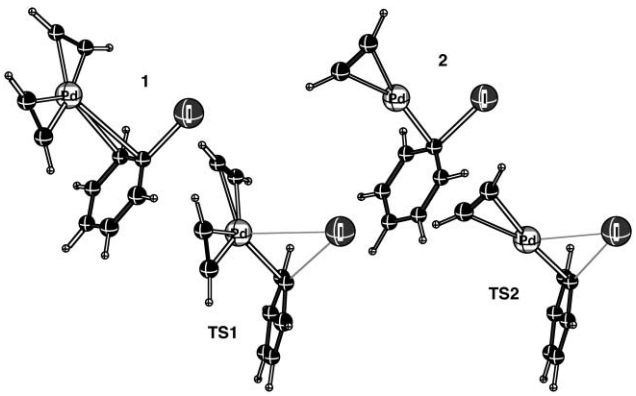

The possibility that complex **1** may dissociate one ligand before the actual oxidative addition has also been considered. Formation of the alternative prereactive complex **2** *via* dissociation of one of the acetylenes is endothermic by 16 kJ/mol relative to **1**. However, the oxidative addition can then take place *via* a concerted transition state (TS2) with a barrier of merely 5 kJ/mol. All together this yields a barrier of 65 kJ/mol from $Pd(HC{\equiv}CH)_2$ and PhI, substantially lower than TS1. In addition, due to the change in molecularity, TS2 is expected to be entropically favored relative to TS1, by approximately 30 kJ/mol at ambient temperature, leading to a very strong preference for TS2. Cundari and coworkers obtained a similar computational result employing phosphine ligands in the gas phase.[14]

We have also considered that anionic ligands may participate in the reaction, as originally suggested by Amatore and Jutand, and later supported by DFT calculations.[10,13] For the reaction of anionic $HCOO^{-}Pd(HC{\equiv}CH)$ with PhI, we were unable to locate a pre-reactive complex, but we could determine a bimolecular TS similar to that for the other paths, TS3, with a calculated barrier of only 69 kJ/mol.

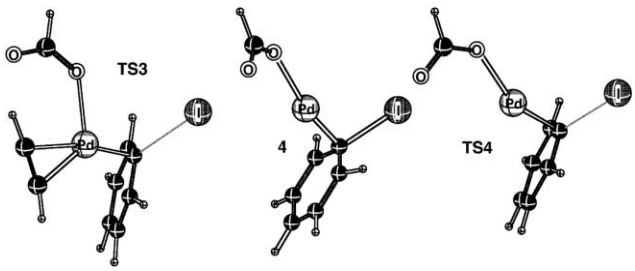

As for the neutral path, one acetylene may dissociate upon coordination of PhI. This exchange yields the anionic species **4** which contains no strongly stabilizing ligand, meaning that acetylene only has acted as a "carrier" of palladium(0). Starting from $HCOO^{-}Pd(HC{\equiv}CH)$ and PhI, the ligand-to-substrate exchange is endothermic by 58 kJ/mol: the palladium species formed is highly reactive and the oxidative addition *via* TS4 takes place with an insignificant barrier of 0.2 kJ/mol.

The calculated potential energy profiles are summarized in Fig. 4. On the free energy surface, both TS1 and TS3 will be destabilized relative to TS2 and TS4 due to the difference in molecularity. Our interpretation is that in the oxidative addition, Pd is only coordinated by the substrate and one additional ligand.

A direct comparison of anionic and neutral paths is strongly dependent on the solvation model, which has not been validated for this type of calculation.† Thus, from the computational results, we cannot conclude whether the neutral or anionic path is preferred. However, for the phosphine system, a strong effect of anions on the rate of oxidative addition has been demonstrated experimentally,[10] and we therefore believe it likely that either TS4 or TS2 can be active, depending on the relative concentration of formate and acetylene in the hydroarylation reaction.

To conclude, alkynes have a substantial stabilizing effect on Pd(0). We predict that alkynes in some cases can be better ligands than phosphines, which are currently the most frequently

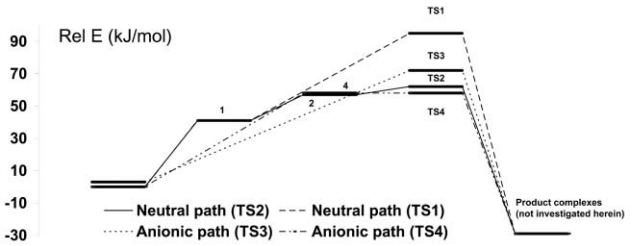

Fig. 4 Calculated reaction paths for oxidative addition to PhI.

employed ligands in reactions catalyzed by Pd(0). Since the use of phosphines brings some practical problems, reactions where alkynes are substrates can in some cases better be performed in the absence of phosphines. Specifically, the success of the "ligand-free" hydroarylation and hydrovinylation of alkynes is rationalized by the current study.[2–5] However, the use of alkynes as ligands in other reactions is limited by the high reactivity of alkynes toward Pd(II) complexes.

Notes and references

‡ We note that direct comparison between neutral and anionic complexes suffers from the low reliability of our solvation model for the difference between localized and metal-centered anions; see ref. 13.

1 E. I. Negishi, Ed., *Handbook of Organopalladium Chemistry for Organic Synthesis*, Wiley-Interscience, New York, 2002.
2 I. P. Beletskaya, *J. Organomet. Chem.*, 1983, **250**, 551; S. Cacchi, G. Fabrizi, F. Marinelli, L. Moro and P. Pace, *Tetrahedron*, 1996, **52**, 10225.
3 A. Arcadi, S. Cacchi, G. Fabrizi, F. Marinelli and P. Pace, *Eur. J. Org. Chem.*, 1999, **12**, 3305.
4 S. Cacchi, M. Felici and B. Pietroni, *Tetrahedron Lett.*, 1984, **25**, 3137.
5 A. Arcadi, E. Bernocchi, A. Burini, S. Cacchi, F. Marinelli and B. Pietroni, *Tetrahedron Lett.*, 1989, **30**, 3465.
6 DFT calculations made with the Jaguar 4.2 program package from Schrödinger Inc., Portland, Oregon: http://www.schrodinger.com. All the calculations were performed at the B3LYP/LACVP* level. The geometries were fully optimized in solvent, simulated with the PB-SCRF model: B. Marten, K. Kim, C. Cortis, R. A. Friesner, R. B. Murphy, M. N. Ringnalda, D. Sitkoff and B. Honig, *J. Phys. Chem.*, 1996, **100**, 11775. The parameters were set to $\varepsilon = 38$ probe radius = 2.47982 to simulate DMF.
7 F. Weinhold and C. Landis, *Valency and Bonding: A Natural Bond Orbital Donor–Acceptor Perspective*, Cambridge University Press, Cambridge, UK, 2005.
8 A. M. Kluwer, C. J. Elsevier, M. Bühl, M. Lutz and A. L. Spek, *Angew. Chem., Int. Ed.*, 2003, **42**, 3501.
9 X. Wang and L. Andrews, *J. Phys. Chem. A*, 2003, **107**, 337; Q. Cui, D. G. Musaev and K. Morokuma, *Organometallics*, 1998, **17**, 1383.
10 C. Amatore, M. Azzabi and A. Jutand, *J. Am. Chem. Soc.*, 1991, **113**, 8375; C. Amatore, M. Azzabi and A. Jutand, *J. Am. Chem. Soc.*, 1991, **113**, 8375; C. Amatore, M. Azzabi and A. Jutand, *J. Am. Chem. Soc.*, 1991, **113**, 8375; S. Kozuch, S. Shaik, A. Jutand and C. Amatore, *Chem. Eur. J.*, 2004, **10**, 3072.
11 L. J. Goossen, D. Koley, H. Hermann and W. Thiel, *Chem. Commun.*, 2004, **19**, 2141; L. J. Goossen, D. Koley, H. Hermann and W. Thiel, *Organometallics*, 2005, **24**, 2398.
12 H. M. Senn and T. Ziegler, *Organometallics*, 2004, **23**, 2980.
13 S. Kozuch, C. Amatore, A. Jutand and S. Shaik, *Organometallics*, 2005, **24**, 2319.
14 T. R. Cundari and J. Deng, *J. Phys. Org. Chem.*, 2005, **18**, 417.

J|A|C|S
ARTICLES
Published on Web 09/09/2006

The Mechanism of the Phosphine-Free Palladium-Catalyzed Hydroarylation of Alkynes

Mårten Ahlquist,[†] Giancarlo Fabrizi,[‡] Sandro Cacchi,[‡] and Per-Ola Norrby*,[†]

Contribution from the Department of Chemistry, Technical University of Denmark, Building 201 Kemitorvet, DK- 2800 Kgs. Lyngby, Denmark, and Dipartimento di Studi di Chimica e Tecnologia delle Sostanze Biologicamente Attive, Università degli Studi "La Sapienza", P.le A. Moro 5, 00185, Rome, Italy

Received March 13, 2006; E-mail: pon@kemi.dtu.dk

Abstract: The mechanism of the Pd-catalyzed hydroarylation and hydrovinylation reaction of alkynes has been studied by a combination of experimental and theoretical methods (B3LYP), with an emphasis on the phosphine-free version. The regioselectivity of the hydroarylation and hydrovinylation shows unexpected differences, which could be attributed mainly to the higher steric demand of the cyclohexenyl group as compared to the phenyl group. Hydroarylation of α,β-acetylenic carbonyl substrates yields a very unusual anti-Michael selectivity, which is shown to result from reaction of the nonconjugated double bond, leaving the conjugation intact. In all cases were the regioselectivities reproduced by the calculations.

Introduction

Over the past decades, palladium-catalyzed reactions have revolutionized synthetic organic chemistry.[1] With reactions such as the Suzuki-coupling[2] and the Heck reaction,[3] completely new tools to construct complex organic molecules have become available. Despite the fact that these methods were developed more than two decades ago, much of the mechanistic detail has not been elucidated to date. Experimental work on phosphine-ligated palladium species improved the understanding of these reactions substantially, although many details are still not fully understood.[4] A number of computational studies on different reaction steps of these reactions have improved the knowledge of the details of different steps in some of the catalytic cycles.[5]

The ligand-free palladium(0)-catalyzed hydroarylation reaction was developed by Cacchi and co-workers (Scheme 1).[6] It contains several challenges and a multitude of steps never described in detail in the literature. The reaction can be viewed as a reductive addition of an aryl iodide to a disubstituted acetylene, with formate acting as the reducing agent. It has been shown that the hydroarylation reaction is an effective protocol for producing trisubstituted alkenes and cyclic derivatives (with properly substituted alkynes) under mild ligand-free reaction conditions. Unfortunately, it has been proven difficult to control the regiochemical outcome of the reaction. Even on acetylenes substituted with a relatively non-bulky aryl on the one end, and a bulky *tert*-butyl group on the other, the addition may be nonregioselective under certain conditions. Quite surprisingly, complete regioselectivity has been observed when reacting a similar *tert*-butyl aryl acetylene, but with the aryl iodide substrate exchanged for a 4-phenyl cyclohexenyl triflate (Scheme 2).[7] In this paper, a rationalization for the observed regiochemical outcome is presented, as well as a full mechanistic investigation of all of the steps in the catalytic cycle of the hydroarylation reaction, by a combination of hybrid density functional (B3LYP) and experimental methods.

Scheme 1. Typical Reaction Conditions for the Phosphine-Free Hydroarylation Reaction

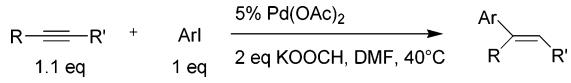

Results and Discussion

Using DFT methods, we have characterized the catalytic cycle of the title reaction, for each step investigating different compositions and geometries. The catalytic cycle consists of oxidative addition, migratory insertion, and reductive elimination as the major steps, but with many possible points on variation,

[†] Technical University of Denmark.
[‡] Università degli Studi "La Sapienza".

(1) Negishi, E. I., Ed. *Handbook of Organopalladium Chemistry for Organic Synthesis*; Wiley-Interscience: New York, 2002.
(2) Miyaura, N.; Yamada, K.; Suzuki, A. *Tetrahedron Lett.* **1979**, *20*, 3437.
(3) (a) Mizoroki, T.; Mori, K.; Ozaki, A. *Bull. Chem. Soc. Jpn.* **1971**, *44*, 581. (b) Heck, R. F.; Nolley, J. P. *J. Org. Chem.* **1972**, *37*, 2320.
(4) (a) Amatore, C.; Pflüger, F. *Organometallics* **1990**, *9*, 2276. (b) Singh, U. K.; Streiter, E. R.; Blackmond, D. G.; Buchwald, S. L. *J. Am. Chem. Soc.* **2002**, *124*, 14104. (c) Casado, A. L.; Espinet, P.; Gallego, A. M.; Martinez-Ilarduya, J. M. *Chem. Commun.* **2001**, 339. (d) Barrios-Landeros, F.; Hartwig, J. F. *J. Am. Chem. Soc.* **2005**, *127*, 6944.
(5) Some selected publications on theoretical palladium chemistry: (a) Siegbahn, P. E. M.; Strömberg, S.; Zetterberg, K. *Organometallics* **1996**, *15*, 5542. (b) Deeth, R. J.; Smith, A.; Hii, K. K.; Brown, J. M. *Tetrahedron Lett.* **1998**, *39*, 3229. (c) Haras, A.; Michalak, A.; Rieger, B.; Ziegler, T. *J. Am. Chem. Soc.* **2005**, *127*, 8765. (d) de Jong, G. T.; Bickelhaupt, F. M. *J. Phys. Chem. A* **2005**, *109*, 9685. (e) Goossen, L. J.; Koley, D.; Hermann, H. L.; Thiel, W. *J. Am. Chem. Soc.* **2005**, *127*, 11102. (f) Popp, B. V.; Thorman, J. L.; Morales, C. M.; Landis, C. R.; Stahl, S. S. *J. Am. Chem. Soc.* **2004**, *126*, 14832. (g) Keith, J. M.; Nielsen, R. J.; Oxgaard, J.; Goddard, W. A., III. *J. Am. Chem. Soc.* **2005**, *127*, 13127.
(6) Cacchi, S.; Fabrizi, G.; Marinelli, F.; Moro, L.; Pace, P. *Tetrahedron* **1996**, *52*, 10225.
(7) Arcadi, A.; Cacchi, S.; Fabrizi, G.; Marinelli, F.; Pace, P. *Eur. J. Org. Chem.* **1999**, *12*, 3305.

10.1021/ja061543x CCC: $33.50

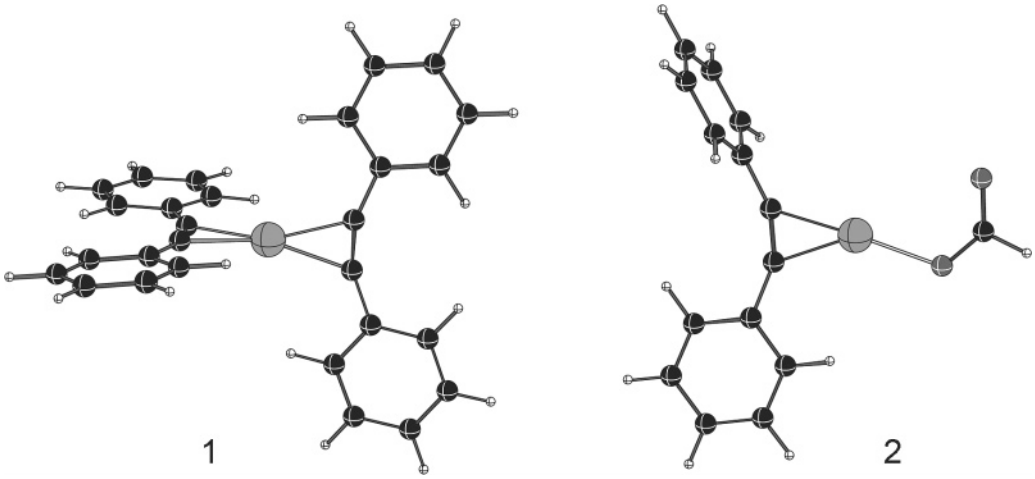

Figure 1. Proposed active species in the hydroarylation, under phosphine-free conditions.

Scheme 2. Regiochemical Outcome of the Hydroarylation and the Hydrovinylation

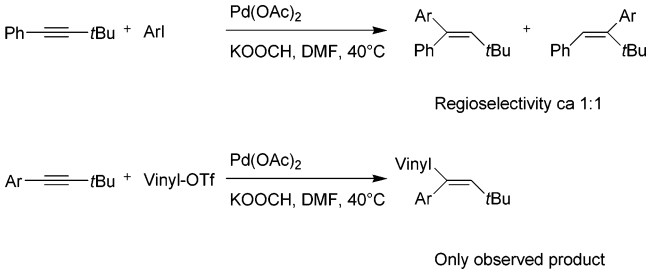

like the exact timing and mechanism of the formate hydride transfer and ligand exchange steps. We will go through the details of each step in order, starting with an analysis of the palladium(0) species present before oxidative addition.

1. Active Catalytic Palladium(0) Species. In the majority of the reactions catalyzed by homogeneous palladium described to date, palladium is ligated to phosphines to keep the active palladium(0) species from precipitating as palladium black. For the hydroarylation reaction, the observation that addition of phosphines did not improve the outcome of the reaction in some cases[6,8] or even can favor the reduction pathway (vide infra) when vinyl triflates are used as the vinyl components[7] led to a change of the protocol. Because the addition of phosphines brings several disadvantages, for example, tedious separation and oxygen sensitivity, the reaction is nowadays mostly performed under ligand-free conditions. As was just mentioned, ligand-free conditions are usually advantageous from a synthetic perspective, but from a theoretical viewpoint it makes the elucidation of the mechanism more challenging. With the phosphines left out, something else must be acting as a stabilizer of palladium(0) to keep active catalyst present in the solution phase. Under typical reaction conditions, there are several possibilities, which include the solvent DMF, the anions formate and iodide, or the substrates aryl iodide and alkyne. The d^{10} electronic configuration of palladium(0) indicates that the ligand should ideally be a strong π-acceptor. In an earlier study of the stability and reactivity of palladium alkyne complexes, it was found that these complexes are surprisingly stable, in some cases even more stable than the palladium phosphine analogues.[9] Two types of complexes were concluded to be the most probable active species, the first one being a neutral complex coordinated to two alkynes, which are strong π-accepting ligands. The second one considered is an anionic complex with one alkyne and one formate ligand because anionic complexes have been proposed as the active species in numerous studies.[9−12] With the theoretical tools employed herein (B3LYP + continuum solvation), we expect a fairly large but systematic error in the absolute solvation energies of anionic species.[13] We have therefore avoided a direct comparison of these two types of complexes, but instead characterized each reaction manifold fully.

In this investigation, we have chosen diphenyl acetylene as the model disubstituted alkyne, because this alkyne has been proven to function well as a substrate in the hydroarylation reaction.[8] The two palladium(0) species most likely to be present in high concentration are then $Pd(PhC{\equiv}CPh)_2$ (**1**) and $[Pd(PhC{\equiv}CPh)OOCH]^-$ (**2**) (Figure 1). The structure of $Pd(PhC{\equiv}CPh)_2$ is such that the two diphenyl acetylene ligands are situated in a perpendicular fashion. The C−C triple bond is prolonged from 1.21 Å in the free diphenyl acetylene to 1.26 Å, as a consequence of the electron backdonation from palladium. In $[Pd(PhC{\equiv}CPh)OOCH]^-$, where the triple bond does not have to compete for the electron density on Pd, the C−C triple bond is slightly longer, 1.27 Å. Both the neutral and the anionic complex are virtually linear across palladium.

2. Oxidative Addition. Oxidative addition of aryl iodides to palladium(0) complexes coordinated to two phosphines has recently been investigated by DFT calculations. Senn and Ziegler described addition to palladium(0) species ligated to a bidentate phosphine.[14] With incorporation of a solvent model in the transition state optimizations, the oxidative addition was shown to proceed via an S_NAr-type mechanism, in contrast to the three-

(8) Cacchi, S.; Felici, M.; Pietroni, B. *Tetrahedron Lett.* **1984**, *25*, 3137.
(9) Ahlquist, M.; Fabrizi, G.; Cacchi, S.; Norrby, P.-O. *Chem. Commun.* **2005**, 4196.
(10) (a) Amatore, C.; Azzabi, M.; Jutand, A. *J. Am. Chem. Soc.* **1991**, *113*, 8375. (b) de Vries, J. G. *Dalton Trans.* **2006**, 421. (c) Amatore, C.; Jutand, A. *Acc. Chem. Res.* **2000**, *33*, 314. (d) Fristrup, P.; Jensen, T.; Hoppe, J.; Norrby, P.-O. *Chem.-Eur. J.* **2006**, *12*, 5352.
(11) (a) Goossen, L. J.; Koley, D.; Hermann, H.; Thiel, W. *Chem. Commun.* **2004**, 2141. (b) Goossen, L. J.; Koley, D.; Hermann, H.; Thiel, W. *Organometallics* **2005**, *24*, 2398. (c) Kozuch, S.; Shaik, S.; Jutand, A.; Amatore, C. *Chem.-Eur. J.* **2004**, *10*, 3072. (d) Kozuch, S.; Amatore, C.; Jutand, A.; Shaik, S. *Organometallics* **2005**, *24*, 2319.
(12) Ahlquist, M.; Fristrup, P.; Tanner, D.; Norrby, P.-O. *Organometallics* **2006**, *25*, 2066.
(13) Ahlquist, M.; Kozuch, S.; Shaik, S.; Tanner, D.; Norrby, P.-O. *Organometallics* **2006**, *25*, 45.
(14) Senn, H. M.; Ziegler, T. *Organometallics* **2004**, *23*, 2980.

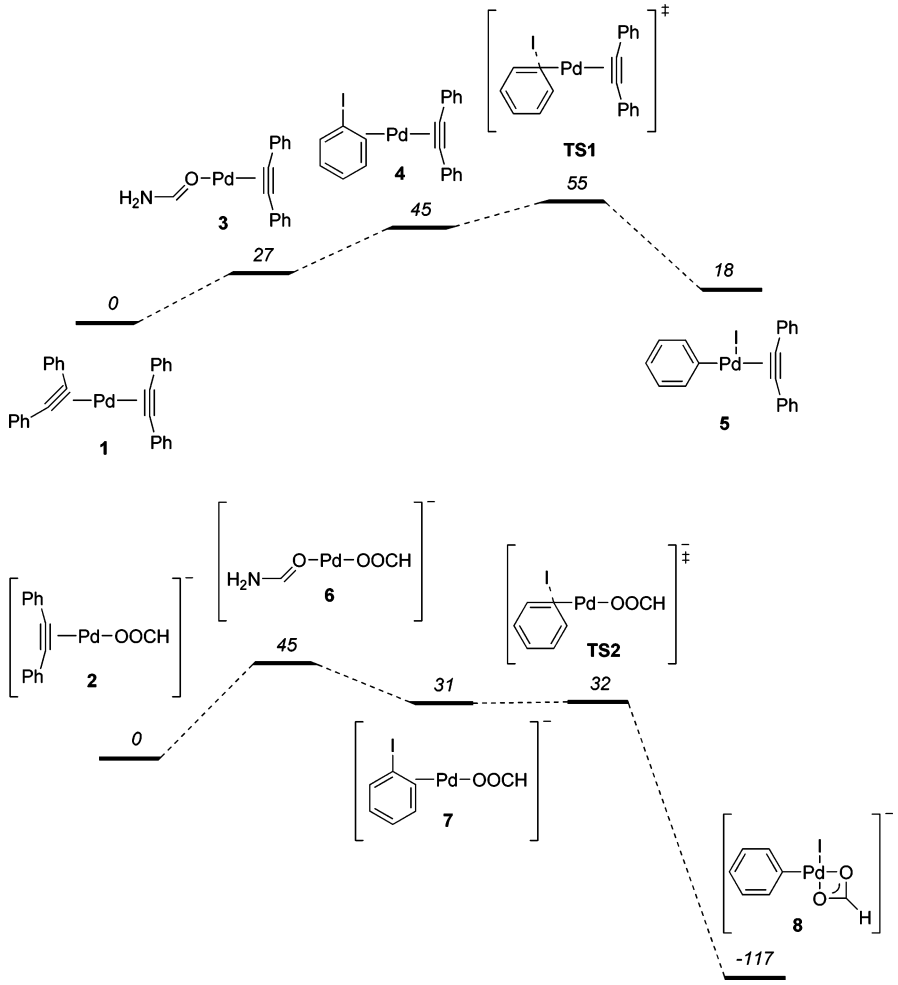

Figure 2. Reaction coordinates for the oxidative addition of phenyl iodide to a neutral and an anionic palladium(0) complex. Numbers in italics represent relative potential energies in kJ/mol.

centered oxidative addition mechanism found in the gas phase, frequently described in text books.[15] Two other groups have studied oxidative addition of phenyl iodide to anionic species of the type $[PdL_2X]^-$, in which the oxidative addition is preceded by decoordination of the anion.[11] Lately, investigations in our group have concluded that the reactive species in palladium-catalyzed oxidative addition of aryl iodide is most likely a low ligated one.[9,12] The reactivity toward oxidative addition of the lower coordinated species, Pd(HC≡CH)(PhI) and $[Pd(OOCH)(PhI)]^-$, was found to be substantially higher than that for the tricoordinate analogues, $Pd(HC{\equiv}CH)_2(PhI)$ and $[Pd(HC{\equiv}CH)(OOCH)(PhI)]^-$.

Ligand exchange at $Pd(PhC{\equiv}CPh)_2$ to dicoordinate complex with a diphenyl acetylene and phenyl iodide Pd(PhC≡CPh)(PhI) is an endothermic reaction by 45 kJ/mol. A possible intermediate in the formation of the prereactive complex is the solvent complex formed by exchange of one of the diphenyl acetylenes by an explicit solvent molecule (formamide has been employed as a model for DMF throughout this investigation). Structurally the prereactive complex **4** is very similar to the previously reported complex Pd(HC≡CH)(PhI),[9] with the phenyl iodide coordinating with the $C_{ipso}C_{ortho}$ double bond to palladium trans to the diphenyl acetylene ligand. The oxidative addition at the prereactive complex Pd(PhC≡CPh)(PhI) takes place via a barrier of 10 kJ/mol (**TS1**). The C−I bond is elongated from 2.20 Å in the prereactive complex to 2.44 Å in the transition state. The product of this reaction is the tricoordinate palladium(II) complex (**5**). Most probably a solvent molecule will fill the free coordination site, to give a complex with the typical square planar structure of d^8-metal complexes.

Another possibility for oxidative addition has also been considered, exchange of the neutral ligand at [Pd(PhC≡CPh)-OOCH]$^-$ to the dicoordinate anionic prereactive complex [Pd(PhI)OOCH]$^-$, possibly via the solvent complex [Pd(formamide)OOCH]$^-$. Formation of the prereactive complex was calculated to be endothermic by 31 kJ/mol. The prereactive complex and the oxidative addition to this species was described in an earlier study,[12] where the oxidative addition was shown to take place basically without any barrier (<1 kJ/mol), which reflects the higher nucleophilicity of the anionic palladium(0) species as compared to the neutral analogue. The immediate product complex is an anionic palladium(II) complex coordinating to phenyl, iodide, and formate in which the formate is coordinating in a bidentate fashion **8**. The exothermicity of the oxidative addition step was calculated to be 117 kJ/mol from the separated reactants and products, respectively. Reaction

(15) (a) Low, J. J.; Goddard, W. A., III. *J. Am. Chem. Soc.* **1986**, *108*, 6115. (b) Ananikov, V. P.; Musaev, D. G.; Morokuma, K. *Organometallics* **2005**, *24*, 715. (c) Sakaki, S.; Biswas, B.; Sugimoto, M. *J. Chem. Soc., Dalton Trans.* **1997**, 803. (d) Sakaki, S.; Kai, S.; Sugimoto, M. *Organometallics* **1999**, *18*, 4825. (e) Sumimoto, M.; Iwane, N.; Takahama, T.; Sakaki, S. *J. Am. Chem. Soc.* **2004**, *126*, 10457.

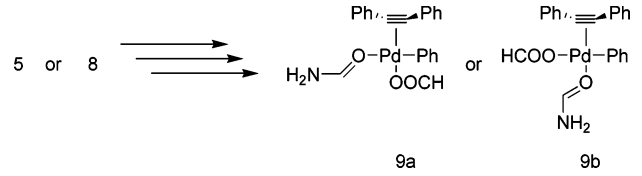

Figure 3. Ligand exchange to the migratory insertion prereactive complex.

coordinates of the oxidative addition reactions are illustrated in Figure 2. As we have shown earlier, the anionic and neutral palladium(0) complexes do not differ significantly in calculated energy.[9] However, the computational comparison depends upon a solvation model using empirically parametrized cavity radii, which to our knowledge has not been validated for comparison of transition metal complexes with differing charge. Thus, the expected uncertainty is larger than the calculated energy difference between the two paths. We will therefore, throughout this work, refrain from direct comparisons between the calculated reaction paths and limit ourselves to the observation that the reaction barrier is lower for the anionic path, in good agreement with the experimental observation that anions increase the rate of oxidative addition to palladium.[10]

3. Ligand Exchange. Before the migratory insertion can take place, a complex with the alkyne in a cis-position to the phenyl must be formed. One of the two coordination sites that do not coordinate the aryl group and the alkyne is likely to coordinate to a formate, because it is present in large excess. To the fourth site of the square planar palladium(II) intermediate, most probably a solvent molecule is coordinated, in this study represented by a formamide. Because the alkyne must be coordinated cis to the aryl, two isomeric complexes should be considered, **9a** and **9b** (Figure 3), which have calculated relative energies of nearly identical magnitude. The coordination mode of the diphenyl acetylene is such that the triple bond is out of the plane.

4. Carbopalladation − Regioselectivity of the Carbopalladation of Alkynes. With the alkyne in a position cis to the aryl group on palladium, a migratory insertion is set to take place. It is in this step that the new carbon−carbon bond is formed and thus also the regiochemical outcome of the reaction is determined. Below follows first a description of the step for the model system, followed by experimental results for different substrates, and finally theoretical results, which rationalize the experimental observations.

4.1. Carbopalladation of PhC≡CPh. Two transition states **TS3a** and **TS3b** for the migratory insertion of PhC≡CPh into the palladium phenyl bond were located, differing only in the relative position of the spectator ligands (formamide and formate). The two transition states were found to be isoenergetic and structurally very similar, and because they are essentially identical in the interesting parts, only the one from the prereactive complex with the formate situated trans to the phenyl will be described. From the structure of the transition state, it

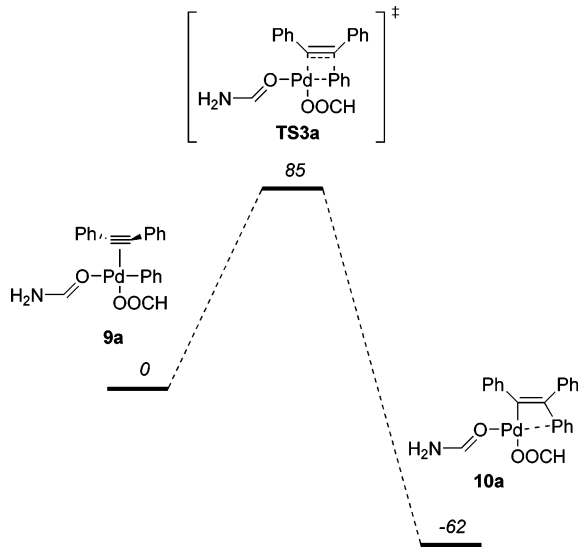

Figure 4. Migratory insertion of PhC≡CPh into the Pd−C_{Phenyl} bond.

appears to be asynchronous. In the transition state, the alkyne has rotated so that it is aligned with its C−C triple bond almost parallel to the Pd−C_{Phenyl} bond. Only a slight elongation of 0.02 to 1.27 Å of the triple bond is observed (1.25 Å in the prereactive complex as compared to 1.35 Å for the resulting double bond in complex **10a**). The Pd−C_{Vinyl} bond, which is formed in this step, is close to being fully formed, with a distance of 2.05 Å (2.00 Å in the resulting vinyl complex). The Pd−C_{Phenyl} bond is, on the other hand, very reactant-like with a bond distance that is basically identical to the one in the prereactive complex, 1.99 and 2.00 Å in **9a** and **TS3a**, respectively. Also, the forming C−C bond is very far from the one in the resulting complex, 2.27 Å in **TS3a** as compared to 1.50 Å in the vinyl complex **10a**. The overall barrier for the carbopalladation step, from the prereactive complex **9a**, was calculated to 86 kJ/mol. The reaction is illustrated in Figure 4.

4.2. Regiochemistry − Experimental. The outcome of the hydroarylation reaction was investigated by reacting phenyl-*t*-Bu-acetylene with 4-iodo-anisole under standard hydroarylation conditions. The overall yield of the reaction was 76%, and the two regioisomers were observed in the ratio outlined in Scheme 3.

The low observed selectivity when one of the substituents on the acetylene is ^{t}Bu is quite surprising. In a previous study of the hydrovinylation reaction, the similar *p*-acetamidphenyl-^{t}Bu-acetylene (**15**) was reacted with 4-phenylcyclohexenyl-triflate (**16**) under the same reaction conditions as above.[7] This yielded product **17** exclusively in 94% yield (Scheme 4).

There are two major differences in the two reactions described above. The first is the change from aryl to vinyl, and the second is the change of leaving group from iodide to triflate. The *para*-substituents on the aryl group of the alkyne have previously been shown to only have a minor influence on the regiochemical

Scheme 3. Product Distribution of the Hydroarylation of Phenyl-^{t}Bu-acetylene

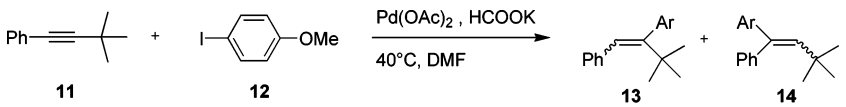

Ratio (**13** : **14**) = 1: 1.1

Scheme 4. Product Distribution in the Hydrovinylation Reaction

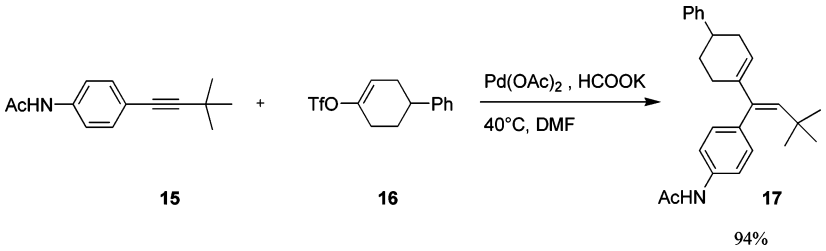

Scheme 5. Product Distribution of the Hydrovinylation Reaction in the Presence of Iodide

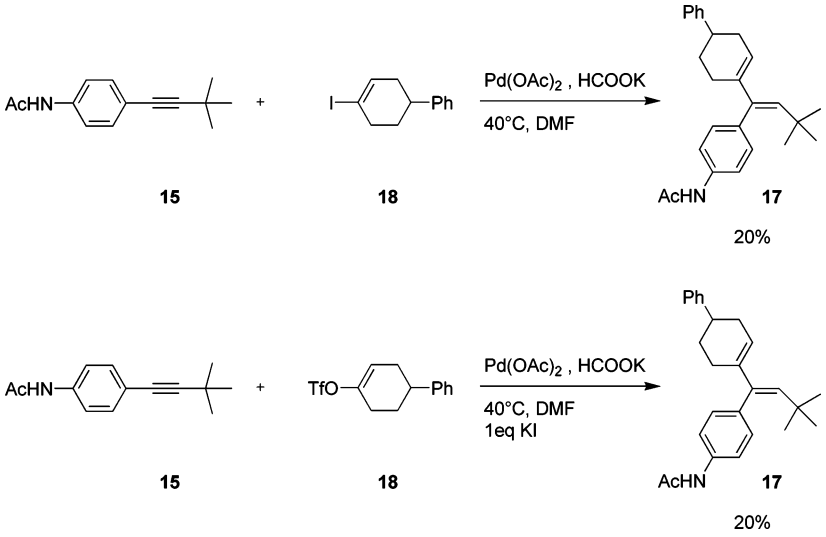

Scheme 6. Observed Regiochemical Outcome of Hydroarylation of **19**[6]

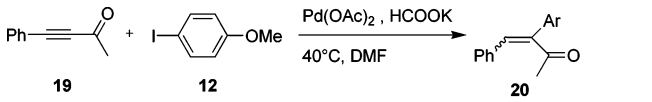

Only isolated regioisomer

Scheme 7. Observed Regiochemical Outcome of the Heck Reaction of **21**[6]

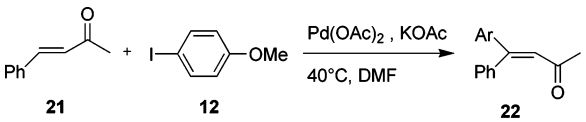

Only isolated regioisomer

outcome.[7] To find out which change in the substrate is responsible for the change in reactivity, two more reactions were conducted. In the first, the vinyl triflate was replaced with the corresponding vinyl iodide **18**, and in the second iodide ion was added as the potassium salt. As Scheme 5 shows, the regio- and stereochemistry is unchanged, and the only hydrovinylation product observed is **17**. The only difference is the yield, which is reduced from 94% to 20%. This is due to reduction of the vinyl electrophile to 4-phenyl-cyclohexene, a frequently observed side reaction under hydroarylation/vinylation reaction conditions. Why the presence of iodide induces reduction of the vinyl−X species is not clear and is not further commented herein. Still, only one regioisomer is observed in the hydrovinylation reaction.

Another interesting observation made previously regarding regiochemical outcome of hydroarylation of alkynes is that α,*β*-acetylenic carbonyls tend to yield the α-addition product and not the more intuitive Michael-addition product (Scheme 6).[6] On the contrary, in the Heck reaction the corresponding alkenes react in the expected manner, yielding the *β*-substituted product (Scheme 7).

4.3. Rationale for the Regiochemistry. 4.3.1. Difference in Regioselectivity between Aryl and Vinyl. A series of transition states for the carbopalladation step of ^{t}BuC≡CPh were characterized by DFT. Both cis/trans isomers with respect to the spectator ligands formate and formamide were studied. For the hydroarylation, phenyl was used as the migrating group, and in the hydrovinylation case 2-butenyl was used as a model for 4-phenyl-cyclohexenyl to include the steric effects induced by the protons present in proximity to the reactive center. The relative energies of the transition states are presented in Figure 5 (only the results of the lowest energy isomers of the respective transition states are reported).

As shown in Figure 5, an excellent agreement was found between the theoretical and the experimental results. In the transition states, the forming carbon−carbon bonds are relatively long, over 2 Å. A consequence of such long distances is that sterics are likely to play a different role than in complexes where the bond distance is closer to what it is in the product. When comparing the geometries of the transition states in Figure 6, three of them appear to have similar steric interactions, **TS4**, **TS5**, and **TS7**. The one that differs is **TS6**, in which introduction of a methyl group in the α-position to the nucleophilic carbon adds substantial steric strain between the methyl group and the *tert*-butyl group of the alkyne.

To further support the hypothesis that the introduction of the α-protons of the 2-butenyl is the cause of the difference in regiochemical outcome, two additional systems were investigated. In the first, the 2-butenyl group was replaced by

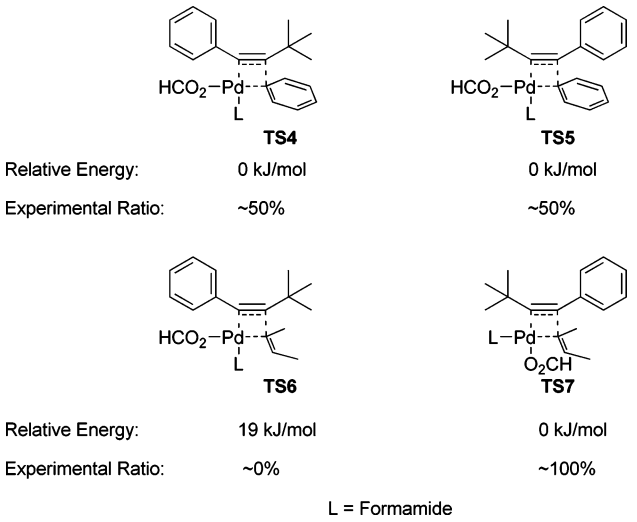

Figure 5. (Top) Relative energies and experimentally observed regioisomer for the migratory insertion of ^{t}BuC≡CPh into a Pd−Aryl bond. (Bottom) Relative energies and experimentally observed regioisomer for the migratory insertion of ^{t}BuC≡CPh into a Pd−2-butenyl bond.

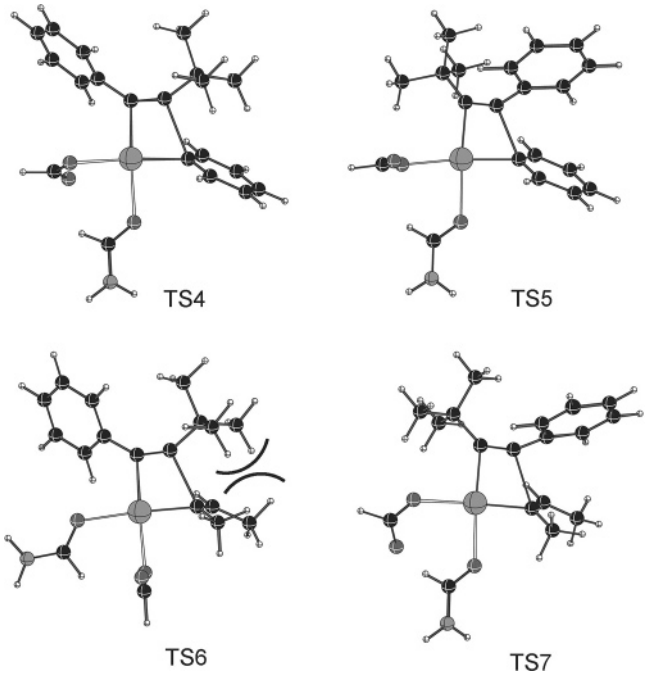

Figure 6. Calculated geometries of hydroarylation and hydrovinylation transition states.

2-butadienyl, a vinylic moiety with steric properties similar to a phenyl. The two regioisomeric transitions states (**TS8** and **TS9**) were found to be close to isoenergetic (Figure 7). In the second system, the ^{t}Bu of the alkyne was replaced by a methyl group, while the 2-butenyl was retained intact. Also, for this system the two regioisomeric transition states (**TS10** and **TS11**) were found to be close to isoenergetic. These results strongly support the view that the sp^3-hybridized carbon substituent on the vinyl group supplies the steric bulk that enables the substrate to differentiate between the ^{t}Bu and Ph substituents and provides a good regioselectivity in the reaction.

4.3.2. α-Insertion versus *β*-Insertion. To model the carbopalladation of α,*β*-acetylenic carbonyls by a Pd−Aryl bond, the

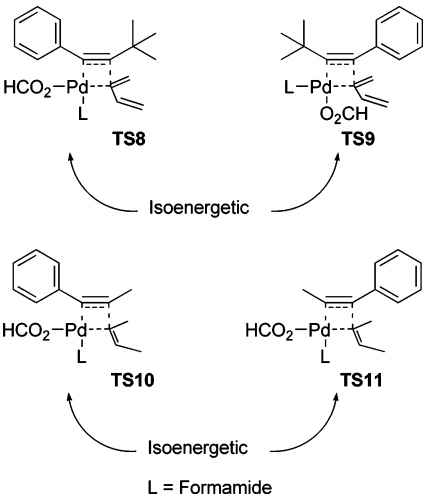

Figure 7. Relative energies of regioisomeric transition states.

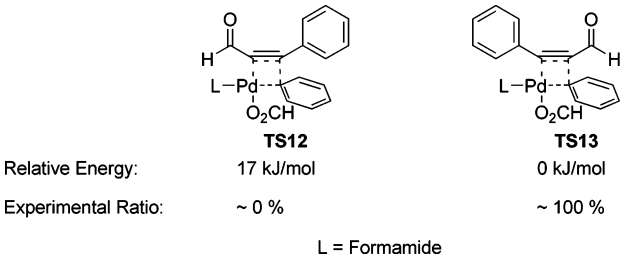

Figure 8. Relative energies and experimentally observed regioisomer for the migratory insertion of PhC≡CCHO into a Pd−Aryl bond (L = formate or formamide).

model alkyne 3-phenyl-pronynal was used. Because two conformations of the carbonyl group are possible, s-cis and s-trans, transition states for both conformations were localized. The results for the s-cis case are shown in Figure 8; the s-trans structures were slightly higher in energy, but gave an almost identical energy difference between the two insertion modes, 15 instead of 17 kJ/mol. As for the system described above, the spectator ligands (formate and formamide) have two possible cis/trans coordination modes, and both isomeric transition states were characterized in every case. In Figure 8, the relative potential energies of the lowest energy forms of the α- and *β*-insertion transition states are shown.

Also for this transformation an excellent agreement between theory and experiments was found, but the rationalization seems to be less straight forward. In most nucleophilic addition reactions to α,*β*-unsaturated carbonyl compounds, one would expect *β*-addition, which is the case in the cuprate additions to the same type of alkynes. Yet, in the hydroarylation the α-addition product is observed experimentally, and also the calculations herein show a clear preference for addition to the α-carbon. While α,*β*-acetylenic carbonyl gives α-addition product, the α,*β*-unsaturated alkene analogue (*E*-benzylideneacetone) reacts mainly at the *β*-carbon in these reactions,[6] indicating some fundamental difference between the alkyne and alkene substrates. In Figure 9, the calculated geometries of one transition state leading to the α- and the *β*-addition products, respectively, are shown. One striking feature is that the reacting *π*-bond of the alkyne is orthogonal to one that is in conjugation with the carbonyl moiety and the *β*-phenyl group. Because the

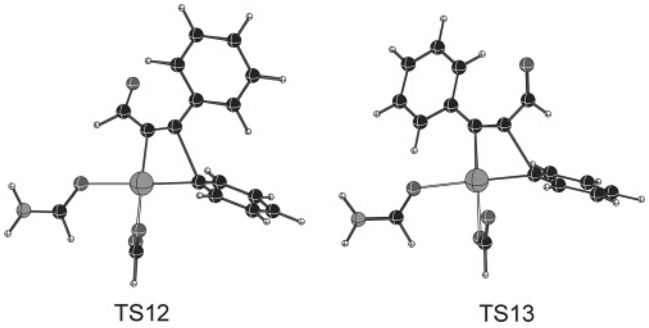

Figure 9. Geometries of transition states for carbopalladation of PhC≡CCHO.

Table 1. Coefficients of π*-Orbitals

molecule	orbital	coefficient α-carbon	coefficient β-carbon
trans-cinnamic aldehyde **23**	π*	0.6869	−0.7267
3-phenyl-propynal **24**	$\pi^*_{\text{conjugated}}$	0.6804	−0.7329
	$\pi^*_{\text{nonconjugated}}$	0.7137	−0.7004

reacting π-bond is not in conjugation with the carbonyl, it is necessary to investigate further the properties of this nonconjugated π-bond.

NBO analyses of *trans*-cinnamic aldehyde (**23**) and 3-phenyl-propynal (**24**), with their respective geometries optimized in planar C_s symmetry, were performed.[16] From these calculations, the coefficients of the p-orbitals that combine to form the π*-orbitals were extracted (Table 1). For the conjugated π*-orbitals, the coefficient is substantially larger on the β-carbon on both **23** and **24**, and thus nucleophilic addition is expected to occur on the β-carbon. This is in accordance with the experimental findings for the Heck reaction of α,β-unsaturated carbonyls,[3b,6] as well as with the observed regiochemistry for cuprate additions.[17] The picture changes completely when looking on the nonconjugated π*-orbital of 4-phenyl-propynal, where the coefficient is actually larger on the α-carbon. The difference is less than for the conjugated π*-orbital, so from an orbital interaction point of view a lower regioselectivity can be expected than for addition to the conjugated π-bond. In a recent investigation of the regioselectivity of the Heck reaction, a dependence of the orbital coefficients as well as of the electrostatic interaction between the reacting atoms was found for the regiochemical outcome of the reaction.[18] The natural charges from the NBO analysis of 3-phenyl-propynal gave values of −0.10 and +0.06 for the α- and β-carbons, respectively. Such partial charges would favor the β-addition product. To summarize, for the alkene substrate **24**, the frontier orbital and charge contributions give a consistent picture in agreement with experiment, whereas for alkyne substrates like **23**, the frontier orbital and charge control arguments are conflicting and inconclusive, and the selectivity seems in fact to be controlled by steric interactions.

5. Palladium Hydride Formation. Before product liberation, a palladium hydride species needs to be formed. One could also envision a mechanism that involves direct hydride transfer from a formate to the vinyl carbon, but no such transition state could be localized. Gradual decrease of the $C_{vinyl}-H_{formate}$ distance in a *cis*-formate-vinyl palladium complex leads to a large increase in energy, yet no complete transfer of the hydride. Instead, a β-hydride elimination mechanism where a hydride is transferred from the formate moiety to palladium was characterized. The starting point was the complex formed in the carbopalladation step, in which the formate is situated in a trans-position to the vinyl **10a**. A transition state was located in which the hydride is transferred to the cis-position relative to the vinyl **TS14**. The geometry of the transition state is such that the formate species is in the plane of the square planar complex, where the hydride is transferring to the site previously coordinating the migrated phenyl group. The barrier was calculated to 71 kJ/mol (94 kJ/mol relative to the most stable formate complex **10b**). Another possibility is hydride formation from the complex in which the formate is situated in a cis-position relative to the vinyl. From here, a different type of transition state was located, **TS15**, one where the formate rotates to form a complex with the formate coordinating with the hydrogen atom to palladium. The barrier for this reaction was calculated to be 99 kJ/mol, and formation of the complex **25** was found to be endothermic by 85 kJ relative to **10b**. Dissociation of CO_2 to yield the palladium hydride complex takes place virtually without any barrier (0.1 kJ/mol). The reactions are outlined in Figure 10.

Both of the transformations described for palladium hydride formation yielded the *cis*-vinyl-hydride palladium species. No transition state for the formation of the *trans*-vinyl-hydride palladium complex could be located. Because the trans-influence of both the vinyl group and the hydride is of substantial magnitude, palladium species with these substituents positioned trans to each other are likely to be highly unstable. To investigate the stabilities of *cis*- and *trans*-vinyl-hydride palladium species, their relative potential energies were investigated for a model system (Figure 11). The results showed that indeed the trans-isomer **28** was much disfavored relative to the cis analogue **27**, by as much as 91 kJ/mol. It is thus concluded that the formation of the hydride does not depend on the formate position in the prereactive complex. The hydride will always end up in the position needed for further reaction, that is, cis to the vinyl moiety.

6. Reductive Elimination − Product Formation. Once the cis palladium hydride vinyl complex (**26a**/**b**) is formed, the final product is obtained through a reductive elimination. A transition state was located (Figure 12), similar to the type described by Diefenbach et al. for the reverse oxidative insertion reaction in the gas phase.[19] From the structure, it is obvious that it is a concerted-type transition state. The forming C−H bond distance was found to be 1.62 Å, a value very close to the ones in the earlier study. The barrier (**TS17**) for the reaction was found to be relatively low, 40 kJ/mol relative to **26b**, and the reaction step can be expected to proceed rapidly. Finally, a palladium(0) alkene complex **29** is formed, and the exothermicity for the transformation of **26b** to **29** was calculated to 96 kJ/mol.

Using a model complex with two formamide molecules coordinated to palladium, no reductive elimination transition state could be located. A gradual decrease of the C−H distance

(16) Glendening, E. D.; Badenhoop, J. K.; Reed, A. E.; Carpenter, J. E.; Weinhold, F. *NBO 4.0*; Theoretical Chemistry Institute, University of Wisconsin: Madison, WI, 1996.
(17) (a) Nilsson, K.; Ullenius, C.; Krause, N. *J. Am. Chem. Soc.* **1996**, *118*, 4194. (b) Ahlquist, M.; Nielsen, T. E.; Le Quement, S.; Tanner, D.; Norrby, P.-O. *Chem.-Eur. J.* **2006**, *12*, 2866.
(18) Deeth, R. J.; Smith, A.; Brown, J. M. *J. Am. Chem. Soc.* **2004**, *126*, 7144.
(19) Diefenbach, A.; de Jong, G. T.; Bickelhaupt, F. M. *J. Chem. Theor. Comput.* **2005**, *1*, 286.

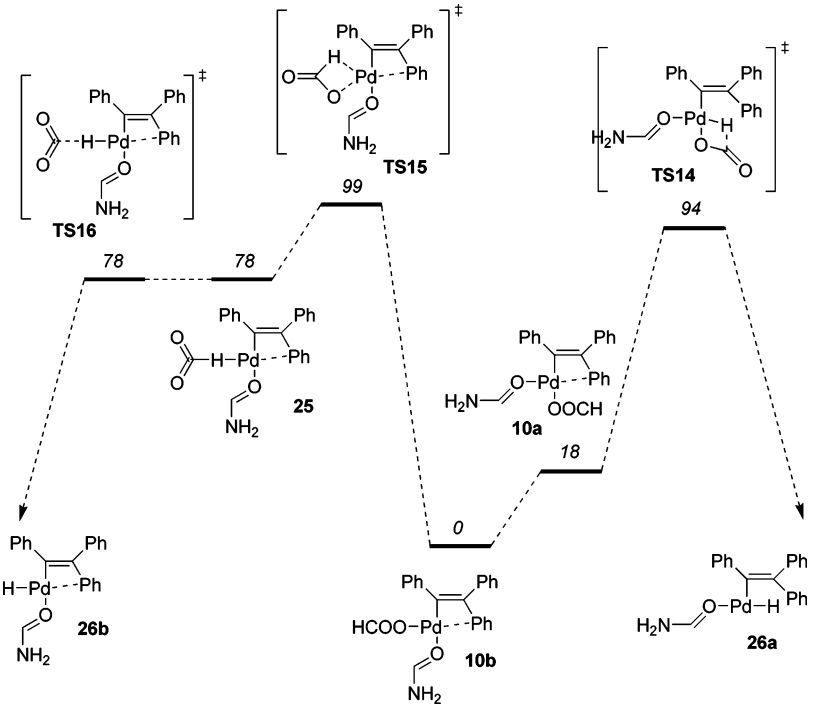

Figure 10. Reaction profile for palladium hydride formation.

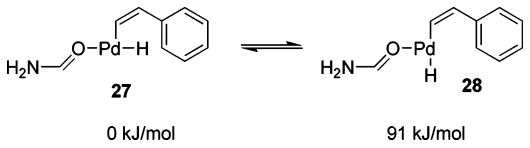

Figure 11. Relative potential energies of cis and trans isomers of a vinyl hydride palladium(II) complex.

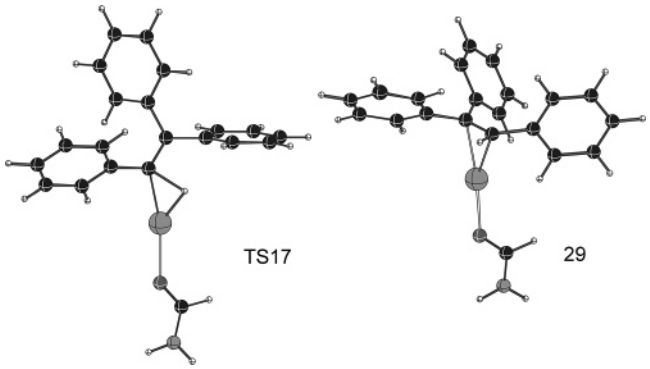

Figure 12. (Left) Geometry of the reductive elimination transition state of the product alkene. (Right) Final palladium(0) alkene complex.

always led to decoordination of one of the formamide ligands. This is likely to be due to the palladium(0)-like structure of the transition state, where a linear dicoordinate structure is expected to be favored.

7. Reductive Path. It has sometimes been observed that instead of formation of the hydroarylation product the aryl is reduced. This is most likely to occur from an intermediate like **9a**, before the *cis*-alkyne-aryl palladium species is formed. A transition state (**TS18**) from **9a** was located. Resulting from this step is a palladium(II) hydride complex **30** where the carbon dioxide is weakly coordinating toward the hydride, similar to the previously described complex **22**. Because the dissociation of CO_2 at **22** has a low barrier and **22** and **30** are structurally very similar, also the dissociation of CO_2 at **30** is assumed to proceed rapidly once **30** is formed. The activation energy for the hydride formation (**TS18**) is 102 kJ/mol, which is higher than the barrier for the migratory insertion and is thus less likely to occur under the reaction conditions described. Caution should be taken, because changing the properties of the reactants or the reaction conditions might very well lead to reduction of the aryl rather than the desired hydroarylation product.

Conclusions

The catalytic cycle for the phosphine-free palladium-catalyzed hydroarylation of alkynes has been characterized by DFT methods. The active catalyst is believed to be Pd^0 ligated by one alkyne and one additional ligand, which can be either another alkyne or a formate. This species can in principle add oxidatively to the electrophilic substrate (e.g., PhI), but we find that oxidative addition is strongly facilitated by loss of one ligand before oxidative addition. This path is also strongly favored by entropy, and we therefore believe it to be of general high importance for oxidative addition reactions.

The favored oxidative addition leads to a tri-coordinate Pd^{II} species, which rapidly adds one additional ligand from solution. Subsequent migratory insertion sets the product regiochemistry. This step has been validated by close reproduction of experimental selectivities in three model reactions, and the differences in regiochemical outcome have been rationalized.

Looking at the electrophilic partner, it is found that aryl groups are insensitive to steric bulk under the conditions that were used, and therefore give a mixture of products, whereas substituted vinyl groups strongly avoid steric hindrance and give substitution at the less hindered position.

The surprising α-substitution observed for carbonyl-substituted alkynes is completely reproduced by the calculations. It

is found that the addition occurs to the nonconjugated double bond in the alkyne, leaving untouched the double bond which is conjugated to the carbonyl, and therefore is determined mostly by steric effects.

The migratory insertion is followed by reaction with formate, expelling carbon dioxide and leaving hydride on palladium. Two different mechanisms were located for this process, one which delivers the hydride to the site occupied by the formate, and one which delivers it to the neighboring site. With these two processes available, the hydride can always be delivered to a position cis to the vinyl group, and this position is also very strongly favored, because both the hydride and the vinyl are strong σ-donors, and therefore avoid being trans to each other. The subsequent reductive elimination occurs with a very low barrier, closing the catalytic cycle.

Experimental Section

All reagents, solvents, and catalysts commercially available were used as received without further purification. Aryl-*t*-butyl-acetylenes were synthesized as described in ref 20. Vinyl triflate **16** was prepared according to the procedure given in ref 21. Vinyl iodide **18** was synthesized from the corresponding vinyl triflate according to ref 22. Reaction products were purified on axially compressed columns, packed with SiO_2 25−40 μm (Macherey Nagel), connected to a Gilson solvent delivery system and to a Gilson refractive index detector, and eluting with *n*-hexane/ethyl acetate mixtures. ^{1}H NMR (400 MHz) and ^{13}C NMR (100.6 MHz) spectra were recorded with a Bruker Avance 400 spectrometer. IR spectra were recorded with a Jasco FT/IR 430 spectrometer.

General Procedure for Hydroarylation/Hydrovinylation of Alkynes. To a stirred solution of **18** (0.139 g, 0.49 mmol) and **15** (0.126 g, 0.59 mmol) in DMF (1.5 mL) were added HCOOK (0.082 g, 0.98 mmol) and $Pd(OAc)_2$ (5.5 mg, 0.024 mmol) under argon. The mixture was stirred at 40 °C. The consumption of starting material **18** was monitored by HPLC. The reaction was quenched when no more **18** remained in the mixture, and subsequently worked up by addition of EtOAc and washing with brine. The organic layer was separated and dried over Na_2SO_4 evaporated under vacuum, and the residue was purified by chromatography on silica gel eluting with a *n*-hexane/AcOEt 70/30 (v/v) mixture to afford 0.037 g of **17** (20% yield), whose IR and NMR spectra are identical to those reported in the literature.[7]

Computational Details

To include both steric interactions as well as the correct electronics, we have included the complete ligand and substrate in all calculations, to avoid artifacts from calculations on small model systems. All calculations were performed with the Jaguar 4.2 program package[23] using the hybrid functional B3LYP.[24] The basis set used was LACVP*, which applies the 6-31G* basis set for all light elements and the Hay−Wadt ECP and basis set for palladium and iodine.[25] To simulate solvent, the Poisson−Boltzmann self-consistent reaction field (PB-SCRF) incorporated in Jaguar 4.2 was used.[26] PB-SCRF is a continuum solvation model, where the molecule is put into a reaction field consisting of surface charges on a solvent accessible surface constructed using a hypothetical spherical solvent probe molecule with the indicated radius.[27] The wavefunction and the reaction field charges are solved iteratively until self-consistency is reached. The parameters for the solvent simulated have been set to 38, probe radius = 2.47982 for DMF.

Transition states were located either by the simple quasi-Newton transition state search starting from a structure resembling that of the transition state, or by a quadratic synchronous transit search. Input geometries for the transition state searches were mostly located by a gradual change of the distances of the bonds forming or breaking.

Acknowledgment. We thank COST for financial support. P.-O.N. is grateful to the Torkil Holm foundation for support.

Supporting Information Available: Cartesian coordinates and absolute energies of calculated geometries. This material is available free of charge via the Internet at http://pubs.acs.org.

JA061543X

(20) Sonogashira, K.; Tohda, Y.; Hagihara, N. *Tetrahedron Lett.* **1975**, 4467.
(21) Stang, P. G.; Treptow, W. *Synthesis* **1980**, 283.
(22) Garcia Martinez, A.; Martinez Alvarez, R.; Garcia Fraile, A.; Subramanian, L. R.; Hanack, M. *Synthesis* **1986**, 222.
(23) DFT calculations were performed with the Jaguar 4.2 program package from Schrödinger Inc., Portland, OR: http://www.schrodinger.com.
(24) Becke, A. D. *J. Chem. Phys.* **1993**, *98*, 5648.
(25) Hay, P. J.; Wadt, W. R. *J. Chem. Phys.* **1985**, *82*, 299.
(26) Marten, B.; Kim, K.; Cortis, C.; Friesner, R. A.; Murphy, R. B.; Ringnalda, M. N.; Sitkoff, D.; Honig, B. *J. Phys. Chem.* **1996**, *100*, 11775.
(27) For a discussion of implicit solvation models, see: Cramer, C. *Essentials of Computational Chemistry: Theories and Models*; Wiley: New York, 2002.

Cross-Coupling

DOI: 10.1002/anie.200600442

Heck Coupling with Nonactivated Alkenyl Tosylates and Phosphates: Examples of Effective 1,2-Migrations of the Alkenyl Palladium(II) Intermediates**

Anders L. Hansen, Jean-Philippe Ebran, Mårten Ahlquist, Per-Ola Norrby, and Troels Skrydstrup**

Considerable efforts have been undertaken by numerous groups in academia and industry over the past decade to expand the repertoire of coupling reagents in palladium(0)-catalyzed cross-coupling reactions.[1] In particular, alkenyl phosphates and tosylates have proven their worth in various cross-coupling reactions, such as the Stille,[2] Suzuki,[2e,f,3] Negishi,[2b] Kumada,[2b,3e,4] Sonogashira,[2b,e,f,5] Buchwald–Hartwig,[4a,6] carbonyl enolate,[3d] and Heck couplings,[7] as effective alternatives to the less stable and typically more expensive alkenyl triflates and nonaflates.[8] However, the majority of this work has focused on the use of activated vinyl phosphates and tosylates, such as α,β-unsaturated systems or α-heteroatom-substituted alkenes, for which the oxidative-addition step is nonproblematic with palladium(0) catalysts bearing aryl phosphine ligands. Less attention has been devoted to nonactivated counterparts, most likely because of the greater difficulty in carrying out the first step of the catalytic cycle, namely the oxidative addition.[3d,4,5,9]

We now report on catalyst systems composed of a palladium complex with a basic, hindered alkyl phosphine that can promote the Heck coupling of nonactivated vinyl tosylates and phosphates with electron-deficient alkenes in good yields, thereby increasing the scope of this important cross-coupling reaction. Furthermore, during these studies we observed an interesting 1,2-isomerization with certain alkenyl tosylates and phosphates under reaction conditions that provide coupling yields as high as 95%. A mechanistic proposal supported by experimental results and DFT calculations is included.

To identify suitable reaction conditions for Heck couplings with nonactivated alkenyl tosylates and phosphates, we examined the use of palladium complexes with the ever increasingly popular bulky electron-rich phosphines.[10] All tosylates and phosphates were prepared from starting ketones by base-promoted proton extraction and reaction with tosyl anhydride (Ts_2O) or $(PhO)_2POCl$, as earlier reported.[4b,11,12] Initial coupling attempts were performed between the tosylate **1** and ethyl acrylate (Scheme 1). After examining a

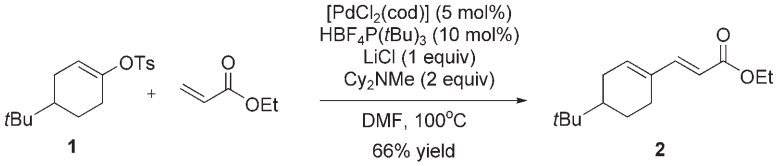

Scheme 1. Heck coupling with a nonactivated vinyl tosylate.

variety of reaction conditions, we noted that a combination of $[PdCl_2(cod)]$ (cod = 1,5-cyclooctadiene; 5 mol%) and the $P(tBu)_3HBF_4$ salt[13] (10 mol%) in the presence of dicyclohexylmethylamine (2 equiv) in dimethylformamide (DMF) at 85°C could furnish the diene **2**, albeit in low yield (approximately 5%). The addition of one equivalent of LiCl, however, had a dramatic effect on the reaction outcome, thus providing a 50% yield of the diene **2** after 24 hours.[14] Increasing the reaction temperature to 100°C improved the coupling yield to 66%. Other reactions conditions, including change of solvent or examination of alternative catalyst combinations, were incapable of promoting the cross-coupling.

To probe the scope of these reaction conditions, we examined the Heck coupling of a variety of alkenyl tosylates

[*] A. L. Hansen, Dr. J.-P. Ebran, Prof. Dr. T. Skrydstrup
The Center for Insoluble Protein Structures (inSPIN)
Department of Chemistry and the Interdisciplinary Nanoscience Center
University of Aarhus
Langelandsgade 140, 8000 Aarhus (Denmark)
Fax: (+45) 8619-6199
E-mail: ts@chem.au.dk
M. Ahlquist, Prof. Dr. P.-O. Norrby
Department of Chemistry, Building 201, Kemitorvet
Technical University of Denmark
DK-2800 Lyngby (Denmark)

[**] We thank the Danish National Science Research Council, the Carlsberg Foundation, and the University of Aarhus for generous financial support of this work.

Supporting information for this article is available on the WWW under http://www.angewandte.org or from the author.

with electron-deficient alkenes and styrene derivatives catalyzed by the $[PdCl_2(cod)]/P(tBu)_3$ combination in the presence of LiCl (Table 1). Generally, all the reactions were completed after 20 h and provided satisfactory coupling yields

Table 1: Heck coupling with nonactivated vinyl tosylates.

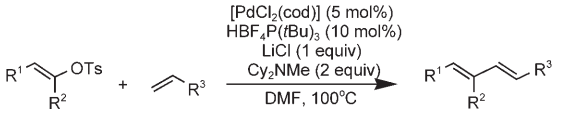

Entry	Vinyl tosylate	t [h]	Product	Yield [%][a]
1	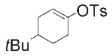	23	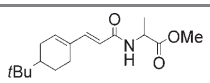	64
2		16	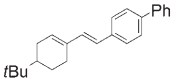	99
3		17	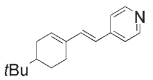	88
4		17	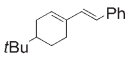	96
5		17	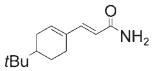	92
6	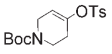	19	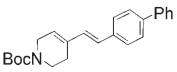	70
7		6	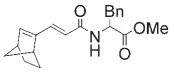	51
8		3	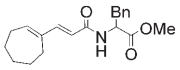	83
9		18	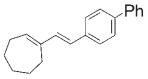	94
10		18	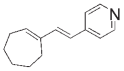	79
11		3	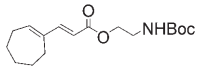	97
12		21	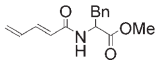	56

[a] Yield of the isolated product.

as high as 99%. Six- and seven-membered cyclic alkenyl tosylates proved particularly effective for these coupling reactions, although reactions with larger rings were unsuccessful. The coupling of the readily available vinyl tosylate to the acrylamide (Table 1, entry 12) demonstrates the potential of this methodology for the simple introduction of a vinyl unit to an α,β-unsaturated amide. Hence, the application of alkenyl tosylates in Heck couplings provides a straightforward means for the preparation of functionalized butadienes from simple starting materials.

Unexpectedly, the normal coupling product was not isolated in the reaction between 1-*tert*-butylvinyl tosylate and styrene. Rather the product from an apparent 1,2-migration of the intermediate alkenyl palladium(II) species was obtained in good yield (79%; Table 2, entry 1).[15] This

Table 2: Heck coupling of alkenyl tosylates with isomerization.

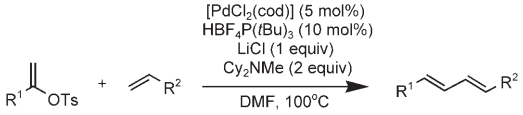

Entry	R^1	t [h]	Product	Yield [%][a]
1	*t*Bu	4	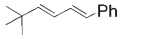	79
2	*t*Bu	20	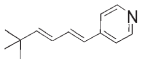	93
3	*t*Bu	23	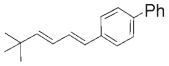	95
4	*t*Bu	20	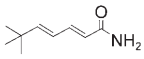	72
5	*t*Bu	3	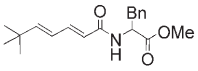	80[b]
6	*t*Bu	24	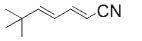	83[c]
7	$SiMe_3$	16	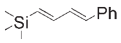	33

[a] Yield of isolated product; unless noted all selectivities of isomerized versus normal Heck products were >95:5. [b] Isomerized/normal products = 10:1. [c] *cis*/*trans* mixture = 1:1.

result is in stark contrast to recent observations by Reissig and co-workers, in which the Heck coupling between the corresponding vinyl nonaflate and methyl acrylate under phosphane-free conditions was reported to give the expected coupling product.[12c] Nevertheless, coupling of the same vinyl tosylate with a variety of alkenes revealed this isomerization to be quite effective with yields attaining 95% and with exclusive *trans* selectivity in all but one case (Table 2, entries 2–6). The use of acrylonitrile (Table 2, entry 6) led to a 1:1 mixture of *cis*/*trans*-isomerized products undoubtedly because of the small size of the nitrile group. One example was attempted with a 1-trimethylsilylvinyl tosylate (Table 2, entry 7). Although its coupling to styrene led to considerable degradation, a 33% yield of the rearranged coupling product could be secured, thus indicating the feasibility of such isomerizations, even with silyl-substituted alkenes, although further optimization is required.[16]

This isomerization–coupling step was also expanded to alkenyl phosphates (Table 3). 1-*tert*-Butylvinyl *O*,*O*-diphenyl phosphate behaved similarly as with the tosylate and coupled effectively to styrene, *p*-phenylstyrene, and 4-vinylpyridine (Table 3, entries 1, 2, and 4, respectively). Interestingly, these reactions proved to be more sensitive to the solvent employed. Whereas dioxane was the solvent of choice in entries 1 and 2, DMF was more adequate in the coupling with the vinyl pyridine. C–C bond formation to the styrene derivatives in DMF only provided coupling yields in the order of 20%. Additional examples with two acrylamides and one acrylate (Table 3, entries 3, 5, and 6) also revealed these substrates to be effective for Heck couplings with isomerization, whereas attempts with acrylonitrile were unsuccessful. In all cases, the diene products were the result of an apparent rearrangement, although in three cases an approximate 9:1 ratio of the isomerized and the normal Heck coupling products was detected (Table 3, entries 3, 5, and 6).

Table 3: Heck coupling of alkenyl phosphates with isomerization.

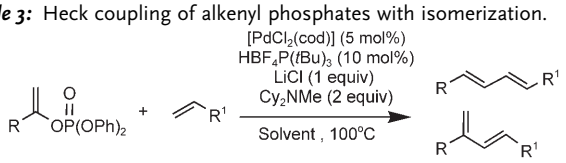

Entry	R	Solvent	*t* [h]	Major product (isomerized/normal)[a]	Yield [%][b]
1	*t*Bu	dioxane	24	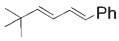	65
2	*t*Bu	dioxane	24	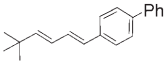	75
3	*t*Bu	DMF	24	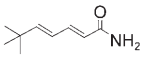	71
4	*t*Bu	DMF	24	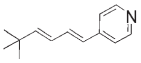 (89:11)	64
5	*t*Bu	DMF	24	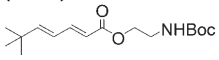 (90:10)	77
6	*t*Bu	DMF	24	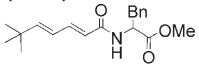 (88:12)	68
7	Ph	dioxane	18	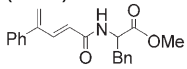	12
8	Ph	DMF	20	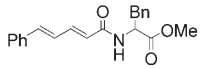 (4:3)	51

[a] Unless noted all selectivities of isomerized versus normal Heck products were > 95:5. [b] Yield of the isolated products.

Finally, a noteworthy solvent effect on the isomerization was observed in the Heck coupling with α-styryl *O*,*O*-diphenylphosphate (Table 3, entries 7 and 8). The reaction of acrylamide with this vinyl phosphate in dioxane was slow but nevertheless afforded 12% yield of the nonisomerized product and recovered starting material after 24 h. In contrast, the same Heck coupling performed in DMF led to a 4:3 mixture of the isomerized and normal Heck products. Recent work by Hartwig and co-workers has shown that isomerization does not take place for Kumada couplings with α-styryl tosylate in toluene.[4b] Hence, it is interesting to note how subtle changes in both structure and solvent can have a marked influence on the isomerization process in these Heck couplings.

A conceivable mechanism for this 1,2-migration involves an initial β-hydride elimination of the palladium(II) species after the oxidative-addition step to give an intermediate alkyne-coordinated palladium hydride species.[17] To gain further insight into the plausibility of this reaction mechanism, a DFT study was conducted for the *tert*-butyl vinyl substrates (Figure 1).[18] The starting point for the calculations was a T-shaped complex **3** that coordinated $P(tBu)_3$, a chloride ion, and the *tert*-butyl vinyl group. Under the experimental reaction conditions, chloride ions are present in the reaction solution; thus, it is likely that a chloride ion displaces the leaving-group anion (tosylate or phosphate). Due to the large steric bulk of the *tert*-butyl alkene and $P(tBu)_3$, they are likely to be positioned *trans* to each other. Palladium(II) complexes containing $P(tBu)_3$ have previously been shown to form tri-coordinate T-shaped complexes rather than the more commonly observed tetra-coordinate square-planar-type complexes.[19] A free coordination site is therefore available to facilitate a potential hydride elimination from any group containing a β hydrogen, as the need for decoordination of a ligand prior to the actual elimination is not present.

From complex **3**, there are then two possibilities, either coordination and insertion of the olefin, or initial 1,2-palladium migration with subsequent coordination and insertion of the olefin. A transition state **TS1** was characterized in which the hydride is transferred to the palladium center, thus yielding the *tert*-butyl acetylene hydride palladium(II) com-

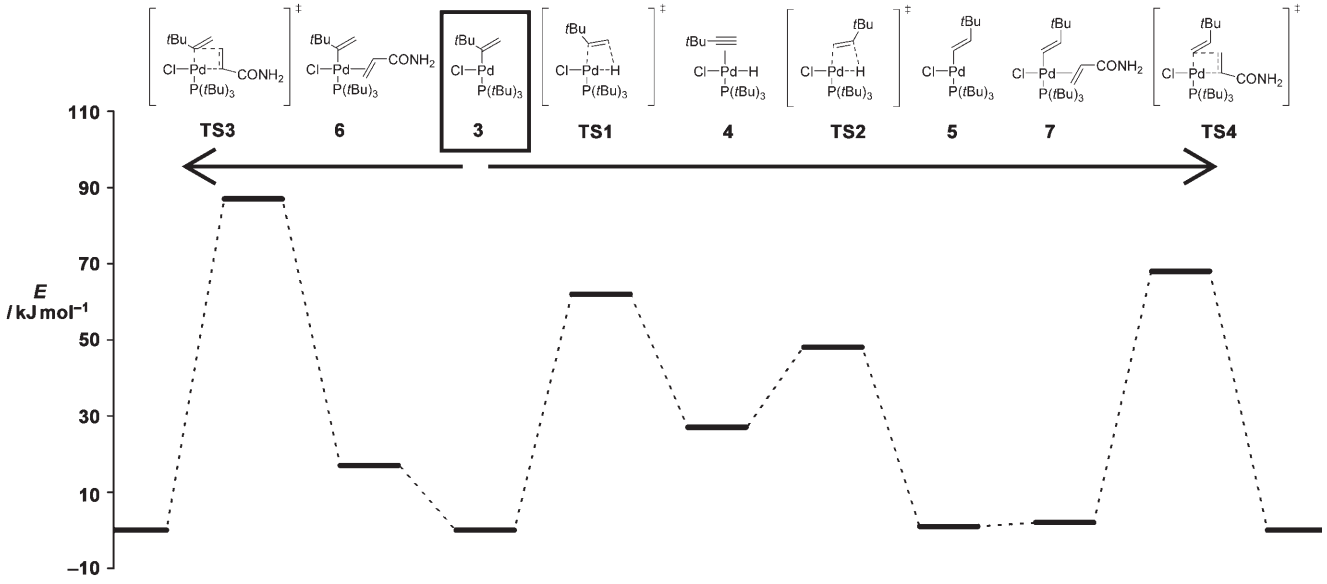

Figure 1. Schematic presentation of the relative energies of the structures **3**–**7** and **TS1**–**TS4**.

plex **4**. The transformation was calculated to proceed with a barrier of 62 kJ mol^{-1}, and the intermediate **4** was found to be 27 kJ mol^{-1} higher in potential energy than **3**. Subsequent insertion of *tert*-butyl acetylene in the Pd–H bond proceeds via **TS2** to yield the isomeric terminal *tert*-butyl vinyl palladium(II) complex **5**. The barrier from **4** was calculated to be 21 kJ mol^{-1}, and the overall isomerization reaction from **3** to **5** is basically thermoneutral, with **5** having a potential energy 1 kJ mol^{-1} above that of **3**. To conclude, the highest barrier for isomerization between the two isomeric palladium–vinyl intermediates was calculated to be 62 kJ mol^{-1} (**TS1**). With such a low barrier, the reaction is likely to proceed rapidly under the reaction conditions. Still, to observe scrambling it is necessary that the barrier for isomerization is lower than the carbopalladation of the olefin. The difference in energy between the barriers for the insertion step then determines the product outcome, thus representing a typical Curtin–Hammett situation.

Further calculations are in support of this hypothesis. Coordination of an olefin (here acrylamide) with **3** yields the prereactive complex **6**, and subsequent insertion takes place via **TS3** with an overall barrier of 87 kJ mol^{-1} relative to **3**. The barrier for the β-hydride elimination described above was found to be 25 kJ mol^{-1} lower in potential energy and is thus several orders of magnitude more rapid than the insertion of acrylamide.[20] At the isomerized complex **5**, coordination of acrylamide results in complex **7**. The insertion occurs via **TS4** with an overall calculated barrier of 68 kJ mol^{-1}, 19 kJ mol^{-1} lower than **TS3**, from which we conclude that the path that leads to the isomerized product is strongly favored.

Finally, some experimental support for this migration was obtained from a coupling experiment between *p*-phenylstyrene and the dideuterated vinyl tosylate **8** (Scheme 2). Under identical coupling conditions with the nonlabeled tosylate, a 72% yield of the diene **9** was isolated in which migration of one deuterium atom was observed.[21]

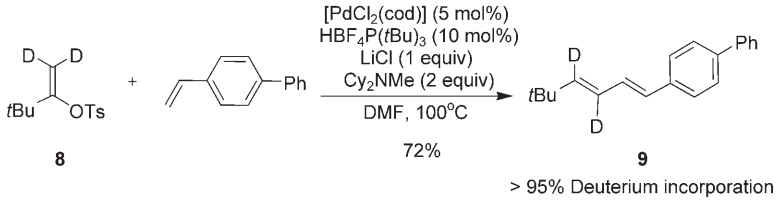

Scheme 2. Isomerization studies with a dideuterated substrate **8**.

In conclusion, we have demonstrated the potential for nonactivated vinyl tosylates and phosphates to be worthy substrates for Heck couplings with electron-poor alkenes and styrene derivatives. Furthermore, effective 1,2-migrations of the alkenyl palladium(II) intermediate has been observed, thus providing a new variation of the Heck coupling. A feasible path for this rearrangement has been located using DFT methods. Further work is currently underway to identify more effective conditions under which the catalyst loading can be lowered and the selectivity to produce either the normal or the isomerized Heck products can be controlled. This work will be reported in due course.

Experimental Section

(*E*)-4-(2-(4-*tert*-Butylcyclohex-1-enyl)vinyl)pyridine: 4-Vinyl pyridine (84 μL, 0.78 mmol), 4-*tert*-butylcyclohex-1-enyl tosylate (60.0 mg, 0.19 mmol), Cy_2NMe (83 μL, 0.38 mmol; Cy = cyclohexyl), LiCl (8.2 mg, 0.19 mmol), and $HBF_4P(tBu)_3$ (5.6 mg, 0.019 mmol) were dissolved in DMF (3 mL). $[PdCl_2(cod)]$ (2.8 mg, 0.0097 mmol) was then added, and the sample vial was fitted with a teflon-sealed screwcap and removed from the glovebox. The reaction mixture was heated for 16 h at 100 °C. After completion, water was added to the crude reaction mixture, followed by extraction with diethyl ether (3 × 25 mL). The organic phases were washed with water (3 × 10 mL) and brine, dried over $MgSO_4$, and concentrated in vacuo. The crude product was purified by flash chromatography on silica gel using ethyl acetate/pentane (1:2) as the eluent, thus affording 41.3 mg of the title compound (88% yield) as a colorless solid. ^{1}H NMR (400 MHz, CD_3CN): $\delta = 8.45$ (d, 2H, $J = 6.4$ Hz), 7.32 (d, 2H, $J = 6.4$ Hz), 7.06 (d, 1H, $J = 16$ Hz), 6.40 (d, 1H, $J = 16$ Hz), 6.05 (t, 1H, $J = 2.8$), 2.47–2.42 (m, 1H), 2.27–2.10 (m, 2H), 2.02–1.93 (m, 2H), 1.32 (ddt, 1H, $J =$ 11.2, 4.8, 1.6 Hz), 1.20 (dq, 1H, $J = 11.2$, 5.2 Hz), 0.90 ppm (s, 9H); ^{13}C NMR (100 MHz, CD_3CN): $\delta = 151.0$, 146.3, 137.2, 136.5, 135.2, 123.31, 121.5, 45.1, 32.8, 28.7, 27.5, 26.5, 24.6 ppm; HRMS $C_{17}H_{23}N$ [M+H$^+$]; calcd: 242.1909; found: 242.1902.

Received: February 2, 2006
Published online: April 11, 2006

Keywords: 1,2-migration · alkenes · Heck reaction · phosphates · tosylates

[1] a) A. de Meijere, F. Diederich, *Metal-Catalyzed Cross-Coupling Reactions*, 2nd ed., Wiley-VCH, Weinheim, **2004**; b) J. Tsuji, *Palladium Reagents and Catalysts, New Perspectives For the 21st Century*, Wiley, Chicester, **2004**; c) *Handbook of Organopalladium Chemistry for Organic Synthesis* (Ed.: E. Negishi), Wiley-Interscience, New York, **2002**.

[2] a) K. C. Nicolaou, G.-Q. Shi, J. L. Gunzner, P. Gärtner, Z. Yang, *J. Am. Chem. Soc.* **1997**, *119*, 5467; b) K. C. Nicolaou, G.-Q. Shi, K. Namoto, F. Bernal, *Chem. Commun.* **1998**, 1757; c) J. Jiang, R. J. DeVita, G. A. Doss, M. T. Goulet, M. J. Wyvratt, *J. Am. Chem. Soc.* **1999**, *121*, 593; d) C. Buon, P. Bouyssou, G. Coudert, *Tetrahedron Lett.* **1999**, *40*, 701; e) F. L. Galbo, E. G. Occhiato, A. Guarna, C. Faggi, *J. Org. Chem.* **2003**, *68*, 6360; f) D. Steinhuebel, J. M. Baxter, M. Palucki, I. W. Davies, *J. Org. Chem.* **2005**, *70*, 10124.

[3] a) F. Lepifre, C. Buon, R. Rabot, P. Bouyssou, G. Coudert, *Tetrahedron Lett.* **1999**, *40*, 6373; b) F. Lepifre, S. Clavier, P. Bouyssou, G. Coudert, *Tetrahedron* **2001**, *57*, 6969; c) J. Wu, L. Wang, R. Fathi, Z. Yang, *Tetrahedron Lett.* **2002**, *43*, 4395; d) H. N. Nguyen, X. Huang, S. Buchwald, *J. Am. Chem. Soc.* **2003**, *125*, 11818; e) U. S. Larsen, L. Martiny, M. Begtrup, *Tetrahedron Lett.* **2005**, *46*, 4261; f) J. M. Baxter, D. Steinhuebel, M. Palucki, I. W. Davies, *Org. Lett.* **2005**, *7*, 215.

[4] a) A. H. Roy, J. F. Hartwig, *J. Am. Chem. Soc.* **2003**, *125*, 8704; b) M. E. Limmert, A. H. Roy, J. F. Hartwig, *J. Org. Chem.* **2005**, *70*, 9364.

[5] D. Gelman, S. L. Buchwald, *Angew. Chem.* **2003**, *115*, 6175; *Angew. Chem. Int. Ed.* **2003**, *42*, 5993.

[6] A. Klapars, K. R. Campos, C.-y. Chen, R. P. Volante, *Org. Lett.* **2005**, *7*, 1185.

[7] a) J. W. Coe, *Org. Lett.* **2000**, *2*, 4205; b) X. Fu, S. Zhang, J. Yin, T. L. McAllister, S. A. Jiang, T. Chou-Hong, K. Thiruvengadam, F. Zhang, *Tetrahedron Lett.* **2002**, *43*, 573; c) A. L. Hansen, T. Skrydstrup, *J. Org. Chem.* **2005**, *70*, 5997; d) A. L. Hansen, T. Skrydstrup, *Org. Lett.* **2005**, *7*, 5585.

[8] For mechanistic studies on oxidative addition with aryl tosylates, see reference [4a] and A. H. Roy, J. F. Hartwig, *Organometallics* **2004**, *23*, 194.
[9] For a few examples of cross-coupling reactions that employ Ni catalysis, see: a) W. R. Baker, J. K. Pratt, *Tetrahedron* **1993**, *49*, 8739; b) Y. Nan, Z. Yang, *Tetrahedron Lett.* **1999**, *40*, 3321; c) J. Wu, Z. Yang, *J. Org. Chem.* **2001**, *66*, 7875.
[10] For references on the development and application of bulky electron-rich phosphines for cross-coupling reactions, notably through the work of Fu, Buchwald, Hartwig, and Beller, see: A. Zapf, M. Beller, *Chem. Commun.* **2005**, 431.
[11] The synthesis of vinyl tosylates and phosphates was prepared according to reference [4b] through proton abstraction of the required ketones with lithium hexamethyldisilazide (LiHMDS) in THF and subsequent treatment with tosyl anhydride or diphenyl chlorophosphate.
[12] The lithium enolate required for the preparation of vinyl tosylate from Table 1, entry 12 was prepared from cyclofragmentation from lithiated THF; see: a) R. B. Bates, L. M. Kroposki, D. E. Potter, *J. Org. Chem.* **1972**, *37*, 560; b) M. E. Jung, R. B. Blum, *Tetrahedron Lett.* **1977**, *18*, 3791; c) I. M. Lyapkalo, M. Webel, H.-U. Reissig, *Eur. J. Org. Chem.* **2001**, 4189.
[13] M. R. Netherton, G. C. Fu, *Org. Lett.* **2001**, *3*, 4295.
[14] The rate acceleration effect of added halide ions to Pd-catalyzed cross-coupling reactions has been proposed to be a result of a medium effect and a more reactive halide-coordinated Pd^0 species; for a recent discussion on the effect of added halide ions with relevant references, see reference [8]. As our previous results in Heck couplings with activated vinyl tosylates suggest that the tosylate is not bound to the alkenyl palladium(II) species after oxidative addition[7c,d] in solvents such as dioxane and, undoubtedly also, DMF, we suggest that added LiCl assures that the reaction passes through a neutral pathway in these Heck couplings by trapping the Pd^{II} cationic intermediate.
[15] A couple of examples of this migration have been reported in two other cross-coupling reactions, although in modest yield; see reference [4b] and J. Takagi, K. Takahashi, T. Ishiyama, N. Miyaura, *J. Am. Chem. Soc.* **2002**, *124*, 8001.
[16] For a recent review on 1,4-migrations, see: S. Ma, Z. Gu, *Angew. Chem.* **2005**, *117*, 7680; *Angew. Chem. Int. Ed.* **2005**, *44*, 7512; .
[17] Along with a mechanism involving β-hydride elimination, an alternative explanation was proposed by Hartwig and co-workers in the 1,2-migration observed for the Kumada couplings with vinyl tosylates.[4b] The presence of a strong base was suggested to induce elimination of the tosylate, thus leading to an alkyne. We do not believe this mechanism holds for these Heck couplings because of the weak base used in these coupling reactions. N. Frydman, R. Bixon, M. Sprecher, Y. Mazur, *J. Chem. Soc. Chem. Commun.* **1969**, 1044.
[18] DFT calculations were carried out with the Jaguar 4.2 program package from Schrödinger Inc., Portland, Oregon: http://www.schrodinger.com. All the calculations were performed at the B3LYP/LACVP* level. The geometries were fully optimized in solvent and simulated with the PB-SCRF model: B. Marten, K. Kim, C. Cortis, R. A. Friesner, R. B. Murphy, M. N. Ringnalda, D. Sitkoff, B. Honig, *J. Phys. Chem.* **1996**, *100*, 11775. The parameters were set to $\varepsilon = 38$, probe radius = 2.47982 to simulate DMF.
[19] J. P. Stambuli, C. D. Incarvito, M. Bühl, J. F. Hartwig, *J. Am. Chem. Soc.* **2004**, *126*, 1184.
[20] As the β-hydride elimination is a unimolecular process, while the olefin insertion is bimolecular, the β-hydride is also strongly favored entropically. Earlier studies have shown that a value of approximately 40–60 kJ mol^{-1} should be added to account for the change in molecularity; see: a) M. S. Searle, M. S. Westwell, D. H. Williams, *J. Chem. Soc. Perkin Trans. 2* **1995**, *1*, 141; b) T. K. Woo, P. E. Blöchl, T. Ziegler, *J. Phys. Chem. A* **2000**, *104*, 121; c) M. Ahlquist, P. Fristrup, D. Tanner, P.-O. Norrby, *Organometallics* **2006**, DOI: 10.1021/om060126q.
[21] A cross-over experiment was also performed with the 1-*tert*-butylvinyl tosylate by the addition of 1-hexyne representing a less hindered alkyne. No hydropalladation and subsequent coupling to an alkene was observed with this alkyne, thus suggesting that the insertion step is probably faster than dissociation of the *tert*-butylacetylene from the palladium hydride intermediate.

Theoretical Evidence for Low-Ligated Palladium(0): [Pd−L] as the Active Species in Oxidative Addition Reactions

Mårten Ahlquist, Peter Fristrup, David Tanner, and Per-Ola Norrby*

Department of Chemistry, Technical University of Denmark, Building 201 Kemitorvet, DK-2800 Kgs. Lyngby, Denmark

Received February 9, 2006

The oxidative addition of PhI to Pd^0 has been studied by DFT with a continuum representation of the solvent. It is shown that the preferred number of ligands on palladium is lower than would be expected from "conventional wisdom" and the 18-electron rule. The most favored oxidative addition is obtained when Pd is coordinated by only the aryl iodide and one additional ligand in a linear arrangement. The calculations indicate that p-orbitals on the central metal are *not* involved in bonding in any of the complexes described herein, in good agreement with classic ligand field theory and also with a recent bonding analysis by Weinhold and Landis, but in apparent violation of the 18-electron rule.

Introduction

Palladium(0) phosphine complexes are among the most versatile transition metal catalysts used for organic synthesis,[1] applications including an array of C−C and C−X cross-coupling reactions,[2,3] and isomerizations of alkenes.[4] One of the most commonly employed palladium phosphine catalysts is $Pd(PPh_3)_n$, which is either generated in situ from a palladium(II) salt or added directly as Pd^0 (some commonly employed sources are $Pd(PPh)_4$ or $Pd(dba)_2 + 2\ PPh_3$). Several studies have dealt with the mechanism of Pd^0-catalyzed reactions, the majority leading to the conclusion that the active species is a "highly unsaturated" 14-electron complex $Pd(PPh_3)_2$, with a low-energy nonreactive "less unsaturated" 16-electron complex $Pd(PPh_3)_3$ as the major species in solution.[5] The first step in the generally accepted catalytic cycle is oxidative addition of ArX (Figure 1), which has sometimes been suggested to be the rate-limiting step, particularly for X = Cl. The use of aryl chlorides is highly desirable for economic reasons, and thus a detailed understanding of the oxidative addition mechanism is important for further methodological improvements. For some Pd^0-catalyzed transformations, addition of anions such as chloride increases the reaction rate, which has been explained by formation of a tricoordinate anionic $[Pd(PPh_3)_2X]^-$ species, which is suggested to be more reactive than the neutral $Pd(PPh_3)_2$ complex.[6] However, under phosphine-free reaction conditions, monoligated palladium has been suggested to be the active species.[7] Recent theoretical results also challenge the generally accepted view on ligation state and stability. It is increasingly becoming recognized that transition metals do *not* employ p-orbitals for bonding and thus have only a valence shell of one s- and five d-orbitals, which can accommodate up to 12 electrons with "normal" bonding. Coordination numbers beyond this depend on the formation of linear three-center−four-electron bonds (ω-bonds), which employ only one metal orbital for bonding to two ligands.[8] Overall, this new view of bonding in metal complexes can rationalize all observations that earlier were perceived as being a result of the 18-electron rule. This new view also quite naturally includes phenomena like square planar d^8-complexes, which have always been viewed as exceptions.

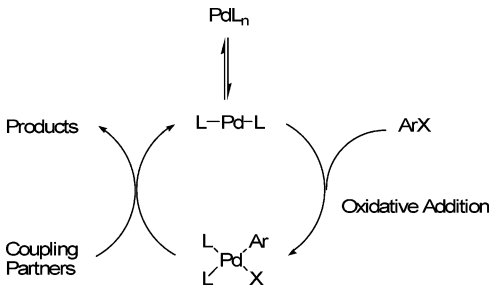

Figure 1. "Textbook" mechanism for palladium(0)-catalyzed cross-coupling reactions.

Herein are reported the results of a theoretical study on the stability of both neutral and anionic palladium complexes containing one, two, or three ligands, as well as the relative reactivity of these complexes toward oxidative addition of phenyl iodide. The effect of the coordination number on stability and reactivity is then discussed in more detail.

Results

Neutral Complexes of the Type PdL_n. For a number of palladium(0) complexes containing n ligands ($n = 1-3$) the

* To whom correspondence should be addressed. Fax: +45 4593 3968. Tel: +45 4525 2123. E-mail: pon@kemi.dtu.dk.

(1) Negishi, E. I., Ed. *Handbook of Organopalladium Chemistry for Organic Synthesis*; Wiley-Interscience: New York, 2002.

(2) (a) Milstein, D.; Stille, J. K. *J. Am. Chem. Soc.* **1978**, *100*, 3636. (b) Miyaura, N.; Yamada, K.; Suzuki, A. *Tetrahedron Lett.* **1979**, *20*, 3437. (c) Negishi, E.; Okukado, N.; King, A. O.; Van Horn, D. E.; Spiegel, B. I. *J. Am. Chem. Soc.* **1978**, *100*, 2254. (d) Mizoroki, T.; Mori, K.; Ozaki, A. *Bull. Chem. Soc. Jpn.* **1971**, *44*, 581, (e) Heck, R. F.; Nolley, J. P. *J. Org. Chem.* **1972**, *37*, 2320. (f) Cacchi, S.; Felici, M.; Pietroni, B. *Tetrahedron Lett.* **1984**, *25*, 3137.

(3) (a) Louie, J.; Hartwig, J. F. *Tetrahedron Lett.* **1995**, *36*, 3609. (b) Guram, A. S.; Rennels, R. A.; Buchwald, S. L. *Angew. Chem., Int. Ed. Engl.* **1995**, *34*, 1348.

(4) Trost, B. M.; Schmidt, T. *J. Am. Chem. Soc.* **1988**, *110*, 2301.

(5) (a) Mann, B. E.; Musco, A. *J. Chem. Soc., Dalton Trans.* **1975**, *16*, 1673. (b) Fauvarque, J-. F.; Pflüger, F.; Troupel, M. *J. Organomet. Chem.* **1981**, *208*, 419. (c) Amatore, C.; Pflüger, F. *Organometallics* **1990**, *9*, 2276.

(6) Amatore, C.; Azzabi, M.; Jutand, A. *J. Am. Chem. Soc.* **1991**, *113*, 8375.

(7) Ahlquist, M.; Fabrizi, G.; Cacchi, S.; Norrby, P.-O. *Chem. Commun.* **2005**, *33*, 4196.

(8) Weinhold, F.; Landis, C. *Valency and Bonding: A Natural Bond Orbital Donor−Acceptor Perspective*; Cambridge University Press, 2005.

10.1021/om060126q CCC: $33.50
Publication on Web 03/17/2006

Scheme 1. Oxidative Addition Takes Place on Either a Di- or Tricoordinate Palladium(0) Complex[a]

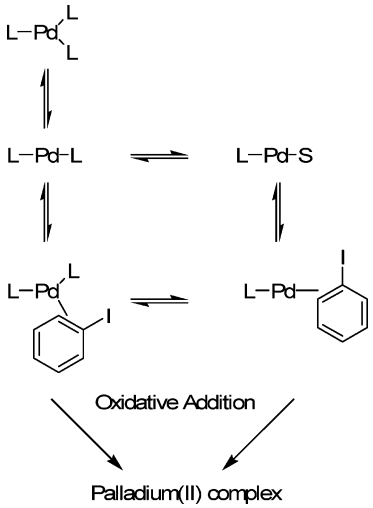

[a] In the current work the stabilities and reactivities of these are investigated.

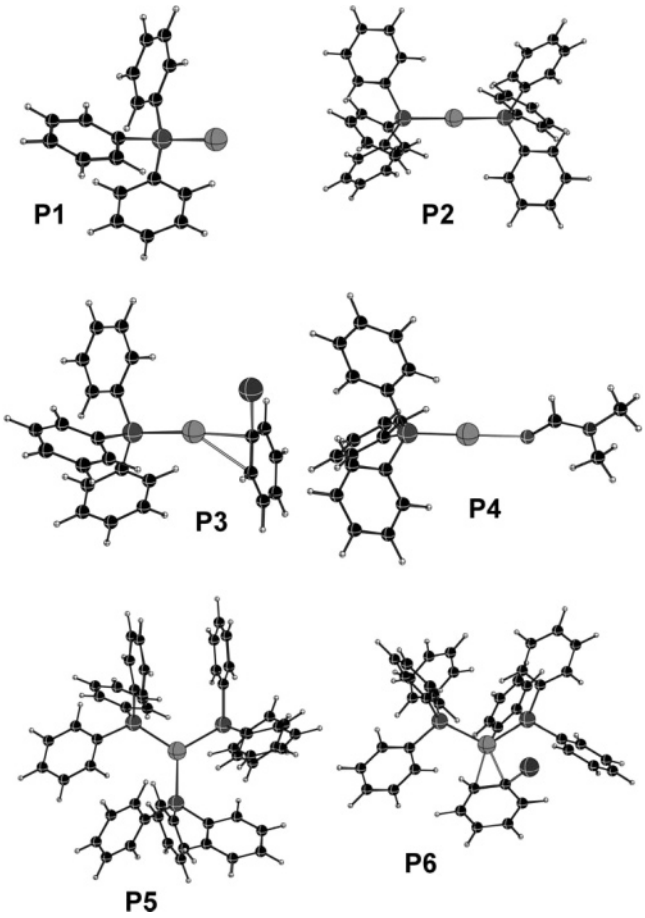

Figure 2. Structures of neutral palladium(0) complexes.

geometries have been optimized both in the gas phase and with a solvent model describing DMF, a commonly employed solvent in these types of reactions (Figure 2). Relative gas-phase free energies, potential energies in solution, and estimated free energies in solution are presented in Table 1.

The gas-phase calculations show a strong stabilization of 82 kJ/mol on going from $PdPPh_3$ to $Pd(PPh_3)_2$. Coordination of a third PPh_3, on the other hand, was found to lead to destabilization by as much as 44 kJ/mol. When applying a solvent model in the calculations, the results are similar when going from $PdPPh_3$ to $Pd(PPh_3)_2$, although less in favor of the dicoordinate species than for the gas-phase calculations. More interesting is that formation of tricoordinate $Pd(PPh_3)_3$ is found to be endergonic by 84 kJ/mol in solution. This value is of such magnitude that it can be expected that the concentration of $Pd(PPh_3)_3$ is basically infinitesimal. Replacing one phosphine in $Pd(PPh_3)_2$ with an explicit DMF solvent molecule was found to be endergonic by 43 kJ/mol. The difference between the monocoordinate complex P1 and the solvent complex P4 gives an indication of the limitations of the continuum solvation model. The continuum cannot give an accurate description of actual coordination of the solvent to the metal, but the effect of including an explicit coordinating solvent molecule is still relatively small, giving a contribution of only 10 kJ/mol.

Table 1. Relative Potential Energies (kJ/mol) of a Series of Neutral Pd^0 Complexes

entry	complex	CN[a]	ΔG_{gas}	ΔE_{DMF}	"ΔG_{DMF}"[b]
P1	$Pd(PPh_3)$	1	82	102	53
P2	$Pd(PPh_3)_2$	2	0	0	0
P3	$Pd(PPh_3)(PhI)$	2	60	53	46
P4	$Pd(PPh_3)DMF$	2	63	40	43
P5	$Pd(PPh_3)_3$	3	44	26	84
P6	$Pd(PPh_3)_2(PhI)$	3	100	68	124

[a] Coordination number of Pd. [b] See Computational Details.

Table 2. Relative Potential Energies (kJ/mol) of $[PdL_nCl]^-$

entry	complex	CN[a]	ΔE_{DMF}	"$\Delta G_{Estimate}$"[b]
Cl1	$[Pd(PPh_3)Cl]^-$	2	0	0
Cl2	$[Pd(PhI)Cl]^-$	2	35	35
Cl3	$[Pd(DMF)Cl]^-$	2	50	50
Cl4	$[Pd(PPh_3)_2Cl]^-$	3	32	72
Cl5	$[Pd(PPh_3)(PhI)Cl]^-$	3	50	90

[a] Coordination number of Pd. [b] See Computational Details.

The monocoordinate complex $Pd(PPh_3)$ has an unexceptional structure, with a Pd−P bond of 2.24 Å. The dicoordinate complexes (Table 1, entries P2 and P3) are all linear, or nearly so. In $Pd(PPh_3)_2$, the Pd−P bonds are elongated by 0.1 to 2.34 Å, due to the trans-influence. In $Pd(PPh_3)$DMF the Pd−P bond is shorter, 2.23 Å, a value that clearly shows the weak trans-influence of a neutral oxygen atom. The two tricoordinate complexes adopt a trigonal structure, almost perfectly so for both $Pd(PPh_3)_3$ and $Pd(PPh_3)_2(PhI)$, in which the P−Pd−P angle is 114°. In the $Pd(PPh_3)_3$ complex the Pd−P distances are calculated to be 2.41, 2.40, and 2.39 Å, respectively. In accordance with the view of Weinhold and Landis,[8] the three phosphines all donate into the *same* 5s-orbital on palladium (a four-center−six-electron bond), weakening the bond to each individual phosphine compared to the dicoordinated state. All the descriptions above are for the complexes optimized in DMF. The gas-phase optimization yielded essentially identical structures.

Anionic Complexes of the Type $[PdL_nCl]^-$. Anionic complexes with n neutral ligands ($n = 1-2$) and one chloride have been characterized. All have been fully optimized with a solvent model using parameters for DMF (Table 2).

A similar trend is seen for the anionic complexes as for the neutral ones; that is, going from a dicoordinate species to a tricoordinate one does not lead to further stabilization, but rather to destabilization. The two dicoordinate complexes that do not contain any triphenylphosphine are found to be relatively stable, not sufficiently so to be present in detectable amounts, but most definitely of a low enough energy to allow them to be intermediates in a catalytic cycle.

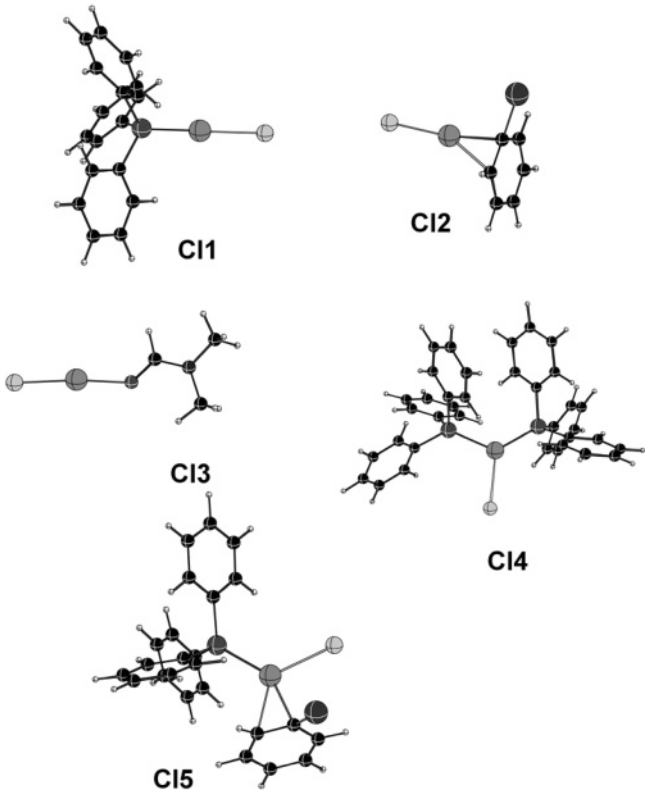

Figure 3. Anionic palladium(0) chloride complexes.

For the anionic complexes the calculated geometries are also in line with what would be expected, with linear geometries for the dicoordinate species and trigonal planar for the tricoordinate ones. In the dicoordinate complex $[Pd(PPh_3)Cl]^-$ the Pd−P bond was found to be 2.23 Å, which is 0.11 Å shorter than the same distance in $Pd(PPh_3)_2$, and likely a consequence of the lower trans-influence of chloride compared to that of triphenylphosphine, while the Pd−Cl bond was calculated to be 2.47 Å. In the solvent complex $[Pd(DMF)Cl]^-$ the Pd−Cl bond was found to be slightly shorter, 2.39 Å, while in the substrate complex $[Pd(PhI)Cl]^-$ it was calculated to be 2.44 Å. The structure of $[Pd(PPh_3)_2Cl]^-$ is distorted such that the two P−Pd−Cl angles are not identical (109° and 124°). The Pd−P distances are 2.31 and 2.38 Å, where the longer bond is to the phosphine with the largest angle to chloride. In this complex the Pd−Cl bond distance is calculated to be as much as 2.73 Å, which is 0.26 Å longer than the Pd−Cl distance in the complex with one phosphine less. This indicates a relatively weak Pd−Cl interaction in $[Pd(PPh_3)_2Cl]^-$. All structures described are for optimizations in DMF and are shown in Figure 3.

Anionic Complexes of the Type $[PdL_n(OOCH)]^-$. Anionic complexes with a formate ligand have been fully optimized with a solvation model describing DMF. Carboxylates are components of many Pd-catalyzed reactions, and the formate can serve as a model for these. In none of the complexes can we see any evidence of steric interactions that would invalidate this model. The relative energies of the palladium formate complexes are displayed in Table 3.

Formation of the tricoordinate species with two triphenylphosphines is found to be endergonic by ca. 50 kJ/mol in DMF (Table 3, entry F1 vs F2). This number differs in magnitude from the same comparison for the chloride system (Table 2, entry Cl1 vs Cl4), which may in part be due to a stabilizing hydrogen-bonding interaction between the formate moiety and one of the phenyl hydrogens. For the formate

Table 3. Relative Potential Energies (kJ/mol) of $[PdLOOCH]^-$

entry	complex	CN[a]	ΔE_{DMF}	"$\Delta G_{Estimate}$"[b]
F1	$[Pd(PPh_3)(OOCH)]^-$	2	0	0
F2	$[Pd(PhI)(OOCH)]^-$	2	25	25
F3	$[Pd(DMF)(OOCH)]^-$	2	33	33
F4	$[Pd(PPh_3)_2(OOCH)]^-$	3	10	50

[a] Coordination number of Pd. [b] See Computational Details.

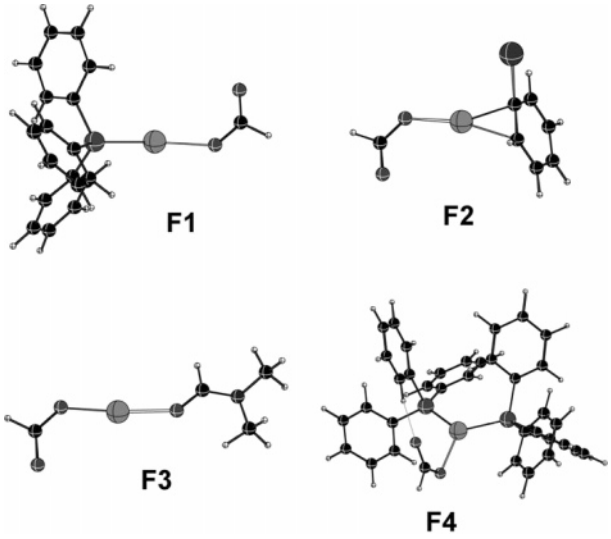

Figure 4. Anionic palladium(0) formate complexes.

complexes a solvent complex $[Pd(DMF)(OOCH)]^-$ was also characterized, and formation of this species was calculated to be endergonic by 33 kJ/mol from $[Pd(PPh_3)(OOCH)]^-$ and DMF.

Structurally the dicoordinate complexes are linear, with the formate coordinating to palladium in an η^1-fashion. The Pd−P distance in $[Pd(PPh_3)(OOCH)]^-$ is identical to the same distance in the chloride analogue, 2.23 Å, while the Pd−O distance is 2.22 Å. In the tricoordinate complex the Pd−P distances are 2.34 and 2.35 Å, while the Pd−O bond is 2.41 Å, which is considerably longer than in the analogue with only one phosphine, thus indicating a weaker Pd−O bond in the tricoordinate complex. All structures described are for optimizations in DMF (Figure 4).

Transition States for Oxidative Addition of Phenyl Iodide to Palladium(0). Two types of transition states have been characterized for the oxidative addition of phenyl iodide to the Pd^0 complexes described above. All have been fully optimized including a solvent model, which has proven to be crucial for these types of species in recent work by Senn and Ziegler, where it was demonstrated that the transition state found in gas-phase calculations did not exist when a solvent model was applied.[9] Similarly, the transition state found when a solvent model was incorporated in the calculations was of a type that could not exist in the gas phase. The first transition state found in the present investigation is one where phenyl iodide has been oxidatively added to $Pd(PPh_3)_2$ (Table 4, entry 1). The second type of transition state found is one where palladium is ligated to only one more ligand than the phenyl iodide (Table 4, entries 2−4).

It is clear that the oxidative addition is facilitated by a lower coordination number on the palladium. While the barrier for oxidative addition to $Pd(PPh_3)_2$ was found to be 13 kJ/mol, oxidative addition to the complexes containing just one more

(9) Senn, H. M.; Ziegler, T. *Organometallics* **2004**, *23*, 2980.

Table 4. Transition State Energies (kJ/mol) Relative to the Respective Prereactive Complexes

entry	oxidative addition transition state complex	CN[a]	ΔE_{DMF}
TS1	$Pd(PPh_3)_2(PhI)$	3	13
TS2	$Pd(PPh_3)(PhI)$	2	2
TS3	$[PdCl(PhI)]^-$	2	1.2
TS4	$[Pd(OOCH)(PhI)]^-$	2	0.2

[a] Coordination number of the corresponding prereactive complex.

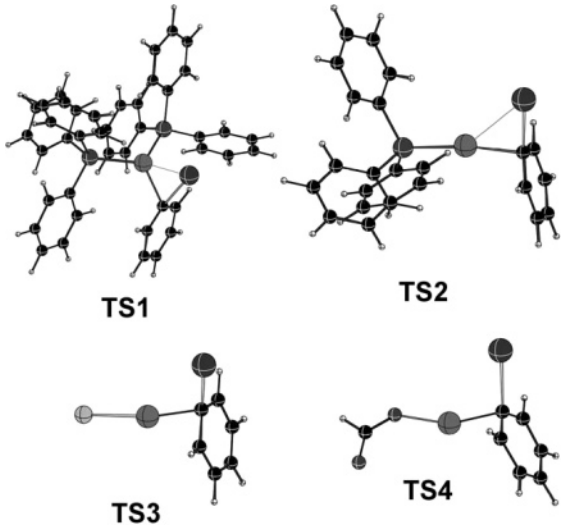

Figure 5. Transition state structures for oxidative addition to palladium(0).

ligand than the phenyl iodide takes place essentially without any barrier (Figure 5). These results are in line with previously published results for palladium(0) alkyne systems, for which it was found that a lower coordination number facilitates oxidative addition.[7] Reactions of complexes with coordination numbers higher than 3 have been studied before and always contain a ligand dissociation from palladium as a crucial prereactive step.[11]

Comparison of Anionic and Neutral Complexes. Since there is a larger degree of uncertainty when comparing neutral and anionic molecules (as opposed to comparison of species of the same charge) when a solvent model is applied, this will be touched upon only briefly here. The equilibrium between $Pd(PPh_3)_2$ and $[Pd(PPh_3)Cl]^-$ is found to be in favor of the former by 58 and 46 kJ/mol in DMF and THF, respectively. For the formate species the numbers are also in favor of $Pd(PPh_3)_2$ but by 41 and 27 kJ/mol for DMF and THF, respectively. At the level of theory used (B3LYP/LACVP*) these values are within the error limit for small anions. In fact, it seems that the continuum model employed here consistently overestimates the solvation energy for the small anions, for example by 63 kJ/mol for Cl^- in DMSO.[10]

Discussion

Di- or Tricoordinate Palladium(0)? From the results above it is obvious that the coordination number of palladium(0) in solution is likely to be lower than what has hitherto been suggested in the literature. In all cases, both in the gas-phase calculations and when applying a solvent model in the calculations, the result is that going from a dicoordinate to a tricoordinate Pd^0 species results in an increase in free energy. The consequence of this is that the often made assumption that tricoordinate complexes are more stabilized than dicoordinate ones is now cast in doubt. Several previous studies have dealt with the stability and reactivity of tricoordinate palladium species,[11] but few have taken into account the possibility of lower coordination,[12] which is probably a consequence of adherence to the time-honored "18-electron rule". However, taking into account the observation that 5p-orbitals are not involved in binding of ligands to Pd, as seen in all our current calculations, the linear 14-electron complex should be regarded as a favored hypervalent state with one ω-bond,[8] analogous to the isoelectronic Ag^+ complexes.

When scrutinizing the early studies of Pd complexes in solution, it becomes apparent that the actual experimental results consist of observation (e.g., by NMR spectroscopy) of multiple species with unclear identity, but with a consistent concentration dependence, allowing a precise determination of the *relative* number of ligands on Pd. However, it is not clear to us how the *absolute* number of coordinating ligands has been determined. In some cases, the assumption has simply been that the highest order complex observed must be identical to either the crystallographically observed coordination or the 18-e complex with four ligands. The current results cast the original assumptions in doubt. The state in the crystal, where the influence of entropy is minor, is determined by the potential energies of the possible complexes and how they pack. On the other hand, in solution, the coordination state is strongly dependent on the entropic contribution, with each ligand loss corresponding to a free energy gain of around 40 kJ/mol at room temperature. Thus, our current results, with higher coordination states being favored by potential energy, but lower coordination states being favored by free energy in solution, are fully compatible with earlier experimental results, but not with the original interpretation of those results.

Looking at the kinetic studies for oxidative addition to palladium, the general observation is that the reaction order in phosphine is negative, usually -1. This has been interpreted as oxidative addition of a PdL_2 complex in equilibrium with a less reactive but more stable PdL_3 species. However, the experimental results basically show only that the rate-determining TS contains fewer phosphine ligands than the resting state of the catalyst and are therefore equally in line with the current results, which indicate that the resting state is PdL_2 and that oxidative addition occurs from complexes of the type L−Pd−PhI, where one ligand again has been lost before reaction.

We also note that only moderately active π-acceptors have been studied here. The calculated difference between di- and triligated Pd is not very large and can probably be reversed by use of strongly electron-accepting ligands such as dba, which would be expected to favor higher coordination states of Pd.[13] In the extreme cases, binding of electron-deficient alkenes to Pd^0 gives a bonding pattern more reminiscent of palladacyclopropane, which would be expected to behave as a Pd^{II} species and accept two ligands trans to the two coordinating alkene carbons.

As stated above, the preference for di- over triligated states mainly arises from an entropic contribution in solution. Thus, chelating ligands would be expected to override this preference. Looking at the geometry of our calculated tricoordinated Pd

(10) Ahlquist, M.; Kozuch, S.; Shaik, S.; Tanner, D.; Norrby, P.-O. *Organometallics* **2006**, *25*, 45.

(11) (a) Kozuch, S.; Shaik, S.; Jutand, A.; Amatore, C. *Chem. Eur. J.* **2004**, *10*, 3072. (b) Goossen, L. J.; Koley, D.; Hermann, H.; Thiel, W. *Chem. Commun.* **2004**, *19*, 2141. (c) Goossen, L. J.; Koley, D.; Hermann, H.; Thiel, W. *Organometallics* **2005**, *24*, 2398. (d) Kozuch, S.; Amatore, C.; Jutand, A.; Shaik, S. *Organometallics* **2005**, *24*, 2319.

(12) (a) Hartwig, J. F.; Paul, F. *J. Am. Chem. Soc.* **1995**, *117*, 5373. (b) Christmann, U.; Vilar, R. *Angew. Chem., Int. Ed.* **2005**, *44*, 366.

(13) Amatore, C.; Jutand, A. *Coord. Chem. Rev.* **1998**, *178*, 511.

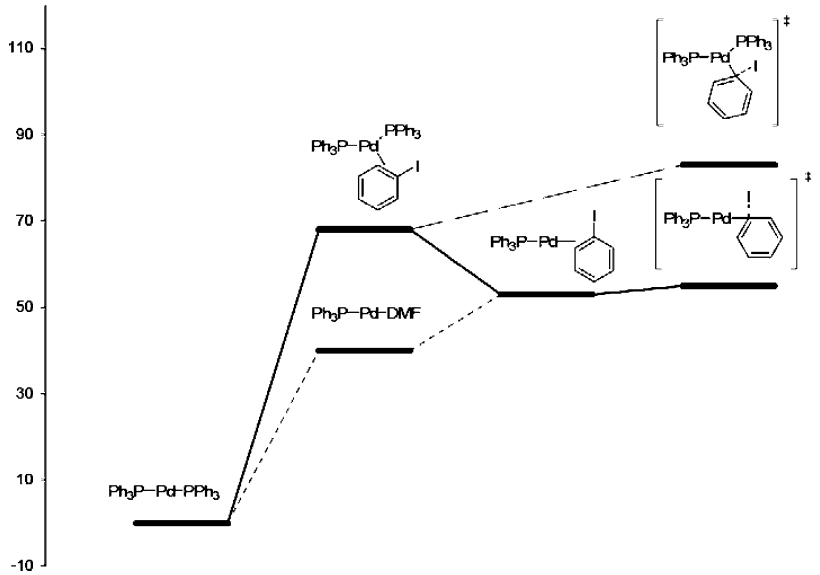

Figure 6. Potential energy diagram for the reaction between $Pd(PPh_3)_2$ and PhI. All energies are in kJ/mol.

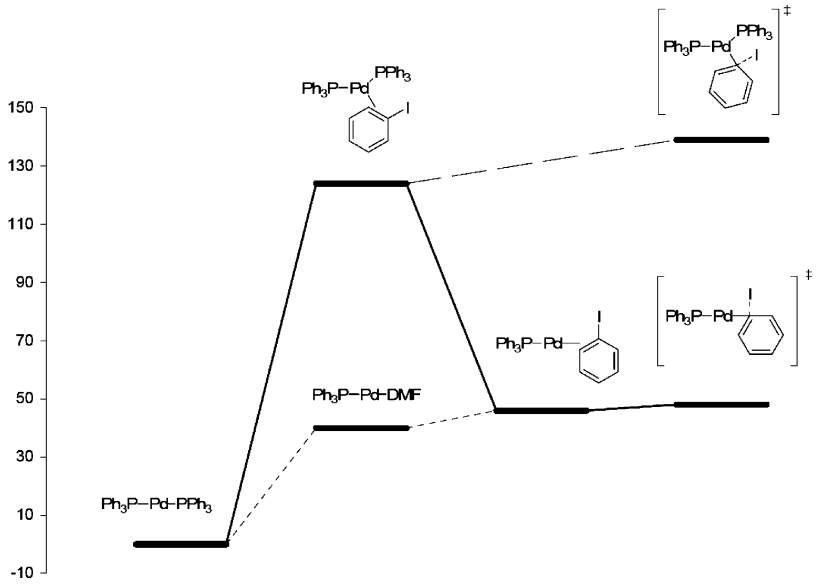

Figure 7. Free energy ("ΔG_{DMF}") diagram of the reaction between $Pd(PPh_3)_2$ and PhI. All energies are in kJ/mol.

complexes, we would expect that a bidentate phosphine with a small or moderate bite angle would accept another ligand trans to one of the phosphines.

Reactivity toward Phenyl Iodide. Oxidative addition is frequently the first step in any *catalytic* cycle involving palladium(0) phosphine species. Although several theoretical studies of oxidative addition have been performed, none have dealt with the possibility of a lower coordinated palladium species, including a solvent model in the calculations.[9,11,14] Our results for the ground states suggest that palladium in solution prefers a dicoordinate structure over a tricoordinate one. A previous study has shown that, in the gas phase, oxidative addition of phenyl bromide to palladium(0) with the model ligand PH_3 is more facile if palladium is coordinated to only one more ligand than phenyl iodide.[15] Since it has been shown that gas-phase calculations do not necessarily yield the same results as solution-phase calculations,[9] we decided to investigate the oxidative addition step including a solvent model. In our experience, utilizing PH_3 as a model for aryl and alkyl phosphines has often proved to give results that differ substantially from the ones for the full system.

For the neutral complexes, the starting point of the reaction is $Pd(PPh_3)_2$ (Figures 6 and 7). For the general case, formation of $Pd(PPh_3)_2(PhI)$ is the first possibility. From here there are basically two paths: either oxidative addition directly on this species or dissociation of one ligand to form the dicoordinate species $Pd(PPh_3)(PhI)$, which could also be formed by a dissociative path via the solvent complex $Pd(PPh_3)DMF$.[12] From the results above the path involving solvent is strongly favored. Oxidative addition involving $Pd(PPh_3)_2(PhI)$ takes place via TS1 with a barrier of 15 kJ/mol. The dicoordinate complex $Pd(PPh_3)$-(PhI), which is found to be more stable than $Pd(PPh_3)_2(PhI)$ by 78 kJ/mol, undergoes oxidative addition via TS2 with virtually no barrier (2 kJ/mol). The consequence of these results is that

(14) (a) Low, J. J.; Goddard, W. A., III. *J. Am. Chem. Soc.* **1986**, *108*, 6115. (b) Ananikov, V. P.; Musaev, D. G.; Morokuma, K. *Organometallics* **2005**, *24*, 715. (c) Sakaki, S.; Biswas, B.; Sugimoto, M. *J. Chem. Soc., Dalton Trans.* **1997**, *5*, 803. (d) Sakaki, S.; Kai, S.; Sugimoto, M. *Organometallics* **1999**, *18*, 4825. (e) Sumimoto, M.; Iwane, N.; Takahama, T.; Sakaki, S. *J. Am. Chem. Soc.* **2004**, *126*, 10457.

(15) Cundari, T. R.; Deng, J. *J. Phys. Org. Chem.* **2005**, *18*, 417.

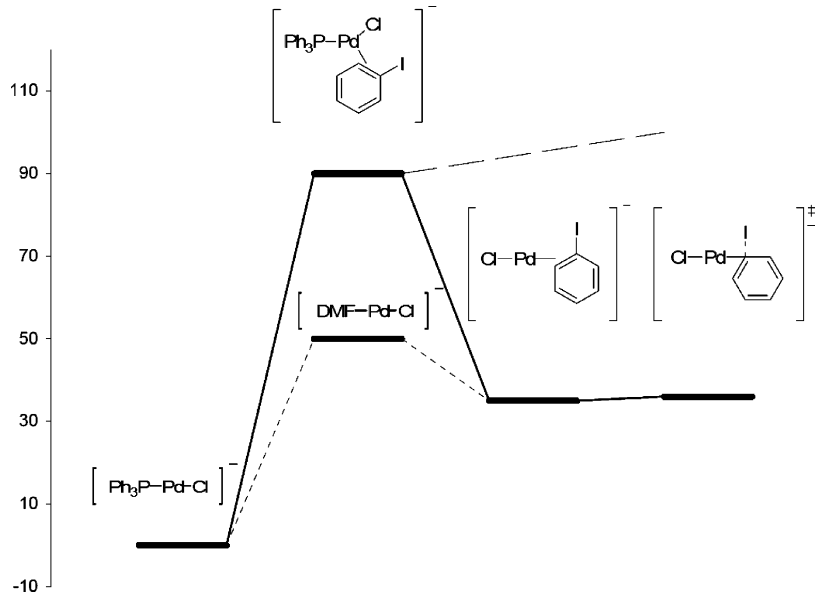

Figure 8. Free energy ("$\Delta G_{\text{Estimate}}$") diagram for oxidative addition to anionic palladium(0) chloride complexes (values in kJ/mol).

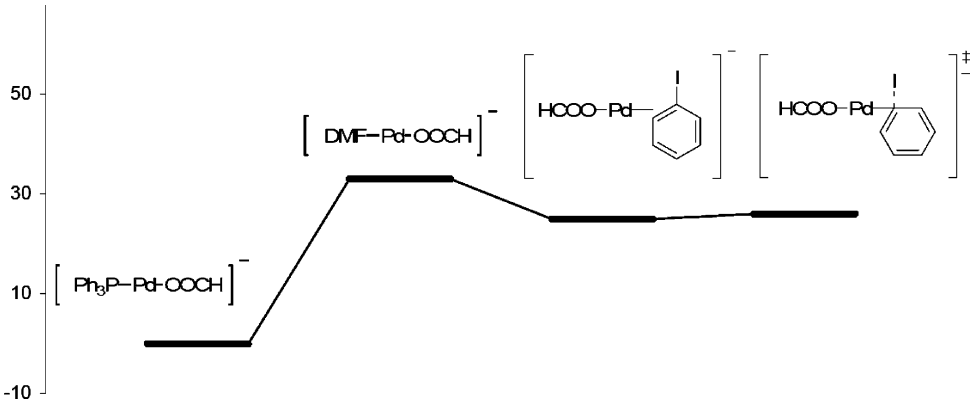

Figure 9. Free energy ("$\Delta G_{\text{Estimate}}$") diagram for oxidative addition to anionic palladium(0) formate complexes (values in kJ/mol).

the species on which the oxidative addition takes place is most likely the one with only one phosphine, $Pd(PPh_3)(PhI)$, which is formed either via ligand exchange on $Pd(PPh_3)_2$ or via the solvent complex $Pd(PPh_3)DMF$. These findings are in line with the theoretical results found recently for palladium acetylene systems, where lower coordination number was shown to increase the reactivity of palladium(0) toward oxidative addition of phenyl iodide.[7] This is also in line with the experimental observations by Beeby et al. that additional triphenylphosphine above 1 equiv relative to the palladium concentration retards the rate of oxidative addition of phenyl bromide.[16] Similar results have been observed by several groups for oxidative addition to palladium(0) complexes containing sterically demanding ligands.[17]

The results for oxidative addition to the anionic palladium(0) species are similar to the ones for neutral analogues (Figure 8). Formation of a tricoordinate complex from $[Pd(PPh_3)Cl]^-$ and phenyl iodide is found to be endergonic by 90 kJ/mol. Dissociation of the phosphine then leads to a more stable complex. This dicoordinate prereactive complex $[Pd(PhI)Cl]^-$ is 35 kJ/mol higher in energy than the corresponding phosphine complex $[Pd(PPh_3)Cl]^-$. Another possible path for the formation of $[Pd(PhI)Cl]^-$ is via the solvent complex $[Pd(DMF)Cl]^-$. Formation of $[Pd(DMF)Cl]^-$ from $[Pd(PPh_3)Cl]^-$ and DMF was found to be endergonic by 50 kJ/mol, compared to the path via the tricoordinate $[Pd(PPh_3)(PhI)Cl]^-$ complex. The solvent complex path is thus favored by 40 kJ/mol. Oxidative addition on the prereactive complex $[Pd(PhI)Cl]^-$ occurs with a very low barrier, 1.2 kJ/mol, via TS3 (Figure 5). Oxidative addition on $[Pd(PPh_3)Cl(PhI)]^-$ was not considered since it is already higher in energy than $[Pd(PhI)Cl]^-$, and the barrier for the neutral analogue was found to be 13 kJ/mol compared to the almost barrier-free oxidative addition on the low-coordinate complexes.

Similarly, the complexes with a formate ligand undergo oxidative addition with a low barrier via a palladium species coordinated to only the formate and the phenyl iodide (Figure 9). Ligand exchange that leads to formation of the solvent complex $[Pd(DMF)OOCH]^-$ is endergonic by 33 kJ/mol. The subsequent formation of the prereactive complex from $[Pd(DMF)OOCH]^-$ and phenyl iodide is exergonic by 7 kJ/mol.

Explanation of the "Anion Effect". For Pd^0-catalyzed processes under certain conditions, an increase in reaction rate has been observed when anions are added to the reaction mixture. This has previously been explained in terms of formation of a highly reactive tricoordinate $[Pd(PPh_3)_2X]^-$ species.[6] However, this explanation is in contradiction to the

(16) Beeby, A.; Bettington, S.; Fairlamb, I. J. S.; Goeta, A. E.; Kapdi, A. R.; Niemelä, E. H.; Thompson, A. L. *New J. Chem.* **2004**, *28*, 600.

(17) (a) Littke, A. F.; Dai, C.; Fu, G. C. *J. Am. Chem. Soc.* **2000**, *122*, 4020. (b) Barder, T. E.; Walker, S. D.; Martinelli, J. R.; Buchwald, S. L. *J. Am. Chem. Soc.* **2005**, *127*, 4685 (c) Barrios-Landeros, F.; Hartwig, J. F. *J. Am. Chem. Soc.* **2005**, *127*, 6944.

present results, since if an anionic species is present in solution it is much more likely to be the dicoordinate complex $[Pd(PPh_3)X]^-$. In our calculation of the chloride system the dicoordinate species is found to have a 72 kJ/mol lower free energy than the tricoodinate one. For the corresponding formate species the difference was calculated to 50 kJ/mol, also here in favor of the dicoordinate species.

When comparing the neutral and anionic complexes, a preference for the neutral ones is found. This, however, might be an effect of an overestimation of the solvation energy of the free anionic ligands. In a study of the solvation energy of small anions with a solvation model describing DMSO, it was found that it overestimates the free energy of solvation by 63 kJ/mol for the chloride anion. Thus, it might very well be so that the $[Pd(PPh_3)Cl]^-$ complex is more stable than $Pd(PPh_3)_2$, but since the solvation model overestimates the stability of the chloride, the result is the opposite in the calculations. It should be noted that this does not affect the equilibrium between the di- and tricoordinate species, since these compare molecules of the same charge.

From the results above it is clear that the "anion effect" is not likely to be due to formation of the previously suggested species $[Pd(PPh_3)_2X]^-$, since it is both a low-concentration species[8] and also less reactive toward oxidative addition than $[Pd(PPh_3)X]^-$. Thus, in the presence of anions there is a possibility for formation of anionic palladium complexes of the type $[Pd(PPh_3)X]^-$. For oxidative addition of phenyl iodide, a relatively poor ligand for palladium(0), two paths can be followed from this complex. The first possibility is formation of a solvent complex ($[Pd(Solv)X]^-$ and then ligand exchange to yield the prereactive complex $[Pd(PhI)X]^-$. The second involves an association of PhI to $[Pd(PPh_3)X]^-$ to yield the prereactive complex via the tricoordinate $[Pd(PPh_3)(PhI)X]^-$. In both the anionic and the neutral mechanisms described above, the barriers for the oxidative addition at the dicoordinate prereactive complexes were found to be very low. Therefore, there has to be another explanation for the "anion effect". One possibility is that the formation of the prereactive complexes is more favored for the anionic complexes than for the neutral analogues, which is exactly what is observed in the calculations described above. The energy required for formation of $Pd(PPh_3)(PhI)$ from $Pd(PPh_3)_2$ was 46 kJ/mol, while formation of $[Pd(PhI)X]^-$ from $[Pd(PPh_3)X]^-$ was endergonic by 35 and 25 kJ/mol for $X = Cl^-$ and HCOO, respectively. A rationale for this observed difference in ability to form the dicoordinate prereactive complex could be that in the neutral complex PPh_3 acts as an electron acceptor. Another electron-accepting ligand such as the electrophile PhI is then disfavored. For the anionic analogues the situation is very different. Since palladium in these cases is coordinated only to an electron-donating ligand (the anionic one), ligation of the electrophile PhI is more favored. The overall effect can be viewed as a push−pull effect between the ligands, where palladium is merely acting as a carrier of electron density from a nucleophilic species to an electrophilic one. An identical effect has been observed for palladium(0) alkyne complexes, where the push−pull effect was so pronounced in some complexes that the palladium(0) was better viewed as being an anionic palladacyclopropene palladium(II) complex (Figure 10).[7]

Conclusions

All our results indicate that it is necessary to re-evaluate the nature of the palladium(0) species present in solution and relevant to many of the most commonly used Pd^0-catalyzed organic reactions. In every case, an increase in potential energy was found when going from a dicoordinate to a tricoordinate palladium(0) species. As a consequence of these findings, the most reactive species in neutral solution is found to be $Pd(PPh_3)(Solv)$, with $Pd(PPh_3)_2$ substantially less reactive, in contrast with earlier proposals where $Pd(PPh_3)_3$ has been assumed to be the dominant species in solution. The often observed effect of "phosphine poisoning" at high phosphine concentrations then originates from the equilibrium between $Pd(PPh_3)_2$ and $Pd(PPh_3)(Solv)$ rather than the equilibrium between $Pd(PPh_3)_3$ and $Pd(PPh_3)_2$. Our results also strongly suggest that anionic Pd^0 complexes, which are presumed to be formed upon addition of chloride, are not of the previously suggested type $[Pd(PPh_3)_2X]^-$, but are much more likely to be species containing only one phosphine ligand, $[Pd(PPh_3)X]^-$. On the basis of this observation, a cogent explanation can be advanced for the "anion effect" sometimes observed in Pd^0-catalyzed organic reactions. Rationalized from the results above, the "anion effect" is found to be due to the fact that formation of a prereactive "push−pull" complex (Figure 10) is more favored for the anionic complexes than for the neutral analogues.

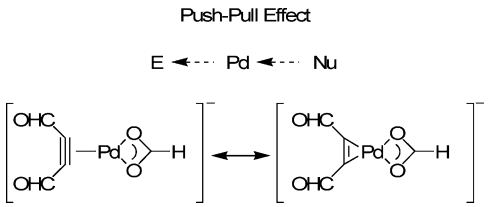

Figure 10. "Push−pull effect" in palladium complexes.

Computational Details

To include both steric interactions and the correct electronics we have included the complete ligand and substrate in all calculations, to avoid artifacts from calculations on small model systems. All calculations were performed with the Jaguar 4.2 program package[18] using the hybrid functional B3LYP.[19] The basis set used was LACVP*, which applies the 6-31G* basis set for all light elements and the Hay−Wadt ECP and basis set for palladium and iodine.[20] To simulate solvent, the Poisson−Boltzmann self-consistent reaction field (PB-SCRF) incorporated in Jaguar 4.2 was used.[21] PB-SCRF is a continuum solvation model, where the molecule is put into a reaction field consisting of surface charges on a solvent-accessible surface constructed using a hypothetical spherical solvent probe molecule with the indicated radius.[22] The wave function and the reaction field charges are solved iteratively until self-consistency is reached. The parameters for the two solvents simulated have been set to $\epsilon = 38$, probe radius $= 2.47982$ for DMF and $\epsilon = 7.43$, probe radius $= 2.52372$ for THF.

To get an estimate of the Gibbs free energy in solution, the vibrational component of the free energy, calculated by harmonic normal-mode analysis employing an analytic Hessian calculated in the gas phase, was added to the free energy calculated by optimization of the geometry in the solvation model. This procedure is valid only when the gas-phase and solvated geometries are very similar, and thus could only be applied to neutral complexes in

(18) DFT calculations made with the Jaguar 4.2 program package from Schrödinger Inc., Portland, OR: http://www.schrodinger.com.

(19) (a) Becke, A. D. *Phys. Rev. A* **1988**, *38*, 3098. (b) Perdew, J. *P. Phys. Rev. B* **1986**, *33*, 8822.

(20) Hay, P. J.; Wadt, W. R. *J. Chem. Phys.* **1985**, *82*, 299.

(21) Marten, B.; Kim, K.; Cortis, C.; Friesner, R. A.; Murphy, R. B.; Ringnalda, M. N.; Sitkoff, D.; Honig, B. *J. Phys. Chem.* **1996**, *100*, 11775.

(22) For a discussion of implicit solvation models, see: Cramer, C. *Essentials of Computational Chemistry: Theories and Models*; Wiley: New York, 2002.

this study. The most significant contribution to the vibrational component was from a change in molecularity, which added 42−58 kJ/mol. Earlier experimental[23] and theoretical[24] studies have yielded similar results. For the anionic complexes, only the molecularity contribution to the free energy was considered. Since no gas-phase calculations were performed for the anionic species, a conservative estimate of 40 kJ/mol to account for molecularity is made.

Acknowledgment. P.O.N. is grateful to Professor Clark Landis for illuminating discussions. We thank the Technical University of Denmark for support.

Supporting Information Available: This material is available free of charge via the Internet at http://pubs.acs.org.

OM060126Q

(23) Searle, M. S.; Westwell, M. S.; Williams, D. H. *J. Chem. Soc., Perkin Trans. 2* **1995**, *1*, 141.

(24) (a) Woo, T. K.; Blöchl, P. E.; Ziegler, T. *J. Phys. Chem. A* **2000**, *104*, 121. (b) Seth, M.; Senn, H. M.; Ziegler, T. *J. Phys. Chem. A* **2005**, *109*, 5136.

Organometallics **2007,** *26,* 550−553

Oxidative Addition of Aryl Chlorides to Monoligated Palladium(0): A DFT-SCRF Study

Mårten Ahlquist[†] and Per-Ola Norrby*[,‡]

Departments of Chemistry, Technical University of Denmark, Building 201 Kemitorvet, DK-2800 Kgs. Lyngby, Denmark, and Göteborg University, Kemigården 4, SE-412 96 Göteborg, Sweden

Received June 5, 2006

Oxidative addition of aryl chlorides to palladium has been investigated by hybrid density functional theory methods (B3LYP), including a continuum model describing the solvent implicitly. A series of para-substituted aryl chlorides were studied to see the influence of electronic effects on the reaction. It was found that the experimentally observed higher reactivity of the more electron deficient aryl chlorides is due to their ability to accept back-donation from Pd^0 and form reasonably strong pre-reactive complexes. This effect is less pronounced in the transition state; when it is measured from the pre-reactive complex, the barrier to oxidative addition is actually higher for the electron-deficient aryl chlorides, but the overall reaction barrier is still lower than for the electron-rich aryl chlorides.

Introduction

Palladium-catalyzed reactions have had a major impact on organic chemistry. A myriad of coupling reactions between aryl halides and nucleophiles have been developed over the last few decades.[1] In the prototypic cross-coupling reaction depicted in Scheme 1, the organometallic reagent RM provides the coupling partner,[2] but similar catalytic cycles are also valid for palladium-catalyzed additions to π systems.[3] A major achievement was the development of catalytic systems that are able to couple aryl chlorides rather than the iodo and bromo analogues.[4] Similar catalyst systems have recently been shown to be able to couple even less reactive substrates such as tosylates and phosphates.[5]

Within this class of reactions, the first step in the catalytic cycle is oxidative addition of an aryl halide to a low-ligated Pd^0 species. This step, and its microscopic reverse, reductive elimination, has been the subject of much investigation.[6] In particular, a number of computational studies of the mechanism of oxidative addition of aryl halides have recently appeared.[7] Of special interest is a study by Senn and Ziegler, demonstrating that the nature of the oxidative addition transition state changes qualitatively when going from calculations in the gas phase to models incorporating an average influence of the solvent (a continuum model).[7a]

Scheme 1. Generic Catalytic Cycle for Pd-Catalyzed Coupling Reactions

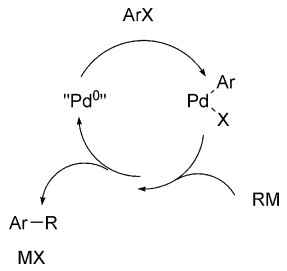

Herein we report a density functional theory investigation of the effect of the electron density of the aryl chloride on the oxidative addition. All calculations were performed at the B3LYP/LACVP* level of theory, applying a Poisson−Boltzmann self-consistent reaction field to describe the solvent implicitly.[8]

Results and Discussion

Oxidative Addition to $Pd(PtBu_3)$. One of the most commonly employed palladium sources for cross-coupling reactions

* To whom correspondence should be addressed. Tel: +46 31 7723848. Fax: +46 31 7723840. E-mail: pon@kemi.dtu.dk.

[†] Technical University of Denmark. Tel: +45 4525 5430. Fax: +45 4593 3968.

[‡] Göteborg University.

(1) (a) Milstein, D.; Stille, J. K. *J. Am. Chem. Soc.* **1978**, *100*, 3636. (b) Miyaura, N.; Yamada, K.; Suzuki, A. *Tetrahedron Lett.* **1979**, *20*, 3437. (c) Negishi, E.; Okukado, N.; King, A. O.; Van Horn, D. E.; Spiegel, B. I. *J. Am. Chem. Soc.* **1978**, *100*, 2254. (d) Mizoroki, T.; Mori, K.; Ozaki, A. *Bull. Chem. Soc. Jpn.* **1971**, *44*, 581. (e) Heck, R. F.; Nolley, J. P. *J. Org. Chem.* **1972**, *37*, 2320. (f) Cacchi, S.; Felici, M.; Pietroni, B. *Tetrahedron Lett.* **1984**, *25*, 3137. (g) Trost, B. M.; Schmidt, T. *J. Am. Chem. Soc.* **1988**, *110*, 2301. (h) For a recent review on palladium catalysis in total synthesis see: Nicolaou, K. C.; Bulger, P. G.; Sarlah, D. *Angew. Chem., Int. Ed.* **2005**, *44*, 4442.

(2) Hassan, J.; Sévignon, M.; Gozzi, C.; Schulz, E.; Lemaire, M. *Chem. Rev.* **2002**, *102*, 1359.

(3) (a) Beletskaya, I. P.; Cheprakov, A. V. *Chem. Rev.* **2000**, *100*, 3009. (b) Cacchi, S.; Fabrizi, G. *Chem. Rev.* **2005**, *105*, 2875.

(4) (a) Littke, A. F.; Dai, C.; Fu, G. C. *J. Am. Chem. Soc.* **2000**, *122*, 4020. (b) Barder, T. E.; Walker, S. D.; Martinelli, J. R.; Buchwald, S. L. *J. Am. Chem. Soc.* **2005**, *127*, 4685. (c) Barrios-Landeros, F.; Hartwig, J. F. *J. Am. Chem. Soc.* **2005**, *127*, 6944.

(5) (a) Roy, A. H.; Hartwig, J. F. *J. Am. Chem. Soc.* **2003**, *125*, 8704. (b) Hansen, A. L.; Ebran, J.-P.; Ahlquist, M.; Norrby, P.-O.; Skrydstrup, T. *Angew. Chem., Int. Ed.* **2006**, *45*, 3349.

(6) (a) Low, J. J.; Goddard, W. A., III. *J. Am. Chem. Soc.* **1986**, *108*, 6115. (b) Ananikov, V. P.; Musaev, D. G.; Morokuma, K. *Organometallics* **2005**, *24*, 715. (c) Sakaki, S.; Biswas, B.; Sugimoto, M.; *J. Chem. Soc., Dalton Trans.* **1997**, 803. (d) Sakaki, S.; Kai, S.; Sugimoto, M. *Organometallics* **1999**, *18*, 4825. (e) Sumimoto, M.; Iwane, N.; Takahama, T.; Sakaki, S. *J. Am. Chem. Soc.* **2004**, *126*, 10457.

(7) (a) Senn, H. M.; Ziegler, T. *Organometallics* **2004**, *23*, 2980. (b) Goossen, L. J.; Koley, D.; Hermann, H.; Thiel, W. *Chem. Commun.* **2004**, 2141. (c) Goossen, L. J.; Koley, D.; Hermann, H.; Thiel, W. *Organometallics* **2005**, *24*, 2398. (d) Cundari, T. R.; Deng, J. *J. Phys. Org. Chem.* **2005**, *18*, 417. (e) Kozuch, S.; Amatore, C.; Jutand, A.; Shaik, S. *Organometallics* **2005**, *24*, 2319. (f) Braga, A. A. C.; Ujaque, G.; Maseras, F. *Organometallics* **2006**, *25*, 3647.

(8) DFT calculations were carried out with the Jaguar 4.2 program package from Schrödinger Inc., Portland, OR (http://www.schrodinger.com). All of the calculations were performed at the B3LYP/LACVP* level. The geometries were fully optimized in solvent, simulated with the PB-SCRF model: Marten, B.; Kim, K.; Cortis, C.; Friesner, R. A.; Murphy, R. B.; Ringnalda, M. N.; Sitkoff, D.; Honig, B. *J. Phys. Chem.* **1996**, *100*, 11775. The parameters were set to $\epsilon = 38$ probe radius $= 2.48$ to simulate DMF.

10.1021/om0604932 CCC: $37.00
Publication on Web 01/03/2007

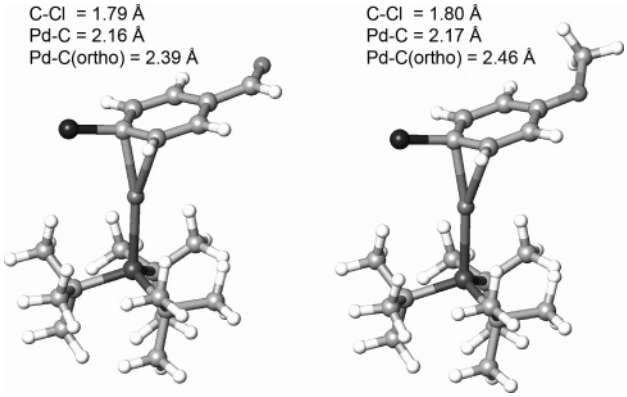

Figure 1. Pre-reactive complexes of Pd(P*t*Bu$_3$) with *p*-chlorobenzaldehyde and *p*-chloroanisole.

of aryl chlorides is Pd(P*t*Bu$_3$)$_2$, a catalytic system originally developed by Fu and co-workers.[9] The 14-electron complex Pd(P*t*Bu$_3$)$_2$ is believed to be the major species in solution and was therefore chosen as the reference complex of our investigation. The calculated geometry of Pd(P*t*Bu$_3$)$_2$ is similar to that of the previously reported triphenylphosphine analogue,[10] in that it adopts a linear structure. The Pd−P bond lengths were found to be slightly longer in Pd(P*t*Bu$_3$)$_2$ than in Pd(PPh$_3$)$_2$: 2.38 Å vs 2.34 Å. We note that this geometry is consistent with the bonding model of Weinhold and Landis: of the 6 s and d valence orbitals on Pd, 5 are occupied by the 10 valence electrons of Pd^0. The last valence orbital can accommodate 2 ligands in a trans relationship by a 3-center−4-electron ω-bond.[11]

Palladium catalysts bearing bulky phosphines have been proposed to react via monocoordinate 12-electron complexes:[12] in the current case, Pd(P*t*Bu$_3$). A significant decrease of the Pd−P distance is observed in Pd(P*t*Bu$_3$), by 0.11 Å to 2.27 Å, a consequence of the strong trans influence of the phosphine (similar results were found for PPh$_3$ complexes in an earlier study[10]). Using the Weinhold−Landis bonding model, the bond is now a standard 2e bond, significantly stronger *per ligand* than the ω bond. Frequently these types of reactions are performed in coordinating solvents, e.g., DMF, and in these cases a solvent molecule is likely to coordinate trans to the single phosphine, in an unsymmetrical ω-bond.

Investigation of the influence of para substituents on the aryl chlorides can give valuable information on electronic effects in chemical reactions. In the current study, we have included six different aryl chlorides, with both electron-withdrawing and -donating substituents. For all of these, we have optimized pre-reactive complexes where one aryl chloride and one phosphine coordinate to Pd. Two of the structures are shown in Figure 1, and the energies relative to Pd(P*t*Bu$_3$)$_2$ of all the complexes are given in Table 1. From the values of the relative energies it is clear that the electron-poor aryl chlorides form much more stable complexes with Pd^0 than do the aryl chlorides with higher electron density. A comparison between the aryl chlorides with the strongest and weakest binding, *p*-OHC-PhCl and *p*-MeO-PhCl, respectively, reveals a difference of as much as 17 kJ mol^{-1}. This trend can be rationalized by the high aptitude of Pd^0 for d−π* back-bonding. A similar trend has previously been observed for binding of alkynes to Pd^0.[13]

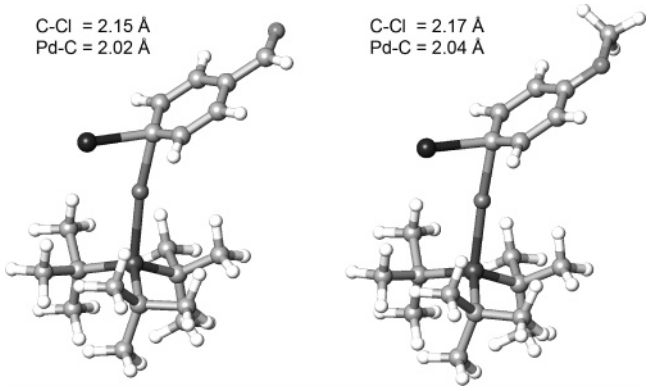

Figure 2. Transition states for the oxidative addition of *p*-chlorobenzaldehyde and *p*-chloroanisole to Pd(P*t*Bu$_3$).

Table 1. Energies of the Pre-reactive Complexes Pd(ArCl)P*t*Bu$_3$ and the Subsequent Oxidative Addition Transition States, Relative to Pd(P*t*Bu$_3$)$_2$, in kJ mol^{-1}

X in *p*-Cl-PhX	pre-reactive complex	transition state
−CHO	64.9	104.6
−CN	65.7	104.8
−H	75.8	112.5
−NH$_2$	74.2	107.0
−Me	76.8	112.6
−OMe	81.7	114.2

The transition states for the oxidative addition of the aryl chlorides reveal an intriguing feature. Relative to the case for the respective pre-reactive complexes the barrier for oxidative addition is calculated to be lower for electron-rich aryl chlorides. For example, the barrier is only 32 kJ mol^{-1} for Pd(P*t*Bu$_3$)(*p*-MeO-PhCl) compared to 40 kJ mol^{-1} for Pd(P*t*Bu$_3$)(*p*-OHC-PhCl) (Figure 2). However, the total barrier (as shown in Table 1), obtained as the sum of the activation barrier for the addition step and the energy of the intermediate, is still substantially lower for the electron-deficient aryl chlorides, with a span of 10 kJ mol^{-1} between the least and most reactive aryl chloride. Thus, the binding advantage of the electron-deficient aryl chlorides is only partially retained in the TS, but this is still sufficient to increase the reactivity.

Oxidative Addition to [PdCl]$^-$. [PdX]$^-$ has been proposed as the active intermediate when applying certain Pd^{II} complexes, e.g., palladacycle and pincer complexes, as a source of highly active Pd^0 species.[15] Recently a theoretical study concluded that the oxidative addition in the presence of phosphines could occur at a [PdX]$^-$ type complex.[10] The reactivity of [PdCl]$^-$ toward the same aryl chlorides as above was therefore investigated. Most of the palladium present is still undoubtedly ligated by at least one phosphine, but as we have shown earlier, loss of the additional ligands before the actual oxidative addition step substantially reduces the free energy barrier.[10] Under some reaction conditions, complexes coordinating one phosphine and an anion have been proposed to be the major species,[14] motivating the choice of [Pd(P*t*Bu$_3$)Cl]$^-$ as the reference complex herein.

Formation of the pre-reactive complexes of the type [Pd(ArCl)Cl]$^-$ follows a trend similar to that for the neutral

(9) Littke, A. F.; Fu, G. C. *Angew. Chem., Int. Ed.* **1998**, *37*, 3387.
(10) Ahlquist, M.; Fristrup, P.; Tanner, D.; Norrby, P.-O. *Organometallics* **2006**, *25*, 2066.
(11) Weinhold, F.; Landis, C. *Valency and Bonding: A Natural Bond Orbital Donor-Acceptor Perspective*; Cambridge University Press: Cambridge, U.K., 2005.
(12) Christmann, U.; Vilar, R. *Angew. Chem., Int. Ed.* **2005**, *44*, 366.
(13) (a) Ahlquist, M.; Fabrizi, G.; Cacchi, S.; Norrby, P.-O. *Chem. Commun.* **2005**, 4196. (b) Ahlquist, M.; Fabrizi, G.; Cacchi, S.; Norrby, P.-O. *J. Am. Chem. Soc.* **2006**, *128*, 12785.
(14) Fristrup, P.; Jensen, T.; Hoppe, J.; Norrby, P.-O. *Chem. Eur. J.* **2006**, *12*, 5352.
(15) (a) Böhm, V. P. W.; Herrmann, W. A. *Chem. Eur. J.* **2001**, *7*, 4191. (b) de Vries, A. H. M.; Parlevliet, F. J.; Schmieder-van der Vondervoort, L.; Mommers, J. H. M.; Henderickx, H. J. W.; Walet, M. A. M.; de Vries, J. G. *Adv. Synth. Catal.* **2002**, *344*, 996.

Table 2. Energies of Pre-reactive Complexes [Pd(ArCl)Cl]$^-$ and the Subsequent Oxidative Addition Transition States Relative to [Pd(P*t*Bu$_3$)Cl]$^-$, in kJ mol^{-1} [a]

X in *p*-Cl-PhX	pre-reactive complex	transition state
−CHO	39.6 (35.3)	78.9 (72.3)
−CN	41.0 (37.6)	78.8 (72.8)
−H	58.8 (56.2)	90.7 (84.9)
−NH$_2$	52.9 (52.0)	90.6 (87.2)
−Me	58.9 (57.6)	91.7 (87.6)
−OMe	59.3 (57.6)	92.9 (88.2)

[a] Given in parentheses are values from single-point calculations including diffuse functions on all heavy elements.

palladium complexes, although a more strongly pronounced electronic effect is observed for the anionic complexes. Also here the relative stability of the pre-reactive complexes with the electron-deficient aryl chlorides is much higher than the stability of the complexes with the electron-rich aryl chlorides, with a difference between the two extremes *p*-OHC-PhCl and *p*-Me-PhCl calculated to be as large as 20 kJ mol^{-1} in favor of the complex with *p*-OHC-PhCl. Geometrically the anionic complexes differ slightly from the neutral phosphine complexes in that the aryl chloride is more tightly bound to Pd. In [Pd(OHC−PhCl)Cl]$^-$ the Pd−C$_{ipso}$ distance is 2.09 Å and the Pd−C$_{ortho}$ distance is 2.22 Å. The C−Cl distances are almost identical in the anionic and neutral complexes: 1.80 and 1.79 Å, respectively.

The barriers from the respective pre-reactive complexes follow the same trend as for the neutral complexes, with the lowest barrier found for the complexes containing electron-rich aryl chlorides (relative to the respective pre-reactive complexes) (Table 2). However, also for the anionic reaction the overall barrier from the separated reactants is substantially lower for the electron-deficient aryl chlorides. The difference between the highest and lowest barrier in the anionic path is calculated to be 14 kJ mol^{-1}, compared to the 10 kJ mol^{-1} span for the neutral path. The higher reactivity difference for the anionic palladium species is in agreement with the experimental observations by Herrmann et al. that reactions under phosphine-free conditions show a higher ρ value than for reactions with phosphines present, which was attributed to the formation of the highly active anionic species [Pd(OAc)]$^-$.[15a]

Rationale for the Reactivity. To further understand which factors are responsible for the reactivity difference, the homolytic bond dissociation energies (BDE) of the aryl chlorides were calculated. In Figure 3 the BDE:s are plotted against σ^p, which gave a good fit. The lowest and the highest BDE values were found for NC-PhCl and H$_2$N-PhCl, respectively, with a 7.65 kJ mol^{-1} lower value for NC-PhCl. In the oxidative addition a similar trend is observed: i.e., electron-deficient aryl chlorides react more readily than the electron-rich analogues. However, the difference in reactivity is much larger than the difference in BDE; the barrier for oxidative addition of NC-PhCl is 14.1 kJ mol^{-1} lower than for MeO-PhCl. A Hammett plot of the activation barriers against σ^- gave a good correlation, whereas σ^p correlated poorly. Although the strength of the C−Cl bond could account for some of the difference in the barriers, additional factors must be present that explain the correlation with σ^- rather than σ^p, as well as the high reactivity difference, despite the lower difference in bond strength. The fact that the barriers correlate with σ^- suggests that the mechanism is best described as an S$_N$Ar type mechanism. An even stronger electronic effect (20 kJ mol^{-1}) is observed in the formation of the pre-reactive complexes as compared to that in the transition state (Figure 4). Structurally the pre-reactive complexes resemble π complexes which are known to be favored by electron-withdrawing substituents that allow for more back-donation from palladium. In the transition states some of the transferred charge is relocalized to the dissociating chloride; hence, the electronic effect remains, but to a lesser extent.

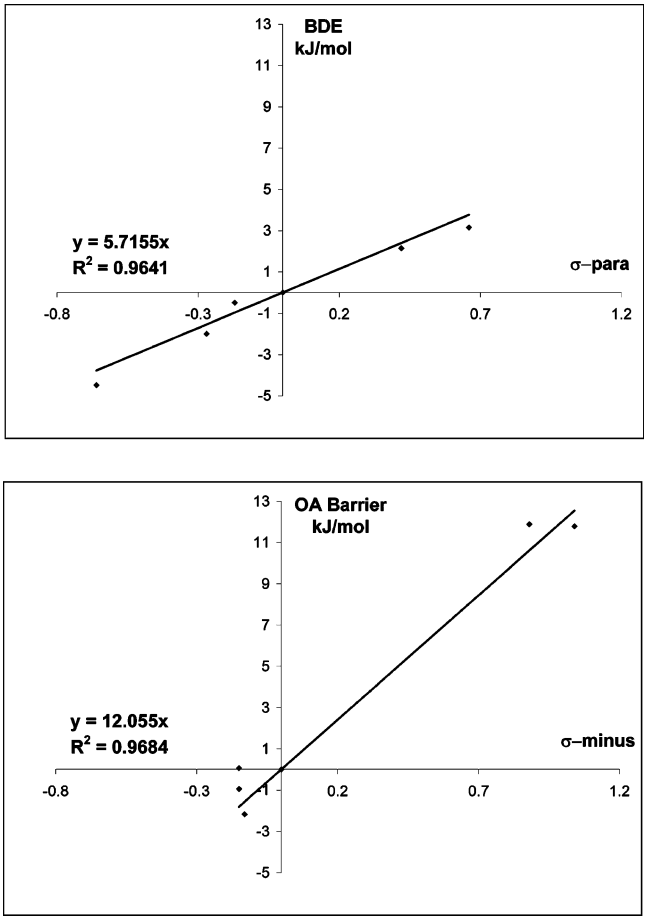

Figure 3. Hammett plots of (top) the C−Cl BDE values of the aryl chlorides and (bottom) the relative potential energies of the transition states for oxidative addition of aryl chlorides to monocoordinate palladium(0).

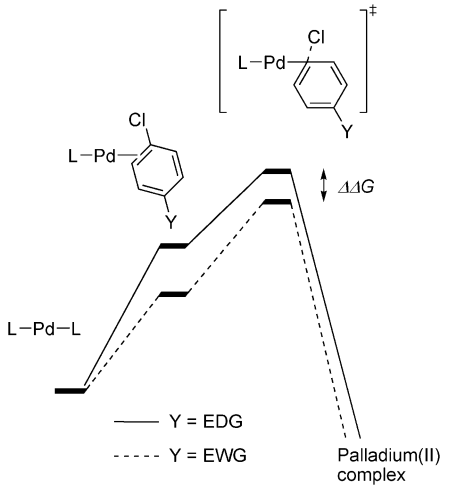

Figure 4. Illustration of the effect of introduction of an electron-withdrawing group in the aryl chloride. The effect of having an electron-deficient aryl chloride is greatest in the prereactive complex but remains to a substantial extent in the oxidative addition transition state.

Catalytic Activity. The oxidative addition barriers of the neutral palladium species are calculated to be in the range 106−

114 kJ mol^{-1} relative to Pd(P*t*Bu$_3$)$_2$, where the lower barriers were obtained for addition of electron-deficient aryl chlorides. This is substantially higher than the previously calculated barriers for phenyl iodide,[7,10] in good agreement with the observation that reactions of aryl chlorides frequently require heating. However, we want to point out that a substantial part of the reaction barrier comes from the necessity to dissociate one of the phosphines from Pd. Reaction conditions allowing formation of monoligated Pd,[12] possibly with a coordinating solvent molecule, would substantially reduce the barrier to oxidative addition.

The anionic path was found to proceed with barriers in the range 79−93 kJ mol^{-1} relative to the anionic complex [Pd(P*t*Bu$_3$)Cl]$^-$.[16] If we start instead from the solvated anionic palladium species [Pd(DMF)Cl]$^-$, the barrier is drastically decreased to 13−27 kJ mol^{-1}. Complexes such as [Pd(DMF)Cl]$^-$ are likely to be highly unstable species, yet even if they are present in only minute concentrations, they would be highly active toward oxidative addition. De Vries and co-workers reported that the anionic Pd(0) complex [Pd(H$_2$O)OAc]$^-$ was detected by ESI-MS under ligand-free conditions, using Pd(OAc)$_2$ as the source of palladium, which suggests that the anionic solvent complexes described in the current study are possible intermediates.

(16) We have avoided comparing the anionic and neutral paths directly, due to the fact that the solvation of small anions sometimes gives results not accurate enough for such a comparison to be reasonable. Due to the cancellation of errors, a comparison of complexes of the same overall charge should yield more reliable results. Ahlquist, M.; Kozuch, S.; Shaik, S.; Tanner, D.; Norrby, P.-O. *Organometallics* **2006**, *25*, 45.

Conclusions

An investigation of the oxidative addition of aryl chlorides to monoligated Pd(0) species has been presented. It was shown that the reactivity difference between electron-deficient and electron-rich aryl chlorides is due to the higher ligating ability of the electron-deficient aryl chlorides. The actual C−Cl bond-breaking step was shown to proceed with a lower barrier for the electron-rich species than for the electron-deficient analogues, relative to the respective pre-reactive complexes. Overall the energy required for the oxidative addition is less for the electron-poor aryl chlorides, in agreement with earlier experimental observations.[4a]

Supporting Information Available: Tables giving *xyz* coordinates and solution-phase energies. This material is available free of charge via the Internet at http://pubs.acs.org.

OM0604932

DOI: 10.1002/anie.200604241

Synthetic Methods

Copper-Catalyzed Synthesis of *N*-Sulfonyl-1,2,3-triazoles: Controlling Selectivity**

Eun Jeong Yoo, Mårten Ahlquist, Seok Hwan Kim, Imhyuck Bae, Valery V. Fokin, K. Barry Sharpless, and Sukbok Chang**

The recent advent of the Cu-catalyzed azide–alkyne cycloaddition (CuAAC),[1] one of the most reliable click reactions,[2] has enabled practical and efficient preparation of 1,4-disubstituted-1,2,3-triazoles from an unprecedented range of substrates with excellent selectivity, which cannot be attained with the traditional Huisgen thermal approaches.[3] In the thermal azide–alkyne cycloaddition, the type of reacting azide is especially important for the control of product distribution. For example, whereas aryl and alkyl azides react with activated alkynes to produce the corresponding 1,2,3-triazoles, *N*-sulfonyltriazoles arising from the reaction of sulfonyl azides with those acetylene compounds can undergo a rearrangement process leading to a mixture of triazoles and their ring-opened tautomers, α-diazoimino species.[4] The reversibility of the ring–chain tautomerism, known as the Dimroth rearrangement,[5] is governed by various factors, which include temperature and reaction medium, in addition to the nature of the ring substituents.[6] The stability of 5-metalated *N*-sulfonyltriazoles is even further reduced[7e] so that CuAAC with sulfonyl azides does not usually produce *N*-sulfonyltriazoles (Scheme 1). Indeed, the facile conversion of 5-cuprated triazole intermediate **A** into the presumed ketenimine species (**C**, R^2 = sulfonyl) results, upon reaction with amines, alcohols, or water, in the formation of amidines, imidates, or amides, respectively (Scheme 1, pathway b).[7] As implied in Scheme 1, the outcome of the reaction is determined by the fate of intermediate **A**. Herein, we describe the development of a copper(I)-catalyzed preparative procedure of *N*-sulfonyl-1,2,3-triazoles[8] on the basis of mechanistic insights and computational studies (pathway a).

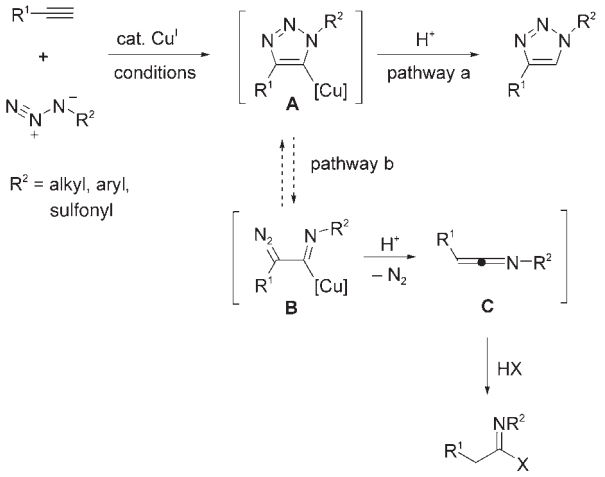

Scheme 1. Copper-catalyzed azide–alkyne cycloaddition (pathway a) and triazole opening process (pathway b)

To investigate the loss of nitrogen gas from the *N*-sulfonyltriazolyl copper intermediate and to compare it with that from the analogous *N*-alkyltriazolyl species, we undertook a computational study (B3LYP/LACV3P*+) of the key reaction steps.[9] Complexes **D** and **G** (Figure 1), which differ only in the substitution of N^1 (**D** has a methylsulfonyl substituent (-SO_2Me) whereas **G** has a methyl group in its place), were chosen as a starting point. A transition state ($\mathbf{E}_{TS}$) for the conversion of **D** into ring-opened tautomer **F**, in which the N^1–N^2 bond is broken, was located. The activation barrier for this transformation was calculated to be 64 kJ mol^{-1} with a N^1–N^2 bond length of 2.11 Å. The formation of diazoimine complex **F** was calculated to be endothermic by 27 kJ mol^{-1}.

Although the loss of nitrogen gas has not been observed when alkyl or aryl azides are used in the reaction, the corresponding step was also investigated for *N*-methyltriazolyl copper complex **G**. The barrier was found to be much higher (148 kJ mol^{-1}; $\mathbf{H}_{TS}$), which could explain why intermediate **I** has not been observed to date. Additionally, resulting diazoimine intermediate **I** was much less stable relative to triazolyl precursor **G**, with a calculated endothermicity for the transformation of 131 kJ mol^{-1}. The N^1–N^2 distance in $\mathbf{H}_{TS}$ was calculated to be 2.42 Å, which indicates a later transition state than that for the sulfonyl-substituted **D**.

According to our hypothesis, the opening of the triazole ring is followed by the loss of nitrogen gas on the path toward

[*] E. J. Yoo, S. H. Kim, Dr. I. Bae, Prof. Dr. S. Chang
Center for Molecular Design and Synthesis (CMDS)
Department of Chemistry and
School of Molecular Science (BK21)
Korea Advanced Institute of Science and Technology (KAIST)
Daejon 305-701 (Korea)
Fax: (+82) 42-869-2810
E-mail: sbchang@kaist.ac.kr
M. Ahlquist
Department of Chemistry
Building 201, Kemitorvet
Technical University of Denmark
2888 Lyngby (Denmark)
Prof. Dr. V. V. Fokin, Prof. Dr. K. B. Sharpless
Department of Chemistry and
The Skaggs Institute of Chemical Biology
The Scripps Research Institute
10550 North Torrey Pines Road, La Jolla, CA 92037 (USA)
Fax: (+1) 858-784-7562
E-mail: fokin@scripps.edu

[**] This research was supported by LG Yonam Foundation and CMDS at KAIST.

Supporting information for this article is available on the WWW under http://www.angewandte.org or from the author.

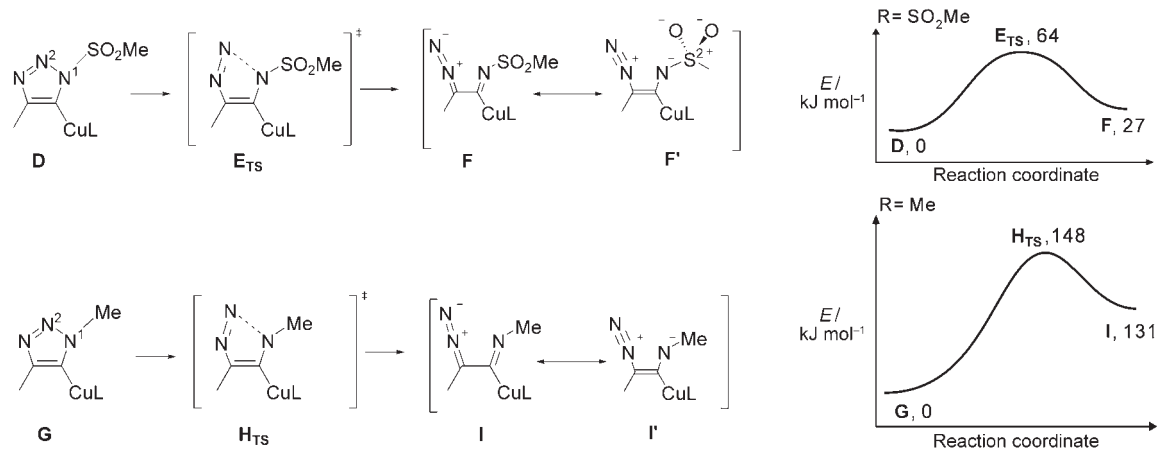

Figure 1. DFT investigation of the cleavage of the N^1–N^2 bond in triazolyl intermediates **D** and **G** (L indicates a spectator ligand, which was water in this case).

the ketenimine. As shown in Scheme 2, a copper-bound transition state in which the C–N^3 bond is broken ($\mathbf{J}_{TS}$) was located. The barrier from corresponding diazoimine intermediate **F** was calculated to be 51 kJ mol^{-1}, which makes the overall barrier for the breakdown of triazolyl **D** to be 78 kJ mol^{-1}. The breaking C–N^3 bond in the transition state is stretched to 1.7 Å. To explore whether this transformation is facilitated in the presence of copper, an analogous process was modeled with a protonated *N*-sulfonyl triazole (**K**). The ring opening of **K** to give diazoimine **L** was calculated to be exothermic by 3 kJ mol^{-1} with a barrier of 69 kJ mol^{-1}, which is only slightly higher than that of Cu triazole species **D** (64 kJ mol^{-1}, Figure 1).

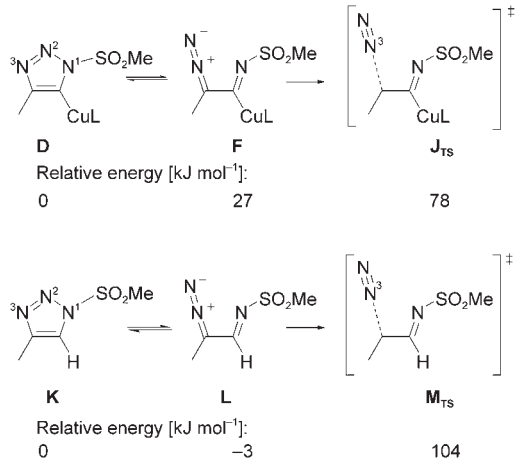

Scheme 2. Relative energy difference between Cu triazole and its protonated analogue in the ring-opening processes.

However, the following step, in which a molecule of N_2 is lost via $\mathbf{M}_{TS}$, showed a barrier that is 56 kJ mol^{-1} higher than that of the corresponding cuprated species. Transition state $\mathbf{M}_{TS}$ appears later than $\mathbf{J}_{TS}$ because the breaking C–N bond was found to be 2.1 Å long compared with 1.7 Å for $\mathbf{J}_{TS}$. In short, the loss of N_2 from the triazolyl copper species (**D**) proceeds with a 26 kJ mol^{-1} lower barrier than that from the protonated species (**K**), which corresponds to a rate difference of 5 orders of magnitude.

The computational insights described above and the previously reported mechanistic studies of the CuACC process[10] revealed to us that by changing the reaction conditions, the triazolyl intermediate could be trapped. By facilitating the protonation of the intermediate and by lowering the temperature to suppress entropically favored processes such as the formation of the dissociative $\mathbf{J}_{TS}$, we believed that triazole formation could be preferred. Consequently, we tested a wide range of reaction parameters, including temperatures and additives, as well as copper catalysts and solvents, in a test reaction of phenylacetylene with *p*-toluenesulfonyl azide (Table 1).

Whereas only a low yield of desired product 1-(*N*-tosyl)-4-phenyl-1,2,3-triazole was obtained under the standard aque-

Table 1: Cu-catalyzed *N*-sulfonyltriazole formation under the various conditions.[a]

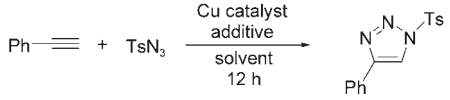

Entry	Catalyst	Additive	Solvent	*T* [°C]	Yield [%][b]
1	$CuSO_4 \cdot 5H_2O$	Na ascorbate[c]	H_2O/ *t*BuOH[d]	25	12
2	CuI	2,6-lutidine	H_2O/ *t*BuOH[d]	25	15
3	CuI	2,6-lutidine	$CHCl_3$	25	37
4	CuI	2,6-lutidine	$CHCl_3$	0	80
5	CuI	2,6-lutidine	$CHCl_3$	70	4
6	CuI	–	$CHCl_3$	0	3
7	CuI	2,6-lutidine[e]	$CHCl_3$	0	73
8	CuI	DIPEA	$CHCl_3$	0	<1

[a] Phenylacetylene (0.60 mmol), TsN_3 (0.50 mmol), additive (0.60 mmol except entries 1, 6, and 7), and [Cu] (0.05 mmol) in solvent (1.0 mL) were used. Ts = *p*-toluenesulfonyl; DIPEA = *N*,*N*-diisopropylethylamine. [b] NMR yield based on an internal standard (1,3-benzodioxole). [c] 0.1 equiv was employed. [d] H_2O/*t*BuOH = 1:2. [e] 0.2 equiv was used.

ous ascorbate conditions (Table 1, entry 1),[1a] variation of the key reaction parameters resulted in significantly improved yields.[11] For example, among several copper salts tested, CuI showed the highest catalytic activity in anhydrous conditions (chloroform). Unsurprisingly, temperature had a dramatic impact on the efficiency of the triazole-forming process (pathway a); the highest yield was obtained at 0 °C and dropped rapidly as the temperature was increased (compare Table 1, entries 3, 4, and 5). Although 2,6-lutidine is required, it can be used in substoichiometric amounts (Table 1, entry 7). Interestingly, 2,6-lutidine was uniquely superior to other organic and inorganic bases we examined.[11]

Under the optimized conditions, a range of terminal alkynes reacted smoothly with several sulfonyl azides to produce 1-(*N*-sulfonyl)-4-substituted 1,2,3-triazoles in good to excellent yields (Table 2). Electronic variation in the phenylacetylene derivatives did not alter the efficiency of the reaction (Table 2, entries 1–4). A heteroaromatic substituent was also readily introduced into the triazole skeleton at the 4-position (Table 2, entry 5). Reaction of a conjugated enyne with a sulfonyl azide took place without difficulty (Table 2, entry 6). Additionally, a range of aliphatic terminal alkynes bearing functional groups readily react with sulfonyl azides under the established conditions (Table 2, entries 7–8). Cycloaddition of terminal propargylic amides and alcohols was also facile and afforded the corresponding functionalized *N*-sulfonyl-1,2,3-triazoles in acceptable yields (Table 2, entries 9 and 10, respectively).

The scope of the reaction with respect to the azide component was also investigated by including a variety of sulfonyl azides (Table 2, entries 11–13). Synthesis of *N*-sulfonyltriazoles was performed on a gram scale without encountering problems.

It has been reported that the introduction of a sulfonyl group into a wide range of heterocyclic compounds results in significant changes in the bioactivity of the compounds.[12] Therefore, the present work of synthesizing sulfonyl triazoles may initiate a new search for bioactive triazole molecules, especially in medicinal chemistry. In addition, because the CuAAC reaction has emerged as a highly efficient means of bioconjugation, especially in recent years,[2] the developed protocol can be utilized to expand the scope of the tool greatly . Moreover, the sulfonyl group could be readily removed under mild conditions by using magnesium in methanol[13] to provide 4-substituted *N*-H-triazoles in excellent yields.[14]

In summary, mechanistic insights and computational studies of the CuAAC reaction enabled the development of a new practical procedure for the preparation of 4-substituted 1-(*N*-sulfonyl)-1,2,3-triazoles. The important heterocycles were obtained regioselectively in good to excellent yield by performing the reactions at low temperature in chloroform in the presence of 2,6-lutidine and a catalytic amount of CuI.

Received: October 17, 2006
Published online: ■■ ■■, ■■■■

Keywords: alkynes · copper · cycloaddition · sulfonyl azides · sulfonyltriazoles

Table 2: Cu-catalyzed cycloaddition of terminal alkynes and sulfonyl azides.[a]

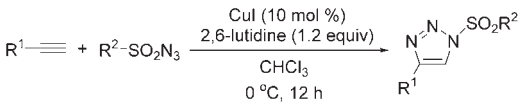

Entry	Product		Yield [%][b]
1	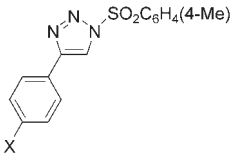	X = H	83
2		Me	78
3		CF_3	84
4		Br	95
5	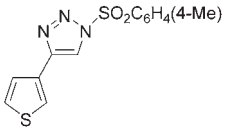		90
6	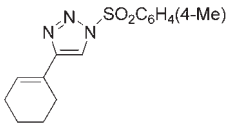		61
7	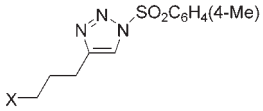	X = Cl	68
8		OC(O)Me	57
9	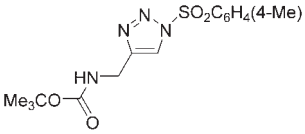		60
10	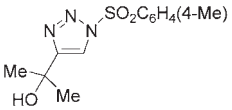		75
11	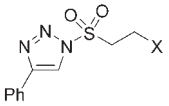	X = Et	80
12		$SiMe_3$	84
13	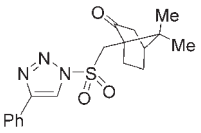		56

[a] A solution of alkyne (0.60 mmol), sulfonyl azide (0.50 mmol), 2,6-lutidine (0.60 mmol), and CuI (0.05 mmol) in $CHCl_3$ (1.0 mL) was stirred for 12 h at 0 °C. [b] Yield of isolated product after column chromatography.

[1] a) V. V. Rostovtsev, L. G. Green, V. V. Fokin, K. B. Sharpless, *Angew. Chem.* **2002**, *114*, 2708; *Angew. Chem. Int. Ed.* **2002**, *41*, 2596; b) C. W. Tornøe, C. Christensen, M. Meldal, *J. Org. Chem.* **2002**, *67*, 3057.

[2] a) H. C. Kolb, K. B. Sharpless, *Drug Discovery Today* **2003**, *8*, 1128; b) V. D. Bock, H. Hiemstra, J. H. van Maarseveen, *Eur. J. Org. Chem.* **2006**, 51.

[3] a) R. Huisgen in *1,3-Dipolar Cycloaddition Chemistry* (Ed.: A. Padwa), Wiley, New York, **1984**, pp. 1–176; b) A. Padwa in *Comprehensive Organic Synthesis, Vol. 4* (Ed.: B. M. Trost), Pergamon, Oxford, **1991**, pp. 1069–1109.

[4] a) P. Grünanger, P. V. Finzi, *Tetrahedron Lett.* **1963**, *4*, 1839; b) P. Grünanger, P. V. Finzi, C. Scotti, *Chem. Ber.* **1965**, *98*, 623; c) R. E. Harmon, F. Stanley, S. K. Gupta, J. Johnson, *J. Org.*

Chem. **1970**, *35*, 3444; d) G. Himbert, D. Frank, M. Regitz, *Chem. Ber.* **1976**, *109*, 370; e) R. Huisgen, *Angew. Chem.* **1980**, *92*, 979; *Angew. Chem. Int. Ed. Engl.* **1980**, *19*, 947.

[5] a) O. Dimroth, *Justus Liebigs Ann. Chem.* **1909**, *364*, 183; b) G. L'abbé, *Bull. Soc. Belg.* **1990**, *99*, 281; c) E. S. H. El Ashry, Y. El Kilany, N. Rashed, H. Assafir, *Adv. Heterocycl. Chem.* **1999**, *75*, 79.

[6] a) M. E. Hermes, F. D. Marsh, *J. Am. Chem. Soc.* **1967**, *89*, 4760; b) C. L. Habraken, C. Erkelens, J. R. Mellema, P. Cohen-Fernandes, *J. Org. Chem.* **1984**, *49*, 2197.

[7] a) I. Bae, H. Han, S. Chang, *J. Am. Chem. Soc.* **2005**, *127*, 2038; b) S. H. Cho, E. J. Yoo, I. Bae, S. Chang, *J. Am. Chem. Soc.* **2005**, *127*, 16046; c) E. J. Yoo, I. Bae, S. H. Cho, H. Han, S. Chang, *Org. Lett.* **2006**, *8*, 1347; d) S. Chang, M. Lee, D. Y. Jung, E. J. Yoo, S. H. Cho, S. K. Han, *J. Am. Chem. Soc.* **2006**, *128*, 12366; e) M. P. Cassidy, J. Raushel, V. V. Fokin, *Angew. Chem.* **2006**, *118*, 3226; *Angew. Chem. Int. Ed.* **2006**, *45*, 3154; f) M. Whitting, V. V. Fokin, *Angew. Chem.* **2006**, *118*, 3229; *Angew. Chem. Int. Ed.* **2006**, *45*, 3157.

[8] V. P. Krivopalov, O. P. Shkurko, *Russ. Chem. Rev.* **2005**, *74*, 339.

[9] All calculations were performed with the use of the B3LYP exchange-correlation functional and the LACV3P*+ basis set as implemented in the Jaguar 6.5 program package by Schrodinger LLC., Portland, OR, 2006. All ground-state and transition-state geometries were fully optimized including the PBF solvent model in Jaguar 6.5, with the default parameters for water. Zero-point energy corrections were estimated from calculation of the harmonic frequencies.

[10] a) F. Himo, T. Lovell, R. Hilgraf, V. V. Rostovtsev, L. Noodleman, K. B. Sharpless, V. V. Fokin, *J. Am. Chem. Soc.* **2005**, *127*, 210; b) V. O. Rodionov, V. V. Fokin, M. G. Finn, *Angew. Chem.* **2005**, *117*, 2250–2255; *Angew. Chem. Int. Ed.* **2005**, *44*, 2210.

[11] See the Supporting Information for details.

[12] a) R. Mahmud, M. D. Tingle, J. L. Maggs, M. T. D. Cronin, J. C. Dearden, B. K. Park, *Toxicology* **1997**, *117*, 1; b) Z. Huang, K. C. Schneider, S. A. Benner, *J. Org. Chem.* **1991**, *56*, 3869.

[13] a) B. Nyasse, L. Grehn, U. Ragnarsson, *Chem. Commun.* **1997**, 1017; b) C. S. Pak, D. S. Lim, *Synth. Commun.* **2001**, *31*, 2209.

[14] a) J. C. Loren, A. Krasiński, V. V. Fokin, K. B. Sharpless, *Synlett* **2005**, 2847; b) T. Jin, S. Kamijo, Y. Yamamoto, *Eur. J. Org. Chem.* **2004**, 3789.

Enhanced Reactivity of Dincucler Copper(I) Acetylides in Dipolar Cycoadditions

Mårten Ahlquist*[,a,b] and Valery V. Fokin,*[,a]

[a]*Department of Chemistry and the Skaggs Institute for Chemical Biology, The Scripps Research Institute, 10550 North Torrey Pines Road,La Jolla, California 92037*

[b]*Department of Chemistry, Technical University of Denmark, Building 201Kemitorvet, 2800 Kgs. Lyngby, Denmark*

RECEIVED DATE (automatically inserted by publisher); fokin@scripps.edu, marten@kemi.dtu.dk

Coordination compounds of copper are ubiquitous in both biological and abiological systems and often contain two or more metal atoms in close association.[1-5] The tendency toward clustering is most apparent among copper(I) species, and the extent of polynucleation has a significant effect on the stability, properties, and catalytic activity of copper(I) complexes. Copper(I) acetylides have a long history, dating back to Glaser's discovery of oxidative dimerization of phenylacetylide of copper in 1869.[6] Transformations involving copper acetylides now extend well beyond the oxidative coupling reactions, yet the precise nature of the reactive alkynyl copper species is not always known, underscoring the facility of the ligand exchange at the copper center and the involvement of multiple equilibria. Nevertheless, that copper(I) complexes with terminal alkynes are usually highly aggregated species, engaging in a range of σ– and π-interactions, has been demonstrated.[7-9]

The copper-catalyzed azide-alkyne cycloaddition (CuAAC)[10,11] reaction is a recent addition to the family of transformations involving alkynyl copper compounds. Therein, copper(I) acetylides are generated *in situ* by the action of a copper(I) complex on a terminal alkyne and are immediately engaged in an efficient sequence leading to the regiospecific formation of a 1,2,3-triazole heterocycle. This catalytic version of the Huisgen's 1,3-dipolar cycloaddition is accelerated by as much as 10^7 comparing to the thermal process, and exhibits excellent scope and exquisite selectivity. A stepwise mechanism involving copper(I) acetylides was proposed[11] (Figure 1, top) and computationally investigated soon thereafter.[12] Here we present the results of a density functional theory (B3LYP) investigation of the reaction between dinuclear copper(I) acetylide complexes and an organic azide, revealing a substantial further drop in the activation barrier already reported for the mono-copper ensemble.

The first DFT treatment of the triazole-forming sequence by Himo et al.,[12] based on a mono-copper acetylide model, correlated well with the observed high regioselectivity and the large rate increase. Formation of the copper metallacycle species **2** (Figure 1) was found to be the rate limiting step (activation energy was calculated to be 18.7 kcal/mol (L = H_2O)). Soon afterward, careful kinetic investigation of the reaction of phenylacetylene and benzyl azide by Rodionov et al. revealed a strict second order dependence on copper under the catalytic conditions.[13] Knowledge of the requirement of two copper atoms in the transition state complex triggered our search for its role. Localization of electron density on C^1 in complex **2**, seen computationally, suggests that the introduction of a second copper atom in proximity to C^1 may offer additional stabilization of this intermediate and of the transition state on the path of **2** to the triazole heterocycle.

Calculations were performed at the B3LYP/LACV3P*+ level of theory as implemented in the Jaguar 6.5 program.[14] All geometries were fully optimized including the PBF-solvation model with the default values of the parameters for simulation of water. Since the treatment of solvation in the PBF model is slightly different from that used in the original calculations, the reaction was remodeled, and the new overall barrier for the union of the azide **3** with the acetylide **4** was calculated at 17 kcal/mol (**TS-mono**). Formation of the resulting metallacycle **2** was found to be endothermic by 11.2 kcal/mol. Both values are in good agreement with those reported previously.

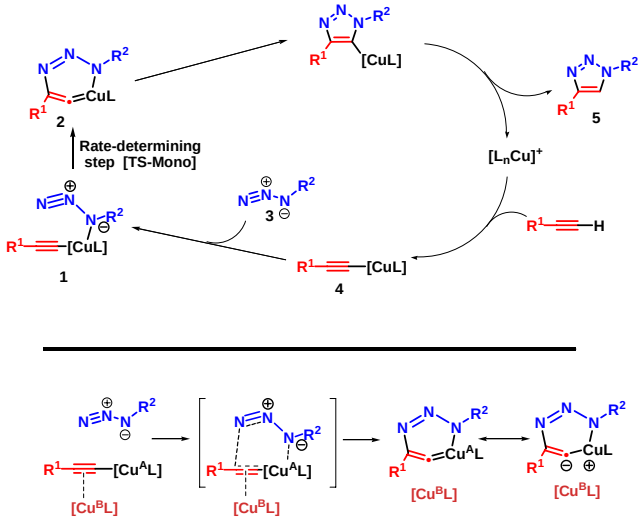

Figure 1. Reported mechanism of the reaction between a mononuclear copper(I) acetylide and an organic azide (top).[12] Introduction of a second copper(I) atom may favorably influence the energetic profile of the reaction (bottom). L = H_2O.

To probe the hypothesis that a second copper center positioned closely to C^1 can have a favorable influence on the transition state leading to the metallacycle **2**, two transition states containing a second copper(I) center were located. The two transition states differed only in the spectator ligand on the second copper atom. In the first, it was an acetylide (**TS-di^{alkyne}**), and in the second the spectator ligand was a chloride (**TS-di^{chloride}**), Figure 2. In both **TS-di^{alkyne}** and **TS-di^{chloride}** the second copper atom, Cu^B, forms a bond with C^1. The distances are calculated at 1.93 Å and 1.90 Å for **TS-di^{alkyne}** and **TS-di^{chloride}**, respectively. This short distance indicates a strong interaction between the 2nd metal atom and the reacting copper acetylide.[15]

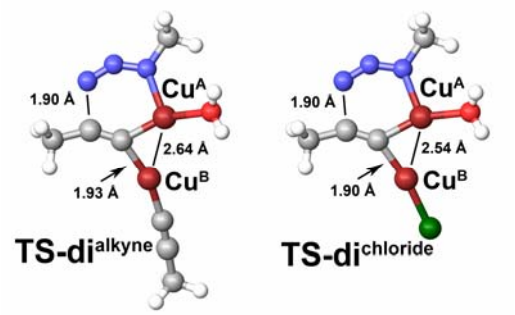

Figure 2. Intercation of the second copper atom with the transition state 1 to 2.

The interaction of the Cu^B with the proposed intermediates in the triazole-forming sequence and with the transition state indicates that a second copper atom is involved in the key steps of the CuAAC process. To compare the reactivity of the dinuclear copper complexes to their mono-copper analog, the transition state energy was compared relative to the azide and dicopper species in isolation. The geometries of dinuclear copper acetylide species $\mathbf{6}^{\mathbf{alkyne}}$ and $\mathbf{6}^{\mathbf{chloride}}$ (Figure 3) were found to be quite similar. The reacting acetylide is σ-coordinated to Cu^A, while the second metal center, Cu^BX (where X is acetylide or chloride), exhibits a stronger interaction with C^1, with possible interactions between Cu^B and C^2 and Cu^A. Interestingly, the μ^2 mode of coordination of the alkyne was not observed unless two identical spectator ligands were present on both copper atoms (e. g. $[MeCC(CuCl)_2]^-$). The barrier for the addition of methyl azide (**3**, R=Me) to the dinuclear copper acetylide complex $\mathbf{6}^{\mathbf{alkyne}}$ was calculated at 12.9 kcal/mol. The corresponding barrier for the chloride analog $\mathbf{6}^{\mathbf{chloride}}$ was found to be even lower, 10.5 kcal/mol. Compared to the mononuclear copper acetylides, for which an overall barrier of 17 kcal/mol was calculated (*vide supra*), the reactivity of the dinuclear complexes is expected to be several orders of magnitude higher.

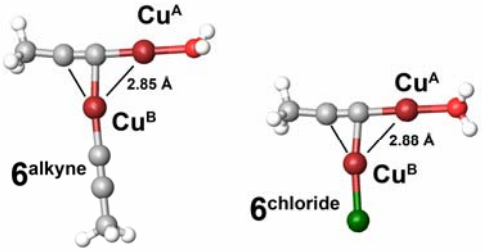

Figure 3. Optimized structures of dinuclear copper acetylides.

Furthermore, a similar effect of the 2nd copper center was observed in the ground state of the six-membered intermediates $\mathbf{7}^{\mathbf{alkyne}}$ and $\mathbf{7}^{\mathbf{chloride}}$ (Figure 4). Both transformations of **6** to **7** were found to be endothermic by 6 and 3.6 kcal/mol for $\mathbf{7}^{\mathbf{alkyne}}$ and $\mathbf{7}^{\mathbf{chloride}}$, respectively—substantially lower endothermicity than for the corresponding mono-copper transformation (11.2 kcal/mol). When the two dinuclear copper complexes $\mathbf{6}^{\mathbf{alkyne}}$ and $\mathbf{6}^{\mathbf{chloride}}$ were compared, $\mathbf{6}^{\mathbf{chloride}}$ was more reactive. This is likely due to the lower trans influence of the chloride comparing to the σ-acetylide ligand, and thus a higher stabilizing ability of the Cu^BX fragment on ligands trans to X, in this case stabilization of the electron density build-up on C^1.

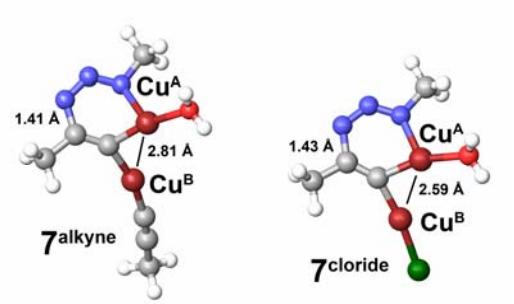

Figure 4. Optimized structures of the dinuclear analogs of the metallacycle **2**.

In addition to providing support for the experimentally observed 2nd order rate law in [Cu],[13] this DFT study points to the more reactive nature of dinuclear copper complexes in dipolar cycloadditions comparing to their monomeric congeners. The involvement of a second copper center in the catalysis may also explain the high activity of heterogeneous catalysts, including bulk copper metal[11,12] and nanoclusters.[16,17] Furthermore, similar dinuclear intermediates are likely involved in other transformations involving copper(I) acetylides, and further examination of their properties should help elucidate the origins of the exceptional reactivity of in situ generated copper(I) acetylides, in particular in aqueous solutions.

Acknowledgements. We are grateful to Profs. K.B. Sharpless and M.G. Finn for stimulating discussions and advice; to Prof. D.A. Case and Dr. V. Pelmenschikov for assistance with the software package, and the Technical University of Denmark (M.A.), and the Skaggs Institute for Chemical Biology and Pfizer, Inc. (V.V.F.) for financial support.

Supporting Information Available: Cartesian coordinates, absolute energies and zero-point energy corrections for all calculated geometries. This material is available free of charge via the Internet at http://pubs.acs.org

(1) Karlin, K. D.; Hayes, J. C.; Gultneh, Y.; Cruse, R. W.; McKown, J. W.; Hutchinson, J. P.; Zubieta, J. *J. Am. Chem. Soc.* **1984**, *106*, 2121.
(2) Karlin, K. D.; Zhu, Z.-Y.; Karlin, S. *J. Biol. Inorg. Chem.* **1998**, *3*, 172.
(3) Chen, P.; Solomon, E. I. *Proc. Natl. Acad. Sci. U. S. A.* **2004**, *101*, 13105.
(4) Liao, Y.; Novoa, J. J.; Arif, A.; Miller, J. S. *Chem. Comm.* **2002**, 3008.
(5) Zheng, S.-L.; Messerschmidt, M.; Coppens, P. *Angew. Chem. Int. Ed.* **2005**, *44*, 4614.
(6) Glaser, C. *Chem. Ber.* **1869**, *2*, 422.
(7) Mykhalichko, B. M.; Temkin, O. N.; Mys'kiv, M. G. *Russ. Chem. Rev.* **2001**, *69*, 957.
(8) Xie, X.; Auel, C.; Henze, W.; Gschwind, R. M. *J. Am. Chem. Soc.* **2003**, *125*, 1595.
(9) Vrieze, K.; van Koten, G. In *Comprehensive Coordination Chemistry*; Pergamon: Oxford, 1987; Vol. 2, pp. 189.
(10) Rae, C. S.; Khor, I. W.; Wang, Q.; Destito, G.; Gonzalez, M. J.; Singh, P.; Thomas, D. M.; Estrada, M. N.; Powell, E.; Finn, M. G.; Manchester, M. *Virology* **2005**, *343*, 224.
(11) Rostovtsev, V. V.; Green, L. G.; Fokin, V. V.; Sharpless, K. B. *Angew. Chem. Int. Ed.* **2002**, *41*, 2596.
(12) Himo, F.; Lovell, T.; Hilgraf, R.; Rostovtsev, V. V.; Noodleman, L.; Sharpless, K. B.; Fokin, V. V. *J. Am. Chem. Soc.* **2005**, *127*, 210.
(13) Rodionov, V. O.; Fokin, V. V.; Finn, M. G. *Angew. Chem. Int. Ed.* **2005**, *44*, 2210.
(14) Jaguar 6.5; Schrodinger LLC., Portland, OR, 2006
(15) Chui, S. S. Y.; Ng, M. F. Y.; Che, C.-M. *Chem. Eur. J.* **2005**, *11*, 1739.
(16) Pachon, L. D.; van Maarseveen, J. H.; Rothenberg, G. *Adv. Synth. Cat.* **2005**, *347*, 811.
(17) Molteni, G.; Bianchi, C. L.; Marinoni, G.; Santo, N.; Ponti, A. *New J. Chem.* **2006**, *30*, 1137.